

UNCLASSIFIED

AD 267 495

*Reproduced
by the*

ARMED SERVICES TECHNICAL INFORMATION AGENCY
ARLINGTON HALL STATION
ARLINGTON 12, VIRGINIA



UNCLASSIFIED

NOTICE: When government or other drawings, specifications or other data are used for any purpose other than in connection with a definitely related government procurement operation, the U. S. Government thereby incurs no responsibility, nor any obligation whatsoever; and the fact that the Government may have formulated, furnished, or in any way supplied the said drawings, specifications, or other data is not to be regarded by implication or otherwise as in any manner licensing the holder or any other person or corporation, or conveying any rights or permission to manufacture, use or sell any patented invention that may in any way be related thereto.

VOLUME 5

NOX

DASA 1300

CATALOGED BY ASTIA 267 495
AS AD No.

267 495

High Altitude Sampling Program

Supplementary

H A S P

Studies

ISOTOPE, INC.



Defense Atomic Support Agency

WASHINGTON 25, D.C.

DASA 1300

THE HIGH ALTITUDE SAMPLING PROGRAM

by

James P. Friend, Editor
Herbert W. Feely, Project Director
Philip W. Krey
Jerome Spar
Alan Walton

VOLUME 5

SUPPLEMENTARY HASP STUDIES

The Final Report on Contract DA-29-044-XZ-609

Prepared for

Defense Atomic Support Agency
Washington 25, D. C.
August 31, 1961

ISOTOPES, INCORPORATED
123 Woodland Avenue
Westwood, New Jersey

GENERAL TABLE OF CONTENTS

Volume 1. HASP Purpose and Methods

Abstract
Preface

Part I. Stratospheric Radioactivity

Chapter 1. Introduction
Chapter 2. The Problem
Chapter 3. Procedures
Appendix A.

Volume 2. Results of Filter Analyses

Part I. (Continued)
Chapter 4. Analytical Results

Volume 3. Discussion of HASP Results

Part I. (Continued)
Chapter 5. The Distribution of Nuclear Debris in the Stratosphere
Chapter 6. Meteorological Processes and Radioactivity

Volume 4. The Application of HASP Data

Part I. (Continued)
Chapter 7. The Surface Burden of World-Wide Fallout
Chapter 8. Remaining Problems in World-Wide Fallout
Chapter 9. The Hazards from Radioactive Fallout
Chapter 10. Summary and Conclusions

Volume 5. Supplementary HASP Studies

Part II. Studies of Stratospheric Particles

Chapter 1. Introduction
Chapter 2. Physical Methods of Particle Studies
Chapter 3. Neutron Activation of Filter Samples
Chapter 4. Analytical Results
Chapter 5. Discussion and Conclusions

Part III. Measurements of Fallout in Man's Environment

Chapter 1. Measurements of Carbon-14 in Tropospheric Air
Chapter 2. Measurement of Tritium in Precipitation
Chapter 3. The Distribution of Radioactivity in Soils
Chapter 4. Plutonium in Man and Environment

VOLUME 5

TABLE OF CONTENTS

Part II. Studies of Stratospheric Particles

Chapter 1. Introduction	1
References	5
Chapter 2. Physical Methods of Particle Studies	6
Description of Particle Collection and Methods of Analysis.	6
Particles in Filter Papers	6
Particles Collected by Impaction	7
Techniques and Analytical Procedures	13
Autoradiographic Techniques	13
Thin Sectioning Techniques	16
Electron Microscopy	20
Light Microscopy Techniques	22
Electron Microscopy Techniques	23
Particle Counting Procedures	24
Chapter 3. Neutron Activation of Filter Samples	26
Neutron Irradiation of Samples	27
Radiochemical Methods	34
The Sequential Separation of Nickel-65, Manganese-56, Copper-64, Chromium-51, Iron-59 and Cobalt-60	37
The Sequential Separation of Phosphorous-32 and Zinc-69.	39
The Radiochemical Analysis of Calcium-45.	40
Calcium-45 Counting Procedure	41
Nickel-65 Purification Procedure	43
Nickel-65 Counting Procedure	44
Manganese-56 Purification Procedure	46
Radiometric Assay	47
Copper-64 Purification Procedure	48
Copper-64 Counting Procedure	49
Iron-59 Purification Procedure	50
Iron-59 Counting Procedure	51
Chromium-51 Purification Procedure	52
Chromium-51 Counting Procedure	53
Cobalt-60 Purification Procedure	55
Cobalt-60 Counting Procedure	56
Zinc-69 Purification Procedure	58
Zinc-69 Counting Procedure	59
Phosphorous-32 Purification Procedure	60

Phosphorous-32 Counting Procedure	61
Results of the Neutron Activation of Filter Papers	62
List of Reagents	64
References	66
Chapter 4. Analytical Results	67
Penetration of Filter Paper by Particles	67
Parallel Sections	68
Normal Sections	72
Physical and Chemical Properties of Stratospheric Aerosols	75
Chemical Composition	76
Particle Classification	82
Particle - Radioactivity Relationships	113
Evaluation of Survey Autoradiograms of Filter Paper	
Samples	113
Size Measurements of Individual Particles Related to	
Survey Autoradiograms.	121
Radioactivity Measurements of Impaction Collector	
Samples	128
References	129
Chapter 5. Discussion and Conclusions	130
The Stratospheric Aerosol	131
Properties of the Stratospheric Aerosol	134
The Particle Size Spectrum	134
The Effect of the Stratospheric Aerosol on World-Wide	
Fallout of Nuclear Debris	141
The Stratospheric Burden of Sulfate	148
Extraterrestrial Material in the Stratosphere	149
Conclusions	152
References	153
Part III. Measurements of Fallout in Man's Environment.	155
Chapter 1. Measurements of Carbon-14 in Tropospheric Air	157
Sample Collection.	158
Analytical Procedures.	159
Sample Preparation.	159
Counting Procedure.	161
Accuracy and Reproducibility	162
Results and Discussion	164
Results	164
Discussion.	167
Summary	172
References.	173

Chapter 2. Measurements of Tritium in Precipitation	174
Experimental Procedures	175
Sample Collection	175
Enrichment of Tritium in Precipitation Samples	175
Deuterium and Tritium Assays	177
Accuracy, Reproducibility and Theoretical Considerations	180
Results and Discussion	183
Summary	191
References	193
 Chapter 3. The Distribution of Radioactivity in Soils	 194
Acknowledgments	196
Description of Soil Samples	197
Sample Collection	215
The Corer.	216
The Core Driving Equipment	216
The Sampling Operation.	216
Sample Pretreatment.	220
The Radiochemical Determination of Strontium-90, Ruthenium-106, Cesium-137 and Cerium-144 in Soils	225
The Sequential Separation of Strontium-90, Cesium-137 Cerium-144	227
Strontium-90 Purification Procedure	230
Yttrium-90 Counting Procedure	231
Cesium-137 Purification Procedure	232
Cesium-137 Counting Procedure.	233
The Determination of Cesium-137 in Soils By Gamma Ray Spectroscopy	235
Cerium-144 Purification Purification	244
Cerium-144 Counting Procedure.	244
Radiochemical Analysis of Ruthenium-106	246
Ruthenium-106 Counting Procedure	248
List of Reagents	249
Quality Control	251
Results and Discussion of Radiochemical Data	255
Variation of Concentrations of Nuclides With Depth In Soils	266
Cumulative Deposits of Radioactivity in New Jersey Soils.	279
Variability of the Total Deposits of Radioactivity in New Jersey Soils.	283
Variability of Nuclide Ratios Within Soils	284
Distribution of Radioactivity in Disturbed and Undisturbed Soils	288
Application of Results to World-Wide Fallout of Strontium-90 and the External Hazard from Fallout Radioactivity	290
Conclusions	294
References	295

Chapter 4. Plutonium in Man and Environment	297
Mode of Entry into Humans	297
Environmental Levels	301
Analytical Procedure	303
Human Tissue Analyses	305
Animal Tissue Analyses	307
Miscellaneous Sample Analyses	308
Summary	311
References	313

VOLUME 5

LIST OF TABLES

Part II

1. 1	Observations of Phenomena Related to Stratospheric Particles. .	2
3. 1	List of Standard Samples for Neutron Irradiation	28
3. 2	Duplicate Determinations of Activated Standard Samples	30
3. 3	Results of Neutron Activation of Filter Papers	63
4. 1	Distribution of Dense Spot Images in 8 Filters	72
4. 2	Results of Neutron Activation Analyses	77
4. 3	Net Quantities of Elements in Dust Samples	77
4. 4	Lattice Constants of Ammonium Sulfate and Ammonium Persulfate	78
4. 5	Impaction Efficiencies for Probe Collector	87
4. 6	Stratospheric Particle Distributions	101-109
4. 7	Calculation of Average Particle Size-Concentration Distributions	110
4. 8	HASP Filters Examined by Survey Autoradiography.	114
4. 9	Comparison of Radiochemical and Autoradiographic Data	120
5. 1	Comparison of AFCRL and HASP Particle Size-Concentration Spectra	137
5. 2	Number and Volume Concentrations of Particles Corresponding to HASP and AFCRL Distributions	138
5. 3	Summary of Particle and Radioactivity Concentrations	144

Part III

1. 1	Radiocarbon Concentrations in Tropospheric Air at Washington Township, New Jersey	165
2. 1	Results of Experiment to Check Enrichment Procedures	181
2. 2	Tritium Concentrations in Precipitation at Westwood, New Jersey	184

3.1	Description of Soil Sampling Sites in New Jersey and Kansas . . .	199
3.2	Comparison of Cesium-137 Analyses by Gamma Ray Spectroscopy and Radiochemical Analysis	239
3.3	Duplicate Analyses.	252
3.4	Deposition of Strontium-90, Ruthenium-106, Cesium-137 and Cerium in New Jersey and Kansas Soils in 1960	259
3.5	Estimations of Cumulative Deposits of Ruthenium-106 and Cerium- 144 in New Jersey Soils on July 1, 1960.	277
3.6	Comparison of Average Cumulative Activities in New Jersey Soils with Estimated Deposits.	278
3.7	Variability of Cumulative Activities of Strontium-90, Ruthenium-106, Cesium-137 and Cerium-144 in New Jersey Soils	282
3.8	Average Percentages of Total Activity in Soils as a Function of Depth	282
3.9	Average Vertical Profile of Strontium-90 in New Jersey Soils . .	287
3.11	Average Nuclide Ratios of Cumulative Activities in New Jersey Soils	287
4.1	Radiation Characteristics of Plutonium-239 and Plutonium-240 . .	298
4.2	Plutonium Analyses of Human Tissue	306
4.3	Plutonium Analyses of Animal Tissue	309
4.4	Miscellaneous Plutonium Analyses	310

VOLUME 5

LIST OF FIGURES

Part II

2.1	Modified Probe Impaction Sampler	10
2.2	U-2 Showing Strut for Probe Mount	11
2.3	Exposure Assembly for Survey Autoradiograms	14
2.4	Filter Paper-Methacrylate Arrangement for Plastic Embedding . .	17
2.5	Microtome Sectioning of a Filter Sample	19
2.6	Selection of 1/8 Inch Diameter Electron Microscope Gride from Probe Window Sample	25
3.1	Scheme of Sequential Analysis of Activated Samples	36
4.1	Parallel Sections and Corresponding Autoradiogram	69
4.2	Variation of Cumulative Collected Radioactivity with Depth of Filter	71
4.3	Distribution of High Density Spot Images in Survey Autoradiograms of Normal Sections of 8 Samples	73
4.4	Normal Sections and Corresponding Autoradiogram	74
4.5	Electron Diffraction Pattern of Ammonium Persulfate Particles . .	79
4.6	Electron Micrograph of Particles of Ammonium Persulfate	79
4.7	Electron Micrograph of Particles of Ammonium Sulfate.	79
4.8	Electron Micrograph Showing Crystalline Ammonium Sulfate Particles	81
4.9	Experimental Impaction Efficiencies of Cylindrical Collectors. . .	84
4.10	Schematic Diagram of Impaction Surface Showing Zone of Maximum Deposition	88
4.11	Electron Micrograph of Stratospheric Particles Showing Evidence of Moisture Condensation	94
4.12	Electron Micrograph of Stratospheric Particles Shadow Cast at an Angle of 10°	97

4. 13	Particle Size-Concentration Distribution	99
4. 14	Electron Micrographs of Non-sulfate Types of Stratospheric Particles	112
4. 15	Survey Autoradiograms of Filter Papers Exposed Simultaneously in the Tropical Stratosphere	116
4. 16	Survey Autoradiograms of Samples Exposed in the Tropical Stratosphere	117
4. 17	Survey Autoradiograms of Samples Exposed in the Polar Stratosphere	118
4. 18	Survey Autoradiograms of Samples Exposed in the Vicinity of the Tropopause Gap	119
4. 19	Beta Count Rates and Autoradiograms of Filter Portions	122
4. 20	Beta Count Rates and Autoradiograms of Thin Sections	122
4. 21	High Resolution Autoradiograms of Large Agglomerated Particles	123
4. 22	High Resolution Autoradiograms of Micron Size Particles	125
4. 23	High Resolution Autoradiograms of Filter Fibers	127
5. 1	Particle Size-Concentration Spectra of Stratospheric Particles	135
5. 2	Vertical Profiles of Particles and Strontium-90, Jan. - Jun. 1960	145

Part III

1. 1	Gas Handling System	160
1. 2	Carbon-14 Counter and Associated Shielding	163
1. 3	Variability of Carbon-14 Concentrations in Tropospheric Carbon- Dioxide at Washington Twp., N. J. and Strontium-90 in Rain at Westwood, N. J.	166
1. 4	Changes in Carbon-14 Concentration in Tropospheric Air During the Period 1954 - 1961	168
2. 1	Gas Handling System for Tritium	179
2. 2	Tritium and Strontium-90 Concentrations in Precipitation at W Westwood, New Jersey	185

2.3	Intercomparison of Tritium Concentrations in Rain From Four Areas	188
3.1	Distribution of Soil Sampling Sites in New Jersey	198
3.2	Sample Corer and Drive Weight	217
3.3	Soil Extruder	219
3.4	Soil and Rock Crusher	222
3.5	Soil and Rock Pulverizer	223
3.6	Patterson-Kelley Blender	224
3.7	Outline of Sequential Analysis	226
3.8	Cs ¹³⁷ Counting Efficiency vs. Soil Weight in Beaker	236
3.9	Total Spectrum of Soil Sample 20-2.	237
3.10	Spectrum of Sample 20-2 Minus Thorium Component	240
3.11	Spectrum of Sample 20-2 Minus Thorium and U Components	241
3.12	Spectrum of Sample 20-2 Minus Th, U and K ⁴⁰ Components.	242
3.13	Ruthenium Distillation Apparatus.	247
3.14	Strontium-90 Concentrations in New Jersey Soils	267
3.15	Ruthenium-106 Concentrations in New Jersey Soils.	268
3.16	Cesium-137 Concentrations in New Jersey Soils	269
3.17	Cerium-144 Concentrations in New Jersey Soils	270
3.18	Average Concentrations of Strontium-90, Ruthenium-106, Cesium-137 and Cerium-144 in New Jersey Soils in 1960	274
3.19	Relative Vertical Profiles of Strontium-90, Ruthenium-106, Cesium-137 and Cerium-144 Concentrations in New Jersey Soils in 1960	275
3.20	Average Cumulative Activities of Sr-90, Ce ¹⁴⁴ , Ru ¹⁰⁶ and Cs ¹³⁷ in New Jersey Soils in 1960	280
3.21	Concentrations of Radioactivity in Disturbed and Undisturbed Soil Samples	289

THE HIGH ALTITUDE SAMPLING PROGRAM

PART II

STUDIES OF STRATOSPHERIC PARTICLES

CHAPTER 1

INTRODUCTION

Studies of particles in the stratosphere were undertaken in HASP in an attempt to shed light on two different aspects of the program; one concerned the efficiency of collection (retentivity) of the HASP filters for radioactive debris in the stratosphere, and the other concerned the physical and chemical properties of the particles on which the radioactive fission products are carried throughout the stratosphere.

At the time when the HASP studies commenced, little was known of particles in the stratosphere. The available information concerning the particulate material was of a qualitative nature based mostly upon indirect measurements of optical phenomena, electrical conductivity, and a few visual observations from manned balloons and aircraft. These observations have been briefly surveyed by Junge, Chagnon and Manson¹. We list here (Table 1.1) the various observations which were made. However, the reader is referred to the above mentioned paper for further discussion. These limited observations provided little information concerning the nature of the particles involved in world-wide fallout in the stratosphere.

By the time HASP was under way, it was widely accepted that the processes which brought world-wide fallout into the troposphere were primarily meteorological-gravitation of the debris - bearing particles being at most a second order effect. Since the size distribution and chemical composition of the stratospheric particles were unknown it was not possible to make a reasonable guess as to whether, once in the troposphere, these particles were incorporated into rain as freezing nuclei or by scavenging due to collision with rain droplets. It was felt that HASP could contribute toward the understanding of these problems and also toward the purely scientific endeavor of man to understand his environment.

Table 1.1 Observations of Stratospheric Particles*

- 1. The occurrence of noctilucent and mother-of-pearl clouds.**
- 2. Increased attenuation in the upper atmosphere in connection with meteor showers.**
- 3. Twilight phenomena.**
- 4. Presence of sodium in the upper atmosphere.**
- 5. Observations of clouds and dust horizons in the stratosphere from aircraft and manned balloons.**
- 6. Measurements of electrical conductivity.**
- 7. Injection of particles into the stratosphere by volcanic eruptions and nuclear explosions.**
- 8. Direct observations of particles by rockets and satellites.**
- 9. Collection of magnetic spherules at the ground.**

*** Table taken from Junge, Chagnon, and Manson, J. Meteor. 18, 81 (1961).**

The routine flights of U-2 aircraft in the lower stratosphere provided a possible means of obtaining particles whose physical and chemical properties could be directly observed.

Early in HASP it was thought possible to observe stratospheric particles collected in the filter samples. Preliminary electron microscope and light microscope examinations of a few samples revealed that dust contamination and pieces of the microfibrils from the filter material precluded unique identification of stratospheric particles. The locations (or distribution) of the collected particles within the filter papers were studied, however, by means of autoradiography performed on

1. large portions of filters (quadrants , halves and sometimes whole papers),
2. microtomed sections of small portions of filters which were embedded in plastic, and
3. individual fibers of filters. This study was pursued in order to obtain information on filter efficiency for the radioactivity collected in the HASP missions.

When it became evident that direct observation of stratospheric particles in filters could not be accomplished, other methods of collection were sought. In the meantime an independent program of particle collection by balloon-borne impactors was being initiated by Air Force Cambridge Research Laboratories in connection with Project Ashcan. In the fall of 1958, Junge² reported the collection of stratospheric particles in this program. It was then decided, in HASP, to attempt to collect particles upon prepared impaction surfaces attached to the upstream face of a filter in the nose sampler of a U-2. A successful collection of particles was obtained in July, 1959, but the method of collection was not amenable to routine sampling. It was desired, then, to initiate a program of

collection of stratospheric particles using HASP aircraft equipped with a particle sampler which could expose impaction surfaces at altitude for any desired time interval. The opportunity for such a program arose when, in a cooperative arrangement, Dr. Christian E. Junge of AFCRL was able to provide the design of an impaction sampler suitable for installation on U-2 aircraft. Through this program, samples suitable for electron microscopic examination were obtained on a routine basis starting in February, 1960.

A special set of filter collections was also obtained in connection with the study of stratospheric particles. These samples were exposed for long time periods in the stratosphere for the purpose of collecting enough particulate material for neutron activation analyses of various elements. It was hoped that these analyses would provide estimates of the amounts of extra-terrestrial material present in the stratosphere.

In Chapter 2 of this part of the report, physical methods employed in the studies of particles in filters and on impactors are described. Chapter 3 describes the procedures and methods employed in the neutron activation studies. In Chapter 4 the results of the various analyses are presented and discussed. Chapter 5 is a discussion of the implications of the results of the particle studies in regard to behavior of nuclear debris. A list of conclusions is also presented.

REFERENCES

1. Junge, C. E., C. W. Chagnon, and J. E. Manson, J. Meteor., 18, 81 (1961).
2. Junge, C. E., "Stratospheric Dust Studies", paper presented at Meeting on AEC Sponsored Research and Development Related to the Collection and Classification of Atmospheric Particulates, General Mills, Inc., Minneapolis, Minn., October, 1958.

CHAPTER 2

PHYSICAL METHODS OF PARTICLE STUDIES

In this chapter, we first describe the methods by which samples for direct observation and detection of stratospheric particles were obtained along with a general description of the analytical methods, and then we describe in detail the various techniques and procedures employed in the analyses of these samples. In particular we are concerned here with describing: a) the autoradiographic studies of particles in the HASP filters and, b) the studies of impacted particles.

DESCRIPTION OF PARTICLE COLLECTION AND METHODS OF ANALYSIS

Particles in Filter Papers

As mentioned in Chapter 1 of this part, the primary purpose of the study of particulate material in filter paper was to determine the degree of penetration of the sampled radioactivity through the fibrous mat, thereby enabling assessment of the efficiency of filtration of the sampled aerosol stream. A few samples, however, were specially studied in an attempt to reach some conclusions concerning the nature of the radioactivity-bearing particles.

The method involved in this study was basically autoradiographic. Portions of HASP filters, ranging in size from a quadrant to a whole filter paper, were contacted, front and back, by x-ray film for periods from about one to three months. The resulting set of autoradiograms constituted a survey of a large area sample. By means of these survey autoradiograms small areas of the sample could be located which contained large concentrations of radioactivity indicated by spots of high optical density in the film ("hot spots"), or alternatively areas with diffuse radioactivity could be located. Once the desired area was

located by reregistration of the survey autoradiograms over the filter paper sample, it was removed from the sample by cutting with scissors or a circular punch. The small portion of the filter paper was then embedded in polybutylmethacrylate and subsequently cut into thin sections (about 10 microns thick) with a microtome. Two types of sections were obtained; one type sliced parallel with the plane of filter face and one type sliced perpendicular to the plane of the face. These sections were laid flat, in serial order, upon a flat lucite plate. From each set of sections from a single small portion of a filter paper, arranged on the lucite plate, another survey autoradiogram (x-ray film) was obtained. By evaluating the optical density associated with each parallel section, an estimate of the distribution of radioactivity with depth in the filter mat was obtained.

The survey autoradiograms from the microtomed sections also served to locate particular sections which were further studied by high resolution autoradiography using liquid emulsion. The liquid emulsion was applied to some vertical sections, also for the purpose of studying particle penetration. From certain filter areas individual fibers of the filter mat were extracted and subjected to high resolution autoradiography. In a few cases when a "hot spot" was detected in a single fiber, the silver grains of the autoradiogram were reduced to permit microscopic examination of the particle, or particles, which contained the radioactivity.

The details of the various techniques employed in this study are given later in this chapter and the results of the study are given in Chapter 4.

Particles Collected by Impaction

a.) Impactors Mounted on Filters

The first successful collection of stratospheric particles in HASP was accomplished by the rather crude method of affixing impaction surfaces to a filter

paper in the nose sampler. The filter paper, and thus the impaction surfaces, were then exposed to stratospheric air in a normal sampling procedure. The sample holder consisted of a one inch diameter disc of 0.005" thick sheet brass. A central hole, 5/16" in diameter, was stamped in the disc, leaving a lip of 1/16" height. A circular piece of 200 mesh copper screen coated with a plastic film was inserted into the central hole and held firmly by household cement and a tight fit. A cylindrical dust cap 5/16" in diameter and 3/8" long fitted over the outer side of the lip, and protected the sample from contamination prior to and after exposure. The back side of the sample was protected from contamination by a piece of gummed paper affixed to the holder. Two small, diagonally opposed holes in the sample holder provided a means for sewing the whole assemblage to the filter paper. Ten samples plus controls were prepared with substrates (impaction surfaces) of Formvar, nitrocellulose, carbon coated nitrocellulose, and Millipore filter. The sample preparation was performed in a "dust free" laboratory. The samples were taken to Plattsburg Air Force Base, New York where they were attached to a nose filter. Immediately before take-off, the dust covers were removed from the sample holders and the filter paper was then rotated into the sampling duct. Shortly after return of the aircraft from the mission, the dust covers were replaced over the samples. The samples were then sent out for electron microscopic examination.

b.) Probe Impactors

By far the most information concerning stratospheric particles was obtained from analyses of samples collected on the probe impactors designed by Junge and Manson of AFCL and flown as part of HASP. Two of the six HASP aircraft were equipped with fixtures and actuators for the installation and operation of the probes. Collection of samples in a routine manner began in February, 1960 and has continued up to the present, although the samples with

which we shall be concerned under HASP were collected up to November, 1960. A total of 17 analyzable samples were obtained for electron microscopy. An equivalent number of samples were obtained for light microscopy and electron microprobe analysis by AFCRL with whom the sampling program was shared. Suitable blank exposures (short time exposures) were obtained by both AFCRL and HASP investigators. Several samples were not analyzable due to malfunctions of the probe actuator, destruction of the substrate and accidental contamination of the sample during handling.

The probe sampler, a modification of which is shown in Figure 2.1, was designed to protect the sample from contamination at all times after preparation of the sample until its return to the laboratory for examination. The probe, on which the HASP samples were collected, differed from that shown in Figure 2.1 in that there was only one sampling surface, the one exposed through the milled window in the body. The large nut at the end of the body was a cover nut. The sampling surfaces consisted of plastic film coated on 200 mesh gold screen which was attached to the stainless steel platen shown in Figure 2.1. The entire probe was constructed of stainless steel except for beryllium-copper spring clips which held the platen to the inner piston. This piston was spring loaded, so that the sampling surface was normally covered by the cylindrical body at the inboard (left) end of the probe. The piston and cylinder were made to close tolerances, thus providing an effective seal against contaminating particles. However, air could slowly diffuse through to the sample along a 1/8 inch long, 0.001 high path between the mating cylinder and piston. The surfaces of the cylinder and piston were coated with a thin film of silicone oil which served three purposes:

- 1.) to capture and hold any particles which entered the space between cylinder and piston,
- 2.) to lubricate the mating surfaces preventing the formation of metal chips during activation and deactivation of the sampler, and

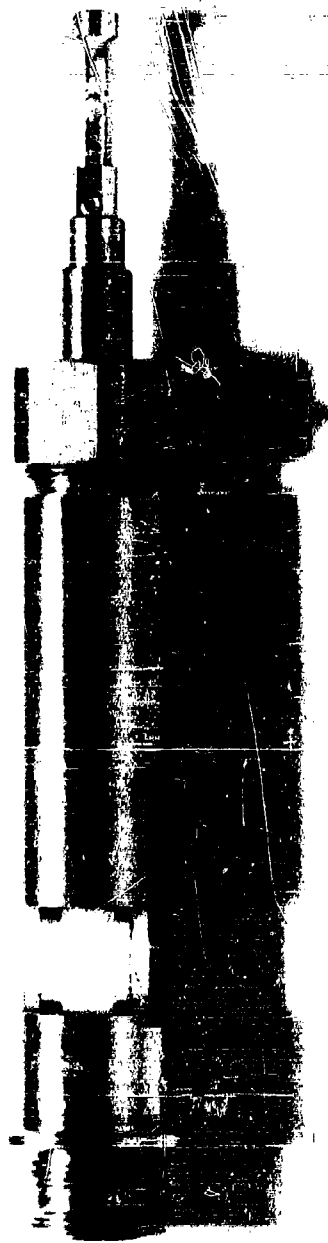


Figure 2.1
Modified Probe Impaction Sampler



Fig. 2.2. U-2 Showing Strut For Probe Mount

- 3.) to prevent icing of the probe during ascent and descent of the aircraft through the moist troposphere.

Flight tests in which the samples were exposed for a very short time (2 minutes) conclusively proved that the design of the probe excluded contamination during shipment, storage, handling in the field, and tropospheric flight.

The probe was mounted on a special strut which was located on the aircraft 132 cm. from the nose, oriented, at an angle of 33° below the horizontal, and extended 15.5 cm from the skin. The sample was therefore about 18 cm from the skin, which permitted sampling of ambient air unperturbed by the structure of the aircraft. The position of the strut can be seen in Figure 2.2. The milled flats in the body of the probe were used for tightening the probe in the strut and for aligning the sampling surface normal to the direction of air flow. The sample was exposed to stratospheric air when the pilot, by means of a switch, caused a push rod within the mounting strut to push against the spring loaded piston, thus moving the sample into the milled window. When the switch was returned to its original position the push rod retracted and the spring forced the piston back to the closed position.

An outline of the history of the sample is given here to illustrate the manner in which the program was performed.

1. The sample was prepared, the probe loaded, placed in a polyethylene bag and packaged for shipment in the "dust free" laboratory of Ernest F. Fullam, Inc.
2. The packaged probe was stored at the base of HASP operations until time for use.
3. At the time of installation on the aircraft, just prior to taxiing to the runway, the probe body and sampling window were kept covered with the polyethylene bag by means of an elastic band.
4. The probe remained covered with the polyethylene bag during taxiing and until just prior to take-off when the bag was removed.
5. The sample was exposed when the aircraft attained sampling altitude in the stratosphere.

6. After the scheduled exposure time had elapsed, the sampler was deactivated. Exposure times ranged from two minutes (for "blank" samples) to about seven hours.
7. Immediately after landing and prior to taxiing off the runway, the probe was re-covered with the polyethylene bag held with an elastic band.
8. The probe was removed from the strut mount and repackaged for delivery to Isotopes, Inc. along with an exposure data sheet.
9. The data sheet was retained at Isotopes, Inc. and the packaged sample was sent on to Ernest F. Fullam, Inc. (EFFI).
10. At EFFI the probe was opened, unloaded, and prepared for electron microscopic examination in a "dust free" atmosphere.
11. The data from the electron microscopy, in the form of data reports and electron micrographs were sent to Isotopes, Inc.

The techniques employed in the various portions of the sample preparation, handling, and analysis are described in the following section of this chapter.

TECHNIQUES AND ANALYTICAL PROCEDURES

Autoradiographic Techniques

(a) Survey Autoradiograms Using Film and Plates

Autoradiograms were produced from HASP filters and plates of thin section of methacrylate embedded HASP filters by exposure in contact with x-ray film (Eastman No-Screen, double coated) or lantern slide plates (Eastman, Contrast) as illustrated in Figure 2, 3. The components were assembled and the films given scribed identification marks under total darkness. The contact pressure was regulated by selection of corrugated spacer thickness to insure even contact without compression of the I. P. C. filter paper. The photographic materials were removed from the sample for the photographic processing steps and subsequently realigned, by means of the registration pins (dowel pins in the case of coated glass photographic

Isotopes, Inc.

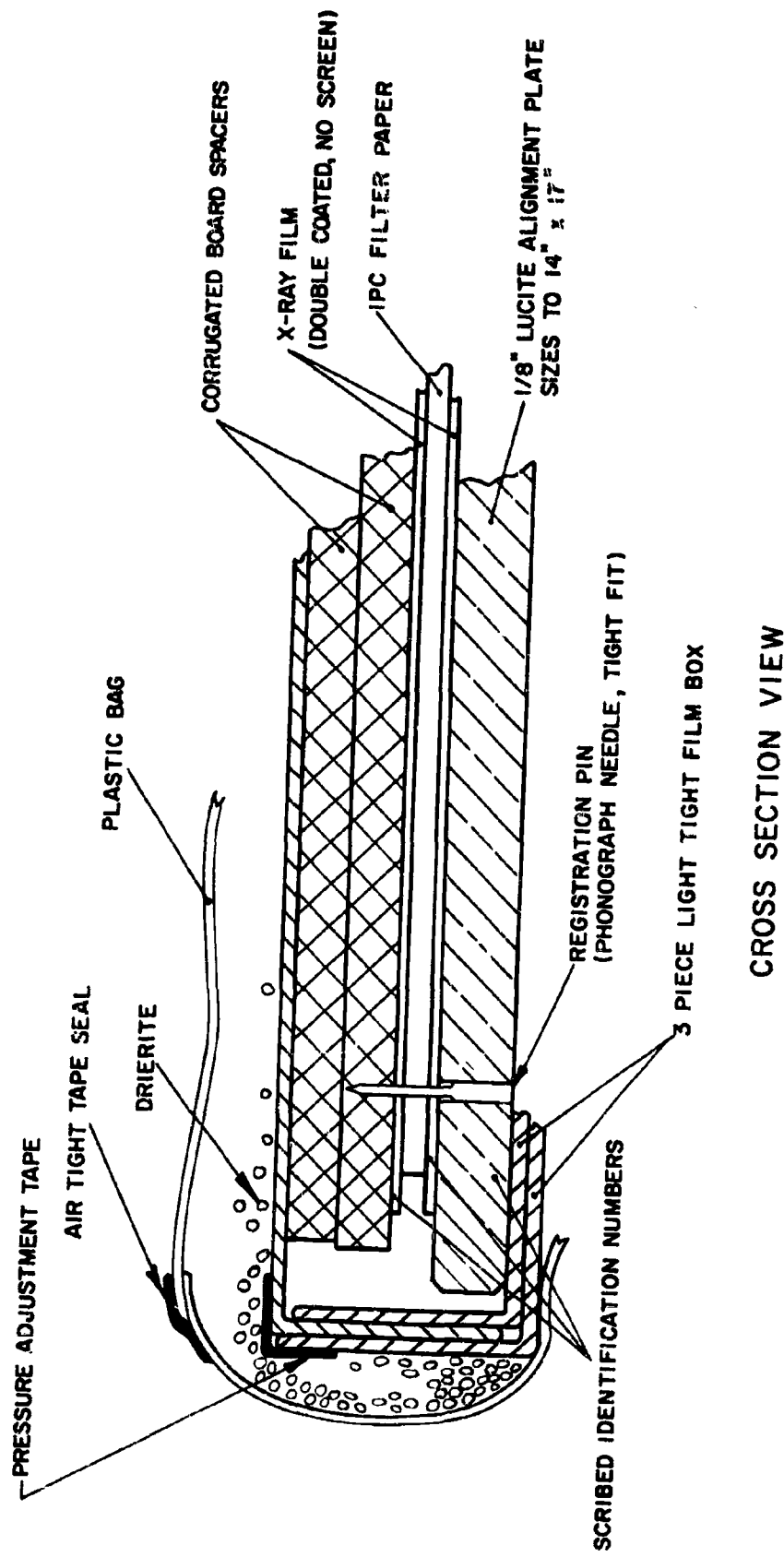


FIG. 2.3 EXPOSURE ASSEMBLY FOR SURVEY AUTORADIOGRAMS

plates), for evaluation of the autoradiographic image. Exposure times for filter papers ranged from several hours to three months. A one month period was found to be the most practical. For thin sections the exposure times ranged from 1 to 12 months. All exposures were made at room temperature ranging from 55 to 85°F. Exposures longer than 1 month were performed in sealed plastic bags containing a desiccant (Indicating Drierite).

Processing was performed with all solutions at $68 \pm 1/2^\circ\text{F}$. Total darkness was maintained until half the time of the acid fixing step had elapsed. The procedure was:

- (1) tray development for 5 minutes in undiluted D-19, with agitation for the first 15 seconds and for the first 5 seconds of each succeeding minute;
- (2) water rinse for 30 seconds with continuous agitation;
- (3) acid fixing for 10 minutes with periodic agitation;
- (4) water wash for 30 minutes in running water;
- (5) air drying by moderately forced air at room temperature.

(b) High Resolution Autoradiograms Using Liquid Emulsion

Melted bulk nuclear track emulsion was coated onto microscope slides which contained individual filter fibers, thin sections of embedded filter, or impaction collector samples in order to achieve a correlation of radioactivity with sample area. Emulsions which were sensitive to all beta energies were used (Eastman NTB-3 and Ilford G-5). The sample slides were handled as follows: Steps 1 thru 3 were carried out under the illumination of 15 watt Wratten OA safelight at a distance of 4 feet.

- (1) Chunks of refrigerated bulk emulsion were placed into a 30 ml beaker.
- (2) The emulsion was heated to fluidity by immersing the beaker in a water bath at 113°F (NTB-3) or 122°F (G-5) and stirring gently with a glass rod.
- (3) A thin layer of emulsion was coated onto the sample slide by the use of a warmed dropper, with care being exercised to prevent the formation of air bubbles in the coated emulsion

Total darkness was maintained from immediately after step 3 until step 6b.

- (4) The coated samples were dried overnight at room temperature.
- (5) The microscope slides were transferred to a light tight box and suspended therein over a desiccant (Indicating Drierite) and the box sealed with tape for the exposure duration.
- (6) The exposed coated samples were processed in D-19 as outlined above for x-ray film, with the following modifications.
 - (a) Development was extended to 10 or 20 minutes and agitation confined to the first 5 seconds of the first and every fifth minute of development.
 - (b) Fixing was for 20 minutes in total darkness followed by nitrogen gas agitation in subdued room light when necessary.
 - (c) The plates were immersed in 1% aqueous solution of glycerol for 1 minute previous to drying at room temperature.

The resultant silver image - radioactive deposit matrix was examined by light microscopy techniques described later in this chapter.

Thin Sectioning Techniques

Portions of HASP filters, selected on the basis of survey autoradiograms, were removed and embedded in plastic preparatory to microtome sectioning. For sectioning parallel with the filter face a 1/8 or 3/16 inch filter disk was removed with a hollow punch, the disk being retrieved from the punch center by grasping its edge with precision tweezers. The filter was backed by 1/8 inch Lucite and the punch driven by a hammer. For sectioning normal to the filter face a strip of filter 1/8 x 5/8 inches was removed using surgical scissors. The punch or scissors were cleaned between samples. The filter specimens were suspended in gelatin capsules containing methacrylate as shown in Figure 2.4.

(a) Methacrylate Embedding

The embedding procedure was:

- (1) Working stocks of butyl and methyl methacrylates were prepared by removing the 0.01% hydroquinone inhibitor from each (by a separatory funnel wash with 2% NaOH followed by 3 distilled water rinses and subsequent filtration through anhydrous Na_2SO_4) and stored in tightly

Isotopes, Inc.

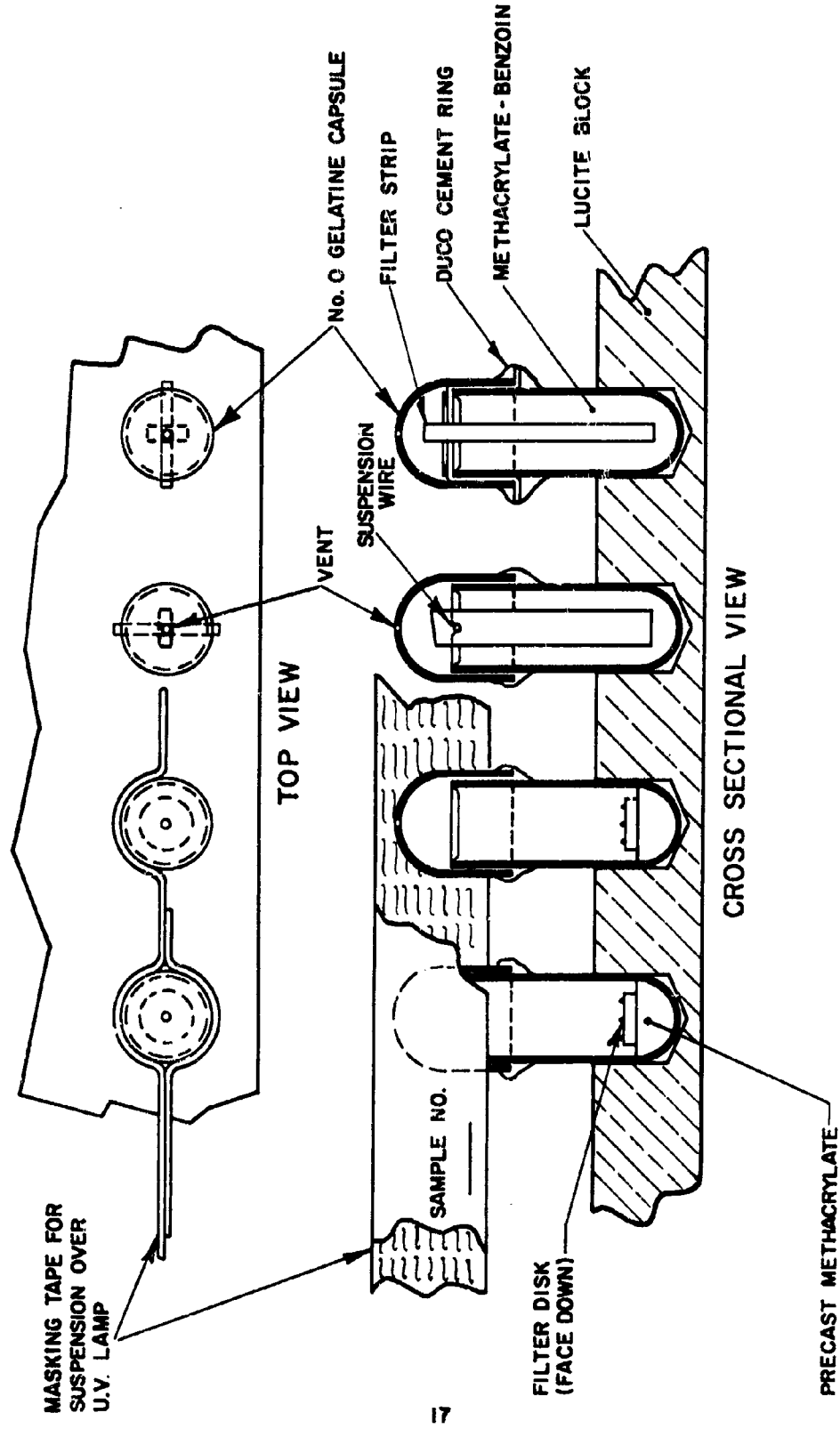


FIG. 2.4 FILTER PAPER - METHACRYLATE ARRANGEMENT FOR PLASTIC EMBEDDING

capped glass bottles in subdued light.

- (2) A mixture of 7 to 10% methyl in butyl methacrylate was made from the purified stocks.
- (3) Benzoin was added to approximately 0.1% concentration (a speck) to initiate polymerization by ultra-violet light.
- (4) Number 0 or 00 gelatin capsules were uncovered and placed upright in a block containing 5/16 inch diameter blind holes (See Figure 2.4). For parallel sections a pre-cast methacrylate solid hemisphere was inserted into the capsule bottom; for normal sections, notches were cut in the capsule wall to accomodate a 0.010" stainless steel suspension wire.
- (5) Sufficient methacrylate-benzoin solution was transferred by pipette to almost fill each capsule.
- (6) The filter portion to be embedded was held at the edge by precision tweezers and inserted slowly into the capsule and oriented to the final position shown in Figure 2.4.
- (7) A small hole was punched in the capsule covers and the covers replaced and sealed to the capsule bottom by a ring of household cement (Duco). When necessary, additional methacrylate was added through the vent to insure a final embedding of approximately 9/16 inch length.
- (8) The block of loaded capsules was placed into a pyrex vacuum desiccator, evacuated slowly with a forepump, and after 15 minutes returned slowly to atmospheric pressure (rapid pumping upset or emptied the capsules).
- (9) Masking tape strips were attached to the capsule covers.
- (10) The array was lifted carefully from the block and suspended 1 1/2 inches above and midway between two 15 watt fluorescent blue lights for a 12 hour polymerization period.
- (11) The gelatin was removed from the solidified plastic pellet by soaking in warm water until the gelatin dissolved or could be peeled.
- (12) The pellet was trimmed to fit the microtome collet and minimize unnecessary microtome sectioning of excess methacrylate.

(b) Microtome Sectioning

The plastic pellet in which the filter was embedded was held in a collet type chuck (Porter Blum) adapted to a rotary microtome (Spencer 820). Clamping of the collet was improved by use of a lever arm inserted into radial holes drilled



Figure 2.5
Microtome Sectioning of a Filter Sampler

in the knurled collet clamping ring. The knife holder was set for zero slice angle and tilt angles of 15° or less. A metal knife was used and sections were cut singly, by hand rotation at approximately one revolution per second. A thickness setting of 10 microns was used to cut cross sections of 25 to 50 square millimeters. Each section was lifted from the knife using precision tweezers (Figure 2.5) and dropped onto a puddle of 25% aqueous solution of acetone standing on a 2" x 3" glass slide, and allowed to flatten and adhere upon drying. Each slide contained up to 48 sections arranged in serial order. The slides containing sections from a single sample were affixed in serial array by means of double coated tape (Scotch Brand No. 400) to 8 x 10 inch plastic registration plates for survey autoradiography. Subsequently, selected thin sections were transferred to glass slides containing "Scotch" tape edge dams and cemented with a 1% gelatin solution preparatory to high resolution autoradiography.

Electron Microscopy

(a) Sampler Preparation

The impaction collector shown in Figure 2.1 was loaded with thin plastic films of nitrocellulose or Formvar supported on gold screen of 200 mesh. The work was performed in the laboratory of Ernest F. Fullam, Inc., in a dust controlled atmosphere, as follows:

- (1) The collectors were dismantled and cleaned in hexane.
- (2) The parts were dipped into a solution of 20mg of silicone oil (100,000 centi-stoke) per milliliter of hexane, and drained dry.
- (3) The collector was reassembled to include the plastic substrate (preparation described below) and inserted into a plastic bag (0.004" polyethylene) and sealed.
- (4) The sampler was rolled in a double thickness of 1/2" thick polyurethane foam and inserted into a double can mailing container the outer can of which was lined with the foam packing.

The plastic films were prepared as follows:

- (5) Plastic solutions of 0.25% Formvar 15/95 in ethylene dichloride and/or 1% nitrocellulose in amyl acetate were prepared (using solvents purified by refluxing over calcium oxide for 4 hours and distilled slowly over a narrow temperature range).
- (6) A 1 x 3 inch glass slide was cleaned by breathing upon and wiping with a lens tissue.
- (7) A thin film of plastic solution was applied by holding a slender dropper horizontally and drawing it along the slide while discharging the solution of plastic.
- (8) The slide was allowed to dry for a few minutes and the edge was then scored with a sharp needle.
- (9) A glass funnel was filled from the bottom with distilled water to the point of overflow, by means of a pressured reservoir.
- (10) A clean water surface was prepared by scraping the water meniscus from the funnel mouth by means of a quick stroke of a clean glass rod.
- (11) The dried plastic coated slide was moistened by breathing on it.
- (12) The slide was inserted slowly, and at a slight angle; under the water surface and the film allowed to float from the glass onto the water surface.
- (13) Gold screening was brought up beneath the film and both lifted vertically from the water.
- (14) The film-gold matrix was blotted at the edge with thin filter paper, and allowed to dry.
- (15) The dried film was handled by the edge with precision tweezers and the film cut to size and cemented at the edge to a stainless steel platen, which fits the collector, by means of a 10% nitrocellulose in amyl acetate cement.
- (16) The platen-substrate assembly was fastened to the collector by means of appropriate spring-clips and stainless machine screws.
- (17) Control films were stored in plastic boxes for subsequent analyses for "background" particles.
- (18) When required to identify "background" particles, the plastic film was vacuum shadowed at near grazing incidence with a thin film of evaporated metal after step 14.

The collector was covered by the plastic bag until seconds before aircraft take off and replaced seconds after landing.

(b) Preparation of Exposed Samples

The collector substrates were removed from the collectors at the Fullam Laboratory as follows:

- (1) The film-gold matrix was removed from the stainless platen by means of a sharp scalpel and precision tweezers.
- (2) The film-fold was backed with 0.003 inch transformer insulating paper and four 1/8 inch diameter disks were punched; as illustrated in Figure 2.6, using a special punch (EFA).
- (3) The grids were placed in individual No. 5 gelatin capsules and then into labeled plastic boxes, for subsequent electron microscopy.
- (4) The remaining sample was cemented at the edges to a glass slide; placed in a plastic box and shipped to Isotopes, Inc. for light microscopy and autoradiography.
- (5) When required for particle thickness determination, the sample was shadowed with evaporated metal after step 1.
- (6) Subsequent to electron microscopy all 1/8 inch sample grids were returned to Isotopes, Inc., cemented to glass slides using an overcoat of 10% nitrocellulose in amyl acetate, dried, and subjected to high resolution autoradiography techniques.

Light Microscopy Techniques

A trinocular phase contrast microscope (American Optical) was modified to include a vertical illuminator and a substage polarizing filter to provide bright field, phase contrast, polarized and pseudo dark field illumination by transmitted light, and bright field or polarized illumination by reflected light. Phase objectives of 5, 10, 43 and 97 times magnification were used with 10 x and 20 x widefield eyepieces. Photographic eyepieces of the negative type (Bausch and Lomb Ultraplane) were used with 4"x5" sheet black and white film and monochromatic light or with 35mm color film and color balanced illuminations. Appropriate magnifications and illuminations were used to examine specially prepared samples for the following:

- (a) Examination of small pieces of IPC paper in order to assess gross porosity of the paper, background particulates, and particulates corresponding to survey autoradiogram images;
- (b) Measurement of the thickness of IPC paper by focusing on the top and bottom planes or by micrometry of carefully cut raw cross sections or thin embedded sections using an eyepiece reticle calibrated by a stage micrometer;
- (c) Study individual filter fibers prepared by removing a mass of fibers by means of precision tweezers, separating on glass slides by means of needles, and flattened and held to the slide by a few drops of acetone;
- (d) Examination and mapping of unique areas of impaction collector sample substrates, both before and after electron microscopy;
- (e) Examination for radioactive particles revealed by high resolution autoradiograms of:
 - (1) filter fibers,
 - (2) thin sections of embedded filter,
 - (3) impaction collector substrates.

The silver image was removed, while viewing through the microscope, by the use of Farmer's Reducer (1% potassium ferrocyanide in 10% sodium thiosulphate) as follows:

- (1) The microscope stage coordinates of a dense autoradiographic image was recorded and a photomicrograph or sketch produced of the field of view.
- (2) Freshly mixed Farmer's Reducer was applied to the image using a drapper; after 1 minute the old drop was removed and replaced by a fresh drop.
- (3) The progress was followed visually and the last particle revealed (or the most central particle) was considered to be the radioactive particle.
- (4) This particle was measured using a calibrated eyepiece reticle.
- (f) Observation of identifying chemical test reactions carried out on impaction probe samples. This has been confined chiefly to a benzidine acetate test for persulphates.

Electron Microscopy Techniques

Electron micrographs of 1/8 inch diameter grids from impaction collector

substrates were produced in an R.C.A. EMV-3F electron microscope by Ernest F. Fullam, Inc. Based on preliminary studies, grids "a" and "b" (Figure 2.6) were examined and representative fields recorded and subsequently enlarged as micrographs representing 5000 x magnification. Grids "c" and "d" were examined at 1500 x magnification and all particles suspected to be of stratospheric origin were recorded.

Particle thickness was determined for several selected grids by means of shadowing the grids in a vacuum with evaporated gold-palladium alloy incident at 10° with the grid surface. Selected area electron diffraction patterns of areas as small as 150 square microns (0.00015 sq. mm.) were recorded, measured and compared with American Society for Testing Materials (ASTM) Standards by Ernest F. Fullam, Inc.

Particle Counting Procedures

Individual particles illustrated in electron micrographs were measured by comparison with a reticle scale calibrated to 0.1 mm., with the aid of a 6 x magnifying lens. The micrograph patterns were divided into small areas to prevent measuring a given particle twice. The particles were classified into two groups based on particle shape and electron optical density.

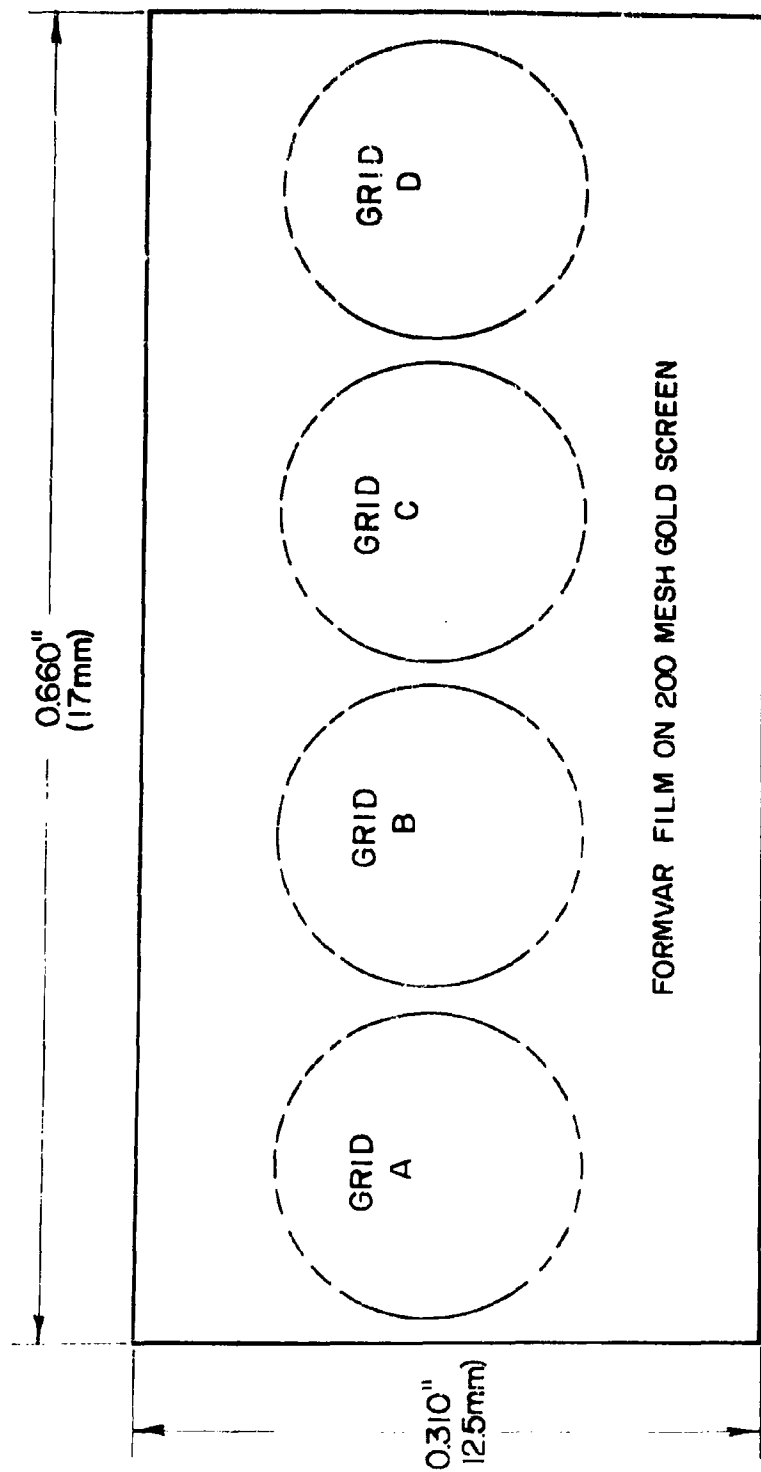


FIGURE 2.6

SELECTION OF 1/8 INCH (3mm) DIAMETER ELECTRON MICROSCOPE GRIDS FROM
PROBE WINDOW SAMPLE

CHAPTER 3

NEUTRON ACTIVATION OF FILTER SAMPLES

As a means of estimating the content of terrestrial and/or extraterrestrial material in the stratosphere, an experiment involving neutron activation analyses of special HASP filter samples was undertaken.

The basic plan of the experiment consisted of obtaining four exposed hatch samples, two from a northbound flight and two from a southbound flight from Minot AFB, North Dakota. Four blank samples from each flight were obtained from filters loaded into the hatch sampler but not exposed to stratospheric air. The activation analyses were thus performed upon twelve samples, four exposed and eight unexposed hatch filters.

The procedure used for handling the filter papers and installing them in the aircraft are as follows:

Two groups of six hatch filters were obtained in their original sealed envelopes; each group represented a different batch of filter paper.

The retaining frames and screens were thoroughly wiped with a washed flannel cloth; each filter was removed from its envelope by personnel wearing talcum powder-free surgical gloves and placed in its retaining frame. Each frame was assembled and placed in the changer mechanism of the hatch sampler. This was accomplished without contacting the filter with anything but the frame. A Philips head screw driver was utilized for punching a small hole in the center of the filter to accommodate a frame retaining screw. The entrance and exit ports of the hatch duct were covered with masking tape; the hatch sampler was

installed in the aircraft and the tape was removed just prior to the time of taxiing for take-off.

On return of the aircraft to the hangar from a southbound course, the hatch sampler was removed and each filter in its frame was placed on a work bench where it was disassembled by personnel wearing surgical gloves. All filters were placed in manilla envelopes for delivery to Isotopes, Inc.

It was originally planned that Isotopes, Inc. personnel would perform all of the filter handling and loading for both north and southbound flights as described above. The plan was carried out for the southbound flight only since the northbound flight did not immediately materialize. However, Air Force personnel were instructed in the procedure and they performed the handling and loading for a subsequent northbound flight.

Neutron Irradiation of Samples

The neutron activation of the twelve filter samples was divided into four irradiations in which nine elements, nickel, manganese, copper, zinc, phosphorous, chromium, iron, calcium and cobalt, were determined. The comparator or comparative assay technique of simultaneous irradiation of samples with standard samples of the elements of interest was utilized in all irradiations.

The first irradiation was undertaken as a dry-run of the techniques and procedures as well as to ascertain the flux homogeneity across the length of the sample container. No filter samples were involved in this experiment. The second irradiation involved four blank, or unexposed, filters. The third and fourth irradiations each involved two exposed and two unexposed filters.

Table 3. 1. List of Standard Samples for Neutron Irradiation*

Element	mg of Standard/ ml of Solution	ml Aliquot	gm Weight of Standard	Activated Product
Co	10. 00	0. 10	1×10^{-3}	Co ⁶⁰
Cr	1. 00	0. 10	1×10^{-4}	Cr ⁵¹
Cu	0. 10	0. 10	1×10^{-5}	Cu ⁶⁴
P	5. 00	0. 20	1×10^{-3}	P ³²
Ca	10. 00	1. 00	1×10^{-2}	Ca ⁴⁵
Fe	10. 00	1. 00	1×10^{-2}	Fe ⁵⁹
Zn	20. 00	0. 10	2×10^{-3}	Zn ⁶⁹
Mn	0. 10	0. 10	1×10^{-5}	Mn ⁵⁶
Fe	10. 00	1. 00	1×10^{-2}	Fe ⁵⁹
Ni	10. 00	0. 10	1×10^{-3}	Ni ⁶⁵
Cu	0. 10	0. 10	1×10^{-5}	Cu ⁶⁴
Co	10. 00	0. 10	1×10^{-3}	Co ⁶⁰

* Listed in order of packing in cylindrical container

In the first irradiation comparator standards of the elements of interest were prepared by evaporating aliquots of standard solutions (see Table 3.1) onto individual Alcoa 1119, 1 1/2 inch by 1 1/2 inch aluminum foils. The foils were folded into small packets and an aluminum cover foil placed over each packet.

The aluminum foils, supplied by Brookhaven specifically for activation analyses, were pre-treated by several 6N nitric acid washings, several distilled water rinsings and finally dried under vacuum to minimize contamination by dust particles. All handling in this and subsequent irradiations were conducted by personnel wearing talcum powder free surgical gloves and in a comparatively "dust free" atmosphere.

The standards were combined in a 7/8 inch diameter by 2 1/2 inch cylindrical aluminum capsule, supplied by Brookhaven National Laboratories, in the order shown in Table 3.1. Duplicate standards were placed at various intervals to ascertain the flux homogeneity. The container was inserted in the W-13 experimental hole, 9 feet 6 inches from the west face of the graphite reactor at Brookhaven National Laboratories, and subjected to a thermal flux of approximately 7.5×10^{12} neutrons per square cm per second for a 48 hour period.

On completion of irradiation, the aluminum packets were unfolded and each foil leached four times with warm 6N nitric acid. The resulting solutions were placed in respective volumetric flasks from which duplicate aliquots of the gamma emitters, Ni^{65} , Mn^{56} , Cu^{64} , Zn^{69} , Cr^{51} , Fe^{59} and Co^{60} , were removed for radioassay by multichannel gamma ray spectrometry.

Table 3.2. Duplicate Determinations of Activated Standard Samples

Activated Duplicate		Irradiation No.	dpm	% Standard Deviation from the Mean
Cu ⁶⁴	No. 1	1	9.93×10^7	0.70%
Cu ⁶⁴	No. 2	1	1.03×10^8	
Fe ⁵⁹	No. 1	1	6.93×10^6	2.10%
Fe ⁵⁹	No. 2	1	7.14×10^6	
Co ⁶⁰	No. 1	1	7.15×10^7	2.05%
Co ⁶⁰	No. 2	1	7.36×10^7	
Fe ⁵⁹	No. 1	4	3.00×10^5	0.80%
Fe ⁵⁹	No. 2	4	3.03×10^5	
Co ⁶⁰	No. 1	4	5.93×10^6	0.71%
Co ⁶⁰	No. 2	4	5.87×10^6	

The radioassay data indicated that all standards were highly contaminated with sodium-24 from the $\text{Al}^{27}(\text{n},\alpha)\text{Na}^{24}$ reaction as well as activation products from impurities in the aluminum foil. Consequently, the duplicate standards were radiochemically purified in order to determine the flux homogeneity. The data are summarized in Table 3.2. All other standards were discarded.

In view of these problems, the use of aluminum foil as the mounting material in subsequent irradiations was abandoned. A second irradiation, employing 2 3/4 inch x 2 3/4 inch squares of Dupont Type C, 25 gauge, "Mylar" polyester film as the mounting material, was undertaken. All Mylar squares were subjected to the same pre-treatment as were the aluminum foils in order to remove any surface contaminant. Comparator standards were prepared by evaporating aliquots of standard solutions (as summarized in Table 3.1 but with no duplicates) on individual Mylar squares. Each square was folded into a smaller square and placed into one of two 1/2 inch diameter by 1 inch cylindrical polyethylene capsules in the order shown below.

<u>Capsule No. 1</u>	<u>Capsule No. 2</u>
Ni	P
Mn	Cr
Cu	Fe
Zn	Ca
	Co

Four unexposed filters were removed from their envelopes and a 3.1 square inch segment, containing the filter identification number, was removed from each filter. A 1 inch diameter circle, containing the hole left by the frame retaining screw, was punched out of the center of each filter and utilized for total beta assay and autoradiography. The filters were cut into small squares approximately 1/2 inch on a side, placed into 150 ml platinum dishes (2/sample) and ashed in a muffle furnace for approximately six hours at 450-460°C. The ash of each sample was quantitatively transferred (one sample was lost during transfer) to a Mylar square. The squares were folded into packets and placed into individual 1/2 inch diameter x 1/2 inch cylindrical polyethylene capsules.

A Mylar square, contained in a similar capsule was prepared as a blank in order to ascertain the background activity attributed to the polyester. The blank capsule, the three sample capsules and two standard capsules, were placed in a 1 1/4 inch diameter by 2 1/4 inch cylindrical polyethylene capsule. This entire unit was irradiated in the W-13 experimental hole of the graphite reactor at Brookhaven National Laboratories in a thermal flux of approximately 1×10^{12} neutrons per sq. cm per second for 22 hours.

Upon completion of irradiation, the ash samples and Mylar blank were removed from their containers with Teflon coated tweezers and each packet placed in a platinum dish containing 5 ml of 48% HF, 5 ml of 70% HClO_4 and 10 ml of H_2O . The packets were opened beneath the surface of the solution with Teflon coated tweezers to prevent the loss of the powdery ash. The solution was brought to boiling; the Mylar square removed from solution, rinsed

with water and transferred to another platinum dish containing a similar solution of HF and HClO_4 . The Mylar square was given three 2 minute leachings in the second hot HF- HClO_4 solution, rinsed with H_2O and transferred to a culture tube where it was radioassayed by multichannel gamma ray spectrometry. If any residual activity from the sample remained, the leaching process and radioassay was repeated until it was removed. However, it was generally found that three initial leachings were ample. All Mylar exhibited an inherent, unknown activated product with a 0.58 Mev gamma ray and an approximate 10 day half-life, which could not be removed by repeated leachings. This activity was disregarded in the radioassay.

The primary and secondary solutions in the first and second platinum dishes were evaporated to fumes of HClO_4 and combined into a 25 ml volumetric flask. The platinum dishes were twice washed with several ml of hot 1N HCl and the washings added to the volumetric flasks. Finally, the solutions were diluted to volume from which suitable aliquots were removed for radiochemical analysis.

The comparator standards were removed from their capsules and each packet opened beneath the surface of a 6N HNO_3 solution with Teflon coated tweezers (standards of Ni^{65} and Mn^{56} were processed immediately because of their short half lives). Each Mylar square was given four 15 minute leachings hot 6N HNO_3 , rinsed with H_2O and placed in a culture tube. The Mylar was radioassayed for residual activity employing the 100 channel gamma ray spectrometer. If any residual standard activity remained, the leachings and radioassay procedure was repeated until less than 1% of the total standard activity

remained. As in the case of the samples, all Mylar exhibited an inherent, unknown activated product which could not be removed by repeated leachings, so this activity was ignored in the radioassay.

The resulting standard solutions were transferred to volumetric flasks, from which appropriate duplicate aliquots of Ni^{65} , Mn^{56} , Cu^{64} , Zn^{69} , Cr^{51} , Fe^{59} and Co^{60} solutions were removed for radioassay by multichannel gamma ray spectrometry. To calibrate the low level beta counters for self-absorption self-scattering effects, appropriate aliquots of the Ni^{65} , P^{32} , Ca^{45} and Co^{60} standard solutions were removed for the preparation of standard samples.

The third and fourth irradiations were performed in exactly the same fashion as the second irradiation. Two exposed and two unexposed filter ash samples along with the comparator standards were encapsulated in each irradiation. Both irradiations were performed in the W-13 hole of the Brookhaven graphite reactor in a thermal flux of approximately 1×10^{12} neutrons per sq. cm per second for 24 hours. Duplicate standards were provided in the fourth irradiation to obtain further data on the neutron flux homogeneity within the sample container. The data, summarized in Table 3.2 with data from the first irradiation, indicate that the flux variation was no more than 2.1% across the sample container.

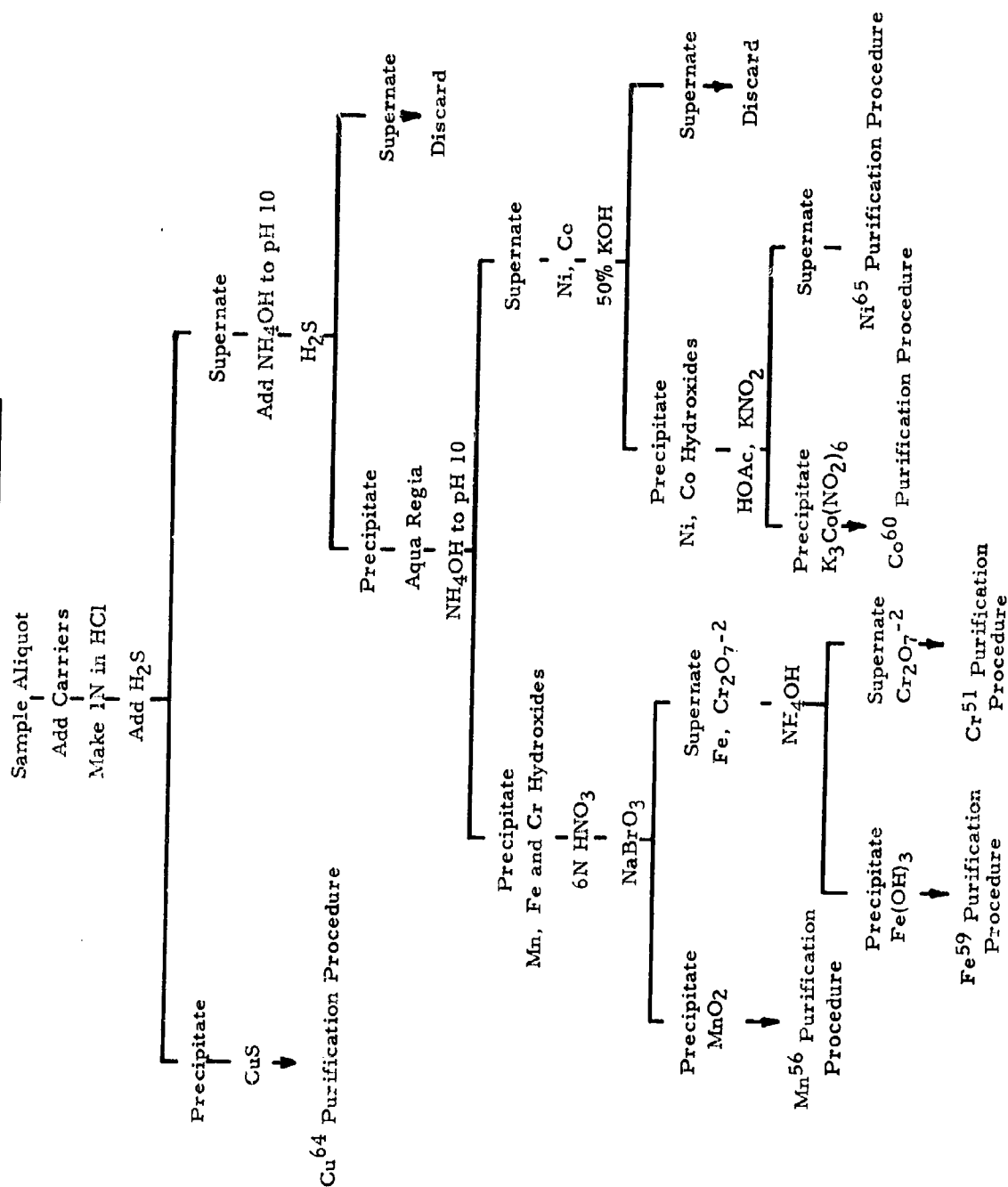
Radiochemical Methods

A sequential scheme was developed for the analysis of the unexposed filter samples of the second irradiation. Nickel-65, manganese-56, copper-64, chromium-51, iron-59 and cobalt-60 were separated sequentially from a 10 ml

aliquot of the sample. The sequential scheme is summarized in Figure 3.1. A 5 ml aliquot was removed for the separation of zinc-69 and phosphorous-32 and another 5 ml aliquot utilized for calcium-45 analysis.

Results of the second irradiation indicated that all the elements of interest except chromium, iron and cobalt were in an abundance to give high levels of activity from smaller aliquots. As a result, in subsequent irradiations, an individual aliquot was removed for the analysis of each radionuclide. A 5 ml aliquot was removed for Ni^{65} analysis, a 3 ml aliquot for Zn^{69} analysis, a 2 ml aliquot for Ca^{45} analysis, 1 ml aliquots for Mn^{56} , Cu^{64} and P^{32} analyses and a 10 ml aliquot for the separation of Cr^{51} , Fe^{59} and Co^{60} by the sequential scheme summarized in Figure 3.1.

Figure 3.1. Scheme of Sequential Analysis of Activated Samples



The Sequential Separation of Nickel-65, Manganese-56, Copper-64, Chromium-51, Iron-59 and Cobalt-60¹

1. To an aliquot of the sample contained in a 40 ml glass centrifuge tube, add 20 mg of nickel, manganese, copper, chromium, iron and cobalt carriers.
2. Make the solution 1N in HCl, digest in a hot water bath for 5 minutes and saturate the solution with H₂S gas for 5 minutes. Centrifuge and reserve the supernate.
3. Wash the CuS precipitate with 5 ml of 1N HCl, centrifuge and discard the wash.
4. Dissolve the precipitate in 8 ml of aqua regia, boil over a flame for several minutes and add 2 mg of Sr, Ba and Fe carriers. Continue with step (b) of the copper-64 purification procedure.
5. To the supernate from step (2), add concentrated NH₄OH to pH ~10 and bubble H₂S gas through the solution for 5 minutes.
6. Again add concentrated NH₄OH to pH ~10 and boil over a flame for 2 minutes to insure the complete precipitation of chromium hydroxide.
7. Cool, again bring the pH to approximately 10 with concentrated NH₄OH, centrifuge and discard the supernate.
8. Dissolve the precipitate with 8 ml of aqua regia, make the solution basic to pH 10 with concentrated NH₄OH, centrifuge and reserve the precipitate for Mn⁵⁶, Cr⁵¹ and Fe⁵⁹ separation. Wash the precipitate with 10 ml of 6N NH₄OH, centrifuge and combine supernates.
9. To the combined supernates, add 20 ml of 50% KOH and boil for 15 minutes to completely precipitate Ni and Co hydroxides. Centrifuge and discard the supernate. Wash the precipitate with 10 ml of H₂O, centrifuge and discard the wash.
10. Dissolve the precipitate in 3 ml of 6M HOAc, heat slightly if the precipitate does not completely dissolve. Dilute to 25 ml with H₂O and cool in an ice bath.
11. Precipitate K₃Co(NO₂)₆ by addition of 6 ml of glacial acetic acid saturated with potassium nitrite; cool for 30 minutes, centrifuge and decant the supernate into a 100 ml beaker.

12. Wash the precipitate with two 20 ml portions of H_2O , centrifuge and combine the washings and supernate. Reserve the combined washings and supernate for step (b) of the Ni^{65} purification procedure.
13. Reserve the precipitate for step (d) of the Co^{60} purification procedure.
14. Dissolve the precipitate from step 8, reserved for Mn^{56} , Cr^{51} and Fe^{59} separation, in 10 ml of 6N HNO_3 and transfer the solution to a 100 ml beaker with 15-20 ml of H_2O . Add 3 ml of saturated NaBrO_3 and heat to incipient boiling for 15 minutes in order to precipitate MnO_2 .
15. Transfer the mixture, portionwise, to a 40 ml centrifuge tube, centrifuge and decant the supernate to a clean 100 ml beaker. Wash the precipitate with 10 ml of 3N HNO_3 , centrifuge and combine the wash and supernate. Reserve the precipitate for step (e) of the Mn^{56} purification procedure.
16. To the combined supernate and wash, add concentrated NH_4OH to a pH of 8.5 to precipitate $\text{Fe}(\text{OH})_3$.
17. Transfer the mixture to a 40 ml glass centrifuge tube, centrifuge and decant the supernate to a 125 ml Erlenmeyer flask. Wash the precipitate with 5 ml of H_2O , centrifuge and combine the wash with the supernate. Reserve the combined wash and supernate for the Cr^{51} purification procedure.
18. Reserve the precipitate for the Fe^{59} purification procedure.

The Sequential Separation of Phosphorous-32 and Zinc-69^{2, 3}

1. To a 5 ml aliquot of the sample contained in a 30 ml beaker, add 5 mg of phosphorous carrier and 20 mg of zinc carrier.
2. Evaporate the solution almost to dryness and transfer the sample to a 60 ml separatory funnel using 20 ml of concentrated HCl as transfer agent.
3. Place the separatory funnel over a Dowex-1 anion exchange column (Note 1) and allow the sample to deposit on the column at the rate of 1 drop every 4 seconds.
4. Collect the effluent, which contains the phosphorous, in a 100 ml beaker. Elute the remaining phosphorous with 50 ml of concentrated HCl and combine effluents.
5. Evaporate the phosphorous fraction almost to dryness, transfer the sample to a 40 ml lusteroid tube with 10 ml of H₂O and proceed to step (c) of the phosphorous purification procedure.
6. Elute the zinc by passing 75 ml of 1M HNO₃ through the column collecting the effluent in a 100 ml beaker.
7. Evaporate the solution to about 5 ml, transfer the solution to a 40 ml glass centrifuge tube using a few ml of water as transfer agent and proceed to step (b) of the zinc-69 purification procedure.

Note 1. The resin is prepared by placing the resin in a 400 ml beaker and adding 200 ml of H₂O. The resin is allowed to settle and the H₂O containing the fine particles of resin is decanted off. This procedure is repeated with an additional four 200 ml portions of H₂O and three 100 ml portions of 6N HCl. After the last 6N HCl wash, the resin is slurried with 12M HCl and placed in a 1.3 cm diameter column to a resin height of 16 cm. About 25 ml of 12M HCl is run through the column as a final washing.

The Radiochemical Analysis of Calcium-45 4, 5, 6

1. To an aliquot of the filter paper solution contained in a 40 ml glass centrifuge tube, add 20 mg of standardized calcium carrier and make the solution strongly ammoniacal with concentrated NH_4OH .
2. Heat in a hot water bath for five minutes, then add 10 ml of saturated $(\text{NH}_4)_2\text{CO}_3$ to precipitate CaCO_3 ; digest until the precipitate settles. Cool, centrifuge and discard the supernate.
3. Dissolve the precipitate in 2 ml of 6N HCl and add 6 drops of Fe carrier (10 mg Fe/ml). Heat over a flame for several minutes to remove all CO_2 . Dilute to 10 ml with H_2O and precipitate $\text{Fe}(\text{OH})_3$ by the dropwise addition of concentrated NH_4OH .
4. Cool, centrifuge, transfer the supernate to a clean 40 ml centrifuge tube and discard the precipitate.
5. Acidify the supernate with concentrated HCl and repeat step 4 twice.
6. Render the supernate from the last $\text{Fe}(\text{OH})_3$ scavenge strongly ammoniacal with concentrated NH_4OH , heat in a hot water bath and add 10 ml of saturated $(\text{NH}_4)_2\text{CO}_3$. Digest until the precipitate of CaCO_3 settles, cool, centrifuge and discard the supernate.
7. Dissolve the CaCO_3 precipitate in 2 ml of 6N HCl, boil over a flame for several minutes to expel CO_2 and dilute to 10 ml with H_2O .
8. Transfer the solution to a 100 ml beaker, dilute to 40 ml with H_2O and add 1N NaOH to pH of 12.
9. Add one-half of a "murexide" tablet, stir until dissolved, and then add dropwise, with stirring, 7.5% EDTA solution until the color changes from red to blue.
10. Carefully adjust the pH to 5.5 with 1N HCl and transfer the solution, without washing, to a 60 ml separatory funnel, the stem of which is directly over a 13 mm OD ion-exchange column containing sodium-cycled "Dowex-50" cation exchange resin (Note 1).
11. Adjust the flows from the separatory funnel and column to 1 drop/second, collecting the effluent in a 250 ml beaker.
12. Elute the column with 150 ml of "calcium wash solution" (1% citric acid-0.75% EDTA, with the pH carefully adjusted to 5.3), collecting the eluent in the same 250 ml beaker.

13. Evaporate the solution on a hot plate to approximately 50 ml and transfer with H₂O washings to 100 ml beaker; evaporate just to dryness.
14. Cautiously add 30 ml of fuming HNO₃ and evaporate just to dryness. Add another 20 ml of fuming HNO₃, evaporate to about 5 ml and cool the beaker in a cold water bath for 5 minutes.
15. Decant the mixture into a 40 ml centrifuge tube, centrifuge and discard the supernate.
16. Dissolve the Ca(NO₃)₂ residue remaining in the beaker with a minimum amount of H₂O and add to the centrifuge tube. Wash the beaker with two 5 ml portions of H₂O and add to the tube.
17. Render the solution strongly ammoniacal with concentrated NH₄OH, heat to boiling over a flame and precipitate CaC₂O₄·H₂O by the dropwise addition of 3 ml of 4%(NH₄)₂C₂O₄. Centrifuge and discard the supernate.
18. Dissolve the precipitate in 2 ml of concentrated HNO₃, add 2 ml of 1M NaBrO₃ and evaporate to 1 ml over a flame.
19. Add 6 drops of Fe carrier (10 mg Fe/ml) and dilute to 15 ml with H₂O. Add concentrated NH₄OH until Fe(OH)₃ precipitates; centrifuge and discard the precipitate.
20. Acidify the solution with concentrated HNO₃ and repeat the Fe(OH)₃ scavenge.
21. Precipitate CaC₂O₄·H₂O as in step 17, filter the precipitate onto a weighed Whatman No. 42 filter disk, wash with two 10 ml portions of H₂O and once with a 10 ml portion of anhydrous "anhydrol." Dry in an oven at 100°C for 15 minutes, cool to room temperature in a desiccator and weigh for chemical yield (approximately 60-70%).

Calcium-45 Counting Procedure

The CaC₂O₄·H₂O mount is counted in a low level beta counter. Radiochemical purity is ascertained by counting without an absorber and then with an aluminum absorber of 6.26 mg/cm² thickness. The ratio of the two count rates is compared by counting absolute standards under the same conditions. If the sample ratio agrees with the standard ratio within the prescribed counting statistics, the sample is accepted as radiochemically pure.

Note 1. The resin is conditioned by three cycles of alternate washings with 5% HCl solution and 5% NaCl solution in a 400 ml beaker. The resin is allowed to settle and the fine particles decanted off after the addition of wash solution. The resin is finally washed free of NaCl with several H₂O washings and approximately 10 ml of wet resin is placed in the column.

Nickel-65 Purification Procedure ⁷

- (a) To an aliquot of the filter paper solution, contained in a 40 ml glass centrifuge tube, add 20 mg of standardized nickel carrier and stir.
- (b) Add 10M KOH until all the nickel is precipitated as the hydroxide. Centrifuge and discard the supernate. Wash the precipitate with 5 ml of H_2O , centrifuge and discard the wash.
- (c) Dissolve the nickel hydroxide precipitate in 5 ml of 6M HCl, add 10 ml of 10% sodium citrate solution and render the solution ammoniacal by the addition of concentrated NH_4OH (Note 1). Dilute to 25 ml with H_2O and precipitate nickel by the addition of 15 ml of 1% alcoholic DMG reagent. Centrifuge and discard the supernate. Wash the precipitate with 30 ml of H_2O containing a drop of concentrated NH_4OH . Centrifuge and discard the wash.
- (d) Dissolve the Ni-DMG precipitate in 2 ml of concentrated HCl and dilute to 15 ml with H_2O (Note 2). Add 10 ml of 10% sodium citrate solution, 5 ml of DMG reagent and precipitate Ni-DMG by the addition of concentrated NH_4OH . Centrifuge and wash the precipitate as in step (c).
- (e) Dissolve the Ni-DMG precipitate in 10 ml of concentrated HNO_3 and transfer the solution to a 250 ml Erlenmeyer flask. Boil the solution to dryness on a hot plate and continue heating to destroy all organic matter (Note 3).
- (f) Dissolve the black NiO by heating in several ml of concentrated HCl. The solution process is aided by the addition of a drop or two of concentrated HNO_3 . Boil until $NiCl_2$ precipitates (Note 4) and then dilute to 20 ml with H_2O .
- (g) To the solution from step (f) add 3 drops of concentrated HCl and 4 drops of Cu carrier (10 mg Cu/ml). Heat almost to boiling in a hot water bath and pass H_2S gas through the solution for 5 minutes. Filter the sulfide precipitate through Whatman No. 42 paper (9 cm in diameter) contained in a 2", 60° glass funnel and collect the filtrate in a clean 40 ml centrifuge tube.
- (h) Boil the filtrate over a flame to remove the excess H_2S , add 4 drops of copper carrier and repeat the sulfide scavenge as in step (g).
- (i) Boil out the H_2S , add 8 drops of Fe carrier (10 mg Fe/ml) and precipitate $Fe(OH)_3$ from hot solution by the addition of concentrated NH_4OH (1 ml in excess). Centrifuge and transfer the supernate to a 40 ml centrifuge tube.

- (j) Acidify the supernate with concentrated HCl, add 8 drops of Fe carrier and repeat step (i).
- (k) To the supernate from the last $\text{Fe}(\text{OH})_3$ scavenge, add 10 ml of 10% sodium citrate solution and 15 ml of 1% alcoholic DMG solution; transfer the solution to a 1 liter separatory funnel containing 500 ml of CHCl_3 .
- (l) Shake the separatory funnel for 3 minutes to extract the Ni-DMG into the chloroform (lower) layer. (Note 5).
- (m) Drain the CHCl_3 extract into a clean 1 liter separatory funnel and wash the extract with two 50 ml portions of H_2O containing a few drops of concentrated NH_4OH . Discard the aqueous phase and washings.
- (n) Back-extract the nickel with 20 ml of 6M HCl (Note 6). Transfer the aqueous phase to a 250 ml Erlenmeyer flask and evaporate the solution nearly to dryness. Add 4 to 5 ml of concentrated HNO_3 and evaporate the solution to near dryness.
- (o) Add 1 ml of concentrated H_2SO_4 and heat the solution to SO_3 fumes; fume strongly for 10 minutes (Note 7). Cool, add 6 ml of H_2O to dissolve the solids and add concentrated NH_4OH to the first permanent blue color; then add 1 ml in excess.
- (p) Add 2 gm of $(\text{NH}_4)_2\text{SO}_4$ and transfer the solution to a plating cell as described in the analysis of Pu^{239} (See Chapter 3 of Part I of this report). Plate the nickel on a weighed, circular platinum foil, 7/8 inch in diameter, for approximately 3 hours at 0.10 amp (Note 8). Add one drop of concentrated NH_4OH about every 30 minutes.
- (q) After plating is complete, wash the disk with H_2O and anhydrous "anhydrol." Air dry, weigh for chemical yield (approximately 60%) and mount on a brass planchet.

Nickel-65 Counting Procedure

The radioactive decay of the Ni mount is monitored by beta counting. The Ni mount is accepted as radiochemically pure if its decay rate is within ± 8.0 minutes of the 153.6 minute-half life of Ni^{65} .

- Note 1. A color change to deep blue-violet indicates that sufficient NH_4OH has been added.
- Note 2. Disregard any DMG which precipitates at this stage.
- Note 3. It is necessary to remove all organic matter in order to precipitate $\text{Fe}(\text{OH})_3$ in step (i).
- Note 4. Be certain that the heating is continued for sufficient time to remove HNO_3 .
- Note 5. Freshly precipitated Ni-DMG ordinarily extracts readily into CHCl_3 . If it does not do so, as indicated by the yellow orange color, add an additional 50 ml of CHCl_3 and shake the funnel vigorously until the aqueous phase is colorless.
- Note 6. The complete disappearance of the yellow-orange color of Ni-DMG in the CHCl_3 layer indicates that back-extraction is complete.
- Note 7. All organic materials and nitrates must be removed for successful plating.
- Note 8. The time required for complete plating depends upon the volume of solution. The best indication of completion of the plating is when the solution becomes colorless.

Manganese-56 Purification Procedure ³

- (a) To an aliquot of the filter paper solution contained in a 150 ml beaker, add 20 mg of standardized manganese carrier, 5 ml of concentrated HNO_3 and heat the solution on a hot plate almost to boiling.
- (b) Add 2 ml of saturated NaBrO_3 solution and digest until all the MnO_2 has precipitated.
- (c) Transfer the mixture to a 40 ml centrifuge tube, centrifuge and discard the supernate. Wash the precipitate with 10 ml of 3N HNO_3 , centrifuge and discard the wash.
- (e) Dissolve the MnO_2 precipitate in 4 ml of concentrated HCl and evaporate the solution to near dryness. If the solution does not turn clear or a very light green during evaporation, again add 4 ml of concentrated HCl and evaporate until the solution turns light green (Note 1). After the light green color is obtained, make the volume up to 4 ml with concentrated HCl .
- (f) Pass the solution over a Dowex-1, 100-200 mesh, 8 or 10% nominally cross-linked, chloride form anion exchange column (Note 2), that has been washed with concentrated HCl , and collect the effluent in a 50 ml Erlenmeyer flask. Wash the column with two 10 ml portions of concentrated HCl , combining the washings with the effluent.
- (g) Evaporate the combined effluent and washings to about 2 ml and transfer the solution to a 40 ml centrifuge tube with about 10 ml of H_2O .
- (h) Add solid Na_2CO_3 to the solution until all the MnCO_3 has precipitated; heat slightly to insure complete precipitation. Centrifuge and discard the supernate. Wash the precipitate with 10 ml of H_2O , centrifuge and discard the wash.
- (i) Dissolve the precipitate in 3 ml of concentrated HNO_3 , add 1 ml of Fe carrier (10 mg Fe/ml) and dilute to 15 ml with H_2O . Cool in an ice bath and add 0.5 gm of NaBiO_3 (with stirring), to oxidize the Mn^{+2} to MnO_4^- . Continue stirring for 1 minute and then add 2 drops of 85% phosphoric acid to stabilize the permanganate.
- (j) Make the solution basic with 6N NaOH (pH 9 to 10 with pH paper), centrifuge and decant the supernate to 100 ml beaker (Note 3). Wash the precipitate with 5 ml of H_2O containing several drops of 6N NaOH , centrifuge and combine the wash with the supernate.
- (k) To the combined supernate and wash from step (j), add 3 ml of concentrated HNO_3 , a few drops of saturated oxalic acid solution and heat on a hot plate until the solution becomes colorless. (Note 4).

- (l) Heat the solution almost to boiling, add 2 ml of saturated NaBrO_3 and heat vigorously until all the MnO_2 has precipitated.
- (m) Transfer the precipitate, to a 10 ml test tube, centrifuge and discard the supernate. Wash the precipitate with 5 ml of H_2O , centrifuge and discard the wash. Stopper the tube and gamma count.
- (n) On completion of the radioassay, slurry the precipitate in H_2O and filter with Whatman No. 42 filter paper (9 cm) contained in a 2", 60° funnel.
- (o) Place the filter paper and precipitate in a tared porcelain crucible and heat gently until the paper is completely charred, making sure that the paper does not ignite.
- (p) Heat the crucible in an electric muffle furnace at 850° for 1 hour, cool in a desicator and determine the chemical yield (60-70%) as Mn_3O_4 .

Radiometric Assay

The test tube containing the MnO_2 precipitate is placed in the well crystal of the gamma ray spectrometer. The net count-rate in the 0.82 Mev photopeak is determined by the area method.

Note 1. If the solution remains a deep green, then add 4 to 6 drops of 1N sodium bisulfite and proceed to step (f).

Note 2. The column is 13 mm OD glass tubing with a resin bed 1/2 to 3/4 inch in depth.

Note 3. The solution should remain deep purple.

Note 4. The MnO_4^- is reduced to Mn^{+2} .

Copper-64 Purification Procedure ⁹

- (a) To an aliquot of the filter paper solution contained in a 40 ml centrifuge tube, add 20 mg of standardized copper carrier and 2 mg of barium, strontium and iron carriers.
- (b) Render the solution ammoniacal with concentrated NH_4OH and add approximately 1 gm of solid K_2CO_3 to precipitate the carbonates. Centrifuge and decant the supernate to a clean 40 ml centrifuge tube.
- (c) Neutralize the supernate with concentrated HCl (until a faint blue color persists) then add solid NaHSO_3 until the blue coloration disappears and SO_2 fumes are evolved.
- (d) Add 1 ml of saturated KCNS , 1 ml of glacial acetic acid and digest in a hot water bath for 15 minutes. Centrifuge and discard the supernate.
- (e) Wash the precipitate with two 5 ml portions of H_2O , centrifuge and discard the washings.
- (f) Dissolve the precipitate in a minimum amount of concentrated HNO_3 (HOOD, Note 1), dilute to 10 ml with H_2O and make the solution basic with concentrated NH_4OH .
- (g) Repeat steps (c) through (e).
- (h) The sample may be prepared for radiometric assay by one of two methods. If the count rate is not great enough for assay in the 100 channel gamma ray spectrometer, the Cu^{64} is plated for beta counting. If the count rate is high enough, then the CuSCN precipitate is utilized as the final mount.
 - (1) Filter the CuSCN precipitate onto a previously washed and weighed Whatman No. 42 filter disk. Wash the precipitate with 10 ml of H_2O and 10 ml of anhydrous "anhydrol". Dry in an oven at 100°C for 15 minutes and cool to room temperature in a desiccator; weigh and record the chemical yield (approximately 70%).
 - (2) Dissolve the CuSCN precipitate in a minimum of concentrated HNO_3 (HOOD, Note 1), dilute to 15 ml with H_2O and heat with stirring. Add 1N NaOH dropwise until a permanent black precipitate forms, then add four to five drops in excess. Centrifuge and discard the supernate. Wash the precipitate with 5 ml of 0.01N NaOH , centrifuge and discard the wash. Dissolve the CuO precipitate in 10 ml of 1.5N H_2SO_4 , add 2 drops of freshly boiled HNO_3 and transfer the solution to a plating cell as described in the analysis of Pu^{239} (Chapter 3, of Part I of this

report). Plate the copper on a weighed disk of platinum foil, 7/8 inch in diameter, for approximately 3 hours at about 3 volts and 100 milliamperes. On completion of plating, wash the disk with H₂O and anhydrous "anhydrol," weigh as copper metal and mount on a brass planchet for beta counting.

Copper-64 Counting Procedure

The radioactive decay of the Cu metal is monitored in a low-level beta counter. If the half life agrees within ± 0.5 hour with the 12.8 hour half life of Cu⁶⁴, the sample is accepted as radiochemically pure.

The CuCNS precipitate is placed in a 10 ml test tube and inserted in the "well" crystal of the gamma ray spectrometer. The net count-rate in the 0.65 Mev photopeak is determined by the area method.

Note 1. CAUTION: Toxic vapors may be involved.

Iron-59 Purification Procedure 10

- (a) Wash the $\text{Fe}(\text{OH})_3$ precipitate from step 18 of the sequential analysis with 15 ml of 1M NH_4OH , centrifuge and discard the wash.
- (b) Dissolve the $\text{Fe}(\text{OH})_3$ precipitate in 15 ml of 10M HNO_3 and 1.5 ml of 30% H_2O_2 with thorough mixing. Add 15 ml of freshly prepared 0.5M 2-thenoyltrifluoroacetone (TTA)-xylene solution and extract the mixture for 10 minutes utilizing a high speed motor stirrer.
- (c) Centrifuge for 1 minute and carefully withdraw and discard the aqueous (lower) phase with a transfer pipette. Wash the sides of the centrifuge tube with several ml of water, centrifuge for 1 minute and withdraw the aqueous wash solution.
- (d) Transfer the organic phase to a clean 40 ml centrifuge tube, add 15 ml of 4M HNO_3 -3% H_2O_2 solution and perform a one minute scrub utilizing the motor stirrer. Centrifuge, withdraw and discard the aqueous scrub solution with a clean transfer pipette.
- (e) Wash the sides of the tube with several ml of H_2O , centrifuge, withdraw and discard the wash.
- (f) Transfer the organic phase to a 60 ml cylindrical separatory funnel, add 5 ml of concentrated HCl , and mix thoroughly with a mechanical stirrer until the organic phase is essentially decolorized (about 10 minutes).
- (g) Withdraw the aqueous (lower) phase into a 40 ml centrifuge tube and precipitate $\text{Fe}(\text{OH})_3$ with excess concentrated NH_4OH . Centrifuge and discard the supernate.
- (h) Transfer the precipitate in small portions, using H_2O as transfer agent, to a 10 ml test tube, centrifuge and discard the supernate. Stopper the tube and gamma count.
- (i) On completion of the radioassay, slurry the precipitate in H_2O and filter with Whatman No. 42 filter paper (9 cm) contained in a 2", 60° funnel.
- (j) Place the filter paper and precipitate in a tared porcelain crucible and heat gently until the paper is completely charred. Heat the crucible in a muffle furnace at 700° for 30 minutes, cool in a desiccator and record the chemical yield as Fe_2O_3 (approximately 70%).

Iron-59 Counting Procedure

The $\text{Fe}(\text{OH})_3$ precipitate is counted in the "well" crystal of the multi channel gamma ray spectrometer. The net count-rates in the 1.10 and 1.30 Mev photopeaks are determined by the area method

Chromium -51 Purification Procedure 11, 12

- (a) Transfer the supernate reserved for Cr^{51} analysis from step 17 of the sequential separation, to a 125 ml Erlenmeyer flask and evaporate the solution to approximately 5 ml.
- (b) Add 5 ml of H_2SO_4 (Note 1) and evaporate the solution to near dryness. Transfer the solution to a 40 ml glass centrifuge tube with about 20 ml of H_2O and precipitate $\text{Cr}(\text{OH})_3$ by the dropwise addition of 10M KOH (Note 2). The base is added until one drop in excess starts to dissolve some of the precipitate. Centrifuge and discard the colorless supernate. Wash the precipitate with 20 ml of H_2O , centrifuge and discard the wash.
- (c) Dissolve the $\text{Cr}(\text{OH})_3$ precipitate in 6-8 drops of concentrated HCl, dilute to 10 ml with H_2O and again precipitate $\text{Cr}(\text{OH})_3$ with 10M KOH as in step (b). Centrifuge and discard the supernate.
- (d) Dissolve the $\text{Cr}(\text{OH})_3$ precipitate in 6-8 drops of concentrated HCl, dilute to 10 ml with H_2O and add 4 drops each of Pd (10 mg Pd/ml) and Cu (10 mg Cu/ml) carriers.
- (e) Heat almost to boiling and bubble H_2S gas through the solution for 5 minutes. Filter the precipitate with Whatman No. 42 (9" diameter) filter paper contained in a 2", 60° glass funnel, collecting the filtrate in a clean 40 ml glass centrifuge tube. Discard the sulfide precipitates.
- (f) Precipitate $\text{Cr}(\text{OH})_3$ from the filtrate as in step (b), centrifuge and discard the supernate. Wash the precipitate with 10 ml of H_2O , centrifuge and discard the wash.
- (g) Dissolve the precipitate in 6-8 drops of concentrated HNO_3 , boil the solution for several minutes and then dilute to 10 ml with H_2O .
- (h) Add 2 ml of saturated NaBrO_3 and heat for 15 minutes to oxidize all the Cr^{+3} to $\text{Cr}_2\text{O}_7^{-2}$.
- (i) Add 5 mg of Fe carrier, precipitate $\text{Fe}(\text{OH})_3$ with concentrated NH_4OH , centrifuge and discard the precipitate.
- (j) Acidify the supernate with concentrated HNO_3 , add 5 mg of Fe carrier and repeat step (i).
- (k) Bring the supernate to boiling and add 3-4 ml of saturated $\text{Ba}(\text{NO}_3)_2$ to precipitate BaCrO_4 . Centrifuge and discard the supernate.

- (l) Wash the precipitate with 30 ml of H_2O , add a few drops of aerosol solution, centrifuge and discard the wash.
- (m) Dissolve the $BaCrO_4$ in 0.5 ml of concentrated HNO_3 and dilute to 10 ml with H_2O . Cool to 0° in an ice-salt bath and transfer the solution to a 125 ml separatory funnel containing 90-100 ml of cold diethyl ether.
- (n) Add 3-4 drops of cold 30% H_2O_2 (Note 3) and immediately extract the blue peroxy compound into the ether (Note 4). Discard the aqueous (lower) phase.
- (o) Wash the ether layer 2 times with 10 ml portions of cold H_2O containing 4-6 drops of concentrated HNO_3 . Discard the washings.
- (p) Back-extract by shaking the ether with approximately 15 ml of H_2O containing 1 ml of concentrated NH_4OH . Transfer the aqueous phase to a centrifuge tube and heat gently in a hot water bath to remove excess ether.
- (q) Add 3-4 ml of saturated $Ba(NO_3)_2$ solution to precipitate $BaCrO_4$. Centrifuge and discard the supernate. Wash the precipitate with 30 ml of H_2O , centrifuge and discard the wash.
- (r) Dissolve the $BaCrO_4$ precipitate in 0.5 ml of concentrated HCl , dilute to 15 ml with H_2O and add 1 ml of 1M $HOAc$. Heat to boiling, add 4-8 ml of 1M NH_4OAc , dropwise to reprecipitate $BaCrO_4$, and let the mixture stand for 5 minutes. Centrifuge and wash the precipitate with two 20 ml portions of H_2O containing a few drops of aerosol solution. Discard the washings.
- (s) Filter the precipitate on a tared regular Whatman No. 42 filter disk using 10 ml of anhydrous "anhydrol" as transfer agent. Dry in an oven at $110^\circ C$ for 20 minutes, cool in a desiccator and weigh for chemical yield (approximately 60%). Place the precipitate in a 10 ml test tube and gamma count.

Chromium-51 Counting Procedure

The test tube containing the $BaCrO_4$ precipitate is inserted in the "well" crystal of the 100 channel gamma ray spectrometer. The net count-rate in the 0.32 Mev photopeak is determined by the area method.

- Note 1. Upon reduction, the solution should turn a dark green.
- Note 2. $\text{Cr}(\text{OH})_3$ precipitates at a pH of 9 to 9.5 and dissolves in excess KOH.
- Note 3. Excess H_2O_2 will catalyze the decomposition of perchromic acid.
- Note 4. The blue perchromic acid is very unstable decomposing to the green Cr^{+3} . Therefore the extractions should be completed as rapidly as possible.

Cobalt-60 Purification Procedure. ¹³

- (a) To the supernate from step 13 of the sequential separation, reserved for cobalt-60 analysis, add 10 mg of Ni carrier and 5 ml of 10M KOH. (Note 1). Boil until the cobalt and nickel hydroxides are precipitated. Centrifuge and discard the supernate. Wash the precipitate with 15 ml of H₂O and discard the wash.
- (b) Dissolve the precipitate in 3 ml of 6M HOAc, heat slightly if necessary. Dilute to 25 ml with H₂O and cool to room temperature.
- (c) Precipitate K₃Co(NO₂)₆ by adding 6 ml of 3M HOAc saturated with KNO₂. Allow about 30 minutes for complete precipitation. Centrifuge and discard the supernate. Wash the precipitate with 30 ml of H₂O, centrifuge and discard the wash.
- (d) Dissolve the K₃Co(NO₂)₆ precipitate in 5 ml of concentrated HCl and boil for several minutes to remove decomposition products. Add 10 mg of Ni carrier and dilute to 25 ml.
- (e) Precipitate Ni and Co hydroxides with 10M KOH.
- (f) Dissolve the precipitate in 3 ml of 6M HOAc and repeat steps (b) and (c).
- (g) Dissolve the K₃Co(NO₂)₆ in 5 ml of concentrated HCl, boil almost to dryness and add 2 drops of Pd carrier (10 mg Pd/ml) and 4 drops of Cu carrier (10 mg Cu/ml). Dilute to 20 ml with H₂O and add 1N HCl to make the solution 0.1N.
- (h) Heat the solution almost to boiling and bubble H₂S gas through the solution for 5 minutes. Filter the sulfide precipitate with Whatman No. 42 filter paper (9 cm) contained in a 2", 60° glass funnel and collect the filtrate in a 125 ml Erlenmeyer flask. Discard the sulfide precipitate.
- (i) Boil the filtrate almost to dryness (Note 2) to remove excess H₂S, dilute to 25 ml with H₂O and transfer the solution to a 40 ml centrifuge tube. Add 4 drops of Fe carrier (10 mg Fe/ml) and precipitate Fe(OH)₃ by addition of concentrated NH₄OH, adding about 0.5 ml of NH₄OH in excess (Note 3). Centrifuge and discard the precipitate.
- (j) Acidify the supernate with 6N HCl, add 4 drops of Fe carrier and repeat the scavenge as in step (i).

- (k) Acidify the supernate with concentrated HCl, adding 1 ml in excess. Transfer the solution to a 125 ml separatory funnel, add 15 g NH_4SCN and shake until all of the solid has dissolved. Extract the Co-SCN complex into 50 ml (1:1) of amyl alcohol-ethyl ether reagent. Discard the aqueous (lower) phase.
- (l) Wash the organic phase with two 10 ml portion of NH_4SCN solution, discarding the washings.
- (m) Back extract the Co into 20 ml of H_2O to which 6 ml of concentrated NH_4OH has been added. Transfer the aqueous phase to a 40 ml centrifuge tube and discard the organic phase.
- (n) Precipitate CoS by bubbling H_2S gas through the solution for 2 minutes, centrifuge and discard the supernate.
- (o) Transfer the CoS precipitate with 5-10 ml of H_2O to a 125 ml Erlenmeyer flask, add 10 ml of concentrated HNO_3 and boil nearly to dryness. (1-2 ml).
- (p) Add 3 ml of concentrated H_2SO_4 and heat to SO_3 fumes. Cool, slowly add 5-10 ml of H_2O and again cool. Neutralize the solution with concentrated NH_4OH and add 1 ml in excess.
- (q) Transfer the solution to a plating cell (as described in the analysis of Pu^{239} , Chapter 3, of Part I of this report), containing about 2 g of $(\text{NH}_4)_2\text{SO}_4$ and electroplate Co on a tared 7/8" diameter Cu disk. Begin plating at 3-4 volts and 0.10 amps. After the first half hour, increase the current to 0.20 amps. and plate for 4-5 hours.
- (r) After plating wash the disk with H_2O and acetone. Dry in a desiccator, weigh for chemical yield (approximately 60%) and mount on a standard brass planchet for beta counting.

Cobalt-60 Counting Procedure

The cobalt mount is counted in a low-level beta counter. Radiochemical purity is determined by counting without an absorber and then with an aluminum absorber of 5.02 mg/cm^2 thickness. The ratio of the two count rates is compared to the ratios obtained by counting absolute standards under the same conditions. If the sample ratio agrees with the standard ratio within the prescribed counting statistics, the sample is accepted as radiochemically pure.

- Note 1. The purpose of the initial precipitation by means of KOH is to remove the Co from strong acid solution. For as complete precipitation of $K_3Co(NO_2)_6$ as possible, mineral acids and oxidizing agents must be absent.
- Note 2. The H_2S is removed to prevent precipitation of CoS in the $Fe(OH)_3$ scavenging step.
- Note 3. If, at the addition of NH_4OH , the green color of $Co(OH)_2$ appears, add HCl until the color disappears and then proceed with the $Fe(OH)_3$ precipitation.

Zinc-69 Purification Procedure

- (a) To an aliquot of the filter paper solution contained in a 40 ml glass centrifuge tube, add 20 mg of standardized zinc carrier.
- (b) Neutralize the solution with 6N NaOH, then add 1 ml in excess. Add 2 mg of Fe carrier, heat to boiling, cool, centrifuge and decant the supernate to a clean 40 ml centrifuge tube.
- (c) Again add 2 mg of Fe carrier, heat to boiling, cool and filter the mixture on Whatman No. 52 filter paper (9 cm diameter) contained in a 2", 60° glass funnel; collect the filtrate in a clean 40 ml centrifuge tube.
- (d) Carefully add 4 ml of 6N HCl (solution should now be 1N in acid), cool in an ice bath and precipitate $\text{ZnHg}(\text{SCN})_4$ by adding 3 ml of $\text{HgCl}_2\text{-KSCN}$ reagent. Cool for 5 minutes with occasional stirring (Note 1).
- (e) To the precipitate from step (d), add 1.5 ml of 6N HNO_3 , 3 ml of H_2O and carefully boil the solution over a micro-burner until a clear solution results; continue boiling for 1 to 2 minutes to remove all products of decomposition.
- (f) Dilute the solution to 10 ml with H_2O , place in a hot water bath and saturate with H_2S gas for 5 minutes to precipitate HgS . Centrifuge and decant the supernate to a 40 ml centrifuge tube.
- (g) To the clear supernate, add 1 ml of 6N NaOH (Note 2) and 5 mg of Bi carrier. Heat in a hot water bath and saturate the solution with H_2S gas for 5 minutes. Centrifuge and decant the supernate to a clean 40 ml glass centrifuge tube.
- (h) Repeat the Bi_2S_3 scavenge as in step (g). Filter the mixture through Whatman No. 42 filter paper (9 cm in diameter) contained in a 2", 60° glass funnel, collecting the filtrate in a clean 40 ml centrifuge tube.
- (i) Boil the solution over a flame for approximately 2 minutes to remove excess H_2S gas.
- (j) Carefully acidify the solution to 1-2N with concentrated HCl, cool in an ice bath and precipitate $\text{ZnHg}(\text{SCN})_4$ as in step (d).
- (k) Repeat step (e)

- (l) Dilute the solution from step (e) to 10 ml with H_2O , cool in an ice bath and precipitate $ZnHg(SCN)_4$ with 3 ml of $HgCl_2$ -KSCN reagent.
- (m) Filter the precipitate on a tared Whatman No. 42 filter disk using 15-20 ml of "zinc wash solution" as transfer agent. Wash with 10 ml of anhydrous "anhydrol," dry in an oven at $105^\circ C$ for 30 minutes, cool in a desiccator and weigh for chemical yield (approximately 65%).

Zinc-69 Counting Procedure

The $ZnHg(SCN)_4$ precipitate is placed in a 10 ml test tube and counted in the "well" crystal of the 100 channel gamma ray spectrometer. The activity of Zn^{69m} is determined by the net count-rate in the 0.44 Mev photopeak obtained by the area method.

- Note 1. It may be necessary to scratch the side of the centrifuge tube to start the formation of the precipitate.
- Note 2. The acid concentration should be approximately 0.3M (\sim pH 0.7) after the addition of 6N NaOH. A white precipitate of ZnS may form but should dissolve with stirring. If the precipitate does not completely dissolve, add 6N HNO_3 drop by drop, with stirring, until the ZnS dissolves.

Phosphorous-32 Purification Procedure 14, 15

- (a) Pipette an aliquot of the filter paper solution into a clean lusteroid tube.
- (b) Add 1 ml of standardized phosphorous carrier (5 mg P/ml) and dilute to 10 ml with H_2O .
- (c) Add 4 ml of concentrated HNO_3 , 5 ml of ammonium molybdate reagent and heat for 5 minutes in a water bath (temperature should not exceed $50^\circ C$). Centrifuge and discard the supernate.
- (d) Wash the precipitate with 5 ml of 3% HNO_3 , centrifuge and discard the wash solution.
- (e) Dissolve the yellow precipitate of ammonium phosphomolybdate in 0.5 ml of conc. NH_4OH (Note 1), add 10 ml of H_2O , 10 drops of 30% H_2O and stir thoroughly.
- (f) Add 10 ml of concentrated HCl , 2 ml of Zr carrier (10 mg Zr/ml) and digest in a hot water bath for 5 minutes. Centrifuge and discard the supernate. Wash the precipitate with 5 ml of H_2O , centrifuge and discard the wash.
- (g) Dissolve the precipitate in 2 drops (Note 2) of conc. HF , add 10 ml of H_2O , 10 drops of 1N HCl , 0.5 ml Cd carrier (10mg Cd/ml), and a few drops of aerosol solution. Heat in a hot water bath for 15 minutes while bubbling H_2S gas through the solution.
- (h) Filter the mixture containing the sulfide precipitate on Whatman No. 42 filter paper (9 cm diameter) contained in a two (2") inch, 60° glass funnel and collect the filtrate in a clean lusteroid tube.
- (i) Add 20 mg (or until no more precipitate forms) of La carrier (10 mg La/ml), centrifuge and transfer the supernate to a clean 40 ml glass centrifuge tube.
- (j) Add 4 ml of concentrated HNO_3 , 5 ml of ammonium molybdate reagent, several drops of aerosol and heat in a water bath for 5 minutes (temperature should not exceed 50°). Centrifuge and discard the supernate.
- (k) Wash the precipitate with 5 ml of 3% HNO_3 , add a few drops of aerosol, centrifuge and discard the wash.
- (l) Dissolve the ammonium phosphomolybdate precipitate in 1 ml of concentrated NH_4OH (Note 3) and add 2 ml of citric acid solution (0.5 g/ml).

- (m) Slowly add 10 ml of magnesia mixture with stirring and concentrated NH_4OH (dropwise) until the solution is just alkaline; then follow with an additional 10 drops of concentrated NH_4OH .
- (n) Stir for 1 minute after the formation of ammonium magnesium phosphate and then add 4 ml of concentrated NH_4OH ; allow the mixture to stand for 4 hours with occasional stirring.
- (o) Filter the NH_4MgPO_4 precipitate on a Whatman No. 42 filter disk using 1:20 NH_4OH and 15 ml of anhydrous "anhydrol" as transfer agents.
- (p) Dry in an oven at 100°C for 10 minutes, cool to room temperature in a desiccator, mount and beta count.
- (q) The chemical yield is determined, upon completion of radiometric assay, by placing the filter paper, pliofilm, and precipitate into a previously weighed porcelain crucible (with cover) and heat cautiously with a Fisher burner until the filter paper is charred. Transfer to an electric muffle furnace and slowly raise the temperature (Note 4) to 1050°C ; maintain this temperature for 1 1/2 hours. Cool in a desiccator, weigh and record the chemical yield (60-70%) of $\text{Mg}_2\text{P}_2\text{O}_7$.

Phosphorous-32 Counting Procedure

The MgNH_4PO_4 mount is counted in a low-level beta counter with an aluminum absorber of 71.58 Mg/cm^2 thickness in order to eliminate any P^{33} activity.

The sample is counted at three day intervals until a representative straight line can be drawn through a semi-logarithmic plot of the data. if the empirically determined half life is 14.3 ± 0.7 days, the sample is radiochemically pure.

- Note 1. If a white or brownish precipitate remains after the yellow precipitate has dissolved, centrifuge and decant the supernate into a clean lusteroid tube; discard the precipitate.
- Note 2. If the precipitate does not completely dissolve, add 1 extra drop of HF. CAUTION: excess HF will retard the precipitation of NH_4PMO_4 .
- Note 3. Same as note 1 except decant the supernate into a clean 40 ml glass centrifuge tube.
- Note 4. All carbon should be burned off before 900°C .

Results of the Neutron Activation of Filter Papers

The results of the neutron activation of filter papers are summarized in Table 3.3. The data represent the quantities of the elements measured in each filter paper sample. The samples are corrected for portions of paper removed prior to ashing. Dotted lines indicate that the sample was lost during analysis. The concentrations of the various elements in stratospheric air as determined by neutron activation will be presented and discussed in Chapters 4 and 5 following.

Table 3.3. Results of Neutron Activation of Filter Papers

Filter No.	Sample	Irradiation Number	Ni (gm)	Mn (gm)	Cu (gm)	Zn (gm)
"Mylar" Blank		2	---	None	4.81×10^{-8}	6.93×10^{-7}
	<u>Minot North</u>					
II 3595	Exposed Outbound	3	4.91×10^{-5}	1.20×10^{-5}	1.72×10^{-5}	6.79×10^{-5}
II 3596	Exposed Inbound	4	5.54×10^{-5}	7.65×10^{-6}	1.72×10^{-5}	2.98×10^{-5}
II 3597	Unexposed	4	1.59×10^{-5}	5.96×10^{-6}	1.16×10^{-5}	3.12×10^{-5}
II 3598	Unexposed	3	---	5.73×10^{-6}	1.28×10^{-5}	2.85×10^{-5}
II 3599	Unexposed	---				
II 3600	Unexposed	2	1.00×10^{-5} *	2.86×10^{-6} **	---	2.50×10^{-5}
	<u>Minot South</u>					
FD-217	Exposed Outbound	3	2.46×10^{-4}	8.36×10^{-6}	2.51×10^{-5}	6.61×10^{-5}
FD-218	Exposed Inbound	4	4.09×10^{-5}	5.73×10^{-6}	6.69×10^{-6}	2.19×10^{-5}
FD-219	Unexposed	4	3.67×10^{-5}	6.29×10^{-6}	---	2.85×10^{-5}
FD-220	Unexposed	3	1.55×10^{-5}	6.45×10^{-6}	2.08×10^{-5}	3.82×10^{-5}
FD-221	Unexposed	2	7.52×10^{-6}	5.70×10^{-6}	1.99×10^{-5}	1.89×10^{-5}
FD-222	Unexposed	2	1.03×10^{-5}	7.42×10^{-6}	2.74×10^{-5}	2.43×10^{-5}

* Questionable half life

** Low chemical yield

Filter No.	P (gm)	Cr (gm)	Fe (gm)	Ca (gm)	Co (gm)
Mylar "Blank"	4.41×10^{-7}	None	None	1.70×10^{-5}	6.03×10^{-9}
II 3595	1.11×10^{-3}	2.69×10^{-5}	6.79×10^{-4}	5.66×10^{-3}	7.32×10^{-7}
II 3596	4.08×10^{-5}	8.78×10^{-6}	4.15×10^{-4}	2.55×10^{-3}	2.66×10^{-7}
II 3597	4.30×10^{-5}	7.67×10^{-6}	3.61×10^{-4}	2.60×10^{-3}	2.18×10^{-7}
II 3598	8.52×10^{-5}	1.19×10^{-5}	1.19×10^{-5}	3.57×10^{-3}	2.56×10^{-7}
II 3599					
II 3600	1.14×10^{-4}	1.22×10^{-5}	3.40×10^{-4}	2.00×10^{-3}	1.95×10^{-7}
FD-217	9.14×10^{-4}	1.08×10^{-5}	5.59×10^{-4}	4.38×10^{-3}	7.16×10^{-7}
FD-218	4.46×10^{-4}	4.18×10^{-6}	2.20×10^{-4}	2.39×10^{-3}	1.99×10^{-7}
FD-219	3.81×10^{-4}	6.32×10^{-6}	3.21×10^{-4}	2.25×10^{-3}	3.46×10^{-7}
FD-220	8.01×10^{-4}	---	3.09×10^{-4}	2.80×10^{-3}	3.38×10^{-7}
FD-221	7.78×10^{-4}	1.63×10^{-5}	4.42×10^{-4}	1.96×10^{-3}	1.60×10^{-7}
FD-222	8.61×10^{-4}	1.17×10^{-5}	4.69×10^{-4}	2.48×10^{-3}	1.87×10^{-7}

LIST OF REAGENTS

(1) Comparator Standards

- (a) Nickel (Nickel Shot), 10 mg Ni/ml
- (b) Manganese (Manganese Metal), 0.10 mg Mn/ml
- (c) Copper (Copper Wire), 0.10 mg Cu/ml
- (d) Zinc (Zinc Metal), 20 mg Zn/ml
- (e) Chromium ($\text{Cr}(\text{NO}_3)_3 \cdot 9\text{H}_2\text{O}$), 1 mg Cr/ml
- (f) Calcium ($\text{Ca}(\text{NO}_3)_2 \cdot 4\text{H}_2\text{O}$), 10 mg Ca/ml
- (g) Iron (Iron Wire), 10 mg Fe/ml
- (h) Phosphorous $[(\text{NH}_4)_2\text{HPO}_4]$, 5 mg P/ml
- (i) Cobalt (Cobalt Metal), 10 mg Co/ml

(2) Carriers

- (a) Nickel ($\text{Ni}(\text{NO}_3)_2 \cdot 6\text{H}_2\text{O}$), 20 mg Ni/ml
- (b) Manganese ($\text{MnCl}_2 \cdot 4\text{H}_2\text{O}$), 20 mg Mn/ml
- (c) Copper ($\text{CuCl}_2 \cdot 2\text{H}_2\text{O}$), 20 mg Cu/ml, 10 mg Cu/ml
- (d) Zinc (Zinc Metal), 20 mg Zn/ml
- (e) Chromium (Na_2CrO_4), 10 mg Cr/ml
- (f) Phosphorous $[(\text{NH}_4)_2\text{HPO}_4]$, 5 mg P/ml
- (g) Calcium ($\text{Ca}(\text{NO}_3)_2 \cdot 4\text{H}_2\text{O}$), 20 mg Ca/ml
- (h) Iron ($\text{FeCl}_3 \cdot 6\text{H}_2\text{O}$), 20 mg Fe/ml, 10 mg Fe/ml
- (i) Cobalt ($\text{Co}(\text{NO}_3)_2 \cdot 6\text{H}_2\text{O}$), 20 mg Co/ml
- (j) Zirconium ($\text{ZrOCl}_2 \cdot 8\text{H}_2\text{O}$), 10 mg Zr/ml
- (k) Cadmium ($\text{Cd}(\text{NO}_3)_2 \cdot 4\text{H}_2\text{O}$), 10 mg Cd/ml
- (l) Lanthanum ($\text{La}(\text{NO}_3)_3 \cdot 6\text{H}_2\text{O}$), 10 mg La/ml
- (m) Bismuth ($\text{Bi}(\text{NO}_3)_3 \cdot 5\text{H}_2\text{O}$), 10 mg Bi/ml
- (n) Barium ($\text{BaCl}_2 \cdot 2\text{H}_2\text{O}$), 2 mg Ba/ml
- (o) Strontium ($\text{SrCl}_2 \cdot 6\text{H}_2\text{O}$), 2 mg Sr/ml
- (p) Palladium (PdCl_2), 10 mg Pd/ml

- (3) Potassium Nitrite (KNO_2)
- (4) Sodium Bromate (NaBrO_3 , Saturated, 1N)
- (5) Saturated Ammonium Carbonate $[(\text{NH}_4)_2\text{CO}_3]$
- (6) "Murexide" Tablet, Acid Ammonium Purpurate
- (7) Disodium Ethylenediamine Tetraacetate, (7.5% EDTA)
- (8) Calcium Wash Solution (1% Citric Acid, 0.75% EDTA)
- (9) Ammonium Oxalate ($(\text{NH}_4)_2\text{C}_2\text{O}_4$, Saturated)
- (10) Sodium Citrate (10% solution)
- (11) Dimethylglyoxime (1% alcoholic solution)
- (12) Chloroform (CHCl_3)
- (13) Ammonium Sulfate ($(\text{NH}_4)_2\text{SO}_4$)

- (14) Sodium Bisulfite ($1N\ NaHSO_3$)
- (15) Sodium Carbonate (Na_2CO_3)
- (16) Sodium Bismuthate ($NaBiO_3$)
- (17) Oxalic Acid (saturated ($COOH$)₂ · 2H₂O)
- (18) Potassium Carbonate (K_2CO_3)
- (19) Potassium Thiocyanate (KCNS, saturated)
- (20) Hydrogen Peroxide (H₂O₂, 30%, 3%)
- (21) 2-Thenolytrifluoroacetone (0.5M in xylene)
- (22) Sulfurous Acid (H₂SO₃)
- (23) Barium Nitrate (saturated Ba(NO₃)₂)
- (24) Diethyl Ether
- (25) Ammonium Acetate (1M NH₄C₂H₃O₂)
- (26) Ammonium Thiocyanate (solid) (1 g NH₄SCN/2 ml of H₂O)
- (27) Amyl Alcohol-Diethyl Ether Reagent (1:1)
- (28) HgCl₂-KSCN Reagent (39 g of Potassium Thiocyanate in 200 ml H₂O.
Stir in 27 g of Mercuric Chloride while diluting to one liter)
- (29) Zinc Wash Solution (20 ml of KSCN-HgCl₂ Reagent/1000 ml of H₂O)
- (30) Ammonium Molybdate Reagent (200 g (NH₄)₆Mo₇O₂₄ · 4H₂O,
800 ml H₂O and 160 ml concentrated NH₄OH)
- (31) Citric Acid (0.5 g/ml)
- (32) Magnesia Mixture (50 g MgCl₂ · 6H₂O, 100 g NH₄Cl, 3-5 drops of HCl and
500 ml of H₂O)
- (33) H₂S Gas
- (34) "Aerosol" Solution (1%, a wetting agent)
- (35) Anhydrous "Anhydrol" (commercial product of denatured 95% ethyl
alcohol available from C. P. Commercial Solvents, Inc., Newark, N. J.)
- (36) Cation Exchange Resin (Dowex-50, 100-200 mesh)
- (37) Anion Exchange Resin (Dowex-1, 100-200 mesh)

REFERENCES

1. Thompson, B. A., Analytical Chemistry, 31, 1492 (1959).
2. Helwig, H. L., Ashikawa, J. K. and Smith, E. R., "Separation of Iron, Cobalt, Zinc and Phosphorous on Synthetic Resin," UCRL-2655 (1955).
3. "Radionuclide Analysis of Environmental Samples," Ed. P. F. Hallbach, U. S. Dept. of Health, Education and Welfare, Technical Report R 59-6, pg. RC-27A-1 (1959).
4. Farabee, L. B., "Proceedings for the Radiochemical Analysis of Strontium and Barium in Human Urine," U. S. AEC, ORNL-1932 (1955).
5. Burgus, W. H., Collected Radiochemical Procedures, LA-1721 (Revised) Ed. J. Kleinberg, 42 (1954).
6. Steinberg, F. P., "Radiochemical Studies: The Fission Products," Edited by C. D. Coryell and N. Sugarman, (McGraw-Hill Book Company, New York, 1951), Book 1, pg. 482.
7. Burgus, W. H., Collected Radiochemical Procedures, LA-1721 (Revised)
8. "Standard Procedure for Radiochemical Analysis on Naval Reactor Plants at Initial and Refueling Startups," WAPD-M (CDA)-212 (Revised), pg. 12.
9. Hutchin, W. H., "Radiochemical Procedures in Use at the University of California Radiation Laboratory (Livermore)" UCRL-4377, Ed. M. Linder, 16 (1954).
10. Moore, F. L., Fairman, W. D., Ganchoff, J. G. and Surak, J. G. Analytical Chemistry, 31, 1148 (1959).
11. Burgus, W. H., Collected Radiochemical Procedures, LA-1721 (Revised) Ed. J. Kleinberg, 54 (1954).
12. Donnelly, M. J., "Information Pertaining to Radiochemistry Studies on Nuclear Submarines Containing Westinghouse Reactors," WAPD-M (CDR)-513.
13. Burgus, W. H., Collected Radiochemical Procedures, LA-1721 (Revised) Ed. J. Kleinberg, 66 (1954).
14. Bonner, N. A. and Potratz, H. A., Collected Radiochemical Procedures, LA-1721 (Revised), Ed. J. Kleinberg, 30 (1954).
15. Hillebrand, W. F. and Lundell, G. E. F., "Applied Inorganic Analysis," (J. Wiley and Sons, N. Y., 1953) Second Edition.

CHAPTER 4

ANALYTICAL RESULTS

In the two preceding chapters, descriptions were given of the methods by which the various particle studies were performed. This chapter will present the results of the studies. It will also explain the physical and mathematical bases upon which the calculations of results from unrefined data rest. In particular, a brief discussion of the application of theory of impaction of particles is given in order to permit the reader to follow the somewhat devious path from raw data to refined "results." The chapter consists of two main sections. One section concerns the study of filter collection efficiency as determined by autoradiography of microtomed sections of the filter paper. The other section concerns the physical and chemical properties of stratospheric particles as determined in the filter paper study, the neutron activation study, and the study of impacted particles by electron diffraction and electron microscopy.

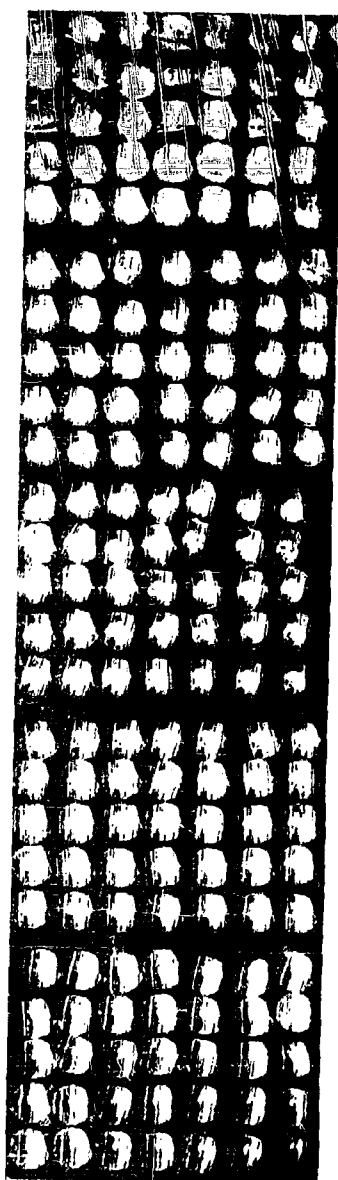
PENETRATION OF FILTER PAPER BY PARTICLES

Evaluation of the survey autoradiograms of microtomed sections of portions of several filter paper samples provided a method for determining the distribution of radioactivity with depth in the filters. Autoradiograms of both parallel and normal sections (described in Chapter 2) were evaluated. The descriptions of the methods of evaluation and the results are given below.

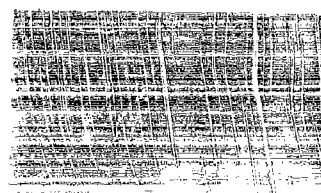
Parallel Sections

The autoradiographic images produced by the thin sections containing portions of fiber matrix were too complex to be evaluated by usual densitometry methods. The images chosen for evaluation were produced by portions of filters for which the initial survey autoradiograms (of quadrants or larger pieces) indicated that the radioactivity was relatively uniformly distributed (i. e. , no "hot spots" were observed in these small areas. However, the individual sections gave small "hot spots" which served to complicate the problem of densitometry.) The survey autoradiogram of the plate containing the sections in serial array was re-registered over the plate and the combination was illuminated from behind with polarized light. The individual sections plus superimposed autoradiograms were viewed with 6X eye magnifier with a polarizing filter. Viewing with "crossed" polarizers made the fibers more apparent, thus readily permitting determination of the sections which contained fibers. This determination was necessary since the microtoming procedures were such that the first and last sections obtained from the plastic pellet came respectively from in front of and from behind the embedded filter paper. The entire matrix of the embedded filter paper usually was contained in about 100 sections of 10 microns thickness. A typical set of sections with corresponding autoradiograms is shown in Figure 4. 1.

A set of autoradiographic images for which the beta activities of the corresponding sections had been measured served as standards for comparison with the images of the sections whose activities were to be determined. The determination consisted in assigning to each image a radioactivity weight factor



10 Micron Thin Sections
of 3/16" Dia. Filter Disk
Embedded in Plastic.



No-Screen X ray Film
Autoradiogram of Sections
on the Left.

FIG. 4.1 PARALLEL SECTIONS AND CORRESPONDING AUTORADIOGRAM

of an integer from zero to ten. Though this is a somewhat subjective procedure, it is felt that the results should have a respectable degree of consistency since all of the evaluation was performed by one person. Furthermore, it is the relative distribution of activity within each set of sections which constitutes the result.

Figure 4.2 shows the results of the autoradiographic determinations on ten different samples of the relative distributions of radioactivity with depth in the filter. The ordinates of the curves are cumulative percent of total activity measured and the abscissae are percent of depth of filter paper based on the number of sections containing fibers. This number varied between 60 and 120. The curves of Figure 4.2 clearly show that none of the measurable activity had penetrated more than 90% of the thickness of the filter papers. In Figure 4.2 a data points from all ten samples are plotted. Figure 4.2 b shows the average of eight samples. The other two samples (299, 535) contained some "hot spots" which caused the distributions to have steeper slopes, as shown in Figure 4.2 c. The sample numbers are listed in Figure 4.2 a along with the exposure time for the autoradiography.

The fact that sections from the backs of the filters representing about 10% of the thickness did not produce autoradiographic images does not mean that there was no activity present in them. The X-ray film used has a detection threshold for 0.7 Mev beta particles of about 10^6 per square centimeter. Using this fact and the measured total beta activities of the filters it is calculated that about 1.5% of the total activity in a filter could be present in the rear 10% of the filter without being detected by the techniques employed in this study.

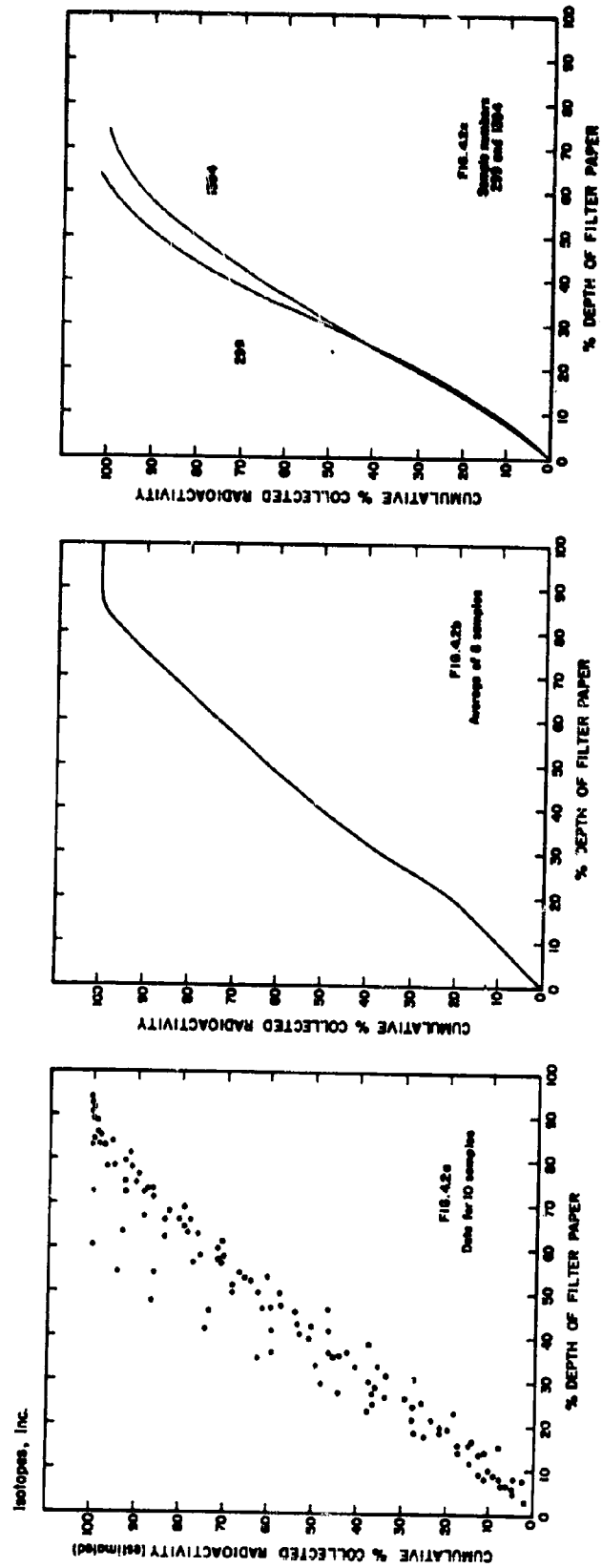


FIGURE 4.2 VARIATION OF CUMULATIVE COLLECTED RADIOACTIVITY WITH DEPTH OF FILTER

Normal Sections

Survey autoradiograms produced from normal sections (cut perpendicular to the plane of the filter face), taken from filter strips which had produced high density spot images in the original survey autoradiograms, were evaluated for eight stratospheric filter samples and three blank filter papers as follows:

1. The radiograms were viewed separately on a light box and all dense spot images were circled with crayon.
2. The radiogram was superimposed on and in registration with the corresponding plate of thin sections.
3. The combination was placed on the viewing box and each marked image with its section was observed with the 6 x magnifier - analyzer.
4. The location of each high density image relative to the filter face was estimated and assigned to one of four class intervals, each of which corresponded to depth increments of 1/4 of the filter thickness.

The survey covered 2,724 thin sections from eight different filters. The distribution of 126 dense spot images is given below in Table 4.1 and in Figure 4.3. Figure 4.3 is a histogram of the number of autoradiographic dense spot images as a function of depth, in terms of fraction of the filter thickness, t.

Table 4.1

Distribution of Dense Spot Images in 8 Filters

Location Depth in Filter	No. of Dense Spot Images Observed
1st Quarter	83
2nd Quarter	30
3rd Quarter	11
4th Quarter	2

CUMULATIVE NUMBER OF DENSE SPOTS

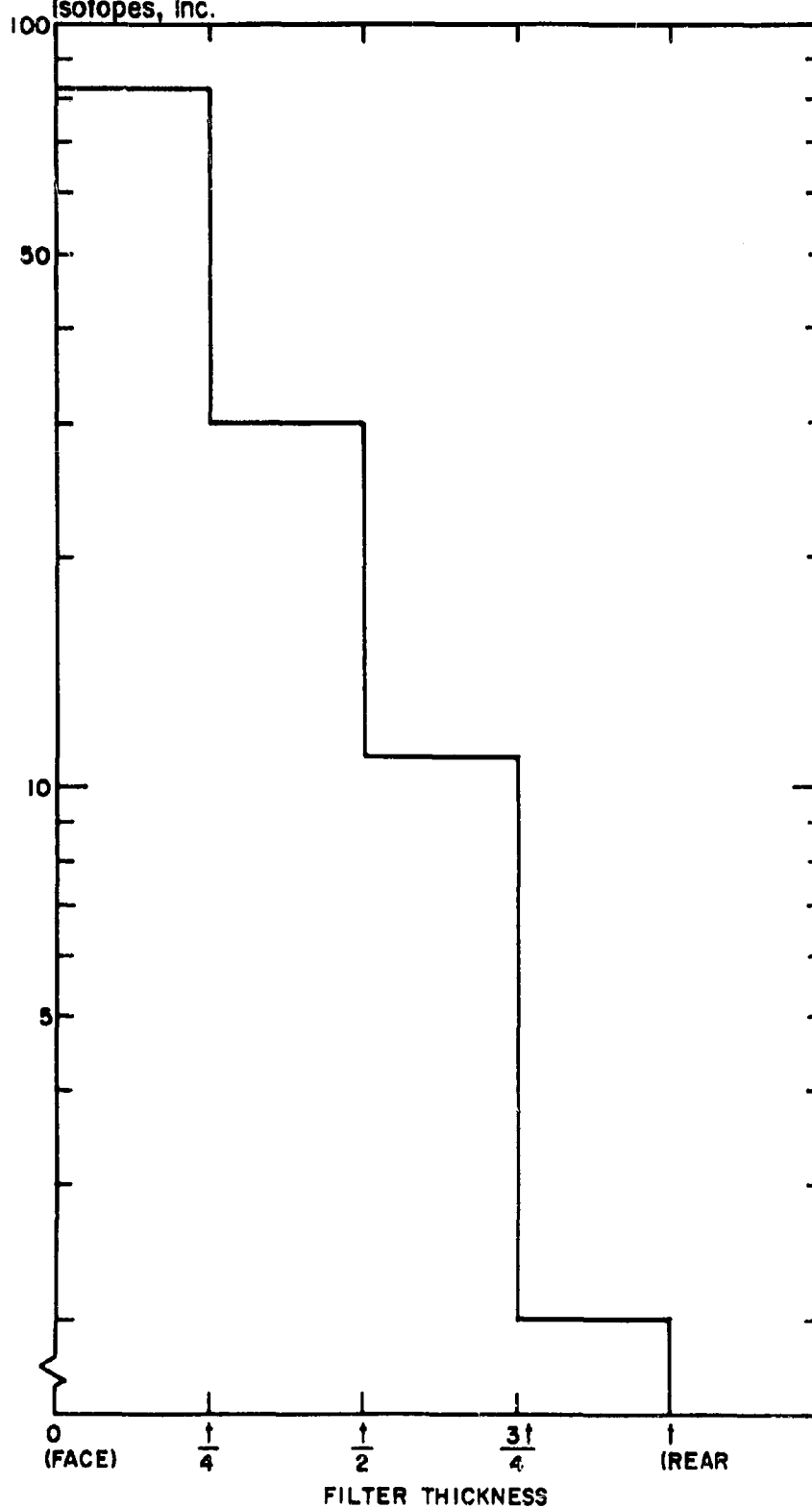
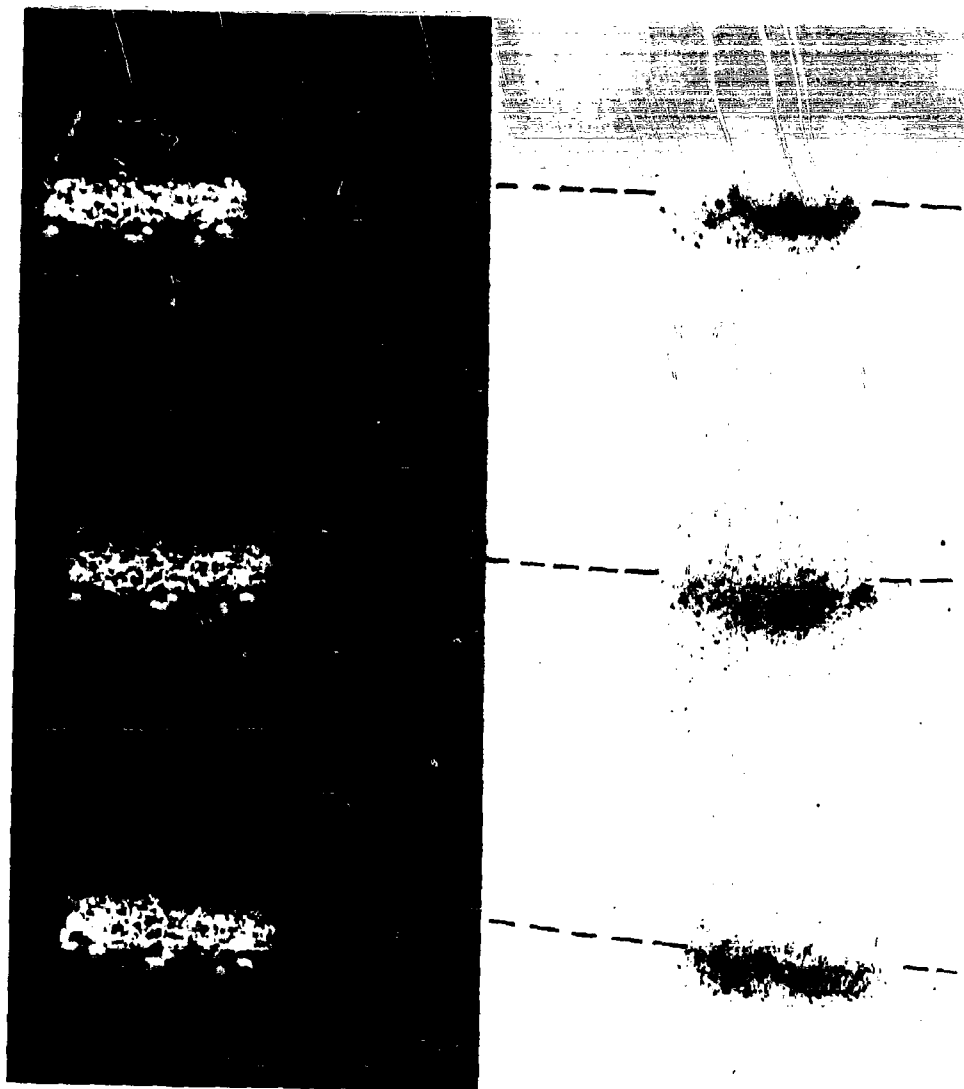


FIG. 4.3 DISTRIBUTION OF HIGH DENSITY SPOT IMAGES IN SURVEY AUTORADIOGRAMS OF NORMAL SECTIONS OF 8 SAMPLES



The Fibrous Filter Mat is 1 mm Thick Excluding
the Backing Gauze Strands. The Dashed Line
Represents the Front Filter Face.

**FIG. 4.4 NORMAL SECTIONS AND CORRESPONDING AUTORADIO-
GRAM**

The sample numbers are also listed in Figure 4.3. A typical normal section and corresponding autoradiogram are shown in Figure 4.4.

An additional qualitative result concerning the compaction of fibers in the filter mat during exposure in the stratosphere was obtained as a by-product of the examination of normal sections. The significance of compaction is discussed in Chapter 3 of Part I of this report. It was observed in many of the normal sections that the fiber packing (number of fibers/unit length) increased with depth in the filter paper. This effect was not discernible in microtomed sections of unexposed (blank) filter paper. The effect was sometime large enough to result in a factor of two increase in the fiber packing. Not all sections displayed this effect, but each sample gave some sections that did.

PHYSICAL AND CHEMICAL PROPERTIES OF STRATOSPHERIC AEROSOLS

The physical properties of stratospheric particles were determined primarily from the microscopic and electron microscopic studies performed on samples collected by the impaction probes. The studies of particles in filter papers by autoradiography and microscopy yielded some qualitative results of the relationship between particle size and radioactivity. The chemical composition of impacted particles was elucidated by electron diffraction. The neutron activation analyses of filter papers served to shed some light on the concentrations of materials which might be expected to comprise portions of extraterrestrial material (or, indeed, terrestrial material) in the stratosphere.

Chemical Composition

a. Neutron Activation

The results of the neutron activation analyses are presented in Table 4.2. This table lists the amounts (in grams) of each element determined in the various exposed filters and blank filters. Also included in Table 4.2 are average values of the amounts of each element found in the blanks. For the northerly flight the blank and sample filters came from the same production batch of filter paper. The filters for the southerly flight also all came from a single batch, but not the same one as for the northerly flight. For this reason, the average blank contents of each element are listed for each set of blank filters.

Table 4.3 lists the net amounts of each element in the samples. These quantities were determined by subtracting the average "blank values" from the total amounts in each sample. In the cases where the total quantity measured was equal to or less than any individual blank value, the net amount listed, as less than or equal to value, represented the limit of detection (based on constancy of blank values). The discussion of these results is presented in Chapter 5, but it is emphasized here that there is a distinct possibility that the samples from both outbound flights (Numbers 3959 and FD-217) could have been contaminated by terrestrial material prior to take-off of the sampling aircraft.

b. Electron Diffraction

Selected area electron diffraction patterns obtained from the impaction probe samples were analyzed at Ernest F. Fullam, Inc. The distances from the center of the ring patterns (see Figure 4.5) are related to the "d - spacings," or distance between lattice planes of the crystal sample. Analysis of the patterns

Table 4.2 Results of Neutron Activation Analyses

Mission/Type	Sample No.	Total Amount (grams)								
		Cu	Zn	P	Cr	Fe	Ca	Co	Ni	Mn
North - Outbound	3595	1.72-5	6.79-4	1.11-3	2.69-5	6.79-4	5.66-3	7.32-7	4.91-5	1.20-5
North - Inbound	3596	1.72-5	2.98-5	4.08-5	8.78-6	4.15-4	2.55-3	2.66-7	5.54-5	7.65-6
Blank	3597	1.16-5	3.12-5	4.30-5	7.67-6	3.61-4	2.60-3	2.18-7	1.59-5	6.26-6
Blank	3598	1.28-5	2.85-5	8.52-5	1.19-5	3.12-4	3.57-3	2.56-7	Lost	5.73-6
Blank	3599	---	---	---	---	---	---	---	---	---
Blank	3600	Lost	2.50-5	1.14-4	1.22-5	3.40-4	2.00-3	1.95-7	<1.00-5	2.86-6
Average Blank		1.22-5	2.82-5	8.07-5	1.07-5	3.38-4	2.72-3	2.24-7	1.3-5	6.35-6
South - Outbound	FD-217	2.51-5	6.61-5	9.14-4	1.08-5	5.59-4	4.38-3	7.16-7	2.46-4	8.36-6
South - Inbound	FD-218	6.69-6	2.19-5	4.46-4	4.18-6	2.20-4	2.39-3	1.99-7	4.09-5	5.73-6
Blank	FD-219	Lost	2.85-5	3.81-4	6.32-6	3.21-4	2.25-3	3.46-7	3.67-5	6.29-6
Blank	FD-220	2.08-5	3.82-5	8.01-4	Lost	3.09-4	2.80-3	3.38-7	1.55-5	6.45-6
Blank	FD-221	1.99-5	1.89-5	7.78-4	1.63-5	4.42-4	1.96-3	1.60-7	7.52-6	5.70-6
Blank	FD-222	2.74-5	2.43-5	8.61-4	1.17-5	4.69-4	2.48-3	1.87-7	1.03-5	7.42-6
Average Blank		2.27-5	2.75-5	7.05-4	1.14-5	3.85-4	2.37-3	2.58-7	1.75-5	6.47-6

Table 4.3 Net Quantities of Elements in Dust Samples

Sample No.	Vol. (cm ³)	Net Amount (grams)								
		Cu	Zn	P	Cr	Fe	Ca	Co	Ni	Mn
3595	1.7910	5.0-6	4.0-5	1.0-3	1.6-5	3.4-4	3.0-3	5.1-7	3.6-5	5.6-6
3596	1.9710	5.0-6	<1.0-5	<4-5	<1.0-5	0.5-4	<2.0-3	<1-7	4.2-5	1.3-6
FD-217	2.1410	<5-6	3.8-5	2.1-4	1.0-5	1.7-4	2.0-3	4.6-7	2.3-4	1.9-6
FD-218	2.0410	<5-6	<2-5	<2-4	<4-6	<0.5-4	<1.0-3	<0.5-7	2.3-5	<0.3-6

gives the interplanar spacings of the sample material, which are then compared with values listed in the X-ray Powder Data File published by the American Society for Testing Materials. The matching of measured spacings with those for a known material can constitute a determination of the composition of the sample material where the accuracy of measurement of the diffraction pattern is sufficient to provide a unique correspondence.

The electron diffraction patterns produced by the particles which constituted the overwhelming majority of the particles collected by the probe samplers corresponded uniquely to those of ammonium sulfate, $(\text{NH}_4)_2\text{SO}_4$, and ammonium persulfate, $(\text{NH}_4)_2\text{S}_2\text{O}_8$. The lattice constants which are related to d-spacings, of these materials are given in Table 4.4 below.

Table 4.4

Lattice Constants of Ammonium Sulfate and Ammonium Persulfate*

Material	Lattice Constants (In Angstrom Units)		
	a	b	c
$(\text{NH}_4)_2\text{SO}_4$	5.951	10.560	7.729
$(\text{NH}_4)_2\text{S}_2\text{O}_8$	7.83	8.04	6.13

Figure 4.5 shows an electron diffraction pattern which was produced by ammonium persulfate particles. Figure 4.6 is an electron micrograph of particles such as those which gave the diffraction pattern shown in Figure 4.5. The electron micrograph shown in Figure 4.7 contains particles identified as ammonium sulfate by means of electron diffraction. Comparison of the particles shown in Figure 4.6 and 4.7 indicates that the sulfate and persulfate particles cannot usually be

* Taken from "Handbook of Chemistry and Physics," Chemical Rubber Publishing Co. (Cleveland, Ohio).

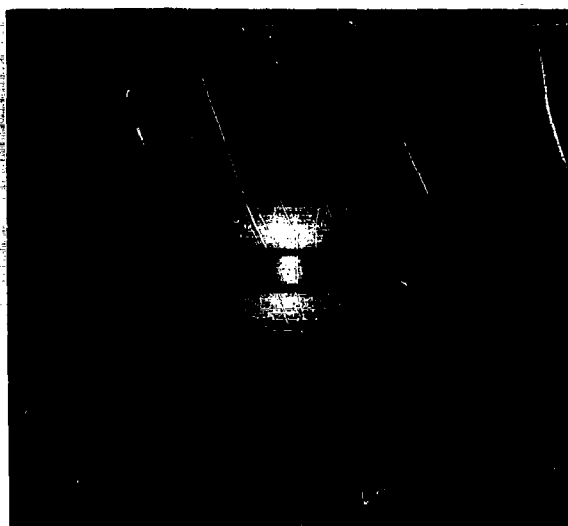


FIG. 4.5 ELECTRON DIFFRACTION PATTERN OF AMMONIUM PERSULFATE PARTICLES

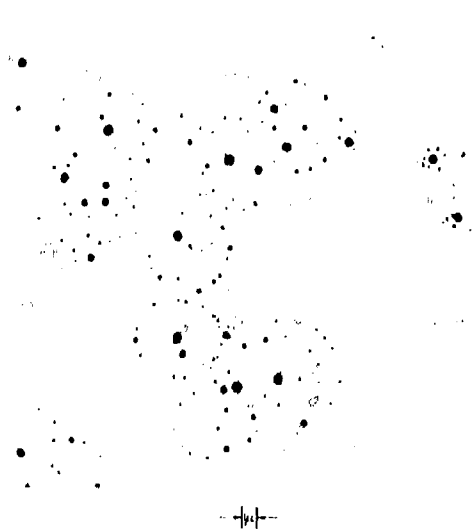


FIG. 4.6 ELECTRON MICROGRAPH OF PARTICLES OF AMMONIUM PERSULFATE

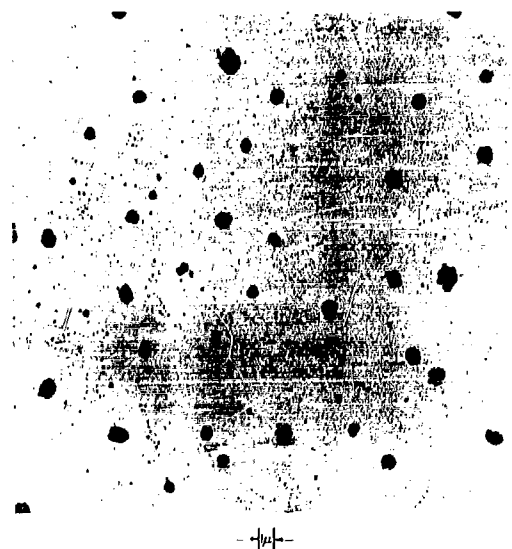


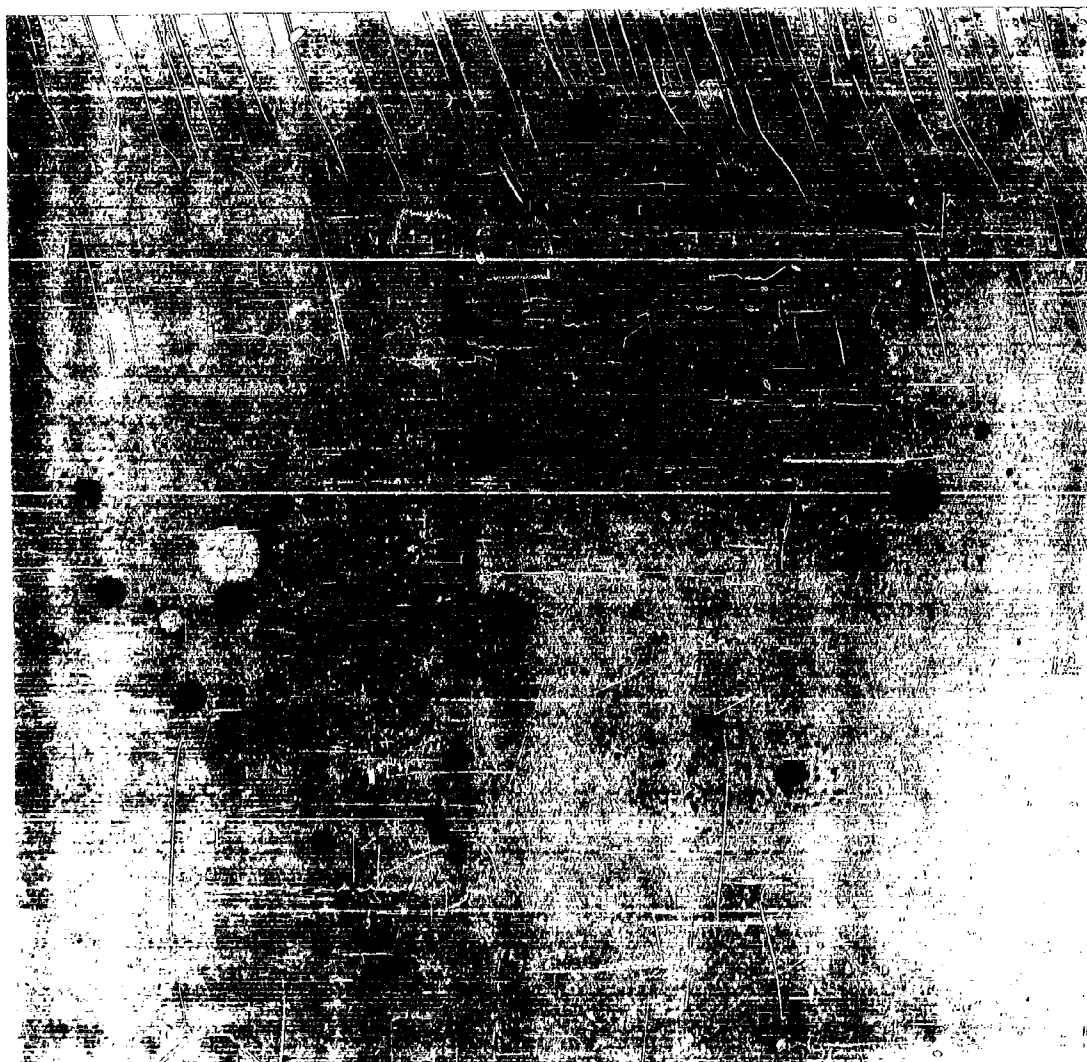
FIG. 4.7 ELECTRON MICROGRAPH OF PARTICLES OF AMMONIUM SULFATE

uniquely identified on a morphological basis. However, a few cases where electron diffraction indicated a composition of ammonium sulfate, some particles were found which displayed distinctly crystalline form where measurements of the angles confirmed the identification. Such particles are shown at the top of Figure 4.8. Other particles shown in the electron micrograph are similar to those more frequently encountered.

The collected particles were found to be hygroscopic, and the hygroscopicity of ammonium sulfate and ammonium persulfate particles have been confirmed in laboratory studies conducted by Junge and Manson⁷. They have firmly established the fact that the stratospheric particles are hygroscopic. However, evidence from the electron micrographs of the particles collected in HASP also confirms their hygroscopicity. The evidence will be discussed in another portion of this chapter.

Of seventeen samples from which electron diffraction data were obtained, three were identified as ammonium persulfate, thirteen as ammonium sulfate, and one contained some of both types. The three samples which contained persulfate only were collected between 16° North and 16° South latitudes. The one sample containing both sulfate and persulfate was collected between 27° and 48° North latitude. The samples containing sulfate were collected from latitudes ranging from equatorial to polar.

It is emphasized here that the vast majority of particles collected were of the sulfate and persulfate type. The following section of this chapter, which deals with particle classification, presents more detail concerning the various types of particles encountered. Also, in Table 4.6, the compositions of the



→1/2←

Fig. 4.8 Electron Micrograph Showing
Crystalline Ammonium Sulphate
Particles.

samples as determined by electron diffraction are given.

Particle Classification

The particles collected by impaction were classified according to radius and type (sulfate, persulfate and other). However, before presenting the results, a brief discussion of the methods used in treating the data is given.

a. Impaction of Particles

In a paper by Ranz and Wong², which has become the standard reference in the subject of inertial impaction of particles, theoretical studies of the efficiencies of collection by impaction of particles from aerosol jets onto various types of surfaces were presented. The theoretical studies were for the most part verified by experiment for the cases of impaction from round and rectangular jets upon a flat surface and from "infinite" jets upon cylindrical and spherical surfaces. The results of the studies by Ranz and Wong show that the process of inertial deposition of particles from jets can be characterized by an impaction parameter, Ψ , defined as follows:

$$\Psi = \frac{C \rho_p V_o D_p^2}{18 \mu D_c} \quad (4.1)$$

where C = Cunningham correction factor for gas resistance experienced by small particles,

$$C = 1 + \left(\frac{2\lambda}{D_p} \right) \left[1.23 + 0.41 \exp \left(-0.44 \frac{D_p}{\lambda} \right) \right] \quad (4.2)$$

for $0.1 < \frac{2\lambda}{D_p} < 134$,

λ = mean free path of gas molecules,
 D_p = diameter of particle,
 D_c = diameter of collector (or width of jet),
 ρ_p = density of particulate material,
 μ = coefficient of viscosity of gaseous medium,
 and V_o = velocity of free aerosol stream relative to collector.

A given case (type of jet plus type of collector) is characterized by a single curve of efficiency, η , versus $\sqrt{\Psi}$. The efficiency is defined as the ratio of the number of particles of diameter D_p deposited on the collection surface to the number of particles with the same diameter existing in the volume of aerosol swept out by the collection surface. For a cylindrical collector exposed to an infinite aerosol stream the curve shown in Figure 4.9 suffices to describe the result of any situation for any permissible set of values of λ , D_p , D_c , ρ_p , μ , and V_o . (Remember that $0.1 < \frac{2\lambda}{D_p} < 134$.) The shape of the curve was mainly determined by experiment except for the region near the minimum value of $\sqrt{\Psi}$ for finite efficiency, which was taken from the theoretical curve of Langmuir and Blodgett³. For values of $\sqrt{\Psi}$ less than the minimum for finite η , mechanisms other than impaction prevail.

For the purposes of evaluating the raw data, in the form of particle size-frequency distributions, from the electron micrographs of the probe samples, we have assumed that the efficiencies of impaction were those for a cylinder. Thus, the curve shown in Figure 4.9 is the basis of the calculations of particle size distributions in the stratosphere.

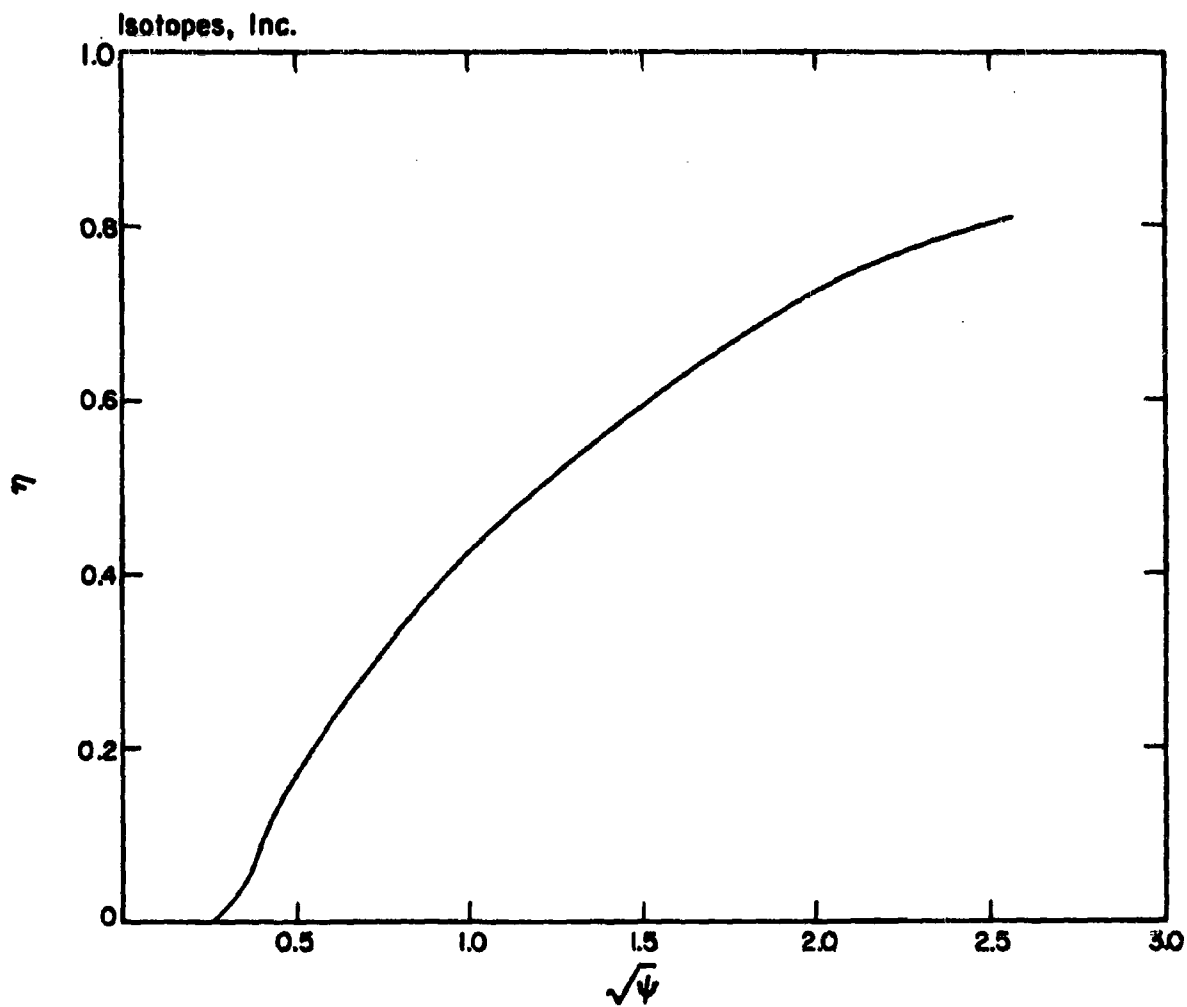


FIG. 4.9 EXPERIMENTAL IMPACTION EFFICIENCIES OF CYLINDRICAL COLLECTORS

The quantities needed to calculate the impaction parameter, Ψ , were obtained from the observed particle size-frequency distribution (D_p), the probe dimensions (D_c), the altitude of collection and air temperature (λ , μ), the aircraft velocity (V_o), and an assumed value for the density of the particulate material (ρ_p).

For particles whose diameters are of the order of the mean free path, and for a given velocity, V_o , the altitude of collection will have the largest effect on efficiency with which the particles are collected. The higher the altitude, the greater is the mean free path of air molecules, λ , the greater is the Cunningham correction factor, C , and thus the greater is the impaction parameter. The viscosity of air, μ , is a slowly varying function of temperature ($\sim T^{1/2}$) and the temperature of the stratosphere does not vary greatly with altitude and time. Therefore, the effect of temperature on the collection efficiency is small compared with that of altitude for stratospheric collections of particles where $D_p \simeq \lambda$. Table 4.5 lists the values of $\sqrt{\Psi}$ and probe collection efficiencies, η , for various particle radii at various altitudes and two different temperatures for the following conditions:

$$D_c = 1.50 \text{ cm},$$

$$\mu = 1.422 \times 10^{-4} \text{ poise (T = 216.66}^\circ\text{K, ARDC Model Atmosphere)} \\ \text{and } 1.36 \times 10^{-4} \text{ poise (T = 205}^\circ\text{K),}$$

$$\lambda = \text{value from ARDC Model Atmosphere for T = 216.66}^\circ\text{K,}$$

$$(\lambda)_{T=205} = (\lambda)_{T=216.66} \left(\frac{205}{216.66} \right),$$

$$V_o = 415 \text{ knots} = 2.13 \times 10^4 \text{ cm/sec.},$$

$$\rho_p = 2 \text{ grams/cm}^3.$$

The table illustrates the dramatic effect of altitude upon the collection efficiencies of particles with radii less than one micron. For radii equal to or greater than one micron the effect of altitude becomes considerably smaller and the effect of temperature becomes larger in comparison to that of altitude.

In general the conditions listed above for the computation of Table 4.5 were those which actually pertained or were assumed to pertain to the collection of the probe samples in HASP. Corrections and interpolations were made when altitude, temperature, and velocity differed significantly from those listed in the table.

b. Calculation of Particle Size-Frequency Distribution

Upon examination of the electron micrographs of the probe samples it became evident that there were several complications which had to be overcome before the actual particle size-concentration distribution of the stratospheric aerosol could be estimated.

The first complication was that the deposition of particles was not uniform over the collection surface in the probe. The particles were deposited in one or sometimes two bands which extended across the sampling surface, parallel to its small dimension, as shown in Figure 4.10. This effect is attributed to the cut of the window in the probe and possibly to a slight deviation of the sampling surface from an orientation normal to the direction of flight.

The presence of the band(s) of particles on the sampling surface did serve, however, to prove that a bona fide collection had been accomplished. If, for instance contaminating tropospheric particles had been present, they would have deposited more or less at random over the surface of the sample, and thus

Table 4.5 Impactation Efficiencies for Probe Collector

Particle Radius $r(\mu)$	50,000 ft.		55,000 ft.		60,000 ft.		65,000 ft.		70,000 ft.	
	$\sqrt{\psi}$	η	$\sqrt{\psi}$	η	$\sqrt{\psi}$	η	$\sqrt{\psi}$	η	$\sqrt{\psi}$	η
A. Temperature = 216.66°K (Model Standard Atmosphere)										
0.100	.186	0	.207	0	.231	0	.260	.004	.291	.016
0.158	.240	0	.270	.008	.296	.016	.331	.032	.371	.056
0.251	.316	.024	.348	.040	.382	.066	.426	.106	.475	.154
0.398	.423	.105	.459	.140	.503	.176	.554	.207	.615	.242
0.631	.583	.226	.623	.250	.675	.276	.731	.306	.802	.340
1.00	.833	.354	.873	.370	.927	.392	.996	.420	1.07	.446
1.58	1.22	.502	1.26	.517	1.32	.536	1.38	.557	1.48	.588
2.51	1.84	.685	1.87	.694	1.95	.712	2.02	.729	2.09	.740
3.98	2.82	.838	2.89	.844	2.93	.846	3.00	.852	3.09	.859
6.31	4.37	.915	4.43	.917	4.47	.918	4.54	.920	4.64	.923
B. Temperature = 205°K										
0.100	---	---	.216	0	.244	0	.273	.010	.311	.022
0.158	---	---	.280	.012	.311	.022	.348	.040	.389	.072
0.251	---	---	.365	.050	.402	.084	.447	.127	.500	.174
0.398	.443	.124	.483	.162	.529	.193	.582	.225	.645	.260
0.631	.612	.241	.654	.267	.709	.294	.768	.324	.843	.358
1.00	.874	.372	.917	.388	.974	.413	1.05	.440	1.13	.470
1.58	1.29	.528	1.32	.536	1.38	.557	1.45	.580	1.56	.612
2.51	1.94	.710	1.96	.714	2.05	.733	2.12	.748	2.20	.762
3.98	2.96	.848	3.04	.854	3.07	.858	3.15	.861	3.25	.868
6.31	4.59	.921	4.65	.923	4.69	.924	4.78	.927	4.87	.929

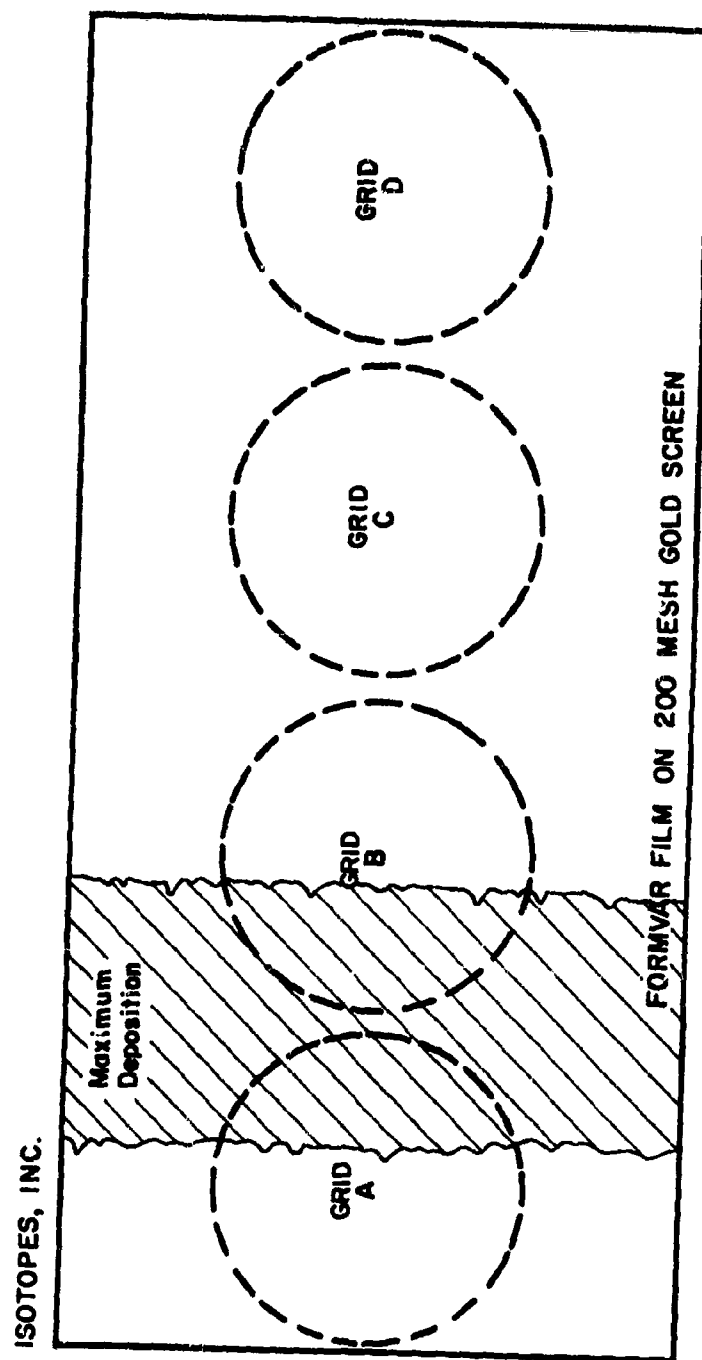


FIG. 4.10 DIAGRAM OF IMPACTION SURFACE SHOWING ZONE OF
MAXIMUM DEPOSITION

readily have been detected. Two separate sample blanks, which were obtained by exposure of a surface prepared in the normal manner to stratospheric air for two minutes, were sent to Ernest F. Fullam, Inc. as regular samples. In each case a very sparse collection of particles of the sulfate type was obtained. There was no evidence of contamination of the samples due to the handling and operation of the probe in the field.

The problems then arose as to how to obtain representative electron micrographs of the sample, how to relate the area of the sample examined to the entire sample, and how to take into account the fact that particles of different size may behave differently with respect to their deposition in the band of high population. The manner in which these problems were met is described in the following paragraphs.

Scanning of the samples in the electron microscope revealed that the zone of maximum deposit contained almost all of the particles whose diameters were smaller than one micron and that these particles were almost entirely of the sulfate and persulfate type. The particles with diameter greater than one micron were found to be far fewer in number than the smaller particles and seemed to show no propensity to deposit on a preferred region of the sampling surface. The scheme of removing four 1/8 inch discs from the sample (see Figure 2.6) was devised to provide representative sampling of the deposit of particles. The position of the zone of heavy deposit was determined by examination of the scrap of screen left after removal of the discs. A map of the zone was made for each sample. Usually the mid-point of the zone fell close to the region between the a and b discs (the discs nearer the inboard end of the sample).

Sometime it was near the center of the a disc. At any rate the map provided a basis for assigning relative weights to the particle counts from the a and b discs.

The following assumptions were made to permit calculation of the particle size-frequency distribution of the sample (uncorrected for impaction efficiency).

1. All particles with diameters less than one micron were deposited within the zone of maximum population but they would have been deposited uniformly over the sample area were it not for the aerodynamic effect due to the cut of the window in the probe.

2. All particles with diameters equal to or greater than one micron were deposited "uniformly" over the sample area. (Actually, the number of such particles deposited on the entire sample was usually small, so that it could hardly be said that the deposit was uniform. A more accurate statement of the assumption is that the particles ($D_p \geq 1$ micron) are not preferentially deposited at any particular location within the sample area.)

Note: If we assume that the layer of air between the sample and the outside surface of the probe is stagnant except for slow eddies which cause the small particles to deposit in a band, then we can estimate the diameter of the particle which would just come to zero velocity at the sampling surface under typical sampling conditions. The maximum thickness of this stagnant layer is 0.635 cm. The distance travelled by a particle in stagnant air with initial velocity V_o and final velocity zero is given by

$$L = \frac{C \rho_p V_o D_p^2}{18\mu}$$

where the quantities are as previously defined. At an altitude of 20 km with

$$\begin{aligned} V_o &= 415 \text{ knots} = 2.13 \times 10^4 \text{ cm/sec,} \\ \rho_p &= 2 \text{ g/cm}^3 \\ \mu &= 1.422 \times 10^{-4} \text{ poise,} \end{aligned}$$

we find that for one micron diameter particles

$$L = \frac{3.71 \times 10^{-8} \times 2 \times 2.13 \times 10^4}{18 \times 1.422 \times 10^{-4}} = 0.617 \text{ cm.}$$

This is very close to the 0.635 cm thickness of the stagnant layer. Thus the notion of a relatively stagnant layer with slow eddy motion and the observation of the segregation on the sampling surface of particles according to size seem compatible.

Typically, all of the electron micrographs of the a and b screens of a single sample covered an area of $4.5 \times 10^{-3} \text{ mm}^2$ while an area of 3.14 mm^2 was scanned to obtain those of the c and d positions. When all of the observed particles had been classified according to radius, the fraction of the sample area occupied by the zone of high population was estimated from the maps. This was obviously a rather crude method. However, the fraction of the area occupied by the zone appeared to be relatively constant between 0.2 and 0.25. Determination of the size-frequency distribution by application of one of the two fractions was accomplished in the following manner.

1. The area, A_1 , occupied by the particles counted in the a and b screens was divided by the fraction, R_1 , of the area occupied by the zone. ($R_1 = 0.2$ or 0.25).
2. The number of particles of a given class, n_{i1} , counted in the a and b screens was divided by the area A_1/R_1 to give the observed frequency per unit area, ν_{i1} . Thus

$$\nu_{i1} = \frac{n_{i1} R_1}{A_1} \quad (i \text{ refers to the particle class}) \quad (4.3)$$

3. The area, A_2 , occupied by the particles counted in the c and d screens was reduced by a factor R_2 such that

$$A_1/R_1 = A_2/R_2 \quad (4.4)$$

4. The observed frequency per unit area of particles of a given class counted in the c and d screens was determined by

$$\nu_{i2} = \frac{n_{i2}}{R_2 A_2} \quad (4.5)$$

where subscript 2 refers to c and d screens.

5. The net distribution was then computed by

$$\nu_i = \nu_{i1} + \nu_{i2} \quad (4.6)$$

where ν_i is the number of particles in the i th class per unit area of the sample. (In most cases where the i th class contained particles with diameters < 1 micron

$$\nu_i \approx \nu_{i1}$$

and when it contained particles with diameters > 1 micron

$$\nu_i \approx \nu_{i2} ,$$

the contribution from the other term being negligible in each case.)

The particles were classified according to radius. The classes were chosen so that $\Delta (\log r) = \text{constant}$: i.e., the intervals of radius were such that $\frac{r_{i+1}}{r_i} = \text{constant}$ where the interval (r_i, r_{i+1}) contains all particles of the $(i+1)$ th class. For the samples evaluated here $\Delta (\log r) = 0.2$. Thus for particles with the range of radius $0.1 \mu \leq r \leq 10 \mu$ there were ten classes. Table 4.6 on pp 101-109 is a compilation of all of the pertinent data concerning the collection of each sample, the composition as determined by electron diffraction, and the particle-size frequency distributions. The tabulated radii are those corresponding to the means of the logarithms of the radii defining the class intervals. The normalized area is that corresponding to A_1/R_1 as described above. The observed frequencies, ν_i , are the number of particles of the i th class found (calculated to be) in the normalized area. The column headed $\frac{f_{\text{obs}} \times 10^5}{V_{01}}$ is 10^5 times ν_i divided by the normalized volume, which is the normalized area times the length of flight path. The quantity $\frac{f_{\text{obs}}}{V_{01}}$ is designated as $\bar{\nu}_i$ and has the units cm^{-3} .

c. Calculation of Particle Size-Concentration Distributions

The column headed $1/\eta$ in Table 4.6 is the reciprocal of the estimated collection efficiency of a particle with the corresponding radius and a density of 2 gm/cm^3 . The quantity \bar{N} is merely the product $\bar{v}_i(\frac{1}{\eta})$ which is the number of particles per cubic centimeter of free air. Thus the column headed by \bar{N} is the particle radius - concentration distribution. The volume concentration, \bar{V} , is obtained by multiplying \bar{N} by $4/3\pi r^3$. It has units of μ^3/cm^3 and represents the volume of particles of the i th class per cm^3 of free air. Summation of the columns of \bar{N} and \bar{V} gives, respectively, the number concentrations and volume concentrations of the aerosol.

The collection efficiencies listed in Table 4.6 were obtained by a somewhat arbitrary procedure based on the impaction efficiencies calculated by the method of Ranz and Wong² as given previously. The problem arose from the observation of many particles collected with diameters smaller than those which should have zero impaction efficiency. (Compare Table 4.6 with Table 4.5.) Also, in this connection, several of the samples appear to have been affected to various degrees by condensation of water. The evidence of condensation is shown in Figure 4.11 where it is seen that each larger particle is surrounded by a "halo" of smaller particles. This appears to have been the result of the following process:

1. During collection of particles in the stratosphere the probe had reached thermal equilibrium with its (cold) environment.
2. After collection when the aircraft descended into the warmer and moister troposphere, though the probe was closed, water vapor diffused through the space between the cylindrical wall and the piston and thence to the sample area.



Fig. 4.11. Electron Micrograph of Strato-
spheric Particles Showing
Evidence of Moisture Condensation

3. The particles of ammonium sulfate or persulfate, being of hygroscopic nature and not having warmed to the temperature of the tropospheric environment, became sites of condensation for the water vapor.
4. The condensed water formed droplets containing the particles, and the particles were partially dissolved in the droplets.
5. At some time after the condensation occurred, the environment became warmer and less humid, the water evaporated, and in so doing, left behind the portions of the original particles which had not dissolved in the droplets plus a residue of material which had been dissolved in the droplets. This residue surrounded each original particle in the form of a halo of very small particles.

It is obvious then, that this condensation-evaporation process could have created many particles which were smaller than the size required for finite impaction efficiencies. In counting and classifying particles from electron micrographs, all of the halo particles were ignored and the central particle or particles were classified when it was apparent that condensation had occurred. No account was taken of the reduction in radius of the central particles as a result of the dissolution process. In the worst cases, the net effect on the "observed" size-frequency distribution of condensation-evaporation and the method of classification was to cause an excess of small particles and a deficiency of larger particles. This effect must be borne in mind in interpreting any of the data presented here.

An additional complication due to condensation of water upon the particles was that they became flattened as the condensed droplet spread over the supporting Formvar substrate. The flattening was pronounced only in those samples where condensation was quite severe. The manner in which this effect was taken into account is described below.

It was noted that the electron optical densities of particles with radii between about 0.2μ and 0.6μ were all about equal. This led to the suspicion that the effect of the spreading of the droplets was to leave particles which had the same thickness regardless of original diameter (except for particles with radii less than 0.2μ). To confirm this suspicion, a few samples were shadow cast with palladium in order that the thickness of the particles could be measured. The results are shown in Figure 4.12 where the shadows were cast at an angle of 10° . Measurements of the distance between the shadow apex and the particle center revealed that many of the particles indeed had thicknesses of about 0.2μ though their radii ranged from 0.2μ to 0.5μ . It was thus felt that, in the cases of severe condensation, the assumption that all particles of the sulfate (and persulfate) type with radii greater than 0.2μ had thicknesses of 0.2μ was justified. The volume of particles in each radius class was computed by

$$V_p = 0.2 \pi r_{oi}^2 (\mu^3) \quad (4.7)$$

and this was placed equal to the volume of the (assumed) original spherical particle. Thus

$$0.2 \pi r_{oi}^2 = 4/3 \pi r_{lj}^3 \quad (4.8)$$

In these two equations r_{oi} is the geometric mean radius of flat particles in class i (class intervals for r_{oi} are determined as previously explained) and r_{lj} is the geometric mean radius of equivalent spherical particles of class j . The radius interval to which r_{lj} is referred is now smaller than that to which r_{oi} is referred as a consequence of equation 4.8. Sample number W-16 in Table 4.6 is an example of the type of classification which results from the above treatment.

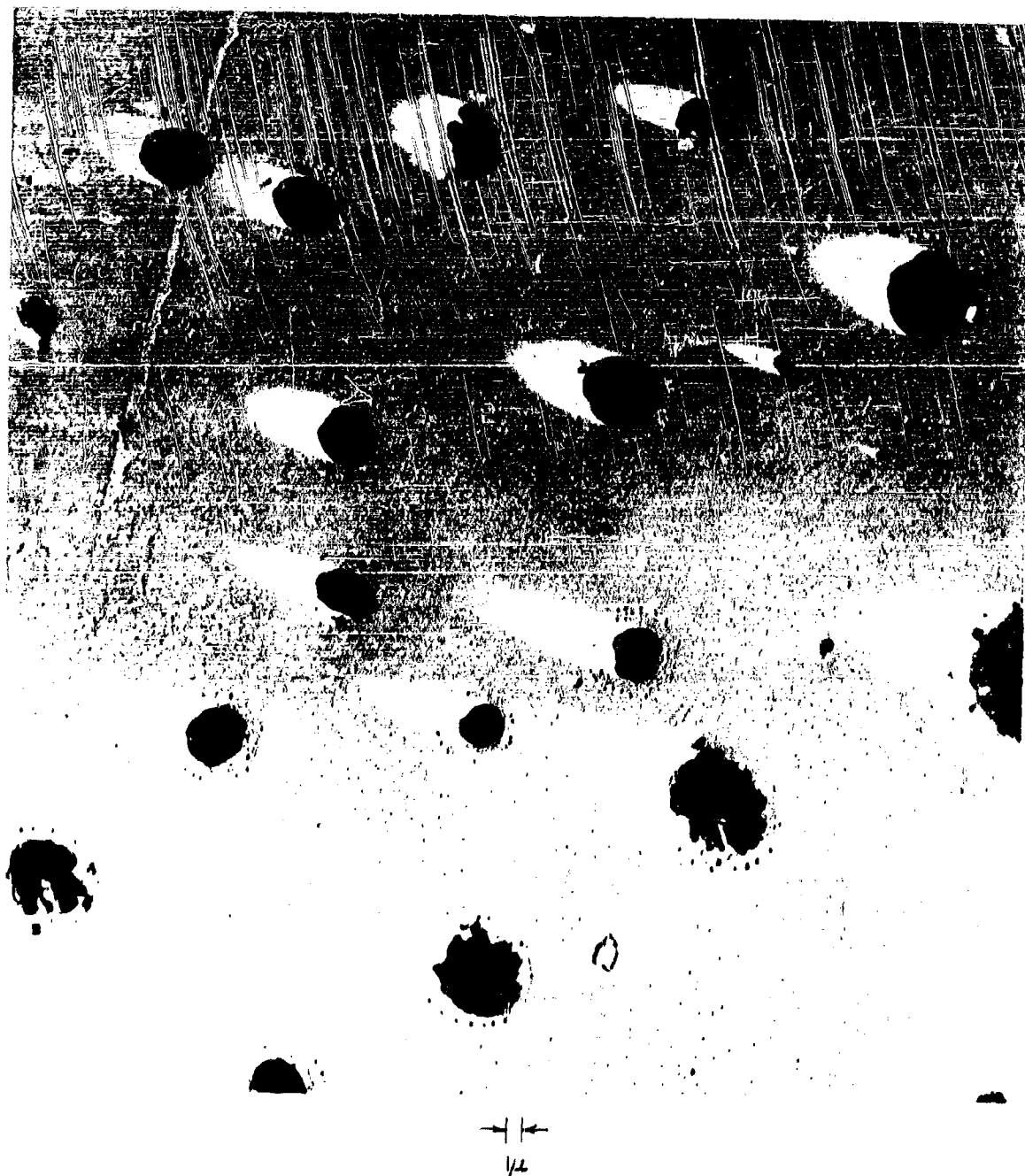


Fig. 4. 12. Electron Micrograph of Strato-
spheric Particles Shadow Cast
At An Angle of 10°

Though the assumption of particles of equal thickness may be rather crude, it will be seen (Table 4.7) that when the corrected distributions are re-expressed in terms of the original class intervals (by a graphical process), the results appear consistent with the other samples.

We now return to our consideration of the method employed for determining the factor $1/\eta$ in Table 4.6. The samples were divided into four categories:

1. seven samples whose mean collection altitudes were near 65,000 feet: sample numbers W-7, W-8, W-10, W-12, W-14, W-16, and W-17.
2. two samples collected at mean altitudes near 67,000 feet: W-3 and W-13.
3. seven samples collected at mean altitudes below 65,000 feet: W-1, W-2, W-5, W-6, W-7, W-11, and W-15.
4. all other samples not listed in the above categories. The particles in these samples could not be classified because of excess condensation or contamination from tropospheric sources.

For the seven samples listed in (1) above the spatial average of the "observed" particle size - concentration distribution, \bar{v}_i vs r , was computed and is shown in curve A of Figure 4.13. For values of r greater than or equal to 0.158 micron the values of $1/\eta$ were those taken from the appropriate columns in Table 4.5. These values were applied to give curve B of Figure 4.13 and \bar{N} in Table 4.6. For $r = 0.100$ micron, the value of $1/\eta$ was obtained by extrapolation of curve B (dashed portion). The ratio of the ordinate of curve B to that of curve A at $r = 0.100$ micron is the value used (135) for $1/\eta$ in Table 4.6. For the samples in category (2), the values of $1/\eta$ were obtained by interpolation in Table 4.5 for all values of r . Thus no extrapolation was necessary.

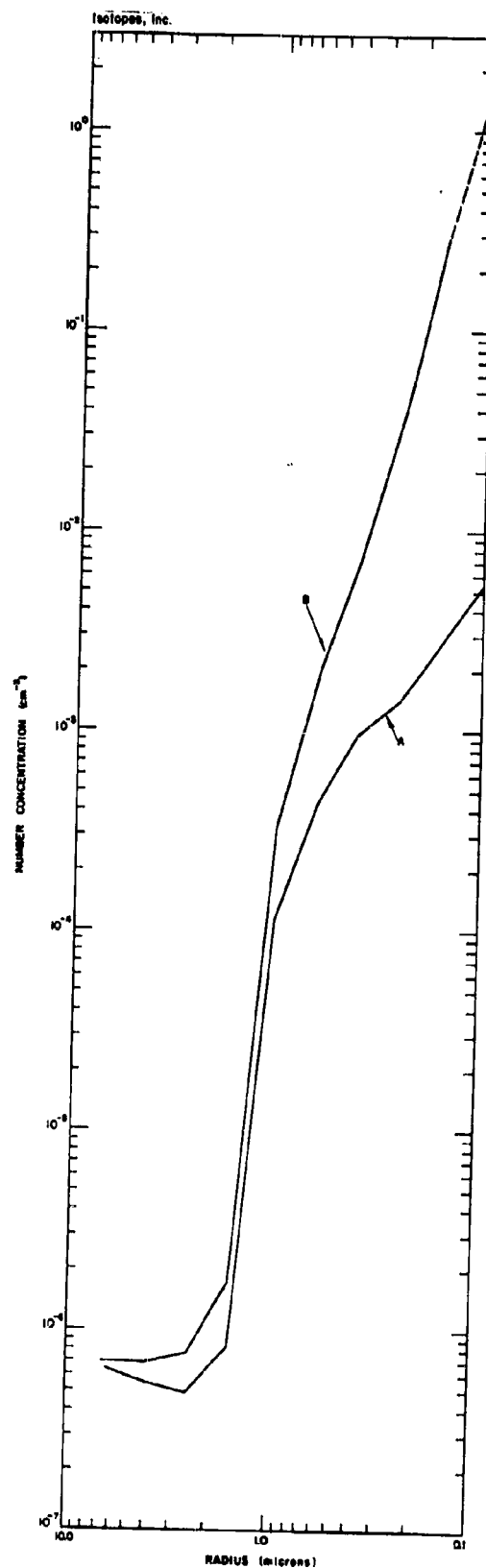


FIG. 4J3 PARTICLE SIZE - CONCENTRATION DISTRIBUTION

For samples in category (3) it was felt that the extrapolation procedure was probably less valid than for (1) and (2). Therefore, the values of \bar{N} were computed from values of $1/\eta$ taken from Table 4.5 for particles with radii greater than 0.158 micron or 0.251 micron depending on the altitude. The entries of dashes in Table 4.6 indicate the values of the radii for which \bar{N} was not obtained.

Table 4.7 summarizes the particle radius-concentration distributions for all of the samples from which suitable data were obtained. The spatial average radius-concentration distribution was obtained by multiplying the values of \bar{N} in a particular class by the corresponding volumetric (volume of sampled air) weight factor, summing these products over all of the samples, and dividing the sum by the sum of the weight factors. As in Table 4.6 the dashes denote undetermined values of \bar{N} . The spatial average volume-concentration distribution was calculated from the radius-concentration distribution by multiplication of the average \bar{N} values by $4/3\pi r^3$. Summation of the average \bar{N} over the classes gives

$$\sum_i \bar{N} = 1.10 \text{ particles/cm}^3$$

for the spatial average number concentration of the stratospheric aerosol.

Similarly, the spatial average volume concentration is

$$\sum_i \bar{V} = 9.62 \times 10^{-3} \mu^3/\text{cm}^3 = 9.62 \times 10^{-15} \text{ cm}^3/\text{cm}^3.$$

d. Particle Size-Type Relations

As has been mentioned, most of the particles observed are of the types which were identified as ammonium sulfate and ammonium persulfate. These particles comprised more than 99% of the particles with radii less than or equal to

Table 4.6 Stratospheric Particle Distributions

Sample No.: 11L07/W-1

Date of Collection: 25 Feb 1960

Latitude	Longitude	Altitude (feet)	IAS (knots)	Temp.	TAS (knots)	Time (min)
27:42 N/13:42 N	98:07 W/82:47 W	60,000	135	-73°C	400	181
13:42 N/27:42 N	82:47 W/98:07 W	65,000	121	-67°C	410	186

Length of Flight Path: 4.60×10^8 cmNormalized Area: $1.69 \times 10^{-4} \text{cm}^2$ Normalized Volume: $7.77 \times 10^4 \text{cm}^3$

Radius (μ)	$\frac{1}{\eta}$	Obs. Frequency	$\frac{f_{\text{obs}} \times 10^5}{\text{Vol.}}$	\bar{N}	\bar{V}
6.31					
3.98					
2.51					
1.58	1.83	5.39^{-3}	6.94^{-3}	1.27^{-7}	2.10^{-6}
1.00	2.40	1.08^{-2}	1.59^{-2}	3.34^{-7}	1.40^{-6}
0.631	3.44	6.57	8.46	2.91^{-4}	3.06^{-4}
0.398	5.21	39.3	50.6	2.63^{-3}	6.94^{-4}
0.251	11.6	126	162	1.88^{-2}	1.24^{-3}
0.158	41.6	369	475	1.98^{-1}	3.26^{-3}
0.100	--	328	422	--	--

Number Conc:

Volume Conc.:

 Sr^{90} Conc.: 2.23×10^{-7} dpm/cm³

Sample No.: 1M07/W-2

Date of Collection: 3 Mar 1960

Latitude	Longitude	Altitude (feet)	IAS (knots)	Temp.	TAS (knots)	Time (min)
71:00N/51:17N	132:30W/102:31W	60,000	135	220°K	419	205

Length of Flight Path: 2.65×10^8 cmNormalized Area: $2.25 \times 10^{-4} \text{cm}^2$ Normalized Volume: $5.97 \times 10^4 \text{cm}^3$

Radius (μ)	$\frac{1}{\eta}$	Obs. Frequency	$\frac{f_{\text{obs}} \times 10^5}{\text{Vol.}}$	\bar{N}	\bar{V}
6.31	1.09	1.43^{-2}	2.40^{-2}	2.61^{-7}	2.74^{-4}
3.98	1.18	1.91^{-2}	3.20^{-2}	3.78^{-7}	1.00^{-4}
2.51	1.40	2.39^{-2}	4.00^{-2}	5.60^{-7}	3.70^{-5}
1.58	1.86	4.29^{-2}	7.19^{-2}	1.34^{-6}	2.21^{-5}
1.00	2.55	2.89^{-2}	4.84^{-2}	1.24^{-6}	5.18^{-6}
0.631	3.62	4.30^{-2}	7.20^{-2}	2.64^{-6}	2.77^{-6}
0.398	5.68	14.6	24.5	1.39^{-3}	3.67^{-4}
0.251	15.2	39.4	66.0	1.00^{-2}	6.66^{-4}
0.158	62.5	281	471	2.94^{-1}	4.86^{-3}
0.100	--	289	484	--	--

Number Conc:

Volume Conc.:

 Sr^{90} Conc.:

Composition: Ammonium Sulfate

Table 4.6 (continued)

Sample No.: 1L09/W-3

Date of Collection: 16 Mar 1960

Latitude	Longitude	Altitude (feet)	IAS (knots)	Temp.	TAS (knots)	Time (min)
25:15N/12:33N	95:03W/81:42W	65,000/66,800		-63°C	415	180
12:33N/27:44N	81:42W/98:07W	66,800/68,500		-63°C	415	177

Length of Flight Path: 4.52×10^8 cmNormalized Area: 2.25×10^{-4} cm²Normalized Volume: 1.02×10^5 cm³

Radius (μ)	$\frac{1}{\eta}$	Obs. Frequency	$\frac{f_{obs} \times 10^5}{Vol.}$	\bar{N}	\bar{V}
6.31	1.08			--	--
3.98	1.16			--	--
2.51	1.32			--	--
1.58	1.68	2.16^{-2}	2.12^{-2}	3.56^{-7}	5.88^{-6}
1.00	2.20	2.40	2.35	5.17^{-5}	2.17^{-4}
0.631	2.93	17.0	16.7	4.90^{-4}	5.15^{-4}
0.398	4.12	89.0	87.3	3.60^{-3}	9.52^{-4}
0.251	6.64	387	379	2.51^{-2}	1.67^{-3}
0.158	17.9	1210	1186	2.12^{-1}	3.50^{-3}
0.100	62.5	2180	2137	1.33^0	5.58^{-3}

Number Conc: 1.57 cm⁻³Volume Conc.: 1.24×10^{-2} μ^3 /cm³Sr⁹⁰ Conc.: 3.61×10^{-7} dpm/cm³

Sample No.: 1L11/W-4

Date of Collection: 22 Mar 1960

Latitude	Longitude	Altitude (feet)	IAS (knots)	Temp.	TAS (knots)	Time (min)
27:43N/48:00N	98:07W	50,000	160	210°K	385	208
48:00N/27:43N	98:07W	55,000	150	210°K	405	176

Length of Flight Path: 4.68×10^8 cmNormalized Area: 1.976 cm²Normalized Volume: 9.24×10^4 cm³

Radius (μ)	$\frac{1}{\eta}$	Obs. Frequency	$\frac{f_{obs} \times 10^5}{Vol.}$	\bar{N}	\bar{V}
0.631					
0.398		23.6	25.5		
0.251	--	33.2	35.9		
0.158	--	153	166		
0.100	--	292	316		

Number Conc:

Volume Conc.:

Sr⁹⁰ Conc.: 1.42×10^{-7} dpm/cm³

Composition: Ammonium Sulfate

Table 4.6 (continued)

Sample No.: 1 M03/W-5

Date of Collection: 29 Mar 1960

Latitude	Longitude	Altitude (feet)	IAS (knots)	Temp.	TAS (knots)	Time (min)
Orbit 43:11N	95.25W	40,000	170	-56°C	335	60
Orbit 43:11N	95.25W	55,000/65,000	155-121	-58°C	420	319

Length of Flight Path: 4.78×10^8 cmNormalized Area: 2.25×10^{-4} cm²Normalized Volume: 1.08×10^5 cm³

Radius (μ)	$\frac{1}{\eta}$	Obs. Frequency	$\frac{f_{obs} \times 10^5}{Vol.}$	\bar{N}	\bar{V}
6.31	1.09			--	--
3.98	1.18	7.15 ⁻³	6.62 ⁻³	7.82 ⁻⁸	2.07 ⁻⁵
2.51	1.40	5.68 ⁻³	5.26 ⁻³	7.36 ⁻⁸	4.88 ⁻⁶
1.58	1.86	1.02 ⁻²	9.44 ⁻³	1.75 ⁻⁷	2.90 ⁻⁶
1.00	2.55	1.43 ⁻²	1.32 ⁻²	3.37 ⁻⁷	1.41 ⁻⁶
0.631	3.62	2.86 ⁻²	2.65 ⁻²	9.69 ⁻⁷	1.02 ⁻⁶
0.531	4.10	2.09 ⁻¹	1.94 ⁻¹	7.96 ⁻⁶	4.99 ⁻⁶
0.391	5.60	2	1.85	1.04 ⁻⁴	2.60 ⁻⁵
0.287	10.7	19	17.6	1.88 ⁻³	1.86 ⁻⁴
0.214	23.7	30	27.8	6.59 ⁻³	2.70 ⁻⁴
0.158	62.5	29	26.9	1.68 ⁻²	2.78 ⁻⁴
0.100	--	381	353	--	--

Number Conc:

Volume Conc.:

Sr⁹⁰ Conc.: 4.92×10^{-7} dpm/cm³

Sample No.: 1M05/W-6

Date of Collection: 31 Mar 1960

Latitude	Longitude	Altitude (feet)	IAS (knots)	Temp.	TAS (knots)	Time (min)
Orbit 43:00N	97:00W	55,000/64,000	151-125	-60°C	415	406

Length of Flight Path: 5.58×10^8 cmNormalized Area: 2.25×10^{-4} cm²Normalized Volume: 1.26×10^5 cm³

Radius (μ)	$\frac{1}{\eta}$	Obs. Frequency	$\frac{f_{obs} \times 10^5}{Vol.}$	\bar{N}	\bar{V}
6.31	1.09	2.15 ⁻²	1.70 ⁻²	1.86 ⁻⁷	1.96 ⁻⁴
3.98	1.18	1.43 ⁻²	1.13 ⁻²	1.33 ⁻⁷	3.51 ⁻⁵
2.51	1.40	6.45 ⁻²	5.12 ⁻²	7.17 ⁻⁷	4.75 ⁻⁵
1.58	1.86	5.02 ⁻²	3.98 ⁻²	7.41 ⁻⁷	1.22 ⁻⁵
1.00	2.55	5.74 ⁻²	4.56 ⁻²	1.16 ⁻⁶	4.86 ⁻⁶
0.631	3.62	3.59 ⁻²	2.85 ⁻²	1.05 ⁻⁶	1.10 ⁻⁶
0.531	4.10	16.4	13.0	5.33 ⁻⁴	3.34 ⁻⁴
0.391	5.60	71.3	56.6	3.17 ⁻³	7.91 ⁻⁴
0.287	10.7	78	61.9	6.61 ⁻³	6.56 ⁻⁴
0.214	23.7	60	47.6	1.13 ⁻²	4.64 ⁻⁴
0.158	62.5	105	83.3	5.21 ⁻²	8.60 ⁻⁴
0.100	--	350	278	--	--

Number Conc:

Volume Conc.:

Sr⁹⁰ Conc.: 4.24×10^{-7} dpm/cm³

Table 4.6 (continued)

Sample No.: 1L03/W-7

Date of Collection: 2 April 1960

Latitude	Longitude	Altitude (feet)	IAS (knots)	Temp.	TAS (knots)	Time (min)
29:23N/18:30N	98:15W/67:10W	65,000	121	-62°C	414	290

Length of Flight Path: 3.71×10^8 cmNormalized Area: 1.81×10^{-4} cm²Normalized Volume: 6.72×10^4 cm³

Radius (μ)	$\frac{1}{\eta}$	Obs. Frequency	$\frac{f_{obs} \times 10^5}{Vol.}$	\bar{N}	\bar{V}
6.31	1.09	---	---	--	--
3.98	1.17	---	---	--	--
2.51	1.37	---	---	--	--
1.58	1.80	2.88 ⁻²	4.29 ⁻²	7.72 ⁻⁷	1.28 ⁻⁵
1.00	2.38	6.90 ⁻²	1.03 ⁻¹	2.45 ⁻⁶	1.03 ⁻⁵
0.631	3.27	3.16 ⁻¹	4.70 ⁻¹	1.54 ⁻⁵	1.62 ⁻⁵
0.398	4.83	86.3	128	6.18 ⁻³	1.63 ⁻³
0.251	9.43	127	189	1.78 ⁻²	1.18 ⁻³
0.158	31.3	229	341	1.07 ⁻¹	1.76 ⁻³
0.100	135	350	521	7.03 ⁻¹	2.94 ⁻³

Number Conc: 0.834 cm⁻³Volume Conc.: 7.55×10^{-3} μ³/cm³Sr⁹⁰ Conc.:

Composition: Ammonium Sulfate

Sample No.: 1L05/W-8

Date of Collection: 5 Apr 1960

Latitude	Longitude	Altitude (feet)	IAS (knots)	Temp.	TAS (knots)	Time (min)
15:00N/08:00S	67:00W	64,500/67,100	122-114	-64°C	415	206
08:00S/15:00N	67:00W	67,100/68,900	114-110	-64°C	415	195

Length of Flight Path: 5.13×10^8 cmNormalized Area: 2.09×10^{-4} cm²Normalized Volume: 1.07×10^5 cm³

Radius (μ)	$\frac{1}{\eta}$	Obs. Frequency	$\frac{f_{obs} \times 10^5}{Vol.}$	\bar{N}	\bar{V}
3.98	1.17	---	---	--	--
2.51	1.37	8.95 ⁻³	8.36 ⁻³	1.14 ⁻⁷	7.58 ⁻⁶
1.58	1.80	1.78 ⁻²	1.66 ⁻²	2.99 ⁻⁷	4.94 ⁻⁶
1.00	2.38	30.6	28.6	6.81 ⁻⁴	2.85 ⁻³
0.631	3.27	75.3	70.4	2.30 ⁻³	2.42 ⁻³
0.398	4.83	95.2	89.0	4.30 ⁻³	1.13 ⁻³
0.251	9.43	96.5	90.2	8.51 ⁻³	6.56 ⁻⁴
0.158	31.3	209	195	6.10 ⁻²	1.01 ⁻³
0.100	135	679	634	8.58 ⁻¹	3.59 ⁻³

Number Conc: 0.935 cm⁻³Volume Conc.: 1.17×10^{-2} μ³/cm³Sr⁹⁰ Conc.: 2.70×10^{-7} dpm/cm³

Composition: Ammonium Sulfate

Table 4.6 (continued)

Sample No.: 1 M09/W-9

Date of Collection: 12 Apr 1960

Latitude	Longitude	Altitude (feet)	IAS (knots)	Temp.	TAS (knots)	Time (min)
67:00N/50:25N	122:10W/102:30W	40,500	170	-48°C	343	171

Length of Flight Path: 1.81×10^8 cmNormalized Area: 2.25×10^{-4} cm²Normalized Volume: 4.07×10^4 cm³

Radius (μ)	$\frac{1}{\eta}$	Obs. Frequency	$\frac{f_{obs} \times 10^5}{Vol.}$	\bar{N}	\bar{V}
2.51	1.49	7.17^{-3}	1.76^{-2}	2.62^{-7}	
1.58	2.07	---		0	
1.00	3.06	2.87^{-2}	7.05^{-2}	2.16^{-6}	
0.631	5.29	2.87^{-2}	7.05^{-2}	3.73^{-6}	
0.531	--	14	34.4		
0.391	--	74	182		
0.287	--	94	231		
0.214	--	39	95.8		
0.158	--	61	150		
0.100	--	146	359		

Number Conc:

Volume Conc.:

Sr⁹⁰ Conc.: 3.84×10^{-7} dpm/cm³

Sample No.: 1 M11/W-10

Date of Collection: 21 Apr 60

Latitude	Longitude	Altitude (feet)	IAS (knots)	Temp.	TAS (knots)	Time (min)
Orbit 48:00N	103:00W	65,000	121	-54°C	419	210

Length of Flight Path: 2.70×10^8 cmNormalized Area: 2.25×10^{-4} Normalized Volume: 6.08×10^4 cm³

Radius (μ)	$\frac{1}{\eta}$	Obs. Frequency	$\frac{f_{obs} \times 10^5}{Vol.}$	\bar{N}	\bar{V}
3.98	1.17	1.43^{-2}	2.35^{-2}	2.75^{-7}	7.26^{-5}
2.51	1.37			--	--
1.58	1.80			--	--
1.00	2.38	8.80	14.5	3.45^{-4}	1.44^{-3}
0.631	3.27	96.7	159	5.20^{-3}	5.47^{-3}
0.398	4.83	143	235	1.13^{-2}	3.00^{-3}
0.251	9.43	309	508	4.78^{-2}	3.16^{-3}
0.158	31.3	911	1499	4.70^{-1}	7.76^{-3}
0.100	135	1365	2245	3.03^0	1.27^{-2}

Number Conc: 3.56 cm⁻³Volume Conc.: 3.36×10^{-2} μ^3 /cm³Sr⁹⁰ Conc.: 6.17×10^{-7} dpm/cm³

Composition: Ammonium Sulfate

Table 4.6 (continued)

Sample No.: 3 L01/W-11

Date of Collection: 21 Apr 1960

Latitude	Longitude	Altitude (feet)	IAS (knots)	Temp.	TAS (knots)	Time (min)
27:43N/48:00N	98:07W	50,000	160	216 °K	392	185
48:00N/27:43N	98:07W	55,000	155	216 °K	421	171

Length of Flight Path: 4.46×10^3 cmNormalized Area: 2.25×10^{-4} cm²Normalized Volume: 1.00×10^5 cm³

Radius (μ)	$\frac{1}{\eta}$	Obs. Frequency	$\frac{f_{obs} \times 10^5}{Vol.}$	\bar{N}	\bar{V}
6.31	1.09	---	---	0	
3.98	1.19	1.60 ⁻¹	1.60 ⁻⁶	1.90 ⁻⁶	
2.51	1.45	3.26 ⁻¹	3.26 ⁻⁶	4.73 ⁻⁶	
1.58	1.96	4.89 ⁻¹	4.89 ⁻⁶	9.58 ⁻⁶	
1.00	2.72	3.35	3.35 ⁻⁵	9.11 ⁻⁵	
0.631	4.20	12.0	1.20 ⁻⁴	5.04 ⁻⁴	
0.398	8.13	21.9	2.19 ⁻⁴	1.78 ⁻³	

Number Conc:

Volume Conc.:

Sr⁹⁰ Conc.:

Composition: Ammonium Sulfate

Sample No.: 1 M01/W-12

Date of Collection: 30 Apr 1960

Latitude	Longitude	Altitude (feet)	IAS (knots)	Temp.	TAS (knots)	Time (min)
65:50N/50:20N	119:50W/102:30W	65,000	124	219 °K	431	147

Length of Flight Path: 1.957×10^8 cmNormalized Area: 1.498 cm²Normalized Volume: 2.93×10^4 cm³

Radius (μ)	$\frac{1}{\eta}$	Obs. Frequency	$\frac{f_{obs} \times 10^5}{Vol.}$	\bar{N}	\bar{V}
1.00	2.38				
0.631	3.27	4 + 4	13.6	4.45 ⁻⁴	4.67 ⁻⁴
0.398	4.83	29	99.0	4.79 ⁻³	1.26 ⁻³
0.251	9.43	41	140	1.32 ⁻²	8.72 ⁻⁴
0.158	31.3	144	491	1.53 ⁻¹	2.54 ⁻³
0.100	135	222	758	1.02 ⁰	4.29 ⁻³

Number Conc: 1.19 cm^{-3} Volume Conc.: $9.43 \times 10^{-3} \mu^3/\text{cm}^3$ Sr⁹⁰ Conc.: $5.02 \times 10^{-7} \text{ dpm}/\text{cm}^3$

Composition: Ammonium Sulfate

Table 4.6 (continued)

Sample No.: 2 L 11/W-13

Date of Collection: 9 May 1960

Latitude	Longitude	Altitude (feet)	IAS (knots)	Temp.	TAS (knots)	Time (min)
15:00N/09:25N	67:00W	64,400/65,400	120	206 °K	407	50
09:25N/03:37N	67:00W	65,500/66,400	118	206 °K	411	51
03:37N/06:41S	67:00W	66,400/68,000	115-113	205 °K	410	99
06:41S/09:11N	67:00W	68,000/70,000	111-106	209 °K	412	141
09:11N/15:00N	67:00W	70,000	105	209 °K	410	45

Length of Flight Path: 4.89×10^8 cmNormalized Area: 6.50×10^{-5} cm²Normalized Volume: 3.18×10^4 cm³

Radius (μ)	$\frac{1}{\eta}$	Obs. Frequency	$\frac{f_{obs} \times 10^5}{Vol.}$	\bar{N}	\bar{V}
6.31	1.08	2.06 ⁻³	6.48 ⁻³	7.00 ⁻⁸	7.36 ⁻⁵
3.98	1.16	6.20 ⁻³	1.95 ⁻²	2.26 ⁻⁷	5.97 ⁻⁵
2.51	1.32	2.07 ⁻³	6.51 ⁻³	8.59 ⁻⁸	5.69 ⁻⁶
1.58	1.68	4.15 ⁻³	1.31 ⁻²	2.20 ⁻⁷	3.63 ⁻⁶
1.00	2.20	1.03 ⁻²	3.24 ⁻²	7.13 ⁻⁷	2.99 ⁻⁶
0.631	2.93	3.30 ⁻²	1.04 ⁻¹	3.05 ⁻⁶	3.21 ⁻⁶
0.398	4.12	24.5	77.0	3.17 ⁻³	8.37 ⁻⁴
0.251	6.64	98	308	2.05 ⁻²	1.36 ⁻³
0.158	17.9	272	855	1.53 ⁻¹	2.53 ⁻³
0.100	62.5	630	1980	1.24 ⁰	5.19 ⁻³

Number Conc: 1.42 cm^{-3} Volume Conc.: $1.01 \times 10^{-2} \mu^3/\text{cm}^3$ Sr⁹⁰ Conc.: $3.03 \times 10^{-7} \text{ dpm}/\text{cm}^3$

Composition: Ammonium Sulfate and Ammonium Persulfate

Sample No.: 2 M03/W-14

Date of Collection: 12 May 1960

Latitude	Longitude	Altitude (feet)	IAS (knots)	Temp.	TAS (knots)	Time (min)
16:25N/35:00S	66:50W/58:30W	63,000/67,000	127-115	210 °C	---	442

Length of Flight Path: 5.66×10^8 cmNormalized Area: 2.25×10^{-4} cm²Normalized Volume: 1.27×10^5 cm³

Radius (μ)	$\frac{1}{\eta}$	Obs. Frequency	$\frac{f_{obs} \times 10^5}{Vol.}$	\bar{N}	\bar{V}
3.98	1.17	5.72 ⁻²	4.50 ⁻²	5.27 ⁻⁷	1.39 ⁻⁴
2.51	1.37	1.44 ⁻²	1.13 ⁻²	1.54 ⁻⁷	1.02 ⁻⁵
1.58	1.80	1.00 ⁻¹	7.87 ⁻²	1.41 ⁻⁶	2.34 ⁻⁵
1.00	2.38	19.9	15.7	3.74 ⁻⁴	1.57 ⁻³
0.631	3.27	139	102	3.33 ⁻³	3.51 ⁻³
0.398	4.83	185	146	7.04 ⁻³	1.86 ⁻³
0.251	9.43	198	156	1.47 ⁻²	9.74 ⁻⁴
0.158	31.3	505	398	1.25 ⁻¹	2.06 ⁻³
0.100	135	672	529	7.13 ⁻¹	2.99 ⁻³

Number Conc: 0.863 cm^{-3} Volume Conc.: $1.31 \times 10^{-2} \mu^3/\text{cm}^3$ Sr⁹⁰ Conc.: $2.84 \times 10^{-7} \text{ dpm}/\text{cm}^3$

Composition: Ammonium Persulfate

Table 4.6 (continued)

Sample No.: 2 L03/W-15

Date of Collection: 19 May 1960

Latitude	Longitude	Altitude (feet)	IAS (knots)	Temp.	TAS (knots)	Time (min)
36:40S/45:00S	59:45W/62:25W	50,000	160	-30 °C	415	193
45:00S/36:40S	62:25W/59:45W	50,000	160	-30 °C	415	184

Length of Flight Path: 4.83×10^8 cmNormalized Area: 2.25×10^{-4} cm²Normalized Volume: 1.09×10^5 cm³

Radius (μ)	$\frac{1}{\eta}$	Obs. Frequency	$\frac{f_{obs} \times 10^5}{Vol.}$	\bar{N}	\bar{V}
6.31	1.09	9.56^{-3}	8.77^{-3}	9.56^{-8}	1.01^{-5}
3.98	1.18	1.43^{-2}	1.31^{-2}	1.54^{-7}	4.07^{-5}
2.51	1.41	2.39^{-2}	2.19^{-2}	3.09^{-7}	2.04^{-5}
1.58	1.89	2.87^{-2}	2.63^{-2}	4.97^{-7}	8.22^{-6}
1.00	2.69	4.30^{-2}	3.94^{-2}	1.06^{-6}	4.45^{-6}
0.631	4.15	1.20^{-1}	1.10^{-1}	4.57^{-6}	4.81^{-6}
0.531	4.93	2.64	2.42	1.19^{-4}	7.42^{-5}
0.391	7.15	19.3	17.7	1.27^{-3}	3.18^{-4}
0.287	--	14.9	13.7	--	--
0.214	--	16.7	15.3	--	--
0.158	--	53.6	49.2	--	--
0.100	--	146	134	--	--

Number Conc:

Volume Conc.:

Sr⁹⁰ Conc.: 2.71×10^{-7} dpm/cm³

Composition: Ammonium Sulfate

Sample No.: 208/W-16

Date of Collection: 17 Nov 1960

Latitude	Longitude	Altitude (feet)	IAS (knots)	Temp.	TAS (knots)	Time (min)
62:00N/32:00N	142:00W/101:00W	60,000/68,600			415	341

Length of Flight Path: 4.37×10^8 cmNormalized Area: 1.99×10^{-4} cm²Normalized Volume: 8.69×10^4 cm³

Radius (μ)	$\frac{1}{\eta}$	Obs. Frequency	$\frac{f_{obs} \times 10^5}{Vol.}$	\bar{N}	\bar{V}
6.31	1.09			--	--
3.98	1.17	6.31^{-3}	7.26^{-3}	8.50^{-8}	2.25^{-5}
2.51	1.37	6.31^{-3}	7.26^{-3}	9.95^{-8}	6.59^{-6}
1.58	1.80			(3.00^{-6})	(4.95^{-5})
1.00	2.38	3.15^{-2}	3.62^{-2}	8.59^{-7}	3.60^{-6}
0.631	3.27	7.57^{-2}	8.71^{-2}	2.85^{-6}	3.00^{-6}
0.531	3.71	28	32.2	1.20^{-3}	7.53^{-4}
0.391	4.93	90	103	5.08^{-3}	1.27^{-3}
0.287	7.50	120	138	1.03^{-2}	1.02^{-3}
0.214	13.5	89	102	1.38^{-2}	5.65^{-4}
0.158	31.3	50	57.5	1.80^{-2}	2.97^{-4}
0.100	135	31	35.7	4.82^{-2}	2.02^{-4}

Number Conc: 0.0966 cm⁻³Volume Conc.: 4.14×10^{-3} μ^3 /cm³Sr⁹⁰ Conc.:

Composition: Ammonium Sulfate

Table 4.6 (continued)

Sample No.: 210/W-17

Date of Collection: 21 Nov 1960

Latitude	Longitude	Altitude (feet)	IAS (knots)	Temp.	TAS (knots)	Time (min)
15:00S/20:00N	178:00W/158:00W	60,000/69,000			415	386

Length of Flight Path: 4.95×10^8 cmNormalized Area: 1.966×10^{-4} cmNormalized Volume: 9.732×10^4 cm³

109

Radius (μ)	$\frac{1}{\eta}$	Obs. Frequency	$\frac{f_{\text{obs}} \times 10^5}{\text{Vol.}}$	\bar{N}	\bar{V}
6.31	1.09	6.24 ⁻²	6.41 ⁻²	6.99 ⁻⁷	7.35 ⁻⁴
3.98	1.17	6.24 ⁻²	6.41 ⁻²	7.51 ⁻⁷	1.98 ⁻⁴
2.51	1.37	1.25 ⁻¹	1.28 ⁻¹	1.75 ⁻⁶	1.16 ⁻⁴
1.58	1.80	1.87 ⁻¹	1.92 ⁻¹	3.45 ⁻⁶	5.71 ⁻⁵
1.00	2.38	7.48 ⁻¹	7.69 ⁻¹	1.83 ⁻⁵	7.67 ⁻⁵
0.631	3.27	1.25	1.28	4.18 ⁻⁵	4.40 ⁻⁵
0.531	3.70	7	7.19	2.67 ⁻⁴	1.68 ⁻⁴
0.391	4.43	23	23.6	1.16 ⁻³	2.91 ⁻⁴
0.287	7.45	120	123	9.23 ⁻³	9.15 ⁻⁴
0.214	13.5	140	144	1.94 ⁻²	7.98 ⁻⁴
0.158	31.3	165	170	5.32 ⁻²	8.80 ⁻⁴
0.100	135	390	401	5.42 ⁻¹	2.27 ⁻³

Number Conc: 0.625 cm^{-3} Volume Conc.: $6.55 \times 10^{-3} \mu^3/\text{cm}^3$ Sr⁹⁰ Conc.:

Composition: Ammonium Persulfate

one micron. In contrast, the vast majority of particles with radii greater than one micron were of a distinctly different type both in morphology and in their electron diffraction patterns. It was also noted in the cases where condensation had occurred to produce halos around the sulfate and persulfate particles, that there was no such effect associated with these other particles. The occurrence of the larger particles in the samples was rather non-uniform, witness the number of zeros entered in Table 4.7. In all, about 250 particles with radii greater than one micron were observed in the samples reported here. Morphologically, three types of larger particles were most frequently observed. These types are shown in Figure 4.14. The first type of particle is spheroidal with high electron optical density. These spheroids were observed in the c and d positions of the samples with radii between about 0.2μ and 2.5μ . They produced no electron diffraction patterns. The second type of particle is somewhat irregular in shape and ranges in size from about 1μ to about 15μ in the largest dimension. Particles of the second type showed wide variation in shape and electron optical density. A few of these particles gave rather poorly defined electron diffraction patterns (indicating the presence of crystalline material) which could not be analyzed. Most of the particles of this type, however, gave no electron diffraction patterns. Undoubtedly the particles of the second category encompass a variety of compositions. The third type of large particle is actually a collection or agglomerate of many very small spherical particles. The size range of the small spheres is from a few thousandths to a few hundredths of a micron. The particles in the collections appear to have been rather loosely held together to form what resembles

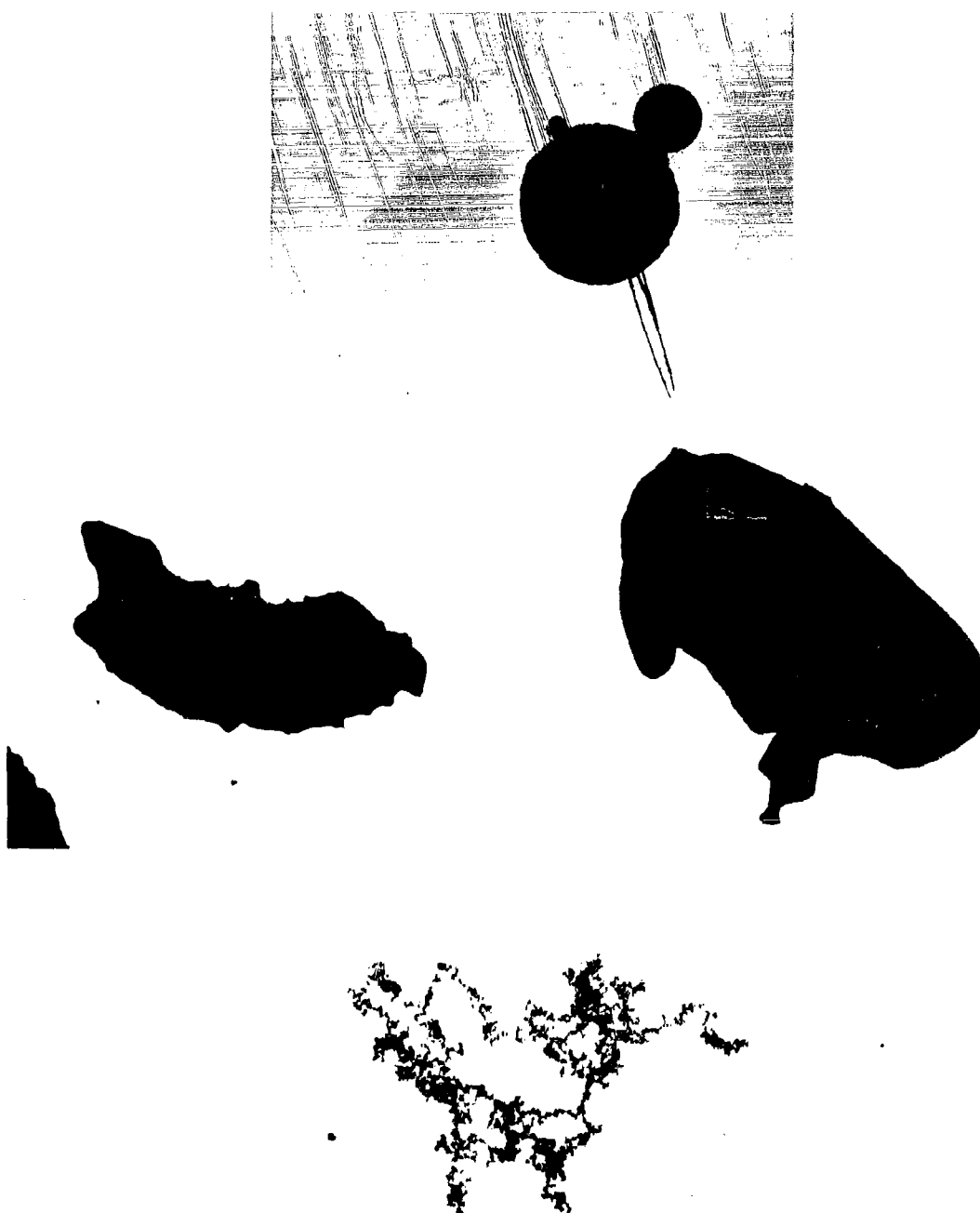


FIG. 4.14 ELECTRON MICROGRAPHS OF NON-SULFATE TYPES OF STRATOSPHERIC PARTICLES

bunches of grapes. The bunches appear to have partially broken apart upon impact. The dimensions of the deposited agglomerates range from about 1 μ to 10 μ . Electron diffraction patterns of some of these particles have been obtained, but no unique identification has been made. Particles of the third type were observed less frequently than those of the other two types. Fewer than fifteen of the 250 large particles were of the third type.

PARTICLE - RADIOACTIVITY RELATIONSHIPS

The autoradiographic studies of filters, portions of filters, microtomed cross sections, individual fibers and impactor samples were performed on HASP samples in an attempt to obtain information which would permit correlation of particle size or type with radioactivity content. In some instances the autoradiography was supplemented by beta counting.

The results of these studies are described below.

Evaluation of Survey Autoradiograms of Filter Paper Samples

Eighty-six filter samples listed in Table 4.8 were examined by survey autoradiography during the course of filter efficiency studies. Twenty-two representative autoradiograms are presented in Figures 4.15 through 4.18 to illustrate the following observations. (Note to the reader: The autoradiograms, as they appear in this report, suffer in fidelity due to the methods of reproduction).

For convenience in comparing the images, data on the location and volume of air sampled and the date and duration of the autoradiographic exposure are listed

Table 4.8. HASP Filters Examined By Survey Autoradiography

90	732	2017	3595	3735
227	751	2025	3596	3749
232	755	2283	3597	3750
299	759	2285	3598	3782
327	910	2436	3599	3783
328	938	2498	3600	3812
329	1012	3394	FD218	3815
330	1035	3401	FD219	3844
403	1306	3473	FD220	3866
404	1354	3479	FD221	3869
405	1355	3480	FD222	3904
406	1383	3502	3601	3905
535	1387	3503	3604	3924
544	1394	3509	3691	3925
557	1699	3538	3696	IPC Blank
608	1815	3553	3698	WE1499 Blank
610	1900	3556	3726	WE1505 Blank
731	1947	3562	3732	

to the right of each image. Radiochemical and radiometric data obtained from the 22 filters are listed in Table 4.9. Caution in interpreting the image patterns is necessary because the size and density of the spot image is a function of the distance between the radioactive particle and the X-ray film as well as of the quantity, type and energy of the radioactive material connected with the particle. The Lantern Slides have approximately one tenth the response of the double coated No-Screen X-ray film with respect to image density.

Quantitative evaluations of the original images are given in Table 4.9 in terms of (1) the diffuse image optical density per 1000 SCF of air sampled and (2) the number of dense spot images per 1000 SCF per 4 cm² of filter. The higher concentrations of dense spot images occurred in samples of fresh debris such as sample 90 containing United Kingdom debris (8 November '57), sample 299 containing Soviet debris (February '58) and 742, 751 and 755 containing Soviet debris (fall '58). Samples of fresh debris collected at different altitudes simultaneously above the northern tropopause gap such as 731, 732 and 751, 755 and 759 produced noticeably different autoradiographic images than the sample collected below the tropopause which produced fewer but somewhat larger spot images. Tropical stratospheric samples 610 and 1035, collected in September 1958 and January 1959, yielded lower concentrations of large spot images than did samples 1306, 1815, 2283 and 2436 which were collected later in 1959 in the tropical stratosphere. Northern polar stratospheric samples collected between 60,000 and 65,000 feet during the summer of 1959, such as 1387, 1947 and 2117, gave higher concentrations of large spot images than did the low altitude sample 1355 or the

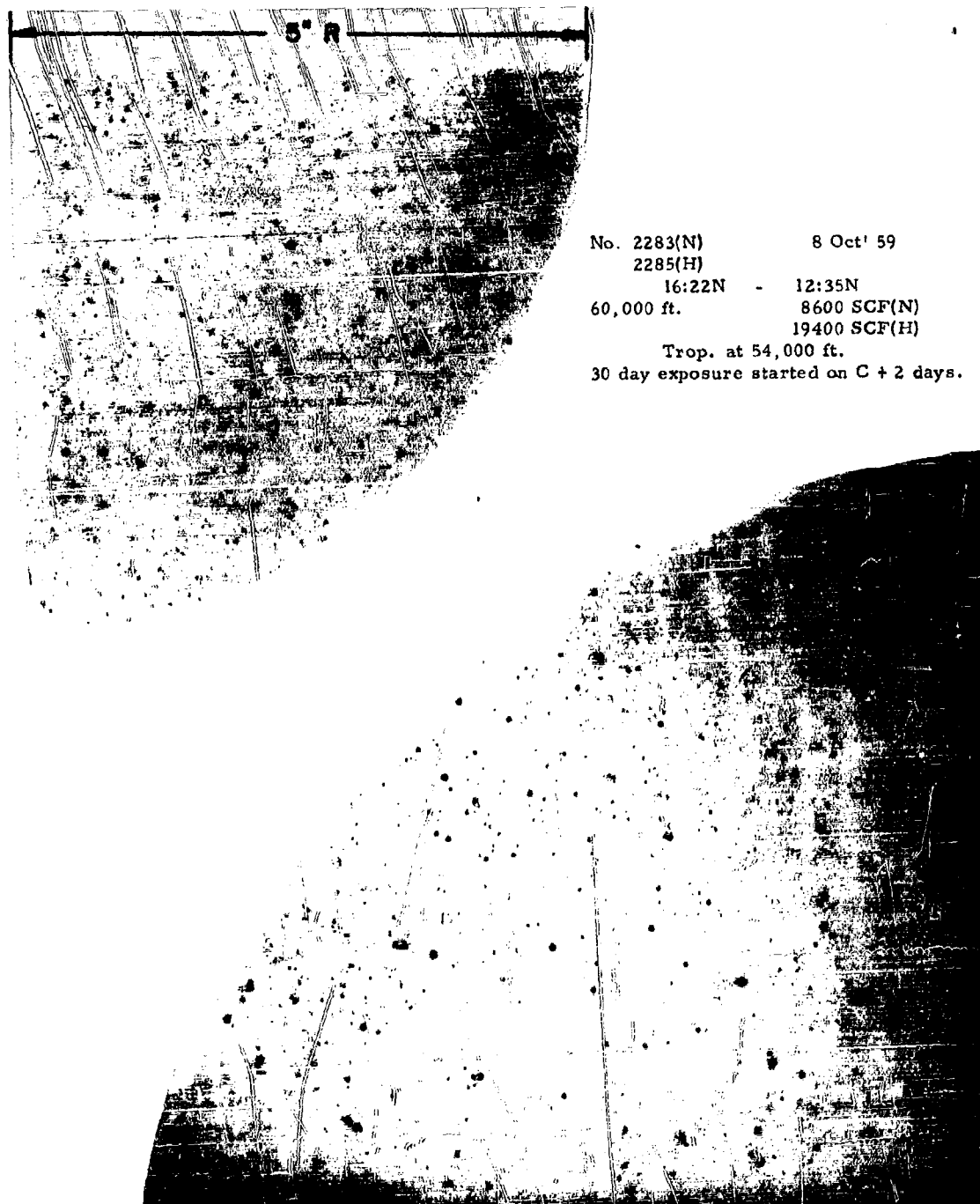
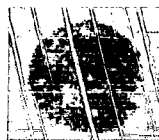


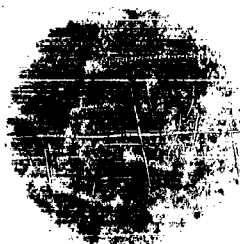
FIG. 4.15 SURVEY AUTORADIOGRAMS OF FILTER PAPERS EXPOSED SIMULTANEOUSLY IN THE TROPICAL STRATOSPHERE



No. 90(H)/22 Nov'57/4:30N-1:05S/
64,000'/7200 SCF/Trop. at
57,000'/13 day exposure started
on C+130 days. (lantern slide)



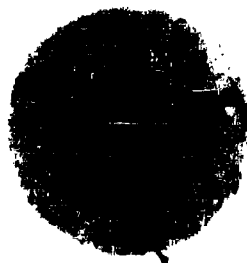
No. 227(N)/7 Feb'58/6:33S-4:13N/
69,000'/9400 SCF/Trop. at
55,000'/13 day exposure started
on C+53 days. (lantern slide)



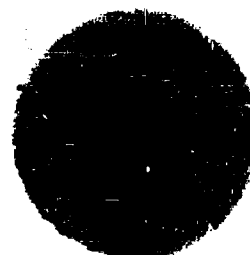
No. 610(N)/16 Sep'58/6:00S-0:41S/
60,000'/8200 SCF/Trop. at
50,000'/30 day exposure started
on C+495 days.



No. 1306(N)/1 Apr'59/10:06N-
15:58N/70,000'/4400 SCF/Trop.
at 53,000'/30 day exposure
started on C+300 days.



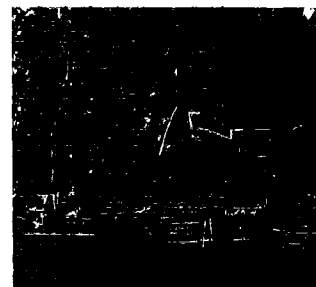
No. 1815(N)/10 Jul'59/4:33N-2:07N
65,000'/8100 SCF/Trop. at
55,000'/30 day exposure started
on C+200 days.



No. 2436(H)/22 Oct'59/9:46N-
15:00N/66,200'/12100 SCF/
Trop. at 55,000'/30 day exposure
started on C+105 days.



No. 3866(N)/12 May'60/4:36N-
6:00S/66,500'/10600 SCF/
Trop. at 54,000'/30 day exposure
started on C+230 days.

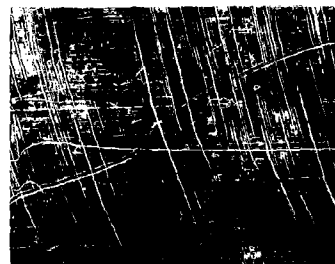


No. 3869(H)/12 May'60/16:25N-
4:50N/64,500'/31900 SCF/
Trop. at 54,000'/136 day
exposure started on C+290 days.

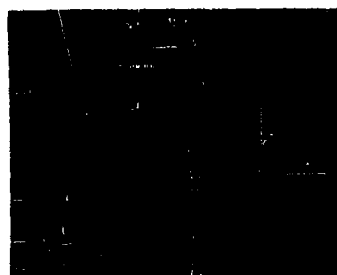
FIG. 4.16 SURVEY AUTORADIOGRAMS OF SAMPLES EXPOSED IN THE TROPICAL STRATOSPHERE



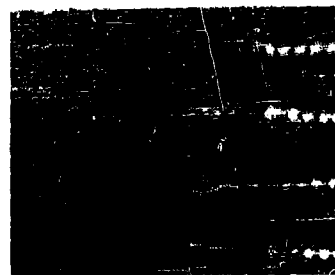
No. 1355(H)/14 Apr'59/65:00N-70:00N/
35,400'/74400 SCF/Trop. at 29,000'/
30 day exposure started on C+190 days.



No. 1387(N)/21 Apr'59/49:35N-54:59N/
60,000'/7500 SCF/Trop. at 30,000'/
15' day exposure started on C+21 days.



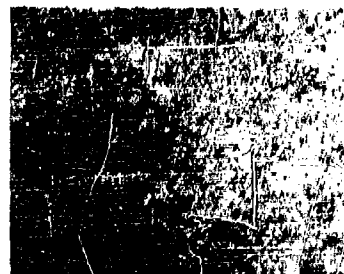
No. 2117(H)/18 Sep'59/65:33N-69:52N/
60,000'/17600 SCF/Trop. at 38,000'/
30 day exposure started on C+21 days.



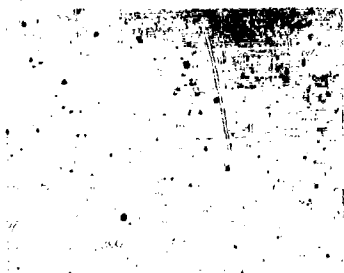
No. 3749(H)/30 Apr'60/65:50N-58:40N/
65,000'/19200 SCF/Trop. below 40,000'/
33 day exposure started on C+270 days.



No. 3750(H)/30 Apr'60/58:30N-50:20N/
65,000'/20980 SCF/Trop. below 40,000'/
120 day exposure started on C+317 days.



No. 3904(H)/24 May'60/66:00N-70:00N/
50,000'/27500 SCF/Trop. at 40,000'/
30 day exposure started on C+30 days.



No. 3924(H)/26 May'60/40:00 ORBIT/
50,000'/33900 SCF/30 day exposure
started on C+30 days.

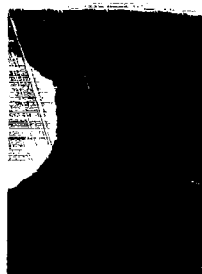
FIG. 4.17 SURVEY AUTORADIOGRAMS OF SAMPLES EXPOSED IN THE
POLAR STRATOSPHERE



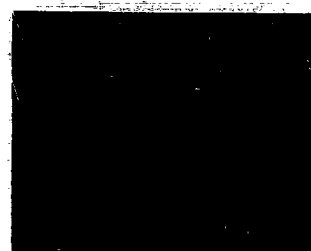
FACE

REAR

No. 299(N)/18 Mar'58/43:29-38:41N/
45,300'/16600 SCF/Trop. at 38,000'/
13 day exposure started on C+13 days.
(lantern slide)



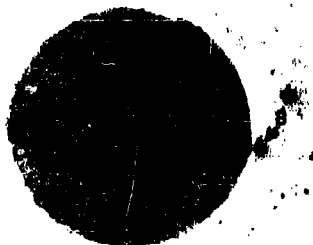
No. 732(N) 22 Oct'58
44:00N ORBIT
60,000 ft. 15600 SCF
Trop. at 53,000 ft.
15 day exposure
started on C + 300
days.



No. 751(N)/29 Oct'58/44:00N-38:10N/
60,000'/8300 SCF/Trop. at 55,000/
30 day exposure started on C+780 days.



No. 731(N) 22 Oct'58
44:00N ORBIT
50,000 ft. 18200 SCF
Trop. at 53,000 ft.
15 day exposure
started on C + 300
days.



No. 755(N) 29 Oct'58
44:00N - 38:10N
55,000 ft. 12100 SCF
Trop. at 55,000 ft.
30 day exposure
started on C + 780
days.



No. 759(N) 29 Oct'58
44:00N - 38:10N
50,000 ft. 15500 ft.
Trop. at 55,000 ft.
30 day exposure
started on C + 780
days
2" disk on C + 330
days.



FIG. 4.18
SURVEY AUTORADIOGRAMS OF SAM-
PLES EXPOSED IN THE VICINITY OF
THE TROPOPAUSE GAP

No. 1035(N) 25 Jan'59
44:00N - 38:26N
60,000 ft. 8500 SCF
Trop at 54,000 ft.
30 day exposure
started on C + 369
days.

No. 1947(N) 26 Jul'59
44:00N - 38:09N
63,500 ft. 8400 SCF
Trop. below 50,000 ft.
30 day exposure
started on C + 180
days.

Table 4. 9. Comparison of Radiochemical and Autoradiographic Data

Sample No. and Type	Collection Date	Mean Lat.	Mean Alt. (feet)	dpm β / SCF (Coll. Date + 10 days)	Date of Autoradio- graphy	Activities on Date of Autoradiography				Autoradiographic Image	
						dpm β SCF	dpm Sr ⁹⁰ 1000 SCF	dpm W ¹⁸⁵ 1000 SCF	dpm Rb ¹⁰² 1000 SCF	Image Density 1000 SCF	No. of Spots / 4 cm ² 1000 SCF
90N	22 Nov '57	2°N	64,000	11,700	1 Apr '58	1,530	2,270	---	---	0.50	83
227N	7 Feb '58	1°S	69,000	380	1 Apr '58	240	1,090	---	---	0.23	19
299N	18 Mar '58	41°N	45,300	560	31 Mar '58	500	370	---	---	0.54	120
610N	16 Sep '58	3°S	60,000	107	24 Jan '60	10	251	213	---	0.035	0.7
731N	22 Oct '58	44°N	50,000	35	18 Aug '59	3.2	39	185	---	0.005	0.5
732N	22 Oct '58	44°N	60,000	1,550	18 Aug '59	93	1,010	357	---	0.127	3.2
751N	29 Oct '58	41°N	60,000	2,900	17 Dec '59	85	1,740	2.1	---	0.135	1.8
755N	29 Oct '58	41°N	55,000	440	17 Dec '59	16	228	4.2	---	0.037	5.0
759N	29 Oct '58	41°N	50,000	38	17 Dec '59	3	114	3.6	---	0.013	0.5
1035N	25 Jan '59	41°N	60,000	49	29 Jan '60	14	262	41	---	0.08	0.7
1306N	1 Apr '59	13°N	70,500	67	25 Jan '60	9.8	400	89	---	0.12	1.8
1355H	14 Apr '59	68°N	35,400	30	21 Oct '59	4.5	128	3.4	---	0.011	0.3
1387N	21 Apr '59	52°N	60,000	~24	12 May '59	~21	~270	---	---	0.075	2.7
1815N	10 Jul '59	1°S	55,000	18	26 Jan '60	10	196	---	---	0.047	1.6
1947N	26 Jul '59	41°N	63,400	15	22 Jan '60	10	208	---	---	0.050	3.1
2117H	18 Sep '59	68°N	60,000	14	9 Oct '59	13	210	29	---	0.013	1.3
2283N	8 Oct '59	14°N	60,000	5.4	10 Oct '59	5.4	70	69	---	0.015	1.2
2285H	8 Oct '59	14°N	60,000	5.9	10 Oct '59	5.9	60	50	---	0.004	0.6
2436H	22 Oct '59	12°N	66,200	12	4 Feb '60	11	188	---	---	0.020	0.8
3749H	30 Apr '60	62°N	65,000	20	25 Jan '61	6.5	194	< 0.2	4.8	0.018	0.1
3750H	30 Apr '60	54°N	65,000	14	13 Mar '61	6.0	176	< 0.2	4.1	0.007	0.1
3866N	12 May '60	1°S	66,500	3.0	28 Dec '60	1.3	95	1.1	---	0.016	0.7
3869H	12 May '60	11°S	64,500	6.2	26 Feb '61	2.2	126	< 0.7	---	0.005	0.4
3904H	24 May '60	68°N	50,000	6.6	23 Jun '60	6.0	119	---	---	0.006	0.3
3924H	26 May '60	40°S	50,000	1.6	25 Jun '60	1.4	40	---	---	0.003	0.6

concurrently collected tropical stratospheric samples. Samples collected during the spring of 1960, such as 3866 and 3869 (tropical stratosphere) and 3904, 3924 (north and south polar stratosphere) yielded low concentrations of spot images. Sample 3749, for the high polar stratosphere failed to produce a large spot image and 3750 produced a small number of them.

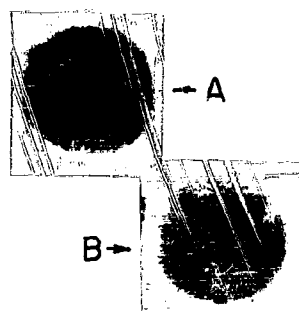
Beta activity values corresponding to large spot images are shown in Figures 4.19 and 4.20. The presence of 4 large particles in sample 731 contributed approximately 14 net counts per minute suggesting an average beta activity per particle somewhere between 12 - 32 disintegrations per minute, depending on counting efficiency, at one year after the collection date of October 1958. Beta counts of thin sections of sample 732, 2 years after the collection date of October 1958, gave net counts of ≤ 2 suggesting particle activities of 10 dpm or less.

The number concentrations of particles which produced large spot images in 22 samples ranged from 0 to 150 particles per 1000 SCF of air sampled. All samples studied which were collected after January 1959 gave results corresponding to less than 0.5 particles per standard cubic foot of air.

Size Measurements of Individual Particles Related to Survey Autoradiograms

Radioactive particles identified by high resolution autoradiography and revealed by subsequent chemical reduction of the spot images are illustrated in Figures 4.21 and 4.22, which include 4 samples of fibers removed from the filter with tweezers and 6 samples of thin sections embedded in plastic.

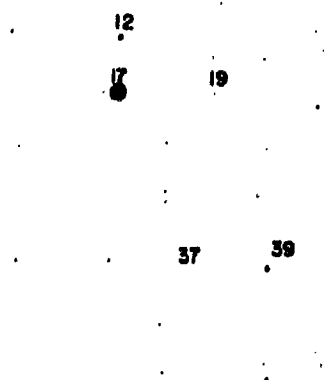
The largest spot images encountered, spot A of sample 759 (Figure 4.18), corresponded to a radioactivity deposit which produced, after microtomy and



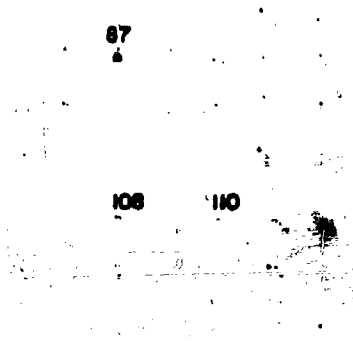
A - 63 ± 1.8 cpm

B - 49 ± 1.3 cpm

FIG. 4.19 BETA COUNT RATES AND AUTORADIOGRAMS OF FILTER PORTIONS

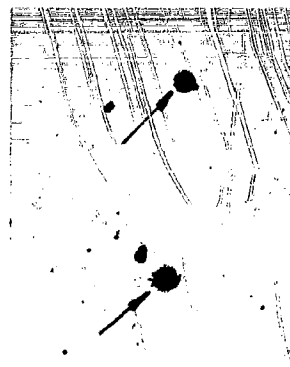


<u>Section No.</u>	<u>Beta Count Rate</u>
12	0.42 cpm
17	2.46 cpm
19	6.37 cpm
37	0.28 cpm
39	0.35 cpm



<u>Section No.</u>	<u>Beta Count Rate</u>
87	0.64 cpm
108	0.24 cpm
110	0.14 cpm

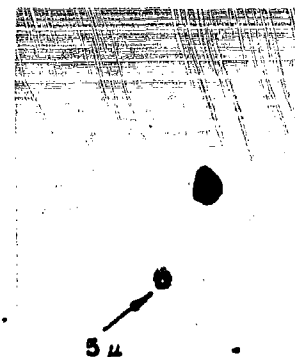
FIG. 4.20 BETA COUNT RATES AND AUTORADIOGRAMS OF THIN SECTIONS



Two Spot Images



Spot Image



Particles Revealed
After Chemical Re-
duction of Spot Image

THIN SECTION FROM SAMPLE 759 SPOT B



Top: Partially Reduced Image
Bot: Further Reduction Revealed
1 Micron Particle (Masked
From View By 14 Micron Amber
Particle)



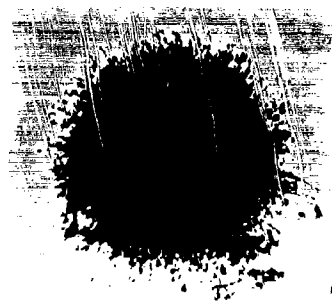
Top: Spot Image
Bot: Agglomerate Revealed After
Reduction of Image

PORTION OF SAMPLE 1947
FIG. 4.21
HIGH RESOLUTION AUTORADIOGRAMS OF LARGE AGGLOMERATED PARTICLES
123

re-autoradiography, spot images from three successive thin sections of 10 micron nominal thickness. Spot B led to two groups of three successive highly active sections. The central section of one set of three was subjected to high resolution and produced 3 spot images shown at the top of Figure 4.21 which were associated with particles of 7, 5 and 5 microns "diameter." As illustrated by the 5 micron diameter particle shown in Figure 4.21, these three particles appear to consist of a transparent body containing dark particles of about 0.5 microns size. Thus the "effective" size of the agglomerates which produced spots A and B appears to be slightly greater than 10 microns although the agglomerates may not have contained radioactive particulates much larger than 1 micron.

Further evidence of activity being associated with very large particles is shown in Figure 4.21. Sample 1947 produced a central particle of 2.5 microns diameter (optically masked in illustration) associated with a 14 micron red-amber particle and a 42 micron transparent object. Sample 1035 contained a collection of 50 to 100 dark particles ranging from 0.5 to 2.0 microns diameter associated with a transparent oblong object of 32 microns length. In each case the transparent object was similar to the filter fibers in appearance but did not produce a light polarization effect.

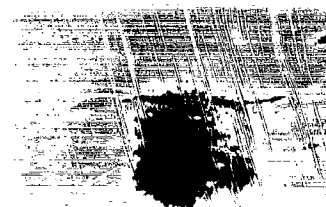
The more common case of spot image such as those marked by arrows on samples 1815, 759, 1035 and 1947 (Figures 4.16 and 4.18) led to a single particle centrally located beneath the coated emulsion spot images. Some spot images at various stages of chemical reduction and some typical radioactive particles so determined are shown in Figure 4.22. Most of the particles were spherical in



THIN SECTION OF 731
1.5 μ Particle



FIBER FROM 732
1.5 μ Particle



FIBER FROM 732
1 μ Particle



FIBER FROM 759
3 μ Particle



SECTION OF 1387
1 μ Particle



FIBER FROM 1815
1 μ Particle

SECTION OF 535
1.3 μ Particle 1 μ Particle



SECTION OF 299
2 μ Particle



SECTION OF 299
Image Partially Reduced Reduction Complete
Image

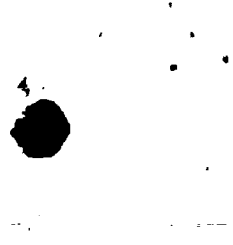


FIG. 4.22 HIGH RESOLUTION AUTORADIOGRAMS OF MICRON SIZE PARTICLES

shape and were opaque, transparent or amber colored transparent in appearance. Extraneous particles and the optical "noise" from the fibers and photographic gelatin made a complete analysis of color, index of refraction and polarization effects impossible. The particles which produced spot images ranged from 0.5 to 3 microns in diameter with most falling in the 1 to 2 micron range. Sample 299 produced several spot images for which no particle was found. One case shown in Figure 4.22, where the partially reduced image-particle matrix assumed a crystalline shaped outline, resulted in four residual particles of approximately 1 micron diameter each after bleaching.

A third type of lesser magnitude spot images occurred in the survey autoradiograms of thin sections exposed for 3 - 12 months. The images have diameters of approximately 0.1 mm and are similar to those illustrated in Figure 4.20. Similar small spot images occurred in the high resolution autoradiograms for which no central particle could be found by light microscopy. It was assumed that these images were caused by particles smaller than the "noise" limit of the sample matrix of 0.5 microns. Since the X-ray film requires approximately 10^8 betas/cm² for a dense image to be produced it was calculated that these particles would have activities on the order of 0.05 disintegrations per minute.

Evidence of still smaller radioactive particles was found in the diffuse image portion of the thin section autoradiograms shown in Figure 4.20 and in the beta tracks occurring in high resolution autoradiograms shown in Figure 4.23. The beta tracks occurred most frequently near the ends or damaged portions of the fibers, and no particulates corresponding to the tracks were found by light microscopy.

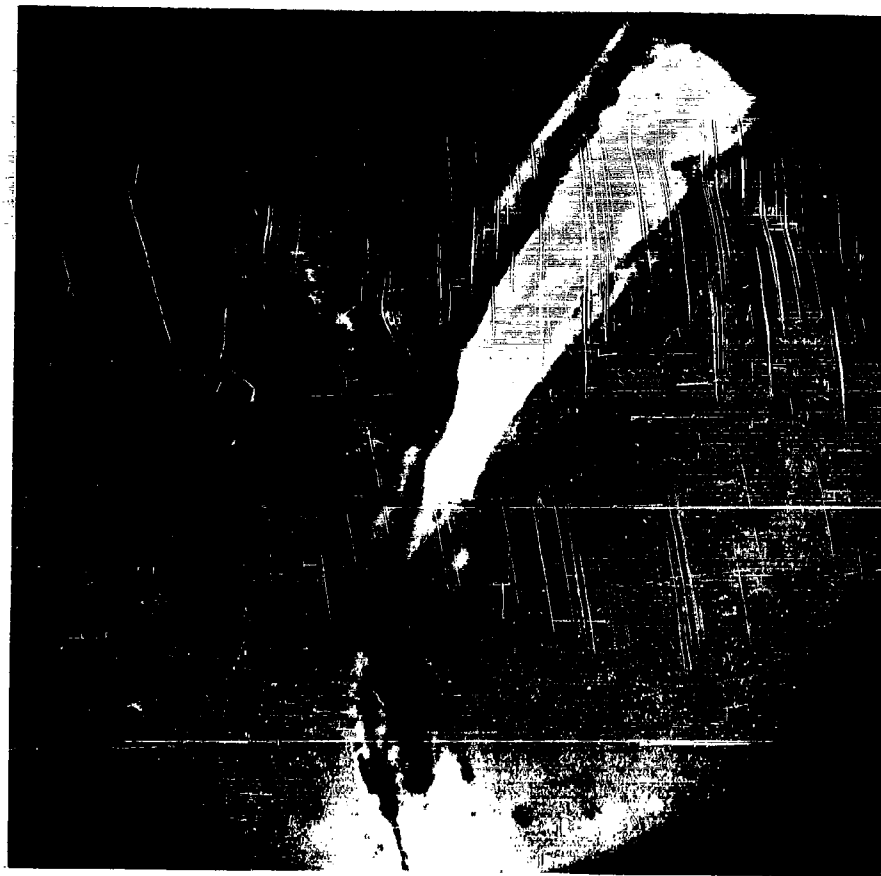


FIG. 4.23 HIGH RESOLUTION AUTORADIOGRAMS OF FILTER FIBERS

Radioactivity Measurements of Impaction Collector Samples

Attempts were made to obtain high resolution autoradiograms of several impactor samples. The results obtained were inconclusive, since the samples gave track counts not significantly different from background after six months exposure.

Two samples were subjected to low level beta determination. Again the results were somewhat inconclusive due to the low activities. There was, however, an indication that the screens from the a and b positions contained higher activities than those of the c and d positions (see Figure 4. 10).

The fact that activity was detected by beta counting and not detected by high resolution autoradiography leads us to conclude that the application of liquid emulsion as practiced in these studies either removed the particles from the sample substrate, or dissolved them, or both.

REFERENCES

1. Junge, C. E. and J. E. Manson, J. Geophys, Research, 66, 2163 (1961).
2. Ranz, W. E. and J. B. Wong, Ind. Eng. Chem. 44, 1371 (1952).
3. Langmuir, I. and K. B. Blodgett, General Electric Research Laboratory, Schenectady, New York, Rept. RL-225, 1944-45.

CHAPTER 5

DISCUSSION AND CONCLUSIONS

HASP has primarily been concerned with the behavior of nuclear debris in the stratosphere. It has been shown¹ that the measured distributions of fission products are a result of

1. weapon yield,
2. weapon test schedule,
3. type of weapon test (ground, air, sea),
4. latitude of test,
5. time (of year) of test,
6. initial meteorological conditions at and shortly after test time.

During a period of frequent testing each of the listed factors contributes such large transient perturbations to the fission product distribution that a complete understanding of the causes of the distribution is unattainable. Even after a time sufficient to allow the transient phenomena to be smoothed, the initial conditions specifying the role of each listed factor must be known in order to understand the particular features of the quasi-steady-state fission product distributions. It may, however, be possible to infer and ultimately to be able to predict quantitatively the behavior of nuclear debris in the stratosphere by studying the particles present there and with which old debris (> 6 months) may be associated. Before entering into the discussion of results of the HASP particle studies, we want to make it clear that there remains much to be proven by definitive measurements and experimentation. The work carried out by HASP investigators and those of Air Force Cambridge

Research Laboratories represents but a beginning in what promises to be a fruitful endeavor in atmospheric chemistry and particle mechanics.

THE STRATOSPHERIC AEROSOL

In 1959 Junge, Chagnon and Manson² collected samples of stratospheric particles by balloon-borne impactors. They also measured concentrations of Aitken nuclei (particles with radii less than 0.1 micron) in the same flights. The number concentrations of the Aitken nuclei decreased from about 100 cm^{-3} at the tropopause to less than 1 cm^{-3} at 20 km. From this fact Junge et al were led to the conclusion that the Aitken nuclei in the stratosphere are of tropospheric origin and the shape of the vertical profile is consistent with a coefficient of vertical eddy diffusion of $2000 \text{ cm}^2/\text{sec}$. Most of the particles collected by their impactors were in the radius range between 0.1 micron and 1.0 micron. (Particles in this size range are often referred to as "large particles.") Particles larger than 1.0 micron radius were detected in small and variable numbers. The particles in the radius range $0.1 \mu \leq r \leq 1.0 \mu$ were found to have a broad maximum in number concentration between about 16 km and 24 km altitude at 45° North latitude. The number concentration in this region was about 1 cm^{-3} . The vertical profiles, number concentrations, and particle radius-concentration distributions of these particles were found to be relatively constant in time and space. Thus Junge, Chagnon and Manson were led to the conclusion that there exists a persistent aerosol layer in the stratosphere whose mass is comprised mainly of particles with

radii between 0.1 micron and 1.0 micron. Electron microprobe analysis of the balloon-collected samples revealed that sulfur was present in higher concentrations than any other detectable constituent of the aerosol particles. It was presumed that the sulfur existed in the form of sulfate.

The work performed under HASP and by AFCRL upon samples obtained by the U-2 impaction probe has firmly established the persistency of the stratospheric aerosol layer. The samples analyzed have represented latitudes between 63°S and 72°N during the period March to November 1960. Altitudes sampled ranged between 40,000 and 70,000 feet, but the predominant altitude of collection was near 65,000 feet (20 kilometers). The electron diffraction studies have shown that the collected particles contain crystalline ammonium sulfate and occasionally ammonium persulfate. Junge and Manson have continued to identify sulfur as the most abundant detectable component by electron microprobe analysis^{3,4}. (The element of lowest atomic weight which could be detected was aluminum. Thus ammonium, which was found by electron diffraction, and sodium, which might have been present, were not detectable in the microprobe studies.) Spot tests on a few samples obtained by AFCRL revealed the presence of NH_4^+ in amounts roughly equivalent to those of $\text{SO}_4^{=}$. Junge and Manson also showed that ammonium sulfate and ammonium persulfate have hygroscopicities similar to that displayed by the collected stratospheric particles. HASP has established that the particles of the type identified as ammonium sulfate (and persulfate) comprise almost all of the particles with radii between 0.1 micron and 1.0 micron. These in turn comprise greater than 90% of the mass of stratospheric particles in the samples.

The evidence described above suffices to prove beyond a reasonable doubt that a stratospheric aerosol exists which has a peak number concentrations between 16 and 24 km altitude in the temperate zones. (Junge⁴ reports vertical profiles of particle number concentrations in the tropics which are similar to those obtained in the temperate latitudes when altitude is considered relative to the tropopause.) The aerosol most probably consists mainly of ammonium sulfate particles with radii in the range $0.1 \mu \leq r \leq 1.0 \mu$. The proposed process by which the aerosol is formed^{2,3} is oxidation in the stratosphere of H₂S and/or SO₂ of terrestrial origin by ozone of stratospheric origin. According to Junge⁵ the SO₂ and NH₃ in non-polluted tropospheric air originate primarily from the oceans. The SO₂ results from oxidation of H₂S which arises from decaying organic material in shallow oceanic waters. Ammonia may result from decomposition of organic surface films on the ocean. The concentrations of SO₂ and NH₃ in high tropospheric air (Mauna Kea) are about 1 γ/m^3 STP⁵. If these gases mix into the stratosphere without appreciable removal by precipitation scavenging then their concentrations at the 20 km level would be about one to two orders of magnitude larger than the estimated concentrations of NH₄⁺ and SO₄⁼ in the stratospheric aerosol. Presumably this would be enough NH₃ and SO₂ to support a steady state concentration of aerosol formed by oxidation of SO₂.

PROPERTIES OF THE STRATOSPHERIC AEROSOL

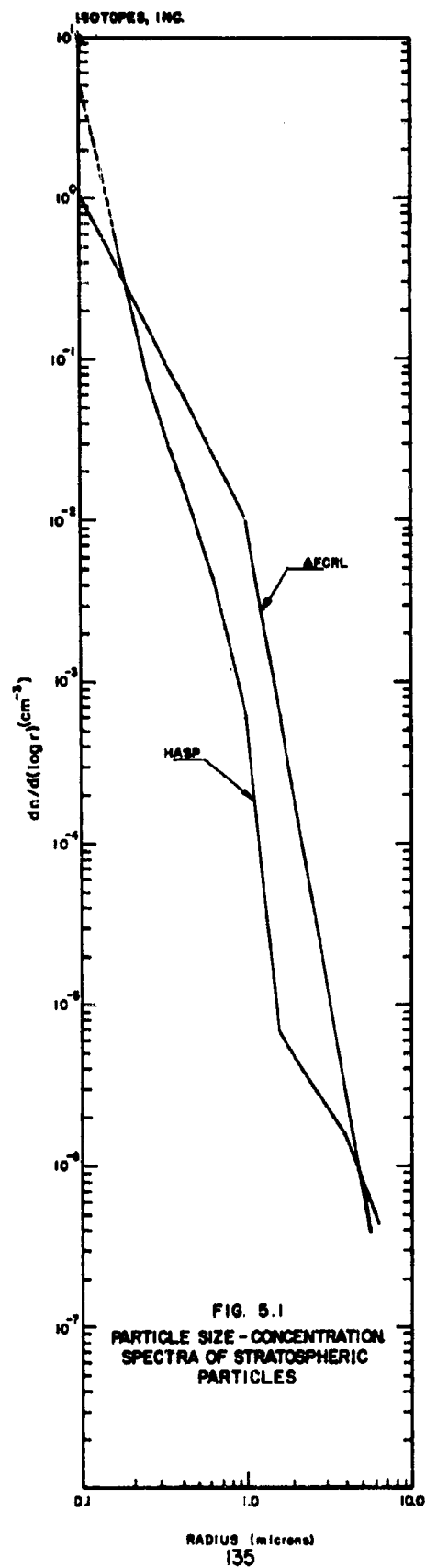
As discussed in the previous section of this chapter, both AFCRL and HASP studies have determined that the mass of the stratospheric aerosol is largely contained in particles with radii between 0.1 micron and 1.0 micron and that the number concentration of particles in this range is about 1 cm^{-3} at the altitude of peak concentration, namely about 20 km. We shall now proceed to discuss the particle size spectrum of the aerosol and then present some conclusions concerning the mass concentrations, the total stratospheric burden of aerosol, and the possible relationships between stratospheric nuclear debris from atomic weapons testing and the aerosol.

The Particle Size Spectrum

In Figure 5.1 are shown the particle size spectra of the stratospheric aerosol as found by AFCRL and HASP. The abscissa is radius in microns and the ordinate is concentration expressed as

$$\frac{dn}{d(\log r)} \quad (\text{cm}^{-3}),$$

where dn is the number of particles per cm^3 of air with radii in the interval defined by $[\log r, \log r + d(\log r)]$. The HASP curve is that which corresponds to the weighted average particle size-concentration distribution given in Table 4.7. The AFCRL curve is taken from the work of Junge and Manson³ and was based on the results of balloon-borne samplers as described in reference (2). It is quite difficult to assess the relative agreement of the two spectra. Junge and Manson have estimated that their spectrum should be correct to within about a factor of two in either



direction with respect to concentration at a given radius between 0.1 micron and 1.0 micron. If we arbitrarily adopt the same estimate for the HASP spectrum, we find that the two curves are in agreement (within a factor of four) for radii between 0.1 micron and 0.45 micron. For the region $0.5 \mu < r < 1.0 \mu$ the discrepancy between the two spectra may be due to failure to take into account flattening of the particles due to condensation of moisture after collection. Junge and Manson suggest that this may be the reason that their measured sulfate deposits gave concentrations about a factor of four lower than those expected by calculation from the particle size spectrum. Another possible source of systematic error may be the peculiar aerodynamic effect of the window in the probe, resulting in efficiencies different from those given by impaction theory. For particles with radii greater than 1.0 micron there exist statistical uncertainties due to the small number of particles collected in a single sample. In view of the fact that, in HASP, the types of particles counted in this size range were not encountered in blank samples, it is suggested that the uncertainty of the HASP spectrum for particles with radii greater than or equal to 1.5 microns is within a factor of four or five. More will be said about these larger particles later in this chapter.

The spectra shown in Figure 5.1 can be approximately represented analytically over given intervals by expressions of the form

$$\frac{dn}{d(\log r)} = c'r^{-b},$$

which is equivalent to

$$\begin{aligned} \frac{dn}{dr} &= cr^{-(b+1)} & (c &= 0.435 c') \\ &= cr^{-a} & (a &= b+1) \end{aligned} \quad (5.1)$$

Table 5.1 below lists the values of c and a for the two spectra shown in Figure 5.1 for the interval $0.1 \mu \leq r \leq 1.0 \mu$.

Table 5.1

	<u>a</u>	<u>c</u>
AFCRL	3	$4.35 \times 10^{-11} \text{ cm}^{-1}$
HASP	4.9	$6.55 \times 10^{-20} \text{ cm}^{-9}$

Integration of equation (5.1) between the appropriate limits of r gives the number concentration of particles. In order to compare the number concentration so obtained with that reported in Table 4.7 for the experimentally determined value care must be taken to use the proper limits for integration. The experimental value of the number concentration, n , was determined by

$$n = \sum_i n_i, \quad (5.2)$$

where n_i is the number concentration of particles in the i^{th} class with radius between r_{i-1} and r_i . Thus the value of n_i corresponds to the geometric mean radius $\bar{r}_i = \sqrt{r_i r_{i-1}}$. In Table 4.7 the radii are the geometric means of radii where the intervals are defined by

$$\log r_i - \log r_{i-1} = 0.2.$$

Thus to compare the value of n obtained by integration of equation 5.1 between two limits ρ_a and ρ_b with that obtained experimentally by summation over intervals defining \bar{r}_i and \bar{r}_j , then we must choose $\rho_a = r_0$ and $\rho_b = r_j$. While we have been considering the interval $0.1 \mu \leq \bar{r} \leq 1.0 \mu$, which really pertains to the

consideration that radius has discrete values rather than continuous values, we must now consider the interval $0.0795 \mu \leq r \leq 1.26 \mu$ in order to treat radius as continuous. As can readily be seen, at 1.0μ radius both curves in Figure 5.1 fall off steeply toward higher values of radius. Thus integration between 1.0 and 1.26 micron will contribute negligibly to the number concentration (and also to the volume concentration to be considered below). Table 5.2 lists the values of number concentration, n , obtained by integration between 0.0795μ and 1.0μ of both curves in Figure 5.1. Also listed are values of the volume concentration, v , obtained by

$$v = \frac{4}{3\pi} \int_{\rho_a}^{\rho_b} r^3 dn \quad , \quad (5.3)$$

where ρ_a and ρ_b are the same limits of radius used in the calculation of n .

The HASP experimental values are listed for comparison to show that the function given by equation (5.1) with the chosen values of a and c actually represents the experimental distribution (Table 4.7 and Figure 5.1) quite closely.

Table 5.2

	<u>$n \text{ (cm}^{-3}\text{)}$</u>	<u>$v \text{ (cm}^3\text{/cm}^3\text{)}$</u>
AFCRL	0.35	1.69×10^{-14}
HASP	1.3	1.06×10^{-14}
HASP (Experimental)	1.1	0.938×10^{-14}

In regard to the volume concentrations of particles with radii greater than 1.0 micron, integration of the AFCRL distribution to infinite radius adds another $0.6 \times 10^{-14} \text{ cm}^3\text{/cm}^3$ whereas summation of HASP experimental results adds only about $0.03 \times 10^{-14} \text{ cm}^3\text{/cm}^3$ to the volume concentrations of particles shown in

Table 5.2. Despite the substantial disagreement between the two distributions for radii greater than 1.0 micron, the volume concentrations of all particles with radii ≥ 0.1 micron are in fair agreement as judged from Table 5.2 and previous statements concerning accuracy of number concentrations.

The studies at AFCRL³ also included determinations of the concentrations of sulfur in the aerosol by electron microprobe measurements of particle deposits on ribbon type impaction surfaces, which were more efficient for small particles than the window impactor used in the HASP studies. The average concentration of sulfur (expressed as grams of sulfate (SO_4) per cm^3) in eleven samples collected at about 20 km altitude was reported as $6.82 \times 10^{-15} \text{ gm/cm}^3$. This concentration was not corrected for impaction efficiency since it was assumed that the AFCRL particle size spectrum was correct. Thus the (approximately) 50% efficiency for 0.1 micron radius particles would not appreciably affect the estimation of the mass deposited since most of the mass corresponding to the assumed spectrum is in particles with radii greater than 0.3 micron, and these have impaction efficiencies greater than 85%. The $6.82 \times 10^{-15} \text{ gm SO}_4/\text{cm}^3$ is to be compared with $13.4 \times 10^{-15} \text{ gm/cm}^3$ for HASP experimental and $24.6 \times 10^{-15} \text{ gm/cm}^3$ for the AFCRL distribution. (These latter figures were calculated from the volume concentrations in Table 5.2 assuming a density of 2 gm/cm^3 and a composition of $(\text{NH}_4)_2\text{SO}_4$. The actual density of ammonium sulfate is 1.8 gm/cm^3 .) As mentioned previously, Junge and Manson suggest that flattening of the particles (see also Chapter 4 of Part II) may be the reason for the factor of nearly four disparity between their measured and computed sulfate concentrations. The

effect of correcting the AFCRL distribution for flattening would be to increase the number of smaller particles because of the low impaction efficiencies and to decrease the number of larger particles which have nearly 100% impaction efficiencies. This would be approximately equivalent to a clockwise rotation of the AFCRL distribution about some point in the 0.2μ to 0.3μ radius region.

If we now assume that the HASP particle size spectrum represents the actual distribution, we calculate from curve 5 of Figure 6 in reference (3) that the AFCRL ribbon impactor contained only about 63% of the sulfate content of the sampled air. Correcting the average sulfate concentration obtained by Junge and Manson brings the average concentration to $11 \times 10^{-15} \text{ gm SO}_4/\text{cm}^3$ which is in close agreement with the value of $13.4 \times 10^{-15} \text{ gm/cm}^3$ obtained in HASP. For this reason we believe that the HASP particle size-concentration spectrum as shown in Figure 5.1 is more nearly correct than the AFCRL spectrum. There still exists, however, a relatively large uncertainty in the spectrum in the region of radius around 0.1 micron. It is in this region that the number concentration is determined. Although nothing is known of the particle size spectrum of Aitken nuclei ($r \leq 0.1 \mu$), their number concentration², namely 1 cm^{-3} , at 20 km altitude agrees with the number concentration given by the HASP spectrum in the region of 0.1 micron radius. If the HASP spectrum is correct, then the number concentration of Aitken nuclei must fall rather steeply with decreasing radius below 0.1 micron.

The Effect of the Stratospheric Aerosol on World-Wide Fallout of Nuclear Debris

When a nuclear device employing fissionable material is detonated near the earth's surface, the fission products, a few moments after the detonation, will be associated with particles ranging from atoms and molecules, through molecular clusters, to micron size and up to a few millimeters. Particles resulting from air bursts may not exceed sizes in the micron range. In general, if the cloud from a nuclear detonation enters the stratosphere, we would expect that as time passes the larger particles will leave the stratosphere by sedimentation and the smaller particles will coagulate with other particles which are present due to their Brownian motion. Particles of an intermediate size may persist for longer periods without appreciable change in size due to growth or without being removed by sedimentation. Thus it is quite apparent that the role played by the particles of the stratospheric aerosol is to remove by coagulation (but not to remove them from the stratosphere) the smallest of the original particles produced by nuclear detonations. The relative importance of this role depends upon the fraction of the total fission products which is carried by the small original particles. Thus, it would be expected that the stratospheric aerosol particles would be associated with a larger portion of the fission products from an air burst than from a surface burst.

The work performed in HASP in connection with the relationships between stratospheric particles and radioactivity was of limited scope and does not permit quantitative estimates of the effects mentioned in the previous paragraph. (We will throughout this discussion use the unqualified term "radioactivity" to mean radioactivity which results from the detonation of fissionable material. We thus

exclude any natural radioactivity such as arises from cosmic rays.) A few general comments concerning the HASP work are considered in order here.

The results from the autoradiographic studies reported at the end of Chapter 4 indicate that the particles which caused the dense spot images were in the size range from about 0.25 micron to about 1.0 or 1.5 microns radius. The fresher the debris, the higher was the concentration of such particles. All collections contained particles with radii smaller than 0.25 micron (the limit of resolution under the prevailing experimental conditions) which produced low density spots and diffuse images in the autoradiograms. The older the debris, the more predominant was the diffuse radioactivity. The two samples studied, Nos. 3749 and 3750, which contained debris from the high altitude rocket detonations Teak and Orange, (see Chapters 4 and 5 of Part 1) gave no dense spot images. One gave only diffuse images while the other gave a few low density spots in addition to diffuse images. This tends to support the previous statements concerning the small sizes of particles from air bursts.

The beta counts of the various positions of two impactor samples indicated that for debris more than a year old more radioactivity resides in smaller particles ($r < 1.0$ micron for density of 2 gm/cm^3), which deposited in the "a" and "b" positions, than in the larger particles, which deposited uniformly over the sample but which are represented by the "c" and "d" positions.

Junge, Chagnon, and Manson² have shown that at or above 20 km altitude individual particles with radii smaller than 0.01 micron introduced into air containing the background particles of the stratospheric aerosol will be attached to

the background population in a time short compared with the time of transport of the air from the stratosphere to the troposphere. Thus radioactive particles with radii greater than a few hundredths of a micron, but small enough to have negligible sedimentation rates, will remain as a separate population intermixed with the aerosol particles. The differences between the HASP and AFCRL particle size spectra are not sufficient to change these conclusions.

The above considerations lead to the expectation that, if nuclear debris is well mixed with the stratospheric aerosol, then air which has a relatively high particle concentration would be expected to have a correspondingly high radioactivity concentration. Table 5.3, which is a summary of Table 4.6, indicates that, at 20 km altitude, this is approximately the case. There is a relatively small variation from sample to sample in the ratio of strontium-90 concentration to the volume (or number) concentration of particles. The larger ratio exhibited by sample W-12 may be explained in part by the presence of strontium-90 from the lower stratospheric injections of the Hardtack test series. Debris from this source was probably the main radioactive component of the particles in the other samples.

By examination of vertical profiles of strontium-90 during the period January-June, 1960 and comparing them with the vertical profile of particles obtained by Junge, Chagnon and Manson², we may gain some indication of the extent to which particles and radioactivity had mixed. These profiles are shown in Figure 5.2. They are plotted relative to the average tropopause heights (36,000 feet for polar and 55,000 feet for tropical) and the units of particle

Table 5.3. Summary of Particle and Radioactivity Concentrations

Sample No.	Date Collected	Latitude	Altitude (feet)	n (cm ⁻³)	v (cm ³ /cm ³)	Sr ⁹⁰ Concentrate (dpm/cm ³)
W-3	3/16/60	27N→12N	67,000	1.57	1.24 x 10 ⁻¹⁴	3.61 x 10 ⁻⁷
W-8	4/5/60	15N→8S	67,000	0.94	1.17 x 10 ⁻¹⁴	2.70 x 10 ⁻⁷
W-10	4/21/60	48N	65,000	3.56	3.36 x 10 ⁻¹⁴	6.17 x 10 ⁻⁷
W-12	4/30/60	66N→50N	65,000	1.19	9.43 x 10 ⁻¹⁵	5.02 x 10 ⁻⁷
W-13	5/9/60	15N→6S	67,000	1.42	1.01 x 10 ⁻¹⁴	3.03 x 10 ⁻⁷
W-14	5/12/60	16N→29S	65,000	0.86	1.31 x 10 ⁻¹⁴	2.84 x 10 ⁻⁷
W-16	11/17/60	62N→32N	64,000	0.10	4.14 x 10 ⁻¹⁵	-----
W-17	11/21/60	15S→20N	65,000	0.63	6.55 x 10 ⁻¹⁵	-----

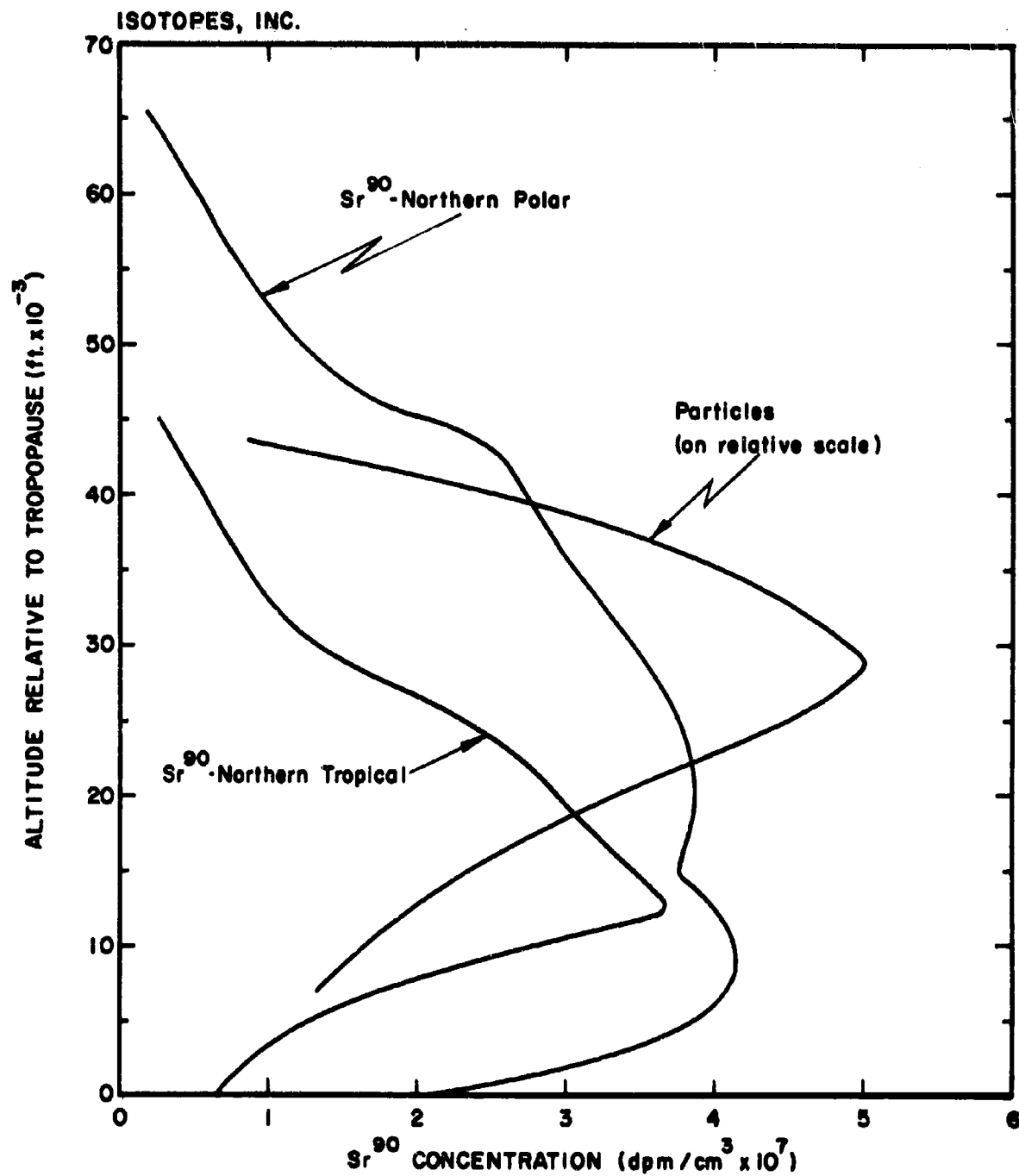


FIG. 5.2 VERTICAL PROFILE OF PROFILE OF PARTICLES AND STRONTIUM - 90, JAN. - JUN. 1960

concentration are relative. The profiles of strontium-90 are taken from Table 6.3 of Chapter 6 of Part 1 and are expressed in dpm per ambient cm^3 . The average strontium-90 concentration at 20 km ($\sim 65,000$ ft.) was 3.1×10^{-7} dpm/ cm^3 which is comparable to the concentrations listed in Table 5.3. The particles and the radioactivity apparently were not well mixed in the tropical stratosphere. They were better mixed in the northern polar stratosphere, however. It is difficult to determine the cause of the non-mixed state in the tropical stratosphere. One possible explanation is that the zone of maximum production of sulfate particles is at a higher altitude than the center of gravity of tropical stratospheric air (about 75,000 ft.) so that no matter how uniformly the air and radioactivity may be mixed, there will always be an excess of particles to radioactivity at altitudes near the zone of maximum aerosol production in comparison to the quantities at lower altitudes.

The foregoing discussion indicated that it is impossible, on the basis of the evidence at hand, to estimate the fraction of radioactivity which is actually contained by particles of the stratospheric aerosol.

The established hygroscopicity of the particles of the stratospheric aerosol may be the factor which causes fallout which is stratospheric in origin to be deposited on the earth primarily in rain. The hygroscopic nature of the sulfate particles presumably would make those with radii less than or equal to 0.1 micron excellent condensation nuclei. While it remains to be proved, it is possible that the larger particles of the stratospheric aerosol may be freezing nuclei, i. e., particles upon which ice crystals can readily form. In the process of cloud

formation, condensation nuclei are the sites for the growth of small water droplets. In order for precipitation from a cloud to occur, it is necessary that freezing nuclei be present so that drops of size sufficient to be influenced appreciably by gravity can form. If particles of the stratospheric aerosol are good freezing nuclei, then it would be expected that stratospheric air which penetrates into the troposphere would have a tendency to initiate rain formation upon mixing with moist tropospheric air. Such a process may account for the observations that rain carries most stratospheric fallout to the ground (see Chapter 7 of Part I.)

The processes involved in rain formation were discussed recently by Fletcher⁶ in connection with the "meteor hypothesis" of rainfall, originally proposed by E. G. Bowen. Fletcher pointed out that measurements made by Australian investigators of freezing nuclei concentrations with balloon-borne equipment and recently by equipment carried by U-2 aircraft have shown that there is, on the average, no tendency for these concentrations to decrease with altitude, and that at 20 kilometers altitude there are also "high" nucleus counts. These observations were offered as "substantial support" for the meteor hypothesis. The reasoning employed was that if the nuclei originate at the earth's surface their concentrations would decrease with altitude and be zero above the tropopause. Since observation contradicted this situation, it was reasoned that the nuclei must be extraterrestrial in origin.

The findings of the HASP particle studies neither confirm nor refute the meteor hypothesis. However, they serve to cast some doubt upon the substantiality of the support offered by the vertical profiles of freezing nuclei. Evidently the

adherents to the meteor hypothesis did not envision the possibility of formation of particles in the stratosphere by chemical reactions of gaseous materials of earthly origin. The overwhelming preponderance of sulfate type particles compared to any other types in the lower stratosphere makes it appear likely that the stratospheric freezing nuclei encountered by the Australian investigators were indeed particles of the stratospheric aerosol. In fact, the freezing nuclei concentrations in the stratosphere and upper troposphere seem to lend support to the ideas advanced in the previous paragraph concerning incorporation of fallout in rainfall.

The Stratospheric Burden of Sulfate

By invoking some rather crude assumptions the total sulfate content of the stratosphere may be estimated by two methods which are outlined below.

1. Assuming that the aerosol and the strontium-90 in the stratosphere had mixed throughout the layer in which the aerosol exists (tropopause to 80,000 feet) both laterally and vertically, then the total SO_4 content of the stratosphere is given by the ratio of the average SO_4 concentration (g/cm^3) at 20 km to the average strontium-90 concentration (dpm/cm^3) at the same altitude multiplied by the total stratospheric burden of strontium-90. The HASP inventory of stratospheric strontium-90 was 0.8 megacurie in January to June, 1960, (see Chapter 6 of Part I) of which less than 10% was estimated to be above 80,000 feet. The mean concentration of strontium-90 at 20 km during that time was $3.1 \times 10^{-7} \text{ dpm}/\text{cm}^3$ (ambient). Assuming the aerosol to be composed of ammonium sulfate, the average SO_4 concentration corresponding to the HASP distribution in Figure 5.1 is $1.34 \times 10^{-14} \text{ gm}/\text{cm}^3$ expressed as SO_4 . The total SO_4 burden of the stratosphere is thus calculated to be 8.1×10^7 kilograms.
2. Assuming the vertical profile of aerosol particles is constant relative to the tropopause over all latitudes and that the aerosol density is proportional to the number concentration as indicated by Junge's work (see Figure 5.2) and by the relative constancy of

the ratio of volume concentration to number concentration in Table 5.3, then integration of the vertical profile over altitude and around the earth yields the total number of particles in the stratosphere (equal to 3.6×10^{24} particles, using an average number concentration of 1 particle/cm³ at 20 km altitude.) This number multiplied by the ratio of average sulfate concentration to average number concentration yields a stratospheric sulfate burden of 4.5×10^7 kilograms.

The difference between the two calculated SO₄ burdens may be some indication of the extent to which the aerosol and radioactivity had not mixed. Since the burden of 8.1×10^7 kg was computed by assuming mixing and that of 4.5×10^7 kg was not, the indication, excluding errors in the other assumptions made, is that the particles and radioactivity were slightly more than 50% mixed throughout the lower stratosphere. However, the errors in the other assumptions certainly obscure the actual extent of mixing.

With the assumptions made in (1) above plus the assumption of a 1.0 year residence half-time for strontium-90 of tropical origin (Chapter 6, Part I), the stratospheric production rate and removal rate may be estimated to be approximately 5.5×10^7 kilograms of SO₄ per year based on a sulfate burden of 8×10^7 kilograms.

Extraterrestrial Material in the Stratosphere

An attempt was made during HASP to obtain information on the presence in the lower stratosphere of particles of extraterrestrial origin by subjecting four specially collected filter samples of stratospheric dust to neutron activation analysis and by careful examination of particles with radii greater than one micron on the impactor samples.

The neutron activation analyses of four filters, each representing about $2 \times 10^4 \text{ m}^3$ of ambient air from the stratosphere, were performed in an attempt to assess the amounts of materials present which may have been extraterrestrial in origin. The results, shown in Tables 4.2 and 4.3 in the previous chapter, indicate, at best, the maximum values of the various elements. The fact that the outbound flights gave higher values of most elements than did the inbound flights indicates that contamination may have been present in the outbound flights, although there is no way to prove it. It is obvious that the filter papers themselves contained amounts of the elements under study which were greater than or equivalent to the amounts collected from the air. Thus, for studies such as this, it is necessary to employ a collection medium which is free of the elements to be detected.

There is a possibility that the larger particles collected by the impactor probes may be extraterrestrial in origin. Junge and co-workers^{2, 3} have pointed out that particles found in the stratosphere with radii greater than a micron or so are most likely to be of extraterrestrial origin. In their studies they encountered a background population of particles on their glass slides, however, and could present little evidence that these large particles were not part of this contamination. As pointed out previously, we believe that the particles with greater than 1.5 micron observed on Formvar substrates were not "background" but an actual collection. The various types of particles observed are described in Chapter 4.

The distribution of particles with radii in the range $1.58 \mu \leq r \leq 6.3 \mu$ has a slope of -2 in Figure 5.1. This is in agreement with the results of Fireman and Kistner⁶ who analyzed stratospheric particles collected by balloon and aircraft. They estimated about 10^{-7} particles/cm³ as the number concentration of particles with radii between 1.5 and 15 microns. The estimates from the HASP data are approximately an order of magnitude higher.

Since the concentrations of material in this size range appear to be quite variable in time and space (see Table 4.7) and collections are quite sparse, we hesitate to draw any conclusions concerning origin and accretion rates of the particles.

CONCLUSIONS

1. The existence of a stratospheric aerosol, originally proposed by Junge, Chagnon and Manson has been confirmed by particle collections under HASP.
2. The aerosol is comprised chiefly of particles with radii in the range 0.1 to 1.0 micron.
3. The composition of the aerosol particles appears to be ammonium sulfate, as determined by electron diffraction, electron microprobe, and chemical spot tests.
4. The particle size-concentration spectrum obtained by electron microscopy studies of the samples appears to agree with the observed number concentrations and the observed sulfur concentrations obtained by Junge, et al.
5. The HASP particle size spectrum gives an average number concentration of 1 particle per cm^3 and an average volume concentration of $9.6 \times 10^{-15} \text{ cm}^3/\text{cm}^3$ for the stratospheric aerosol at 20 km altitude.
6. The aerosol particles probably contained a significant fraction of the nuclear debris present in the stratosphere in the first half of 1960, although no quantitative estimates of the fraction could be made.
7. The stratospheric burden of sulfate as SO_4 was estimated to be 8×10^7 kilograms based on the HASP particle size spectrum, the HASP strontium-90 inventories and the assumption of complete mixing of particles and strontium-90.
8. The studies of penetration of radioactivity through the filter samples indicate that less than 1.5% of the collected activity penetrated 90% of the filter thickness. This is strong evidence for 100% retention of stratospheric particles by HASP filter samples.

REFERENCES

1. cf. Chapters 5, 6, and 8 of Part 1.
2. Junge, C. E. , C. W. Chagnon, and J. E. Manson, J. Meteor. , 18, 81 (1961).
3. Junge, C. E. and J. E. Manson, J. Geophys. Research, 66, 2163 (1961).
4. Junge, C. E. , Private Communication.
5. Junge, C. E. , "Atmospheric Chemistry," Advances in Geophysics, 4, Academic Press, Inc. , New York (1958).
6. Fletcher, N. H. , Science, 134, 361 (1961).
7. Fireman, E. L. and G. A. Kistner, Geochim. et Cosmochim. Acta, 24, 10 (1961).

BLANK PAGE

THE HIGH ALTITUDE SAMPLING PROGRAM

Part III

MEASUREMENTS OF FALLOUT IN MAN'S ENVIRONMENT

CHAPTER 1

MEASUREMENTS OF CARBON-14 IN TROPOSPHERIC AIR

The major efforts toward determining the fate of radioactivity produced in nuclear weapons testing have been restricted to research on the fallout of particulate matter. The amount of attention given to the production, present distribution and future distribution of the gaseous by-products of testing has constituted only a small fraction of the total output. Perhaps one of the main reasons for this lack of interest has been the belief that the gaseous products did not constitute a hazard to the human population. Recent work, however, has tended to attach more significance to the possible hazards from these products. But considerable doubts still remain regarding the ultimate consequences of the radiation dose to mankind.

One of the nuclides produced during weapons testing, not in the fission process but by the reaction of escaping neutrons with the nitrogen of the atmosphere, is carbon-14. The atoms of carbon-14 react immediately with the oxygen in the atmosphere to form carbon dioxide which then becomes a part of the carbon cycle. In addition to the carbon-14 produced in weapons testing, this nuclide is being continually created in the upper atmosphere by natural processes, and the resultant mixture of carbon-14 from both sources enters into the normal processes of exchange between the stratosphere and troposphere, incorporation into the biosphere, exchange between the troposphere and oceans and the subsequent removal from the exchangeable reservoir by formation of limestone, etc. The amount of radiocarbon produced by nuclear tests has resulted in detectable increases in the normal concentrations of carbon-14 in the atmosphere, biosphere and hydrosphere.

Much has been said regarding the similarity in behavior of the gaseous and particulate products of testing. Such phenomena as the rate of removal of radioactivity from the stratosphere to the troposphere and removal of activity from the troposphere are quite well-documented for particulate matter but not so for gaseous materials. There are theories which suggest that the removal of gaseous products such as carbon-14 from the stratosphere does not occur at the same rate as the particulates such as strontium-90 and cesium-137. There is also some question as to whether the bomb carbon-14 exhibits a "seasonal effect" in the changes in concentration in tropospheric air².

Because of the limited aims of the work to be described, only a very small part of the overall problem of the behavior of carbon-14 from nuclear tests has been investigated. We have endeavoured to follow the changes in carbon-14 concentration in tropospheric carbon dioxide over a period of about 1 1/2 years. The results give some information on the rate of absorption of carbon dioxide from the atmosphere by the oceans, the magnitude of seasonal introductions of carbon-14 - free carbon dioxide from fossil fuels, and the introduction of bomb carbon-14 from the stratosphere into the troposphere.

SAMPLE COLLECTION

The procedure used to collect a sample of tropospheric carbon dioxide involved the removal of the gas from the air by absorption in solutions of potassium hydroxide. Samples were collected daily and combined over a seven day period to form an integrated weekly collection.

The collectors used for the absorption of carbon dioxide were three 10 cm diameter petri dishes, each containing about 50 ml of 3 to 4 molar potassium hydroxide solution and surrounded by an enclosure to prevent the entrance of rain. A combined weekly sample of 1000 ml of potassium hydroxide solution was found to yield about 10 liters of carbon dioxide under standard conditions of temperature and pressure.

Prior to being used for sampling, the potassium hydroxide solution was freed of previously absorbed carbon dioxide by precipitation with barium chloride ($K_2CO_3 + BaCl_2 \longrightarrow 2KCl + BaCO_3$). The precipitated barium carbonate was filtered out and the carbonate-free potassium hydroxide solution was ready for use. A one-month supply of potassium hydroxide solution was prepared at one time and stored in a closed container.

Samples collected for analysis were stored in closed polyethylene bottles.

ANALYTICAL PROCEDURES

Sample Preparation

The carbon dioxide dissolved in the potassium hydroxide solution is released by hydrolysis with phosphoric acid in a vacuum system shown in Figure 1.1. The potassium hydroxide solution is placed in flask A and attached to the vacuum system at ground glass joint H. The system is then evacuated through stopcock D or J to a pressure of approximately 20 cm Hg. The system is then isolated from the vacuum pump and liquid nitrogen is placed on trap C. The magnetic stirrer K is started and phosphoric acid from reservoir B is admitted slowly into flask A. As the carbon dioxide is evolved from the solution, ($3K_2CO_3 + 2H_3PO_4 \longrightarrow 3CO_2 + 3H_2O + 2K_3PO_4$) it is frozen out in trap C. The reaction is considered complete when gas ceases to evolve from the solution upon further addition of acid. A few minutes are then allowed to elapse to ensure complete condensation of the carbon dioxide before stopcock L is closed and the frozen carbon dioxide pumped for 10-30 minutes to remove any volatile impurities such as oxygen and nitrogen, which may be present at this temperature. The carbon dioxide is then transferred to trap G by removing the liquid nitrogen

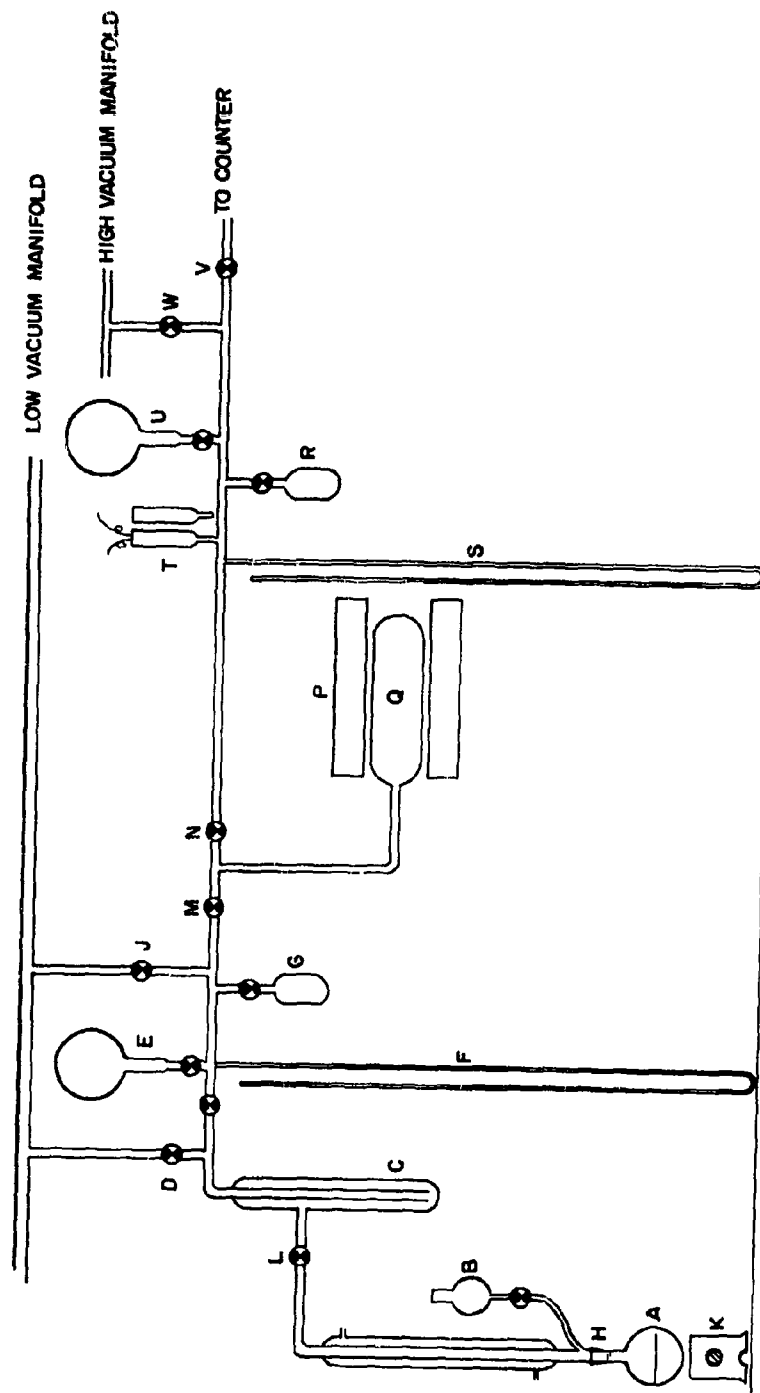


FIG. 1.1 GAS HANDLING SYSTEM
(CARBON-14)

from trap C and placing it on trap G. As C warms up the gas expands from C and is frozen out in G. The gas is then allowed to expand into bulb E where it is stored until ready for further treatment. At this stage, the carbon dioxide is usually fairly pure except for the presence of some water vapor, and radon. These are removed by causing the carbon dioxide to react with calcium oxide in a quartz bulb Q at 750°C to form calcium carbonate; the radon and water vapor, which do not react with the calcium oxide, are subsequently pumped away. The full procedure is as follows. The carbon dioxide is first frozen into trap G, the furnace section is isolated from the remainder of the vacuum system and stopcock M opened to the calcium oxide bulb. The reaction proceeds at about the same rate as the carbon dioxide expands from the trap after removal of the liquid nitrogen. When the reaction is complete, as indicated by a stable reading on the manometer F, the temperature of furnace P is lowered to 400-450°C. Stopcock M is then closed and stopcock N is opened to the high vacuum manifold. The sample is then pumped to a vacuum of less than 1 μ as indicated on Pirani gauge T. When this pressure is attained, the temperature of furnace P is raised to 950°C. The system is isolated from the high vacuum pump by closing stopcock W when the temperature reaches about 550°C. Liquid nitrogen is placed on trap R and the carbon dioxide released from the decomposition of the calcium carbonate at 950°C is frozen in the trap. The decomposition is considered complete when no pressure buildup is observed in the system with trap R isolated. The carbon dioxide is now pure and free from radon and ready to be stored in a bulb such as U, or transferred into the counter to be counted. The sample is transferred into the previously-evacuated counter through stopcock V to a pressure of 1520 mm as read on manometer S.

Counting Procedure

The proportional counter in which the activity of the purified carbon

dioxide sample is assayed is constructed of electrolytic copper. The active volume of the counter is just under two liters. To provide a low background it is shielded by one inch of mercury, a ring of 23 G-M cosmic ray counters operated in anti-coincidence with the sample counter, 4 inches of paraffin wax, and 18 inches of hot rolled steel (Figure 1.2). The background of the counter with this arrangement is 9.2 counts/min. The associated electronics were specially constructed at Isotopes, Inc., in connection with the radiocarbon dating program.

Each sample is counted for two 8 to 15 hour periods several days apart to verify the reproducibility of the counts. All activities are corrected to correspond to a standard temperature of 273°K.

Accuracy and Reproducibility

The U. S. National Bureau of Standards supplies an oxalic acid modern standard for radiocarbon dating laboratories. At the 1959 conference on radio-carbon in Gröningen a value of 0.95 times the activity of this oxalic acid standard was adopted as the modern reference value for radiocarbon dating. The carbon-14 activities of all samples measured in this program are compared with this standard value. The activity (at 273°K) of carbon dioxide from this standard, when filled to a pressure of 1520 mm Hg in our counter, is 24.00 ± 0.18 counts/min. This standard gas is usually assayed once a week and its activity is reproducible to within the statistical error of the count. Background carbon dioxide, from carbonaceous materials older than 50,000 years, is counted several times a week and is usually stable to within the statistical error.

All chemical reactions involved in the analysis are essentially quantitative and therefore no significant isotopic fractionation is to be expected. Background carbon dioxide was prepared several times and the values obtained were identical. In addition, carbon dioxide was prepared from the oxalic acid standard several

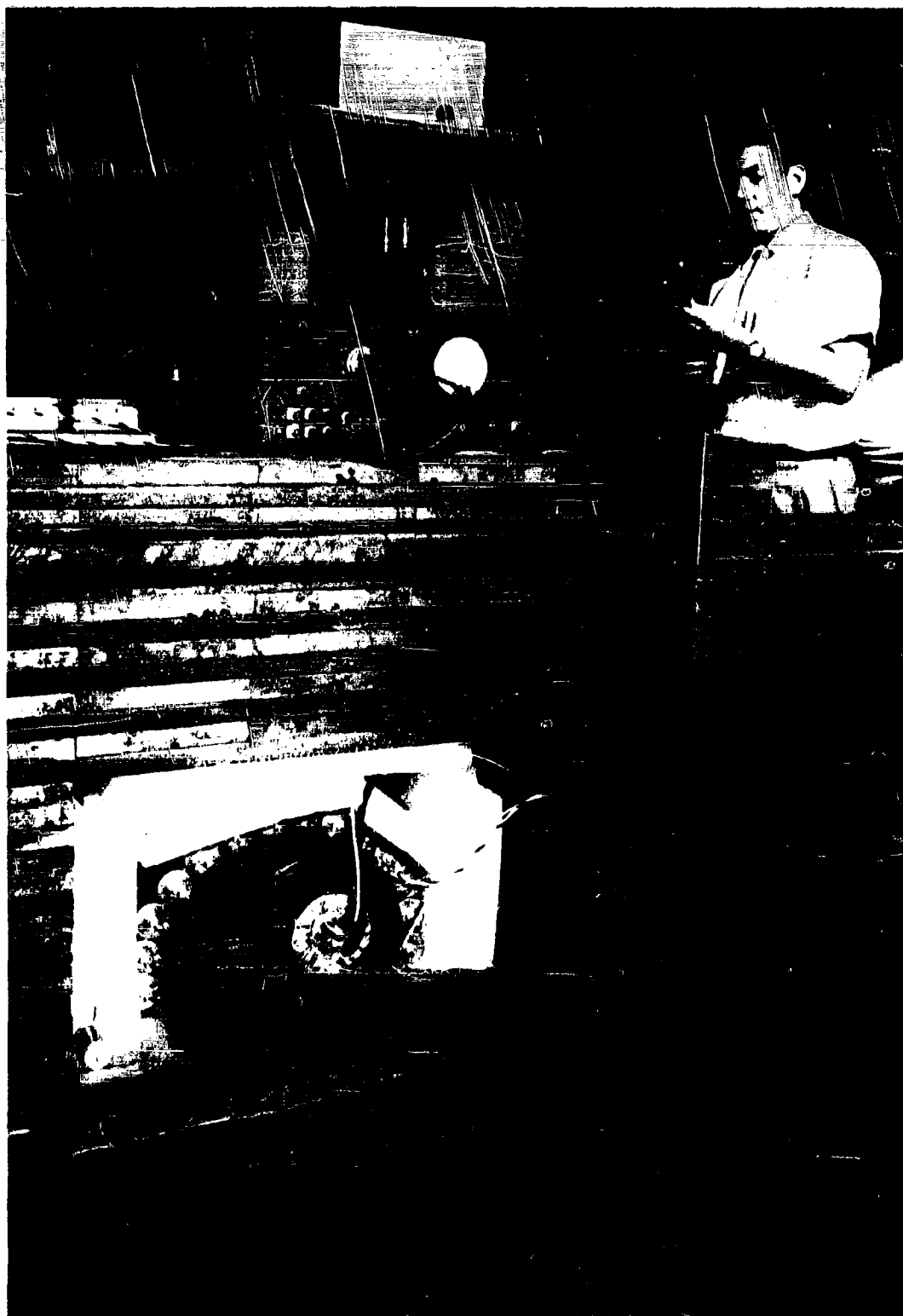


Figure 1.2
Carbon-14 Counter and Associated Shielding

times with the standard activity remaining constant within the statistical error. The statistical errors of the results are based on counting statistics only. All other errors are considered to be negligible.

RESULTS AND DISCUSSION

Results

The results of the analyses of carbon-14 concentrations in tropospheric air at Washington Township, New Jersey for the period January 1960 through April 1961, are summarized in Table 1.1 and graphically represented in Figure 1.3. To facilitate comparison of our data with similar results obtained at other laboratories the following presentation was adopted. The carbon-14 concentrations are expressed with reference to the commonly used NBS oxalic acid according to the formula

$$\delta C^{14} = \frac{A_{\text{sample}} - 0.95 A^{\circ}\text{oxalic acid}}{0.95 A^{\circ}\text{oxalic acid}} \times 100$$

where A_{sample} is the measured carbon-14 activity of the sample and $A^{\circ}\text{oxalic acid}$ is the carbon-14 activity of the NBS oxalic acid standard corrected for radioactive decay between 1 January 1958 and the date of measurement of its activity. (This correction is virtually negligible.) Strictly speaking it is not possible to compare the δC^{14} data in carbon dioxide samples with δC^{14} in plants because of possible isotopic fractionation processes occurring during the photosynthetic process. This is usually overcome by monitoring the C^{13}/C^{12} ratios in all samples and finally normalizing all results to a common C^{13}/C^{12} ratio. Unfortunately this was not possible with our data but it may be pointed out that this could mean a reduction of about 3% in the carbon-14 results of Washington Township carbon dioxide when compared to the data of Broecker and Walton³, and Broecker and

Table 1.1 Radiocarbon Concentrations in Tropospheric Air at Washington Township, New Jersey

<u>Collection Period</u>	<u>δC^{14}</u>
19 Jan - 25 Jan 1960	+ 20.85%
2 Feb - 9 Feb 1960	+ 20.00%
23 Feb - 1 March 1960	+ 18.45%
1 March - 8 March 1960	+ 22.43%
29 March - 5 April 1960	+ 22.40%
5 April - 12 April 1960	+ 16.00%
26 April - 3 May 1960	+ 18.24%
24 May - 31 May 1960	+ 20.82%
28 May 1960 (oak leaves)	+ 17.78%
21 June - 26 June 1960	+ 19.73%
26 July - 2 Aug 1960	+ 20.76%
23 Aug - 6 Sept 1960	+ 18.10%
6 Sept - 20 Sept 1960	+ 19.57%
27 Sept - 4 Oct 1960	+ 17.19%
4 Oct - 11 Oct 1960	+ 17.19%
1 Nov - 17 Nov 1960	+ 14.09%
1 Dec - 11 Dec 1960	+ 12.02%
31 Dec 1960 - 18 Jan 1961	+ 9.04%
18 Jan - 25 Jan 1961	+ 15.42%
18 Jan - 25 Jan 1961 (Closter, N. J.)	
1 Feb - 8 Feb 1961	+ 19.13%
16 March - 3 Apr 1961	+ 20.42%
16 Apr - 1 May 1961	+ 15.63%

Counting error = + 1.5% except for samples collected 5-12 April 1960, and 18 Jan - 25 Jan 1961 (Closter, N. J.) which, because of small size, had an error of $\pm 2.5\%$

FIG. 1.3

VARIABILITY OF CARBON-14 CONCENTRATIONS IN TROPOSPHERIC CARBON-DIOXIDE AT WASHINGTON TWP., N. J. AND STRONTIUM-90 IN RAIN AT WESTWOOD, N. J.

Month	^{14}C (percent) (Open Circles)	^{14}C (percent) (Solid Circles)
J	18.0	30.0
F	18.5	28.0
M	19.0	25.0
A	19.5	22.0
M	20.0	20.0
J	20.5	18.0
J	21.0	16.0
A	21.5	14.0
S	22.0	12.0
O	22.5	10.0
N	23.0	8.0
D	23.5	6.0
J	24.0	4.0
F	24.5	2.0
M	25.0	1.0

VARIABILITY OF CARBON-14 CONCENTRATIONS IN TROPOSPHERIC CARBON-DIOXIDE AT WASHINGTON TWP, N. J. AND STRONTIUM-90 IN RAIN AT WESTWOOD, N. J.

STRONTIUM-90 CONCENTRATIONS IN RAIN
($\mu\text{Ci}/\text{mi}^2/\text{in}$)

0615

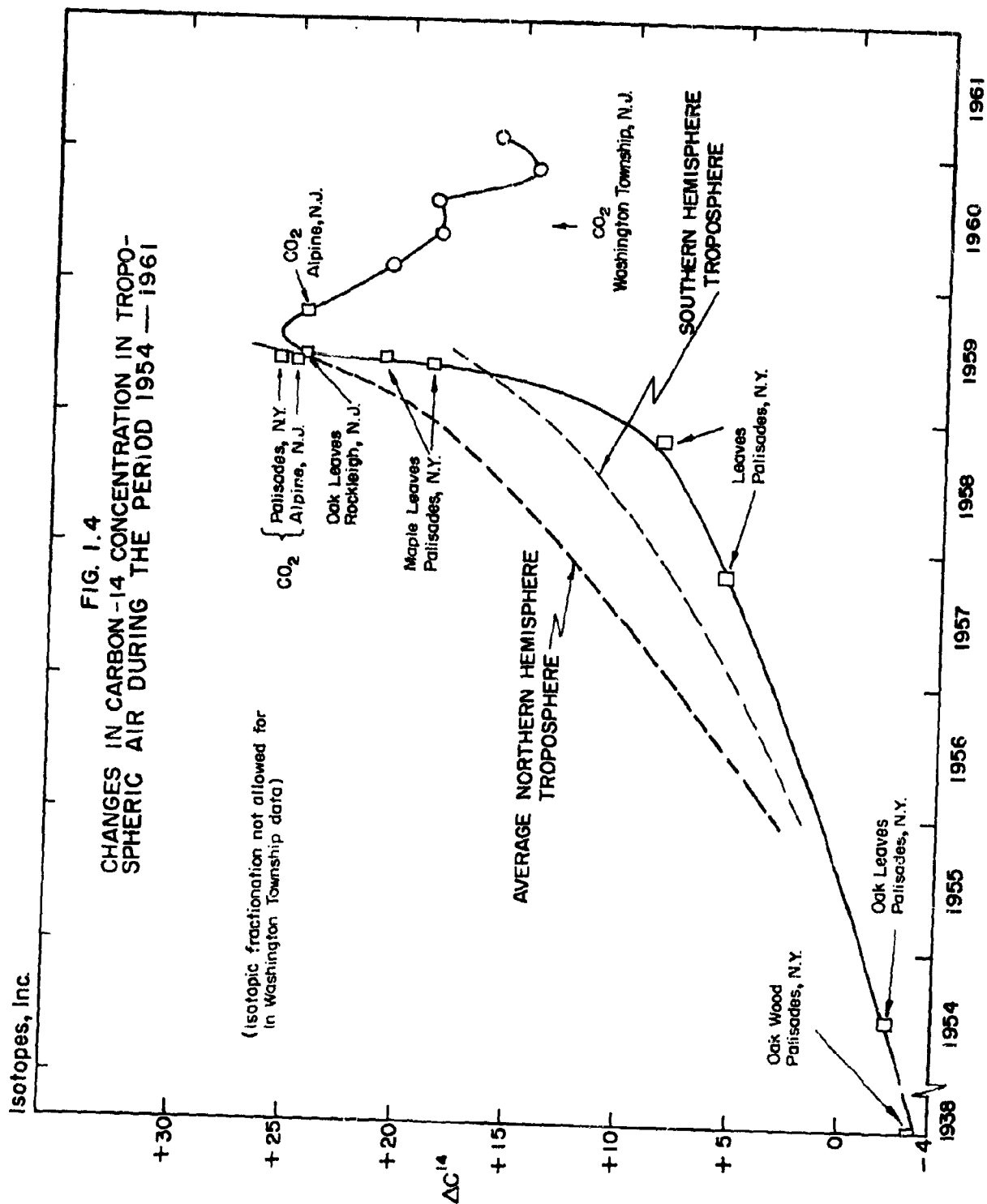
1961

0961

Olson⁴, which are also given in Figure 1.4. In this diagram our data are represented as quarterly averages of the carbon-14 concentrations in tropospheric air. Also indicated in Figure 1.3 is the variability of strontium-90 concentrations in precipitation at Westwood, New Jersey, observed during 1960 and early 1961. This area is close to the regions for which carbon-14 results are available (Washington Township, New Jersey, Palisades, New York, Rockleigh, New Jersey and Alpine, New Jersey) and further serves to show the rate at which nuclear debris entered the troposphere from the stratosphere during this period under examination.

Discussion

Two features of the variability of carbon-14 concentrations in tropospheric air are distinguishable in Figures 1.3 and 1.4. First the concentrations at Washington Township do not exhibit smooth variations with time. There is a pronounced minimum in the curve of concentrations with time during the month of January 1961. It appears that the decline in carbon-14 activity in air, as shown in Figure 1.3 commenced probably in August with only an intermittent rise occurring in September 1960. Following the minimum in January 1961, the radiocarbon concentrations in tropospheric air at Washington Township underwent a sharp increase which continued through March 1961. Although the strontium-90 concentrations in precipitation in the immediate vicinity⁵ indicate that there was a definite increase in the rate of influx of stratospheric debris into the troposphere during the spring of 1960, the carbon-14 concentrations give no apparent indication of a similar behavior. Indeed, if such an injection of carbon-14 from the stratosphere did occur then it was masked by removal or dilution of carbon-14 during the period of injection. There is additional evidence in favor of spring increase in the release of weapons debris from the stratosphere



manifesting itself in the form of higher concentrations of tritium in precipitation of Westwood, New Jersey. These data will be discussed in the following chapter.

The solid curve in Figure 4.1 appears to indicate that the decrease in carbon-14 concentration in tropospheric air which occurred in 1960 at Washington Township, New Jersey was part of a more general decrease in this area which commenced in late 1959. The question of most importance is whether the data obtained at 41°N latitude reflect the behavior of bomb carbon-14 in the northern hemisphere or whether the changes observed are typical only of a restricted area. Superimposed on the results from the New York metropolitan area are two curves taken from a recent U. N. publication⁶ which represent average concentrations for the two hemispheres for the period of interest. Admittedly these curves are drawn from limited data, and therefore they must be considered as idealized. The reason for the New York area results lying somewhat below the average for the northern hemisphere has been attributed to a latitudinal effect in the influx of bomb carbon-14 into the troposphere from the stratosphere.⁹ Some of the earlier results, however, appear to lie below the idealized curve for the southern hemisphere.

If the curve shown in Figure 1.4 for the New York area is typical for the northern hemisphere, there are certain far-reaching implications. It is generally assumed that the bomb carbon-14 now present in the stratosphere and troposphere will gradually equilibrate with the carbon in other reservoirs, the largest of which is the ocean. The rates at which this equilibration will occur with the ocean have been calculated from the steady state distribution of naturally occurring carbon-14 and the Suess effect⁷. It is possible to estimate this rate of exchange with the oceans from our data and the results of Broecker and Olson⁴ for 1959. In the simplest situation, if it is assumed that there has been no further addition of bomb

carbon-14 to the troposphere from mid-1959 to mid-1960 and there is no net return of bomb carbon-14 from the oceans to the troposphere, the following first order equation describing the rate of change of the number of carbon-14 atoms in the troposphere may be applied.

$$\frac{dN_T}{dt} = -k N_T$$

Since the bomb carbon-14 concentrations decreased by almost of a factor of 2 from mid-1959 to mid-1960 the value of the constant k is $0.7(\text{year})^{-1}$, and thus the mean life of carbon-14 in the troposphere before transfer to the oceans is calculated to be 1.4 years. Of course any addition of bomb carbon-14 from the stratosphere or oceans to the troposphere will reduce this mean residence time. This result is considerably lower than found by previous and more refined calculations which yielded values in the region of 5-7 years. In addition to the aforementioned assumptions it is also tacitly assumed that there was no mixing between the northern and southern hemispheres. Broecker and Olson⁴ endeavoured to construct a model of the exchangeable carbon reservoirs and predict the fate of bomb carbon-14 using the best estimates of time constants which were available. Their predictions indicated a rise for the concentrations of carbon-14 in the troposphere of the northern and southern hemispheres for 1960 and not a decrease as observed in our results. It appears, therefore, that if previous data on the rates of exchange between the atmosphere and ocean are correct, then our findings must be the result of some local effects and this area cannot be considered typical for any calculations on a world-wide basis.

A possible local effect which could cause such a decrease in carbon-14 concentrations in the troposphere during 1959-60 is the release of large amounts of carbon-14-free carbon dioxide by the burning of fossil fuels. The presence of heavy industry in New York and New Jersey lends credence to the possibility that this could be important in restricted zones. On a larger scale it is possible to predict the instantaneous effect of the release of given amounts of carbon dioxide. Revelle and Suess⁸ have estimated that in 1959 approximately 10^{16} g carbon dioxide or 3×10^{15} g carbon were released to the atmosphere. If this were confined to the 40°-60°N latitude band (in which most of the fossil fuel is probably burnt) and released instantaneously to the atmosphere it would produce an immediate reduction in the carbon-14 concentration of 5 percent in this latitude band. Mixing outside the bands and the fact that the release is not instantaneous will naturally serve to reduce this effect considerably. If a smaller area is considered, in particular a heavily populated and industrialized zone, it appears feasible that a transient reduction of about 10 percent in the carbon-14 concentration in the troposphere could occur. It would, of course, require optimum meteorological conditions to prevail and this may be restrictive. There is definite evidence, however, which suggests that local effects of the burning of fossil fuel could be important. Indeed Suess effects of 3.5 - 4 percent reduction in the carbon-14 concentration in the biosphere have been observed, as opposed to other areas where the effect amounts to a reduction of only 1.5 - 2 percent.

SUMMARY

From this very limited study it may be concluded that the simple theories describing the uniform addition of carbon-14 from the stratosphere to the troposphere and removal by the oceans, etc. are not applicable in restricted areas. Data from the New York area are in conflict with accepted theories on the rate of exchange of carbon dioxide between the atmosphere and oceans. It is likely that the rapid decreases in carbon-14 concentrations in tropospheric air at Washington Township are the result of local "Suess Effects" and future concentrations should increase from the minimum observed in January 1961. Continued observation of tropospheric air concentrations of carbon-14 will be valuable not only for determining the fate of nuclear bomb radiocarbon, but also for throwing light on the possible variation of Suess Effects which may have occurred prior to testing. This latter information is particularly valuable in radiocarbon dating problems.

REFERENCES

1. Hagemann, F. T., Gray Jr., J., Machta, L., and Turkevich, A., "The Stratospheric Content of Carbon-14, Carbon Dioxide and Tritium," *Science*, 130, 542 (1959)
2. Munnich, K. O., and Vogel, J. C., Paper given at Radiocarbon Conference, Groningen, September, 1959.
3. Broecker, W. S., and Walton, A., "Radiocarbon from Nuclear Tests," *Science*, 130, 309 (1959)
4. Broecker, W. S., and Olson, E. A., "Radiocarbon from Nuclear Tests II," *Science*, 132, 712 (1960)
5. Walton, A., "Tungsten-185 in Precipitation and the Seasonal Variations in Fall-out," *Nature*, 188, 220 (1960)
6. "Radiocarbon from Nuclear Tests," A/AC.82/R.105 United Nations Scientific Committee on the Effects of Atomic Radiation, 14 July 1960.
7. Suess, H. E., "Radiocarbon Concentration in Modern Wood," *Science*, 122, 415 (1955)
8. Revelle, R., and Suess, H. E., *Tellus*, 9, 18 (1957)
9. Tauber, H., "Latitudinal Effect in the Transfer of Radiocarbon from Stratosphere to Troposphere," *Science*, 133, 461 (1961).

CHAPTER 2

MEASUREMENTS OF TRITIUM IN PRECIPITATION

Studies of tritium concentrations in precipitation at various sites throughout the world are important from two standpoints. Firstly, if the studies are conducted on a continuous basis during and after weapons testing the results will yield information on both stratospheric and tropospheric mixing processes. Secondly, the results, in conjunction with other data on tritium distribution, may be used to obtain much information on the hydrological cycle on a local and world-wide scale.

Like carbon-14, tritium is also produced in the upper atmosphere by natural processes, and thus we have a constant tritium background in precipitation, surface and ground waters. Natural tritium has been used in investigations of the physical processes of the hydrological cycle in much the same manner as bomb-produced tritium. Because of the higher tritium concentrations experienced during weapons testing periods, which make the measurement of this nuclide much easier, and the fact that these elevated concentrations have appeared in pulses, the uses of bomb tritium have outnumbered those of natural tritium. Unfortunately, however, the lack of documentation of tritium concentrations in precipitation has prevented the more widespread use of this tool.

In the work which has been conducted as part of HASP, we have concentrated more on the application of the results to the fallout problem rather than on the hydrological implications. Comparison of the tritium and strontium-90

concentrations in precipitation at Westwood, New Jersey indicates a remarkable similarity in behavior of the two nuclides. It is believed that the observed variations indicate that the tritium produced in weapons tests behaves in a manner which is rather strongly dependent on the type and place of detonation of the shot, i. e., whether it is an air or ground burst, and whether it is detonated in the humid tropics or the drier areas to the north. Comparison of our data with those from other laboratories confirms the levels of the concentrations in this area, with the exception that rains in Bedford, Massachusetts appear to have had tritium concentrations which were almost an order of magnitude lower than those at Westwood, New Jersey, Chicago and Ottawa.

EXPERIMENTAL PROCEDURES

Sample Collection

All precipitation samples were collected in receivers on the roof of the building at Isotopes, Inc., in Westwood, New Jersey. Individual rains were usually collected in a polyethylene tub 30 inches by 15 inches by 6 inches deep situated alongside other collectors which were being exposed as part of the AEC fallout program. After the sample was collected it was transferred to a smaller glass or polyethylene container for storage while awaiting analysis.

Enrichment of Tritium in Precipitation Samples

In the majority of precipitation samples the tritium concentration was so low that it could not immediately assayed. It was necessary, therefore, to

enrich the tritium relative to the other hydrogen isotopes in water to the point where the tritium concentration in a given volume of water was much higher than in a similar volume of the original precipitation sample and could be determined with ease. The amount of tritium enrichment which occurs in such a process can be followed by monitoring the deuterium concentration in the sample both before and after enrichment. The enrichment procedure used at Isotopes, Inc., is a well-known electrolytic method developed by Kaufman and Libby¹ and is described in the following sections.

The precipitation sample is first distilled to remove suspended and dissolved impurities and a few milliliters are reserved for deuterium assay. A 250 ml aliquot of the distillate is then placed in a glass enrichment cell and 1 gram of sodium peroxide, which serves as the electrolyte, is added. The cell is placed in a cooling bath which maintains the temperature of the solution at about 10°C during the electrolysis. The iron cathode and nickel anode are inserted and the sample is electrolyzed with about 5-7 amperes direct current. About 8 samples can be processed together and the desired volume reduction occurs in 3 to 4 days.

When the sample has been reduced in volume to about 5 ml, the solution is neutralized by bubbling carbon dioxide through it to prevent excessive loss of hydrogen as sodium hydroxide. After neutralization, the sample is distilled to dryness and the final volume of water is measured. The distilled sample is stored in a tightly capped vial until deuterium and tritium analyses can be performed.

Deuterium and Tritium Assays

Deuterium analyses which, as mentioned previously, are required to determine accurately the tritium enrichment factors, are performed using the well-established falling drop method. The procedure used has been described in detail by Kirshenbaum². Essentially the method depends upon the relationship between the density of the water sample and its deuterium concentration. For a constant drop size the rate of fall of a given drop of water through a liquid, immiscible with and less dense than water, is directly related to the deuterium concentration of the water. A micro-pipette is used to deliver the water drops and a constant temperature bath is used to maintain the temperature of the immiscible organic liquid (in our case o-fluorotoluene) at $27 \pm 0.05^{\circ}\text{C}$. With this system the standard deviation of the determination is about $\pm 5\%$.

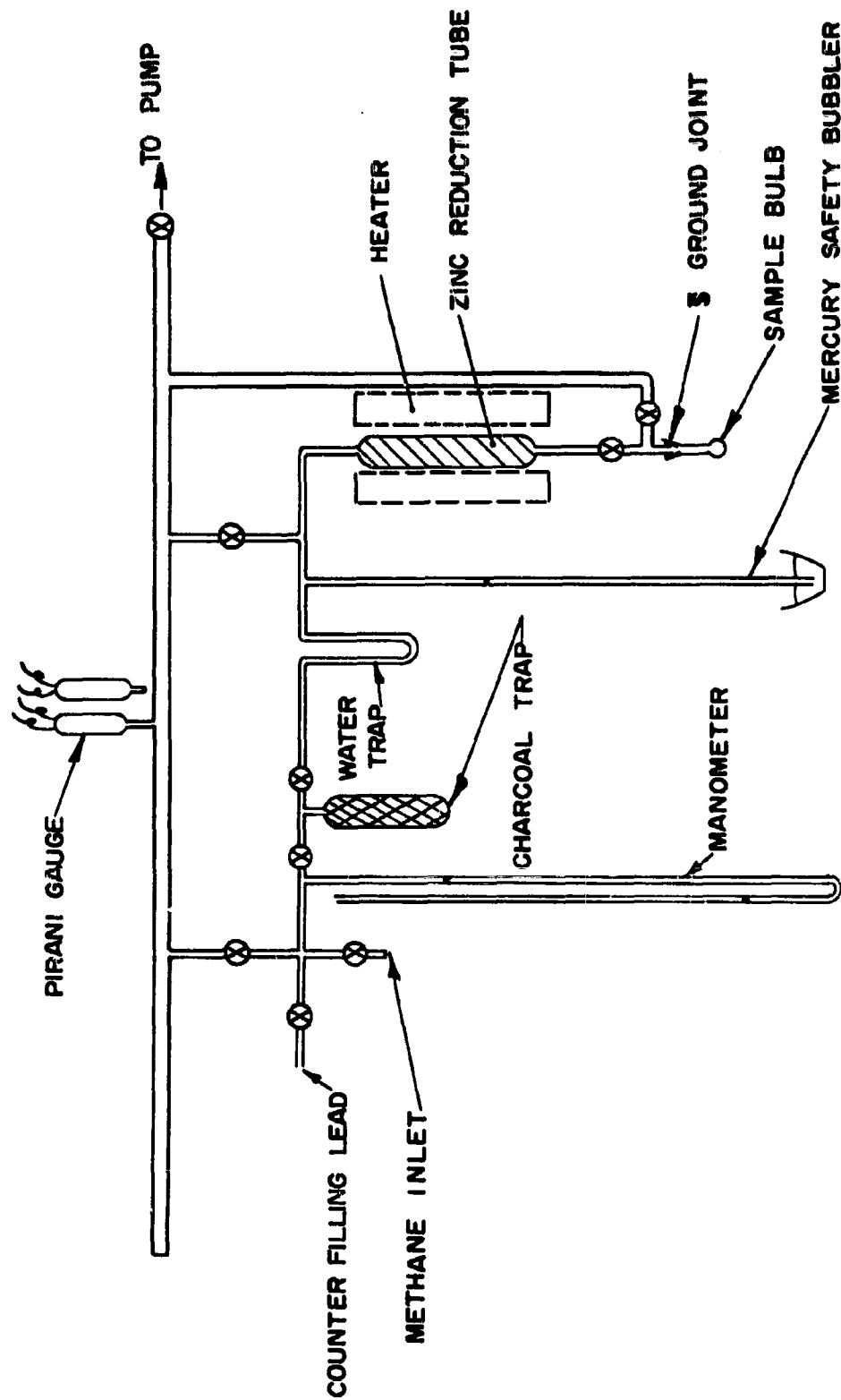
The above method has one limitation in that it is extremely difficult to determine accurately low concentrations of deuterium such as are present in the original precipitation sample. A mass spectrometric assay is to be preferred at these concentrations. Since this was not available at the time, the natural abundance of deuterium in precipitation, 0.015 mole percent, was assumed. Any deviations from this value for the deuterium concentration in precipitation are not likely to cause an error of more than ± 3 percent in the enrichment factor used in the calculation of the tritium concentrations in the precipitation. This estimation of the uncertainty is based on the observed variability of deuterium concentrations in rains determined by Friedman and Smith³.

Following the electrolysis, another aliquot of 1.1 ml of the distilled water is converted to hydrogen by passing it over reagent grade, 20 mesh granular zinc at 400 °C (see Figure 2. 1). The possibility of any isotopic fractionation occurring during this reaction is eliminated because the reaction is quantitative. The hydrogen produced is adsorbed on activated charcoal at liquid nitrogen temperatures so as to maintain a low pressure within the conversion system. When the reaction is complete the liquid nitrogen is removed from the charcoal trap and the hydrogen allowed to desorb and enter an evacuated proportional counter. C. P. grade methane is added to the hydrogen in the counter until a ratio of about 75 percent hydrogen, 25 percent methane is attained at a total pressure of 1000 mm Hg. Recordings of the temperature and pressure of the hydrogen are made to enable the exact volume of hydrogen in the counter to be calculated. It has been determined that the counting efficiency for tritium, under the above conditions, is not affected significantly by varying the percentage of hydrogen in the counting mixture over a range from 10 to 98 percent.

Two identical counters are used for the tritium activity measurements. The counters have an active volume of 1.01 liters and are surrounded by one inch of mercury, a ring of 23 G-M cosmic ray counters operated in anti-coincidence with the sample counters, 4 inches of paraffin wax, and 18 inches of hot rolled steel. The associated electronics were specially constructed at Isotopes, Inc., in connection with other programs which involved measurement of natural tritium concentrations.

Each sample is counted for a period sufficient to reduce the statistical error of counting to less than ± 3 percent. With the backgrounds of the two

FIG. 2.1 GAS HANDLING SYSTEM FOR TRITIUM



counters being 18.0 and 20.0 counts/min these statistics are usually obtained by counting the samples overnight. Background measurements are performed daily with C. P. grade tank hydrogen as the counter filling gas. Comparison of this gas with hydrogen from unenriched deep sea-water samples indicates the absence of any measurable activity.

Accuracy, Reproducibility and Theoretical Considerations

The counters are calibrated routinely about once every four weeks with an NBS standard tritium solution. Based on this standard our counters have an efficiency of 85 ± 2 percent. The count rates of the standard have been found to be reproducible to within ± 2 percent.

As a check on the enrichment procedure a sample of the NBS tritium standard was spiked with deuterium to a concentration which was directly measurable by the falling-drop method. Three aliquots were then enriched separately according to the above procedures and the final tritium and deuterium concentrations were measured. The original tritium concentration was then calculated from the final tritium measurement and the known deuterium enrichment which occurred during the electrolysis. The results of these experiments are shown in Table 2.1. It is observed that there is excellent agreement between the three enriched samples but all three are consistently lower than the unenriched tritium standard by about 13-14 percent. The reason for this discrepancy is not clear at the present time but it may be related to the fact that our enrichment procedure is not exactly the same as Libby's original system. Consequently the enrichment factors may be slightly different. Nevertheless, the fact that our data may be low by about 13

Table 2.1. Results of Experiment to Check Enrichment Procedures

Sample	Procedure	Original Tritium Concentration (T. U.)
R	Unenriched	2200
R-1	Enriched	1920
R-2	Enriched	1930
R-3	Enriched	1890

percent or so does not seriously alter any of our conclusions.

It has been mentioned previously that the extent of the tritium enrichment which occurs during the electrolysis is calculated from the measured enrichment of deuterium which occurs at the same time. These quantities are related as follows:

$$\frac{dP}{P} = \alpha \frac{dD}{D} = \beta \frac{dT}{T} ,$$

where P = number of moles of protium,
 D = number of moles of deuterium,
 T = number of moles of tritium.

If this equation is integrated over the limits of initial and final conditions where $P \gg D \gg T$,

$$\frac{V}{V_0} = \left(\frac{D}{D_0} \right)^\alpha = \left(\frac{T}{T_0} \right)^\beta ,$$

$$\text{or } T_0' = T' \frac{V}{V_0} \left[\frac{D_0' V_0'}{D' V} \right]^{\alpha/\beta} .$$

The primed quantities are now in molar fractions, V_0 is the initial volume, D_0' and T_0' the initial deuterium and tritium concentrations respectively. The remaining quantities, with the exception of α and β , represent the final values after enrichment. For the conditions of these experiments Kaufman and Libby¹ have shown that the value of β/α is equal to 2.1 ± 0.1 and this value was used in our calculations.

RESULTS AND DISCUSSION

The results of the tritium determinations in precipitation at Westwood, New Jersey are given in Table 2.2. Tritium concentrations are expressed in tritium units (T. U.), where 1 T. U. is equivalent to 1 tritium atom per 10^{18} hydrogen atoms. Also given in Table 2.2 are the dates when the rains occurred at Westwood and the quantity of rain which fell during the storm, as measured in a standard 8 inch rain gauge.

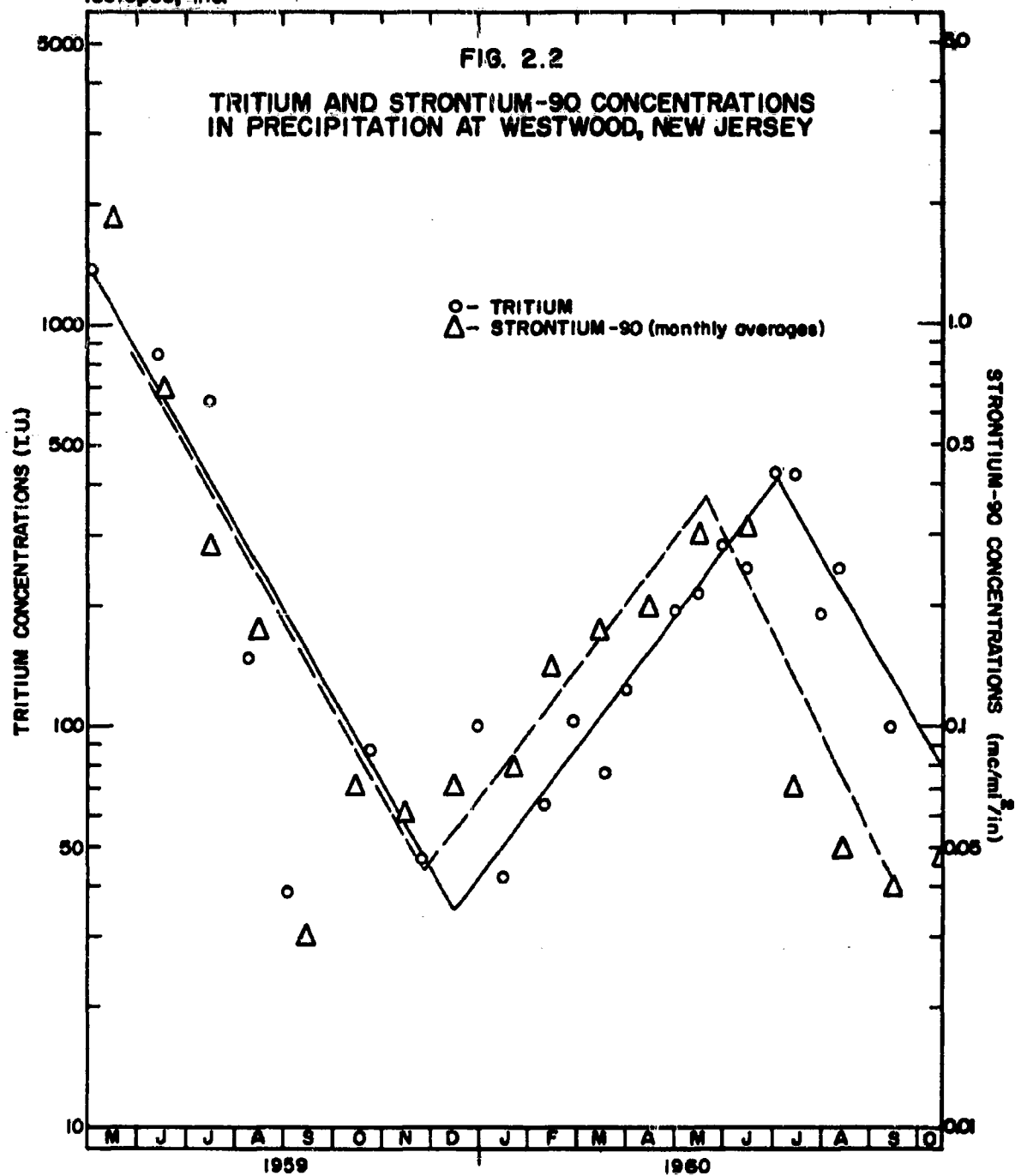
In Figure 2.2 the tritium concentrations are plotted as a function of time together with the average monthly concentrations of strontium-90 observed during the same period. From the spring of 1959 to the fall of 1960 it is clear that there is remarkable agreement in the variability of the concentrations of the two nuclides. One is led to the obvious conclusion that at this time the strontium-90 and tritium in rain are governed by similar mechanisms. Since the major fraction of the bomb debris deposited in this area during the spring of 1959 was derived from the Soviet tests carried out in the Arctic regions in the fall of 1958⁴, it is likely that the majority of the tritium can also be attributed to this source for 1959. The spring peak in nuclide concentrations observed in 1960 can be explained in a straight forward manner for strontium-90 but not so for tritium. It is believed that the strontium-90 is derived mainly from tests, other than Soviet, which were conducted in 1958, i. e., U. S. A. Hardtack series and U. K. Grapple series. Probably included also in the strontium-90 fallout is a small contribution from the high altitude detonations Teak and Orange. The source of the tritium in 1960 is not so clear. According to the early theory of Begemann and Libby⁵, the tritium

Table 2. 2. Tritium Concentrations in Precipitation at Westwood, New Jersey

Collection Date	Inches of Rain	Tritium Units (T/H x 10 ¹⁸)
28 Apr 59	0.95	1435
1 May 59	0.34	1370
13 Jun 59	1.00	843
14 Jul 59	0.22	650
9 Aug 59	2.10	148
2 Sep 59	0.92	38.5
24 Oct 59	1.41	86.5
25 Nov 59	1.33	46.5
29 Dec 59	1.10	100
14 Jan 60	0.82	42.0
11 Feb 60 *	1.02	62.9
11 Feb 60 *		65.6
26 Feb 60	1.07	102
18 Mar 60	0.28	76.0
31 Mar 60	0.74	123
27 Apr 60	0.40	193
12 May 60	0.28	213
31 May 60	0.30	282
18 Jun 60	0.20	249
2 Jul 60	0.48	432
15 Jul 60	0.84	431
31 Jul 60	2.80	190
11 Aug 60	1.49	249
13 Sep 60	5.01	100
17 Oct 60	0.50	75

Analytical error is about $\pm 10\%$

* Duplicate analysis



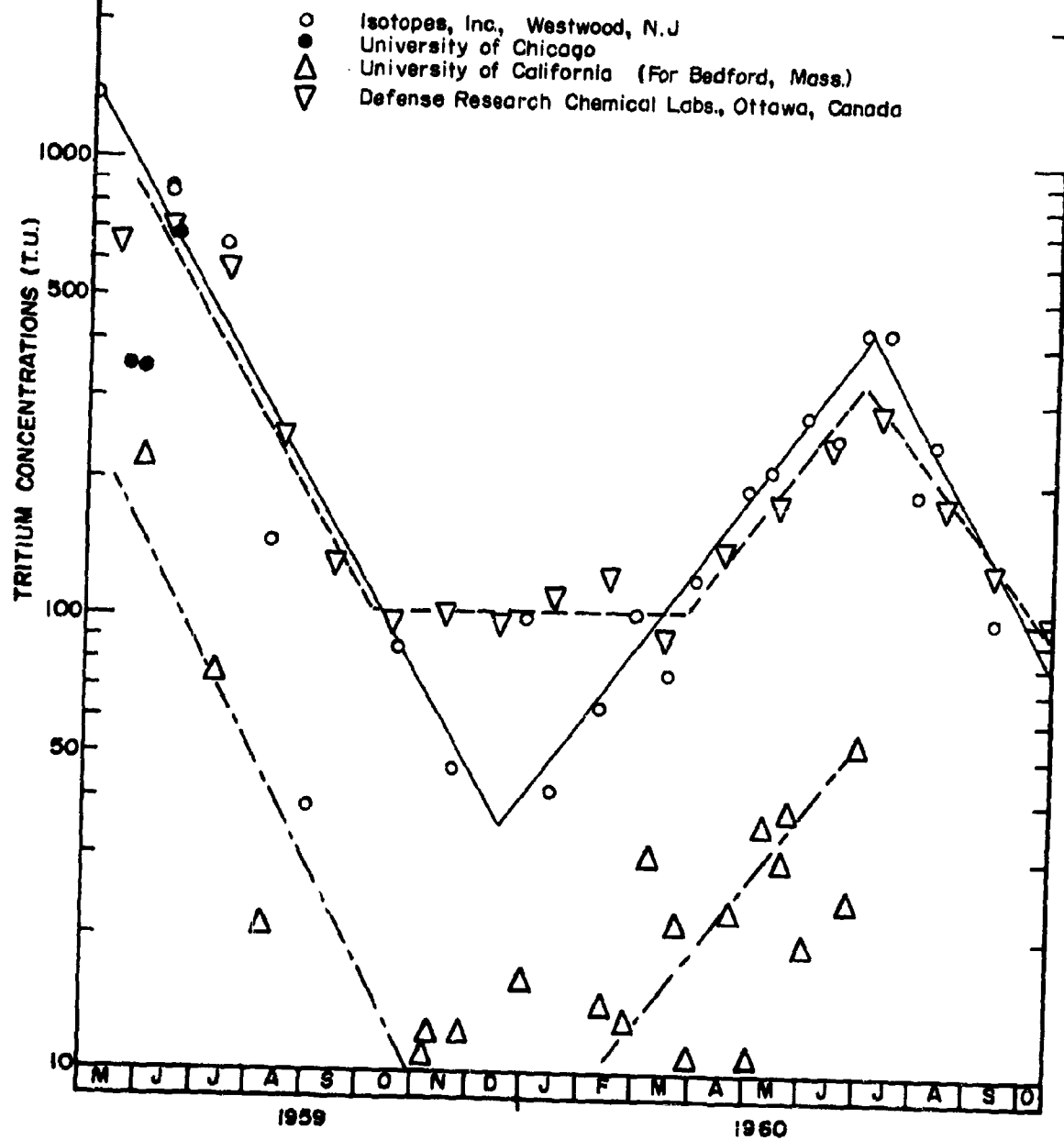
produced in weapons tests possesses a much shorter residence time in the stratosphere than the fission products. It is believed that the tritium, which is produced, or is present in the weapon, is rapidly oxidized to water, and in the case of the Castle test series the large amounts of water vaporized by the weapon thus became labelled with tritium. Since the particles of ice and supercooled water were much larger than those containing the fission products, they settled rapidly, descended into the troposphere where they melted and were precipitated in rain. Libby⁵ suggests that the exponential decay of tritium concentrations in precipitation in 1954 following the Castle series (with a mean residence time $\tau \sim 40$ days) is indicative of the stratospheric residence time rather than a tropospheric residence time of similar magnitude found for particulate debris. Von Buttlar and Libby⁶ cite a value of 3 days for the residence time of moisture in the troposphere. The existence of a spring peak in tritium concentrations in precipitation in 1959, not apparent in our data but clearly visible in the results of Brown⁷, and again in 1960 are indications that the Begemann and Libby picture is not adequate to explain all results, since the last major detonation of a nuclear device took place in October 1958. An alternative explanation may be proposed to explain the tritium concentrations observed in precipitation from 1954 through 1959. If, as is quite likely, the rate of removal of stratospheric tritium is dependent on the type and the place of detonation, most of the tritium data may be explained. When a device is exploded in the tropics, as was the case for many of the United States and United Kingdom tests, then there is much water vapor carried up into the stratosphere with the remainder of the debris.

The cooler temperatures prevailing at higher altitudes cause the water to freeze or supercool and fall out rapidly in much the same way as proposed by Begemann and Libby. Exploding the device on a barge at sea in these low latitudes will increase the possibility of occurrence of this mechanism. On the other hand, if the device is detonated at higher latitudes in less humid conditions and, in particular, if it is an air burst, there is much less moisture carried into the stratosphere with the other debris. Consequently any tritium present as water now has a much better chance of remaining in the vapor phase in the stratosphere. Fallout of tritium would, therefore, not be as rapid under these latter conditions. Such a mechanism would adequately explain the peak concentrations observed in precipitation during the spring of 1959 five months after the last major explosion. As mentioned previously, most of the radioactivity deposited in the northern hemisphere at that time originated from the Soviet tests of 1958, which were performed in the relatively dry Arctic regions.

The 1960 spring peak in tritium, as shown in Figure 2.2, is much lower than in 1959. That this observation is also related to meteorological phenomena is much clearer from additional data obtained by Brown (see Figure 2.3) than from our results. Prior to testing the concentration of tritium in Ottawa rains was 15 T. U., but with subsequent releases of tritium the base level between peaks gradually rose to 100 T. U. Brown accounts for this rise by evaporative recycling of surface waters, which in late 1959 possessed a tritium concentration in the Ottawa region of 300 T. U. Thus, the remaining 200 T. U. must be the result of further injections of tritium from the stratosphere. In the New York area it is

Isotopes, Inc.

FIG. 2.3
INTERCOMPARISON OF TRITIUM CONCENTRATIONS
IN RAIN FROM FOUR AREAS



likely that the base level of tritium in rain is somewhat lower than the 100 T. U. because of greater contributions of Atlantic Ocean water, with a much lower tritium content than 300 T. U., to the precipitation in our area. This is also apparent from the fact that our results for late 1959 decrease to a value of about 40 T. U. compared to 100 T. U. for the same period in Ottawa⁷ (see Figure 2.3). It must therefore be concluded that the most likely reason for the high tritium concentrations experienced in the spring of 1960 is a further injection of tritium from the stratosphere in a manner similar to that experienced by particulate debris. The exact source or sources of this material is more difficult to establish, particularly since we have no stratospheric data available for tritium. If such information were available it might be possible to assess whether Teak and Orange, the high altitude detonations, are contributing much to the tritium fallout at this time. There is no doubt, however, that the 1960 tritium must have been derived from past tests and is probably a complex mixture of material with the majority coming from the 1958 test series.

It must be pointed out that the above suggestions imply that tritiated water, when it enters the troposphere from the stratosphere, behaves in a manner similar to any accompanying particulate material. The 1959 results from Westwood suggest that the mean residence time (T) of water in the troposphere is 40 days, the same as for strontium-90 (Figure 2.2). If it is accepted that the tritium from the Castle test series also exhibited such a residence period in the troposphere, an extremely rapid northward movement of tritium must be visualized following the detonation for the peak tritium concentrations to appear at Chicago so soon after

the explosion. The residence time for this particular tritium in the stratosphere must, therefore, be only a few hours to a few days. It is interesting to note from the above considerations that the residence times of tritium in the stratosphere appear to be much shorter than those for particulate material from the same detonations.

The results from Westwood, New Jersey may be compared with similar data obtained elsewhere. In Figure 2.3 our tritium results are plotted as a function of time together with measurements performed at Chicago⁸, Ottawa, and the University of California⁹. The rains measured at the latter station were actually collected at Bedford, Massachusetts, and should be almost directly comparable with the results from Westwood because similar meteorological conditions govern the weather in the two areas. It is noted, however, that the Bedford results are almost an order of magnitude lower than the data obtained at comparable times at Westwood. Furthermore, it is obvious that good agreement exists between the tritium concentrations in rain at Westwood and those measured at a more northerly station than Bedford, Massachusetts, namely Ottawa, Canada. It would appear, therefore, that unless unique meteorological conditions influence the tritium concentrations in rain at Bedford, there is a consistent difference in the results from the four stations. Since the agreement is good for three of the stations it may be concluded that the results from Bedford, Massachusetts are probably low because of a calibration uncertainty. Further intercalibrations among the four laboratories appear necessary before any other deductions are made.

SUMMARY

The fallout of tritium in 1959 and 1960 was found to follow very closely the deposition of strontium-90 during these years thus indicating that similar factors probably govern the release of these materials from the stratosphere and their removal from the troposphere. Since the peak concentrations in the spring of 1959 and 1960 occur several months after the cessation of nuclear tests, it is suggested that the fallout rate of tritium must be related to the area and type of detonation. It is further hypothesized that tests conducted in the humid tropics, and particularly so if they occur in barges at sea, will result in a very rapid removal of tritium from the upper atmosphere. Those tests performed in drier areas will yield much longer residence times for tritium in the stratosphere. The former suggestion is similar to that proposed by Begemann and Libby to explain the fallout of tritium following the Castle shot except that we believe that the exponential decay of tritium concentrations in precipitation following the peak is related to the rate of cleansing of the troposphere rather than to the removal from the stratosphere. In all cases, between 1954 and 1960, when tritium concentration reach a peak, it has been noted⁷ that the decrease of concentration from the peak value followed an exponential decay with a half-time of about 28 days.

From a comparison of the data obtained at four laboratories during 1959 and 1960 it is suggested that the results from Bedford, Massachusetts are too low. Further intercalibration between laboratories may reveal the reason for this discrepancy.

It would be useful, in establishing the source of tritium in precipitation during 1960 and future years, to have more information on tritium in the stratosphere for this period. In spite of this lack of data it is likely that the 1960 peak in tritium concentrations, which is almost certainly a result of influx of tritium from the stratosphere, is derived from a number of nuclear tests conducted in 1958, with some contribution from the high altitude rocket detonations Teak and Orange and from tests of previous years.

REFERENCES

1. Kaufman, S., and Libby, W. F., "The Natural Distribution of Tritium," *Phys. Rev.*, 93, 1337 (1954).
2. Kirshenbaum, I., "Physical Properties and Analysis of Heavy Water," McGraw Hill Book Co., 324 (1951).
3. Friedman, I., and Smith, R. L., "The Deuterium Content of Water in some Volcanic Glasses," *Geochim. et Cosmochim. Acta*, 15, 218 (1958).
4. Walton, A., "Studies of Nuclear Debris in Precipitation," *Isotopes, Inc.*, 4th Progress Report, Contract AT(30-1)-2415, USAEC, July 15, 1960.
5. Begemann, F., and Libby, W. F., "Continental water balance, ground water inventory and storage times, surface ocean mixing rates and world-wide water circulation patterns from cosmic-ray and bomb tritium," *Geochim. et Cosmochim. Acta*, 12, 277 (1957).
6. Von Buttlar, H., and Libby, W. F., "Natural Distribution of Cosmic-ray Produced Tritium, II," *J. Inorg. Nucl. Chem.*, 1, 75 (1955).
7. Brown, R. M., "Hydrology of Tritium in the Ottawa Valley," *Geochim. et Cosmochim. Acta*, 21, 199 (1961). Also paper presented at A. G. U. Meetings, Washington, D. C., 20 April 1961.
8. Barrett, E. W., and Huebner, L., "Atmospheric Tritium Analysis," Technical Progress Report No. 2, Department of Meteorology, University of Chicago, Contract AT(11-1)636, USAEC, 16 February 1960.
9. Libby, W. F., "Tritium Water List," December 1, 1960, communication to the author.

CHAPTER 3

THE DISTRIBUTION OF RADIOACTIVITY IN SOILS

Prior to this work in HASP research on the deposition of radioactivity in soils has been designed primarily to ascertain the total amount of strontium-90 present on the surface of the earth as a result of nuclear weapons testing. Measurements of the vertical distribution of strontium-90 in soils were performed mainly to establish that it was sufficient to procure a core of soil to a depth of about six inches to ensure that almost all of the strontium-90 fallout was being sampled. Only isolated field experiments have been conducted to determine the factors which govern the distribution of strontium-90 with depth and the future disposition of this nuclide in soils. Such information is important to determine the probability of contamination of food products by radioactivity within the soils and this problem has generally been attacked by laboratory and small-scale field experiments.

From the point of view of the external radiological health hazard it is obviously most important to know the deposition and distribution in soils of the gamma emitting nuclides such as cesium-137. Such information has generally been inferred from the strontium-90 deposits and the theoretical production ratios of the gamma active nuclides to strontium-90 in the fission process. Although this approach is reasonably satisfactory when only the total amount of deposited radioactivity is required, it is obviously of little use when the vertical distribution of the gamma activity is the unknown factor. Such information cannot, of course, be deduced immediately from the vertical distribution of strontium-90 within soils because of the different chemical properties of strontium and the other nuclides. In the case of cesium-137 an activity production ratio of Cs^{137}/Sr^{90} of 1.7 ± 0.5 can be assumed and thus the total cesium-137 deposit within the soils can be calculated by multiplication of the strontium-90 deposit by the above ratio. However,

because of the greater adsorption of cesium-137 on clay minerals compared to strontium-90, it is expected that the cesium-137 will tend to be more concentrated in the upper layers of the soils than the strontium-90. The exact distribution of cesium-137 with depth in soils can only be determined, therefore, by direct radiochemical or gamma-ray spectroscopic analyses.

Several chemical and physical parameters probably influence the vertical distribution of fallout radioactivity within soils. These factors include, type and amount of precipitation deposited on the soil, drainage and permeability of the material, topography of the area being sampled, shadowing effect of nearby buildings and trees etc, organic content of the soil, pH, extent of disturbance of the upper layers (for example by plowing), composition of the soils and any peculiar chemical properties of the soil, such as a high glauconite content exhibited by certain soils in the state of New Jersey. How important these factors are in influencing the deposit and distribution of radioactivity within the soil is well-established for some but poorly known for others. It is fairly widely accepted, although by no means certain, that precipitation is the main carrier for the deposition of radioactive fallout. Hence, the type, amount, and occurrence of rainfall is an extremely important factor influencing the distribution of radioactivity in soils. On the other hand, there are few data on the effects of drainage and permeability of the soil. One of the objectives of the present investigation was therefore, to define at least some of the factors responsible for the distribution of radioactivity in soils. Fortunately within New Jersey there exists a wide range of soil types covering areas of excellent and poor drainage, high and low permeability, high and low organic content, and, of course, disturbed and undisturbed sites. The undisturbed sites are those which have been subject only to natural processes during the past 10 years or so since radioactive fallout from nuclear weapons testing became appreciable. For these reasons several soil samples were collected

in New Jersey during the summer of 1960. In addition a few samples were collected in the state of Kansas, an area of contrasting major soil classification.

Samples were collected in the above areas with a specially designed coring device. The soils were then returned to the laboratory, where they were removed from the corer by an extrusion process, crushed, ground, and blended. Aliquots from several depths in the core were then separated for radiochemical analysis. In the following sections full descriptions of the the above procedures are presented and the results of the analyses are given. The significance of the data from the radiological hazard point of view and the light they shed on the factors governing the vertical distribution of radioactivity within the soils are also discussed.

ACKNOWLEDGMENTS

In the course of this work we have received considerable assistance from numerous individuals who were not directly associated with the project. Their untiring efforts, sometimes under adverse circumstances in the field during surveillance of the sites and at the times of collection of the soil samples, are deeply appreciated. Our gratitude is extended particularly to K. P. Wilson, Soil Conservation Service, U.S. D. A., New Brunswick whose aid in the choice of suitable sites in New Jersey was invaluable to this project. A. P. Nelson, Soil Conservationist, Salina, Kansas gave similar valuable assistance in Kansas. Even before a preliminary selection of soil sites could be made, considerable discussion of the aims of the work with the above persons and many others, including Dr. J. C. F. Tedrow, Rutgers University, N. J., G. A. Quackenbush, and S. L. Tinsley, Soil Conservation Service, U.S.D.A., N. J., M. Bolline, Soil Conservation Service, Salina, Kansas and Dr. L. T. Alexander, U.S.D.A. Beltsville, Maryland, was necessary. Without their aid this work could not have been accomplished. In addition to the above mentioned scientists, the assistance of



those Soil Conservation Service employees who accompanied us to the soil sites and prepared descriptions of the soil profiles is not forgotten. These personnel included S. J. Fletcher, M. Hawkins, C. Jablonski, M. L. Markley, and V. R. Powley in New Jersey, and H. Penner, J. Rockers and D. Rott in Kansas. We are also grateful to the many landowners cited in the descriptions of the soil sites whose contribution of earth to the cause of scientific research permitted our aims to be partially fulfilled.

DESCRIPTION OF SOIL SAMPLES

The following descriptions of soil samples collected in New Jersey and Kansas during the summer of 1960 include only those samples which were subsequently chosen for radiochemical analysis. Figure 3.1 indicates the sample sites chosen in New Jersey. This figure indicates the major land type areas in New Jersey and was taken from a more comprehensive map compiled by the New Jersey Agricultural Experimental Station, Rutgers University and the Soil Conservation Service, U.S.D.A., N. J., in 1954.

FIGURE 3.1

DISTRIBUTION OF SOIL
SAMPLING SITES
IN NEW JERSEY

 River and Coastal Terraces
 Tidal Marshes

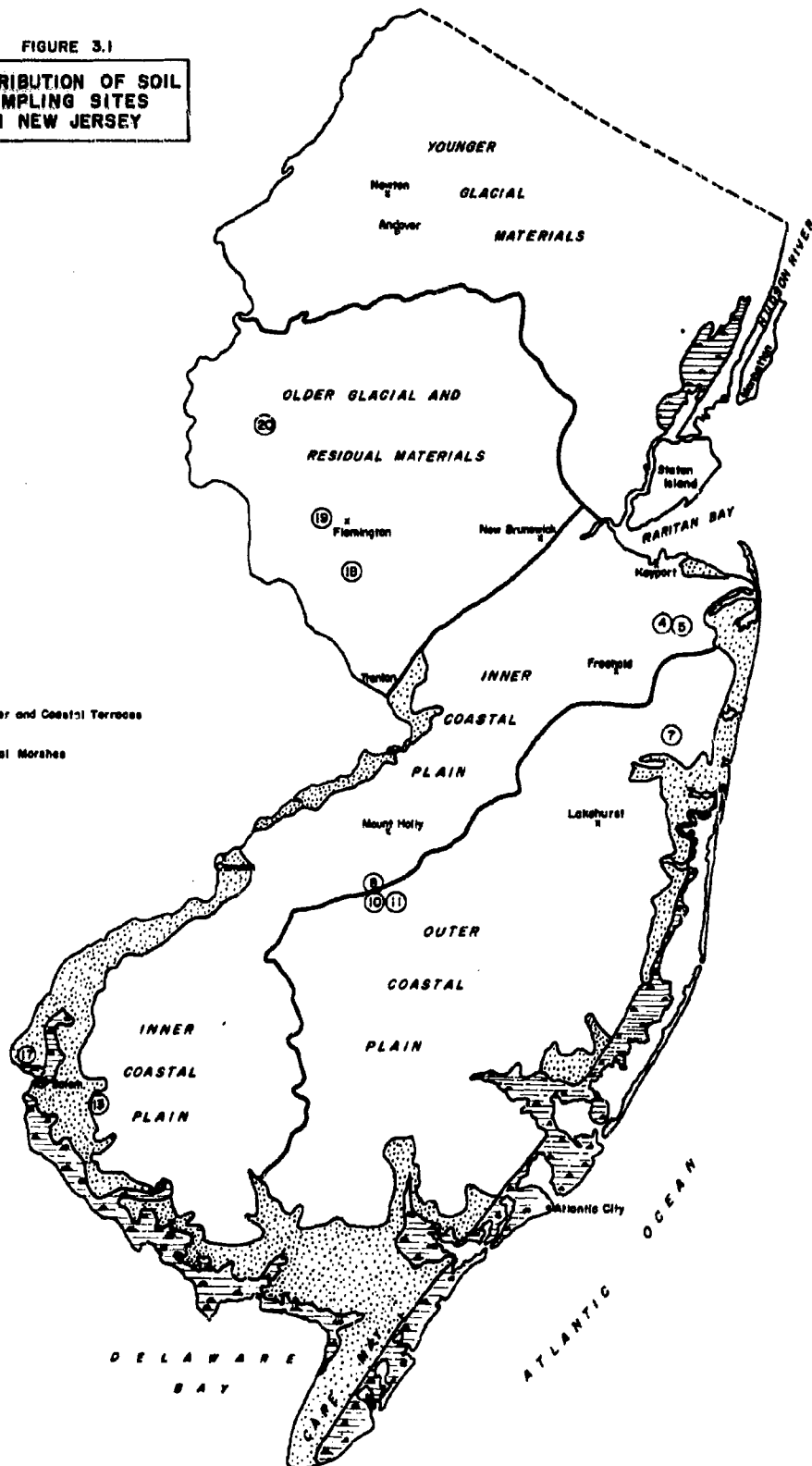


Table 3.1 Description of Soil Sampling Sites in New Jersey and Kansas

Isotopes, Inc. Soil Sample Number 4

Location: New Jersey - 70 yards west of N. J. Route #34, 100 yards north of Holmdel Nursing Home, Holmdel, Monmouth County.

Site: Undisturbed, untreated pastureland located in inner (heavier) belt of northern Atlantic Coastal Plain. Well-drained site on gently sloping (4%) upland not subject to appreciable ponding, overflow, high water table, soil accumulation or erosion. Permeable, sandy loam surface soil with texturally contrasting, moderately permeable, sandy clay loam subsoil overlying sandier, more rapidly permeable substratum.

Date of Sampling: August 3, 1960

Soil Type and Classification: Collington Sandy Loam, Gray-Brown Podzolic

Described by: M. A. Hawkins and C. F. Eby

Soil Zone	Description
A _p 0-10"	Very dark grayish brown (10YR 3/2)* sandy loam; weak medium subangular blocky breaking to weak fine subangular blocky structure; friable when moist; relatively free of gravel; many fine roots; few worm channels; horizon terminates in a pebble line; abrupt, smooth boundary. 10" thick.
A ₁ D ₁ 10-15"	Dark brown (10YR 3/3) gravelly sandy loam; weak fine subangular block breaking to weak medium to fine crumb structure; when moist; few fine roots; abundant quartzose gravel (1/4 to 3" in diameter); gradual wavy boundary. 5" thick.
B ₁ D ₂ 15-24"	Dark yellowish brown (10YR 4/4) gravelly sand loam ground mass; dark brown (10YR 3/3) organic staining; weak medium subangular blocky breaking to weak fine subangular blocky structure; friable when moist; quartzose (1/2-2" in dia.) gravels; very noticable absence of clay coating on sand grains, some greensand (glauconite) has clay coatings; clear wavy boundary. 9" thick.
B ₂ D ₂ 24-34"	Dark yellowish brown (10YR 4/4) sandy clay loam; moderate coarse subangular blocky breaking to moderate medium subangular blocky breaking to weak fine subangular blocky structures; firm in place, friable when removed; moist; thin incomplete or discontinuous clay films on ped surfaces; few fine pores; abrupt smooth boundary. 10" thick.

Sample Number 4 (continued)

Soil Zone	Description
D ₃ 34-38"	Yellowish brown (10YR 5/8) gravelly sandy loam; weak medium subangular blocky structure; friable when moist; no roots; no worm channels; greensand predominates ground mass; some reworked iron stone; diffused wavy boundary. 4 inches thick.
D ₄ 38"+	Greensand (not covered in Munsel Color Chart); "sandy sandy loam"; weak fine crumb structure; friable when moist.

Remarks: Soil contains moderate amount of glauconite (10-30 percent) in upper two feet. Soil colours determined by use of Munsel Color Chart.

* Soil described here was very moist. Colors for dry soil one to two units higher in value.

Isotopes, Inc., Soil Sampling Site Number 5

Location: New Jersey - In cornfield 30 yards east of N. J. Route #34 directly across from Holmdel Nursing Home (see Number 4).

Site: Disturbed site regularly cultivated during past 8 years including liming and fertilizing and located within the inner (heavier) belt of northern Atlantic Coastal Plain. Well-drained site on gently sloping (2%) upland not subject to appreciable ponding, overflow, high water table, soil accumulation or erosion. Permeable, sandy loam surface soil with texturally contrasting, moderately permeable, clayey sandy loam subsoil overlying sandier, more rapidly permeable substratum.

Date of Sampling: August 3, 1960

Soil Type and Classification: Collington Sandy Loam, Gray-Brown Podzolic

Described by: M. A. Hawkins and C. F. Eby

Soil Zone	Description
A _p 0-10"	Very dark grayish (10YR 3/2) sandy loam, weak medium subangular blocky breaking to weak fine crumb structure; friable when moist; relatively free of gravel; few worm channels; few fine roots; abrupt smooth boundary. 10" thick.
B ₂ 10-22"	Dark yellowish brown (10YR 4/4) clayey sandy loam; moderate medium angular to subangular blocky breaking to weak fine subangular block structure; friable when moist; few fine roots; no apparent clay skins; gradual wavy boundary. 12" thick.
C 22-36"	Yellowish brown (10YR 5/6) sandy loam; weak coarse angular blocky breaking to weak fine subangular blocky structure; friable when moist; few discontinuous oxidized bands 1/8-14" thick; clear smooth boundary. 14" thick.
D 36"	Yellowish brown (10YR 5/6) "sandy sandy loam", (50% green-sand) weak coarse angular blocky breaking to weak fine crumb structure; friable when moist; a definite pebble line intermixed with upper part of horizon (2-3" thick) with quartzose gravel 1/2" in dia.; greensand increases with depth; no roots; no work channels; no clay films.

Remarks: Material is high to medium in glauconite content mixed with sand. Soil colors determined by use of Munsel Color Chart while moist.

Isotopes, Inc. , Soil Sample Number 7

Location: New Jersey - 50 yards southeast of County Route 549, 300 yards southeast of County Rout 547 on Horace Migill Farm, Squankum, Monmouth County.

Site: Undisturbed pastureland, probably limed and fertilized regularly, located in outer (sandier) belt of northern Atlantic Coastal Plain. Very poorly drained profile but at time of sampling water table was below 4 feet. Probably tile drained so that water table probably now never higher than 1 foot below surface. Low slope(1%) not subject to appreciable ponding, overflow, soil accumulation or erosion. Rapidly permeable, thick (17"), highly organic, fine sandy soil overlying very rapidly permeable, fine sandy subsoil and substratum. No orterde or ortstein in profile.

Date of Sampling: August 4, 1960

Soil Type and Classification: Rutledge fine sandy loam, Half Bog

Described by: M. A. Hawkins and C. F. Eby

Soil Zone	Description
A _p 0-10"	Black (N 2/0) loamy fine sand and organic matter; weak medium subangular blocky breaking to weak medium crumb; friable when moist; many fine roots; few quartzitic pebbles (1/4-1/2" dia.); few worm channels; abrupt smooth boundary. 10" thick.
A ₁₁ 10-14"	Dark gray (N 4/0) loamy fine sand; single grain; loose when moist; sand grains did not have clay coats; relatively clean; no pebbles; no roots; no worm channels; clear wavy boundary. 4" thick.
A ₁₂ 14-17"	Very dark brown (10YR 2/2) loamy fine sand; single grain; very friable when moist; no roots; no pebbles; no worm channels; humus very pronounced; gradual wavy boundary. 3" thick.
B _{2g} 17-25"	Mottled yellowish brown (10YR 5/8) and gray (10YR 6/1)sandy, fine sandy loam many coarse, prominent mottles; very weak medium subangular blocky breaking to weak fine crumb structure; friable when moist; no pebbles; no roots; no roots; no worm channels; clear wavy boundary. 6" thick.

Sample Number 7 (continued)

C_g 25" + Mottled brown (7.5YR 5/2) and yellowish brown (10YR 5/8) loamy fine sand; medium prominent mottles common; single grain structure; friable when moist.

Remarks: Soil colors determined by use of Munsel Color Chart

Isotopes, Inc., Soil Sample Number 8

Location: New Jersey - In English Setter Club, 1/2 mile north of Medford, Burlington County

Site: Undisturbed grass; weeds and shrubs mowed high for dog field trials. No lime, fertilization or cultivation for at least 8 years. Located in inner (heavier) belt of northern Atlantic Coastal Plain. Well-drained site on gently sloping upland not subject to appreciable ponding, overflow, high water table, soil accumulation or erosion. Topsoil moderately permeable, subsoil slow, substratum moderately permeable.

Date of Sampling: August 8, 1960

Soil Type and Classification: Marlton sandy loam, Gray-Brown Podzolic

Described by: M. A. Hawkins and C. F. Eby

Soil Zone	Description
A _p 0-6"	Dark olive gray (5Y 3/2) sandy loam, weak fine granular structure; very friable when moist; abundant roots; about 5% rounded quartz pebbles; abrupt, smooth boundary.
A ₂ 6-10"	Dark olive (5Y 3/3) sandy loam; weak fine granular structure; friable when moist; many roots; about 5% rounded quartz pebbles; gradual smooth boundary.
B ₂ 10-30"	Dark olive (5Y 3/3) or a little greener clay; strong coarse blocky toward prismatic; very firm when moist, very plastic when wet; roots common in upper part, few in lower; abundant, continuous clay films on ped surfaces; gradual, smooth boundary.

Sample Number 8 (continued)

B₃ 30-44" Stratified alternating layers of dark olive (5Y 3/3) sandy clay and sandy clay loam; massive but granules of glauconite dominate; firm to friable when moist, plastic when wet; few roots; many small granular iron concretions; gradual, smooth boundary.

C 44-54" Dark olive (5Y 3/3) sandy clay loam; massive but granules of glauconite dominate; firm in place, friable when removed, plastic when wet; very few roots; a few small granular iron concretions.

Remarks: Soil contains abundant (more than 30%) glauconite throughout, Soil colors determined by use of Munsel Color Chart.

Isotopes, Inc. , Soil Sample Number 10

Location: New Jersey - Next to Wharton Tract, 3 miles south of Medford and 1 mile north of Jackson, Burlington County. Owner-

Site: Undisturbed in weeds and perennial shrubs adjacent to cranberry bog, mowed to reduce frost hazard. Never limed or fertilized. Located in outer (very sandy) belt of northern Atlantic Coastal Plain. State geologic map designates area as being underlain by Cohansey Sand. Excessively well-drained site on gently sloping top of a sand mound bordering the bog area. Not subject to ponding, overflow, high water table, soil accumulation or erosion. Very rapidly permeable sand throughout.

Date of Sampling: August 8, 1960

Soil Type and Classification: Lakewood sand, Podzol.

Soil Zone

Description

A₁ 0-4" Very dark gray (N 3/0) sand; single grain structure; loose; roots common; individual sand grains light gray; abrupt, smooth boundary.

A₂ 4-10" Light grayish brown (7.5YR 6/2) sand; single grain structure loose; few roots; abrupt irregular (tongued) boundary.

B 10-28" Yellowish brown (10YR 5/6) sand with many tongues of material from horizon above; single grain structure; loose; few roots; gradual wavy boundary.

Sample Number 10 (continued)

C 28-54" Light yellowish-brown (10YR 6/4) sand with few, fine, faint mottles in lower part; single grain structure; loose; few roots. No free water to 54".

Remarks: Soil colors determined by use of Munsel Color Chart.

Isotopes, Inc., Soil Sample Number 11

Location: New Jersey - adjacent to sample 10, next to Wharton Tract, 3 miles south of Medford, 1 mile north of Jackson, Burlington County. Owner-Brick.

Site: Undisturbed in perennial grasses and shrubs, mowed to reduce frost hazard. Not cultivated, limed or fertilized for at least 8 years. Located in outer (very sandy) belt of northern Atlantic Coastal Plain. Poorly drained site with water table at or near surface for a large portion of the year, but at 50" when sampled. In a shallow depression but not subject to appreciable ponding, overflow, soil accumulation or erosion. Very rapid permeable throughout.

Date of Sampling: August 8, 1960

Soil Type and
Classification: Leon sand, ground water Podzol.

Described by: M. L. Markley

Soil Zone	Description
A ₁ 0-5"	Dark gray (N 4/0) sand; single grain structure; loose; roots common; individual sand grains light gray; abrupt, smooth boundary.
A ₂ 5-20"	Pinkish-gray (5YR 6/2) sand; single grain structure; loose; few roots; abrupt smooth boundary.
B _{2h} 20-22"	Very dark brown (10YR 2/2) sandy loam; massive; friable; roots common; abrupt smooth boundary.
B _{2ir} 22-24"	Dark reddish-brown (5YR 3/3) sandy loam; massive; friable; roots common, abrupt, smooth boundary.

Sample Number 11 (continued)

B ₃	24-36"	Yellowish-brown (10YR 5/4) sand; single grain structure; loose; few roots; gradual smooth boundary.
C	36-50"	Brown (10YR 5/3) sand; single grain structure; loose; few roots; dark brown, weakly cemented, stringers or lenses 2-4" thick.
	50"	Free water.
Remarks:		Soil colors determined by use of Munsel Color Chart.

Isotopes, Inc., Soil Sample Number 13

Location: New Jersey - 100 yards south of silo on E. J. Crouse farm on Commissioners Pike, Salem County.

Site: Undisturbed site of grass, weeds, red cedar saplings, located in inner (heavy) belt of northern Atlantic Coastal Plain. Seasonally wet (moderately well-drained to somewhat poorly drained) gentle slope 2 to 3%, not subject to overflow, soil accumulation or active erosion. Soil was developed from non-glaucconitic clays and is slowly permeable throughout.

Date of Sampling: August 10, 1960

Soil Type and Classification: Keyport sandy clay, Red Yellow Podzolic intergrading to Gray Brown Podzolic.

Described by: V. R. Powley

Soil Zone	Description
A _{p1} 0-2"	Dark brown (10YR 3/3) sandy clay; weak fine subangular blocky structure; plastic when wet. 1 1/2 - 2" thick.
A _{p2} 2-7"	Strong brown (7.5YR 5/6) unmottled sandy clay; very weak, medium subangular blocky structure; plastic when wet; 4-5" thick.
B ₂₁ 7-11"	Strong brown (7.5YR 5/6) clay with few, fine, distinct, yellowish-red (5YR 5/6) and pale brown (10YR 8/3) to light gray mottles; strong, very fine to medium subangular blocky structure; very plastic when wet.

Sample Number 13 (continued)

- B_{22g}** 11-16" Strong brown (7.5YR 5/6) clay with common, fine, distinct, yellowish red (5YR 5/6) and pale brown mottles, strong, medium to fine, subangular blocky structure; very plastic when wet; roots common.
- C_g** 16-46" Strong brown (7.5YR 5/6) clay with many fine to coarse, distinct yellowish red (5YR 5/6) and pale brown (10YR 8/3) mottles; structure obscure; plastic when wet. Slightly sandier than horizon above.

Remarks: Soil colors determined by use of Munsel Color Chart.

Isotopes, Inc., Soil Sample Number 17

- Location:** New Jersey - 1/2 mile north on Lehigh Road from intersection with Fort Mott Road, Salem County.
- Site:** Undisturbed with brome sedge, weeds, very small wild cherry and sumac, located on Delaware Bay terrace in the northern Atlantic Coastal Plain. Moderately well-drained toward well-drained, on gently sloping 2% terrace, approximately 10 feet above tide. Not subject to overflow, soil accumulation, or erosion. Fluctuating water table between 4 and 6 feet depth. Permeable sandy loam surface, moderately to rapidly permeable subsoil, rapidly permeable substratum. Soil developed on non-glaucconitic estuarine sandy loam materials, strongly acid.
- Date of Sampling:** August 9, 1960
- Soil Type and Classification:** Woodstown sandy loam, Gray Brown Podzolic intergrading to Red Yellow Podzolic.
- Described by:** V. R. Powley

Soil Zone	Description
A_{p1} 0-1 1/4"	Brown (10YR 4/3) moist (sandy), sandy loam; single grain structure; very friable; abrupt smooth boundary. 1-1 1/4" thick.
A_{p2} 1 1/4-6"	Yellowish-brown (10YR 5/6) moist sandy loam; single grain structure; very friable; clear smooth boundary. 4-3/4-5" thick.

Sample Number 17 (continued)

- B₁ 6-10" Transitional to strong brown (7.5YR 5/6) moist slightly clayey sandy loam; massive; friable; gradual smooth boundary. 2-4" thick.
- B₂ 10-22" Strong brown (7.5YR 5/6) moist sandy, sandy clay loam; weak, medium subangular blocky structure; friable; gradual smooth boundary.
- B₃ 22-25" Strong brown (7.5YR 5/6) moist sandy, sandy clay loam with few, coarse, prominent pale brown (10 YR 6/3) and somewhat finer rust mottles; massive; friable; clear boundary.
- C₁ 25-28" Strong brown (7.5YR 5/6) moist (sandy), sandy loam, unmottled; single grain structure; very friable; clear smooth boundary.
- C₂ 28-37" Strong brown (7.5YR 5/6) moist (sandy), loam with a few coarse distinct (10YR 6/4) and fine to coarse rust mottles.

Remarks: Soil colors determined by use of Munsel Color Chart.

Isotopes, Inc., Soil Sample Number 18

Location: New Jersey - 1 1/2 miles due west of Ringoes, Hunterdon County.

Site: Undisturbed site in hay field not plowed for at least 15-20 years. Limed, fertilized and mowed regularly and located in the unglaciated Triassic lowlands of New Jersey. Well-drained, slope 1 percent, not subject to overflow, soil accumulation, erosion or high water table. Moderately permeable silt loam soil, subsoil and bedrock. Soil developed from silty (Aeolian?) mantle overlying red silty shale bedrock at about 4 feet.

Date of Sampling: August 30, 1960

Soil Type and Classification: Bucks silt loam, silty overlay, Gray Brown Podzolic intergrading to Sol Brun Acides.

Described by: C. F. Jablonski

Sample Number 18 (continued)

Soil Zone	Description
A _p 0-9"	Dark yellowish brown (10YR 3/4) moist silt loam; moderate, medium crumb structure; friable in place, very friable when removed; abundance of roots; pH 6.6; clear boundary.
B ₂₁ 9-15"	Reddish brown (5YR 4/4) moist clayey silt loam; very weak, medium subangular blocky structure; firm in place, friable when removed; some evidence of clay flows along ped faces and along root channels; many roots, organic staining along root channels; pH 5.6; diffused boundary.
B ₂₂ 15-25"	Yellowish red (5YR 4/6) moist clayey silt loam; moderate coarse, subangular blocky structure, breaking to moderate medium, subangular blocky structure; moderately firm; many fine roots; occasional soft shale fragments; clay flows are much more evident along ped faces and root channels than in horizon above; faint organic staining along worm holes and root channels, shale fragments increase toward bottom of horizon; pH 5.2-5.4.
B _{2D} 25-37"	Reddish brown to yellowish red (5YR 4/4-4/6) wet shaly, slightly clayey silt loam; weak very coarse platy structure; slightly sticky; pH 5.0 or less; diffused boundary.
B _{3D} 37-45"	(2.5YR 3/4-3/6) moist shaly loam; massive; very firm in place, friable when removed; shale increases with depth; pH 5.0 or less.
D ₂ 45"+	Red shale bedrock.
Remarks:	Soil colors determined by use of Munsell Color Chart.

Isotopes, Inc., Soil Sample Number 19

Location: New Jersey - 1/4 mile south of Croton, Hunterdon County, in outfield of baseball field.

Site: Undisturbed for 10-15 years, grass and weeds mowed regularly to 4 inches. No lime or fertilizer used. Location on the Hunterdon Plateau in Triassic Lowland of New Jersey, Poorly drained, level, not subject to overflow, soil accumulation or erosion. Water table held close to surface most of the year by impervious argillite rock. Very slowly permeable soil, subsoil, substratum and bedrock. Soil developed from dark gray or dark red massive, hard, slightly calcareous argillite bedrock of the Lockatong formation.

Date of Sampling: August 30, 1960

Soil Type and Classification: Croton silt loam, Humic Gley

Described by: C. F. Jablonski

Soil Zone	Description
A _p 0-9"	Dark grayish-brown (10YR 4/2) with 5% faint greyish mottles, wet, heavy silt loam; moderate, medium to fine crumb structure slightly sticky when wet, friable when moist; many roots; organic staining along root channels, pH 5.2-5.4; clear boundary.
A _{2g} 9-16"	Mottled light brownish-gray and yellowish-brown (10YR 6/2 and 10YR 5/8) wet silty clay loam; weak, very coarse platy structure; sticky; few fine roots; pH 5.2-5.4; clear boundary.
B _{2g} 16-26"	Many fine and coarse, prominent mottles of reddish-brown, light brown, pinkish-white (2.5YR 5/4-4/4, 10YR 6/2, 7.5YR 6/2) moist silty clay loam; very weak, very coarse platy structure breaking to strong, coarse subangular blocky structure; sticky when wet, firm to very firm when moist, hard when dry; fine roots rare; pH 6.4-6.6.
B _{3g} 26-38"+	Dark brown (7.5YR 4/4) moist; fine and coarse prominent mottles 30-40% of surface (7.5YR 6/2-5YR 6/2-6/3) silty clay loam to silt loam; massive; extremely firm in place; pH 6.4-6.6.

Remarks: Soil colors determined by use of Munsel Color Chart.

Isotopes, Inc., Soil Sample Number 20

Location: New Jersey - De Boor Farm, West Portal, Hunterdon County, 3 miles north of West Portal and U. S. Route #22.

Site: Undisturbed pastureland, not limed but fertilized. Located in area of old Jerseyan (Kansan?) glacial till, south of Wisconsin terminal moraine in the Reading Prong of the New England Physiographic Province. Soil material overlies limestone bedrock to a depth of 10-20 feet. Site is well-drained on gently sloping (2 to 3%) upland not subject to appreciable ponding, overflow, high water table, soil accumulation or erosion. Soil is moderately permeable throughout. Parent soil material considered to be composed of limestone and gneissic materials.

Date of Sampling: August 30, 1960

Soil Type and Classification: Washington loam, Gray Brown Podzolic

Described by: C. F. Jablonski

Soil Zone	Description
A _p 0-9"	Dark yellowish-brown (10YR 3/4) moist silt loam; moderate, medium granular structure; friable in place, very friable when removed; abundant roots; pH 6.8 to 7.0 boundary clear.
B ₂₁ 9-17"	Strong brown (7.5YR 5/6) moist clayey loam; moderate, fine to medium subangular blocky structure; friable to firm in place, friable when removed; many roots; some evidence of clay flows; some very small gneiss fragments; numerous worm holes filled with organic stained soil; pH 7.0 plus; boundary diffused.
B ₂₂ 17-29"	Strong brown (7.5YR 5/6) or slightly yellower moist clay loam; strong, medium to coarse subangular blocky structure breaking to moderate medium subangular to angular blocky structure; friable; occasional fine roots; some clay flows along ped faces and along worm holes; some very rotted gneiss particles as well as some less weathered ones ranging in size from 1/4 to 1-1/4" diameter; many worm channels with organic stained filling; pH 7.0 plus; boundary diffused.

Sample Number 20 (continued)

- B₂₃ 29-42" Strong brown (7.5YR 5/6) to yellowish-brown (10YR 5/6) moist, gritty clay loam; moderate medium subangular to angular blocky structure; much manganese (?) staining; numerous quartz pebbles 2-3" in size, plus some limestone fragments; pH 7.0 plus; boundary diffused.
- B₃ 42-52"+ About as B₂₃ horizon above but more gritty with a little less clay; pH 7.0 plus.

Remarks: Soil colors determined by use of Munsell Color Chart

Isotopes, Inc., Soil Sample Number 28

Location: Kansas - 1970 feet west and 2600 feet north of the southeast corner of Section 33-T22S-R5W, Reno County. Owner - Kansas Power and Light Company.

Site: Undisturbed site in upland, eolian sand on undulating topography. Tall native grass, Bluestem, Indian and Switch. Soil exhibits low runoff and is well-drained internally.

Date of Sampling: September 26, 1960

Soil Type and
Classification: Pratt loamy sand

Described by: James J. Rockers

Soil Zone	Description
A ₁ 0-7"	Dark gray brown (10YR 4/2d) very dark brown (10YR 2/2m); loamy sand; weak fine granular; soft when dry, very friable when moist; numerous roots; pH 6.0; grades within about 2" to
A ₃ 7-12"	Brown (10YR 5/3d) dark brown (10YR 3/3m); loamy sand; moderate fine granular; soft when dry; very friable when moist; numerous roots; pH 6.0; grades within about 3" to
B ₂ 12-24"	Light yellowish brown (10YR 6/4d) dark yellowish brown (10YR 4/4m); heavy loamy sand; moderate fine granular; slightly hard when dry, friable when moist; numerous roots; pH 6.0; grades within about 4" to

Sample Number 28 (continued)

- C 24-40" Pale brown (10YR 6/3d) yellowish brown (10YR 5/4m); loamy sand; single grain, loose when dry or moist; numerous roots; pH 5.5.
- C 40-52" Same as horizon above, except moist color is light yellowish brown (10YR 6/4).

Remarks: pH determined using a Hellige kit. Soil colors determined by use of Munsel Color Chart.

Isotopes, Inc., Soil Sample Number 29

Location: Kansas - 1330 feet south and 660 feet west of the north east corner of Section 8-T22S-R4W, Reno County. Owner Eldo Prieb.

Site: Undisturbed site located on upland (elevation approximately 1700 feet) in blue-grama and Buffalo grass. Soil is well-drained, permeability is moderately slow. The grass is overgrazed and under virgin conditions or better management the vegetation would be expected to be Bluestem, Indian and Switch grass.

Date of Sampling: September 27, 1960

Soil Type and Classification: Bethany silt loam (Native grass)

Described by: James J. Rockers

Soil Zone	Description
A ₁ 0-12"	Dark brown (10YR 3/3d) very dark brown (10YR 2/2m) silt loam; moderate medium granular; slightly hard when dry, very friable when moist; many fine grass roots; pH 5.8; grades within 2" to
A ₃ 12-18"	Dark brown (10YR 4/3d) (10YR 3/3m) light silty clay loam; strong medium granular; hard when dry, friable when moist; fine roots are common; pH 6.0; grades within about 2" to

Sample Number 29 (continued)

B ₂₁ 18-37"	Dark gray brown (10YR 4/2d) very dark gray brown (10YR 3/2m) silty clay; weak medium sub-angular blocky with slickensides of ten centimeters in diameter; extremely hard when dry, very firm when moist; few roots; pH 6.5; grades within about 5" to
B ₂₂ 37-45"	Gray brown (2.5Y 5/2d) olive brown (2.5Y 4/4m) silty clay loam; weak medium granular to massive; very hard when dry, firm when moist; mildly calcareous with scattered calcareous concretions some 5mm in diameter.
Remarks:	A Hellige-Truog soil reaction tester was used to determine pH. Soil colors determined by use of Munsel Color Chart.

SAMPLE COLLECTION

In order to collect the large soil samples studied in this program it was necessary to design and fabricate special equipment. The design of the equipment and the procedures for sample handling and pretreatment were conceived and directed toward the minimization of the possibilities of cross-contamination of samples and contamination within any one sample from one depth to another.

The soil sampling equipment consisted of two main portions; (1) the corer which was placed on the surface of the ground at the sampling site and driven into the ground by (2) the corer driving rig. A description of the sampling equipment and its operation is given below.

The Corer

The corer, designed and fabricated at Isotopes, Inc., was basically a steel cylinder with a 1/4 inch wall thickness, two feet long and one foot in diameter. A diagram of the corer with accessory fittings is shown in Figure 3.2. One end of the cylinder was chamfered at a 45 degree angle, providing a cutting edge to facilitate driving the corer into the ground. At the other end of the cylinder, a flange in the form of a 12.5 inch outside diameter annulus was butt welded. The inside of the annulus was then machined flush with the inside wall of the cylinder. A tight fitting metal cap, which was secured to the flange by three countersunk 1/4" - 20 hex cap screws, served to prevent loss of sample both during and after the sampling operations. Two tapped holes in the cap, which were used in fastening a bar handle for extraction of the corer from the ground, served as an air relief during insertion of the corer.

The Core Driving Equipment

The core driving equipment consisted of: (a) the drive pipe, (b) the drive hammer, and (c) the tripod winch. The drive pipe was a 2 inch i. p. s. galvanized iron pipe 4.5 feet long. It was threaded at one end to fit into a 2 inch thick x 11 inch diameter steel flange. This flange, in turn, rested on the cap of the corer and both the flange and the cap were joined together by means of 3 two-inch hexagon socket screws. The function of the drive pipe was to guide the drive hammer during its stroke to gain maximum impact on the corer.

The drive hammer was a cast iron cylindrical block with a 2 1/2 inch center hole, forged steel eye-bolts and an extra heavy chain for safe handling. The dimensions of the hammer were 13 inches high and 11 inches in diameter and it weighed 300 pounds.

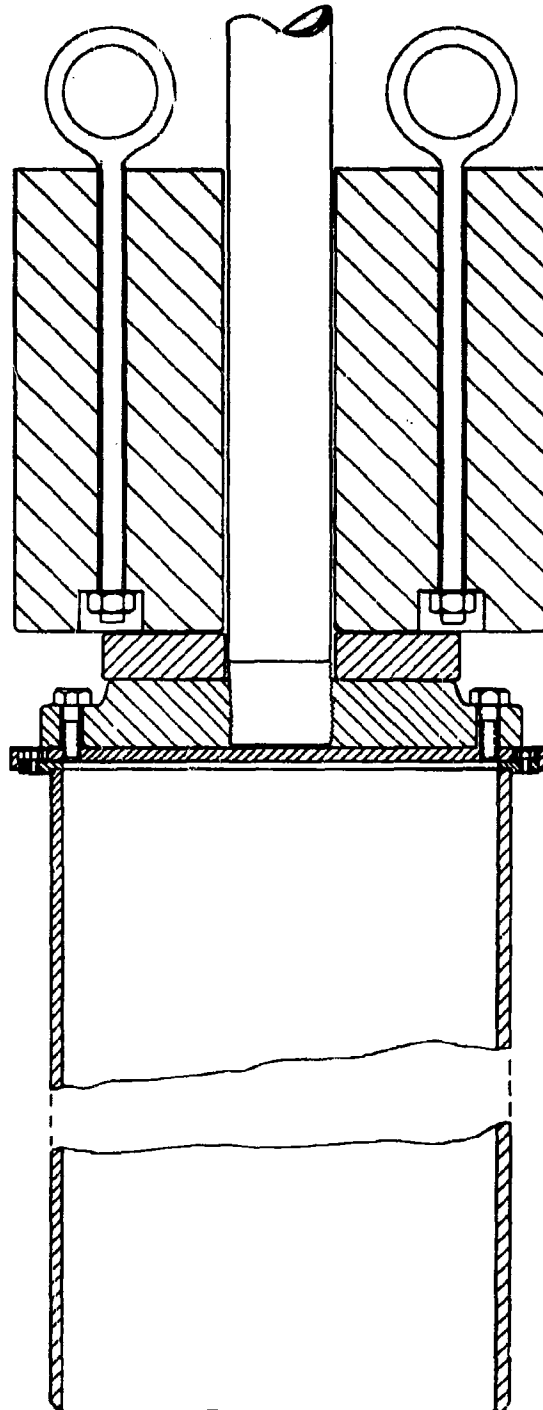
A 9 pound steel drive ring with a 3 inch center hole was placed between the driver hammer and the steel flange to protect the bottom face of the hammer. The actual assemblage of the drive pipe, drive hammer, drive ring, and corer is shown in Figure 3. 2.

The tripod-winch was a Lug-All, Model 1508 with 1500 pounds capacity and a lifting distance from the ground of 7 feet 2 inches. The winch was side-mounted to provide more head room and consisted of a crank with a two-speed arrangement, a positive action brake which permitted controlled lowering, a separate handbrake for lowering without the crank, a high grade steel cable, and a simple overhead pulley arrangement.

The Sampling Operation

All the equipment, the drive pipe, the drive hammer and the tripod-winch plus the corer, was assembled in the field in less than 30 minutes. The actual sampling was carried out by 2 or 3 men in the following manner:

FIG. 3.2 SOIL CORER AND DRIVE WEIGHT



The tripod winch was set at its maximum operating height directly above the chosen sampling site and the cable hook was lowered to lock on the chain of the 300 pound weight which had been placed to one side of the sampling site. Precautions were taken not to disturb the sampling surface by making sure that the weight did not scrape along the surface of the ground as it was being raised. Once the weight was raised about 3 feet off the ground, the corer was placed underneath with further caution against disturbing the sampling surface. The drive ring was centered on the flange, and the drive hammer was cautiously lowered and permitted to rest on the drive ring. The drive pipe was then inserted through the drive hammer and ring and threaded into the flange.

The equipment was then ready for the actual sampling. This process was performed in two phases: (a) insertion of the corer into the ground and (b) removal of the corer and sample from the ground. The first operation was carried out by repeated hammering of the weight on the top of the corer. Initially, the hammering was done with short strokes, 6-12 inches, to guide the corer vertically until it assumed the desired direction. Then the driving operation was intensified by making the weight travel up and down the length of the pipe until the corer was entirely driven into the ground. The drive pipe was unthreaded, the 300 pound weight and drive ring were pulled to one side and the steel flange was removed. A cross bar-handle was secured to the cap of the cover by means of two screws and the cable hook was secured to the bar-handle.

The second operation or extraction was done in one of two ways: if the texture and sorting properties of the soil (i.e. clay) indicated a well packed sample inside the corer, then the sample and corer were pulled directly with the aid of the tripod winch. However, in the case of a loosely packed sample (i.e. sand), a ditch, 1-2 feet wide, was dug around the corer until the bottom of the corer became visible. The corer was then cautiously hoisted up and a cover

FIG. 3.3 SOIL EXTRUDER

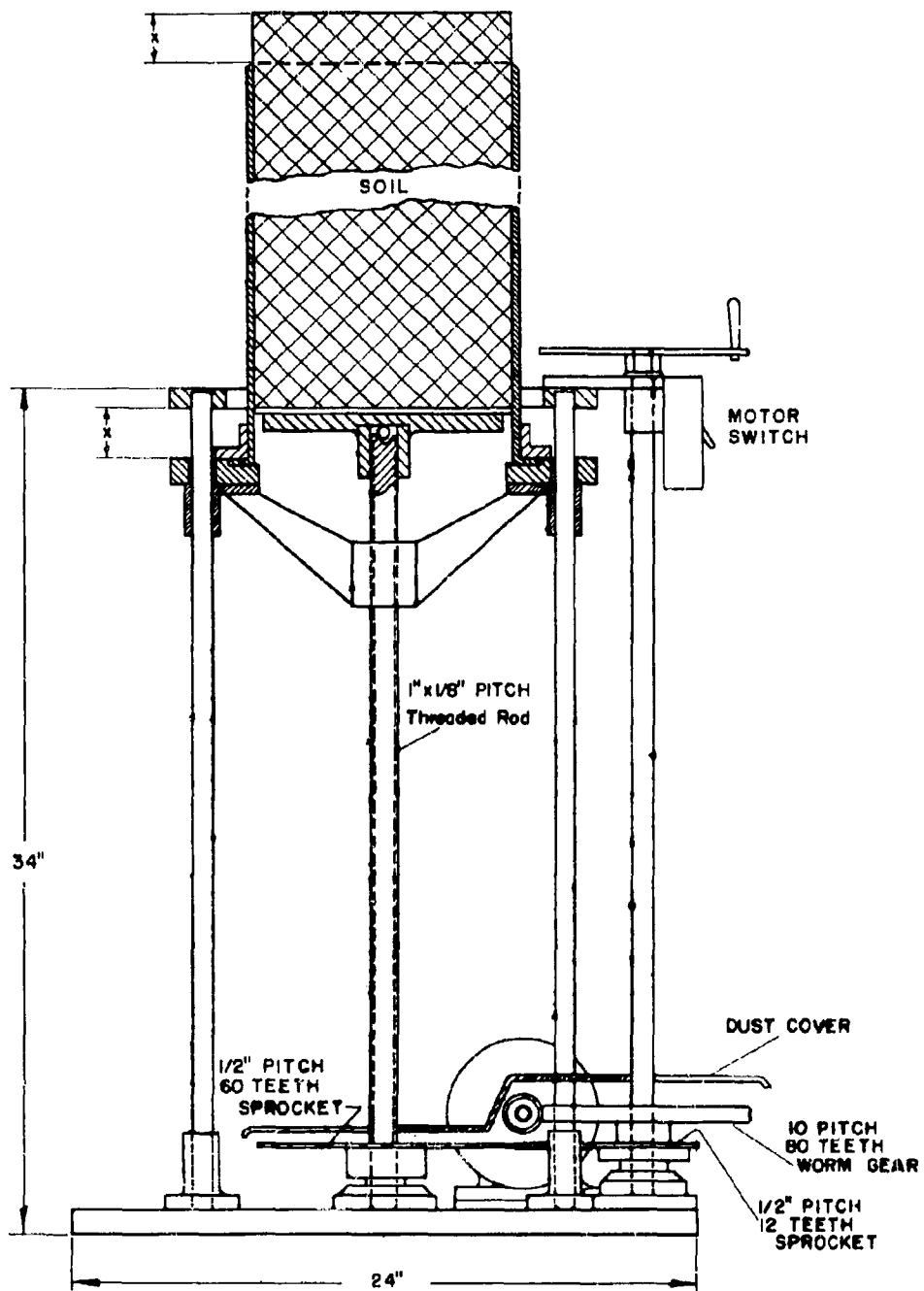


plate was placed underneath to prevent losses due to shaking and handling. In every case, the type of soil was predetermined by "soil striking" around the site with a small cork screw auger sampler.

Sampling was completed by assigning a sample number and covering both ends of the corer with plastic film. The film was taped around the rim of the corer to prevent loss of sample as well as contamination from the outside.

SAMPLE PRETREATMENT

Upon its arrival at Isotopes, Inc. and subsequent to recording the collection data, the soil sample was extruded from the steel corer. This operation was performed with an extruder especially designed and built at Isotopes, Inc. The design was based on a model originally used at Sandia Base, Sandia Corporation, Albuquerque, New Mexico. Plans of such a model were made available to Isotopes, Inc. by Dr. Foster and Dr. Cowan of Sandia Corporation.

The extruder shown in Figure 3.3 was built on the principle of a stationary piston against which a piston chamber was pulled down. In order to extrude a sample, the bottom end (the end representing the lowest depth) of the corer was placed on and fastened to the piston plate by means of a flange ring. The piston plate was held axially by a threaded hub on to a threaded rod. It was further supported radially by three equidistant guide rods with guide bushings. By the downward movement of the piston plate which was caused by rotating the threaded rod, the sample was displaced upward along the length of the corer. The extrusion was carried out in increments of several thicknesses, the first of which represented the surface of the sample. In general, the sequence of increments, starting at the surface, was 0-1/2, 1/2-1, 2-3, 3-4, 4-6, 6-9, 9-12, 12-18 and 18-24 inches. As each section emerged, a sharp edged steel cylinder, 8 inches in diameter and with a height equal to the thickness of the increment, was driven down into the increment. The sample outside the steel cylinder was

discarded and only the 8 inch cut was weighed, given a sample and increment number, and reserved for subsequent operations. This procedure eliminated any cross contamination of the lower depths by upper layers of soil as a result of entrainment of material by the walls of the corer during sampling.

In the case of a few samples, the mode of extrusion was altered to meet the problem of compaction. Because of the texture of some samples, it was impossible to extrude the 24 inch cores. It then became necessary to split the cores into two 12 inch sections by means of a band saw. In this manner, the extruder had no difficulty in handling half a core and extrusion was continued as in the case of a whole core.

After it had been spread on an evaporating pan, the soil increment was dried overnight in an oven at 110°C and again weighed to determine its moisture content. The sample was then passed through the jaw-openings of a D. F. C. Laboratory Crusher, Model 20840. (See Figure 3.4.) The 4 mesh effluent was further reduced to 100 mesh by passing it through the Iler Disc Pulverizer twice. The fine material was collected in a sample pan located below the grinding discs (see Figure 3.5). Finally the sample, depending on its size, was introduced into a 2, 4 or 8 quart capacity plexiglass twin-shell of a Patterson-Kelley Blender (see Figure 3.6). The sample was blended for 1 hour, collected in a plastic bag, weighed, and reserved for radiochemical analysis.

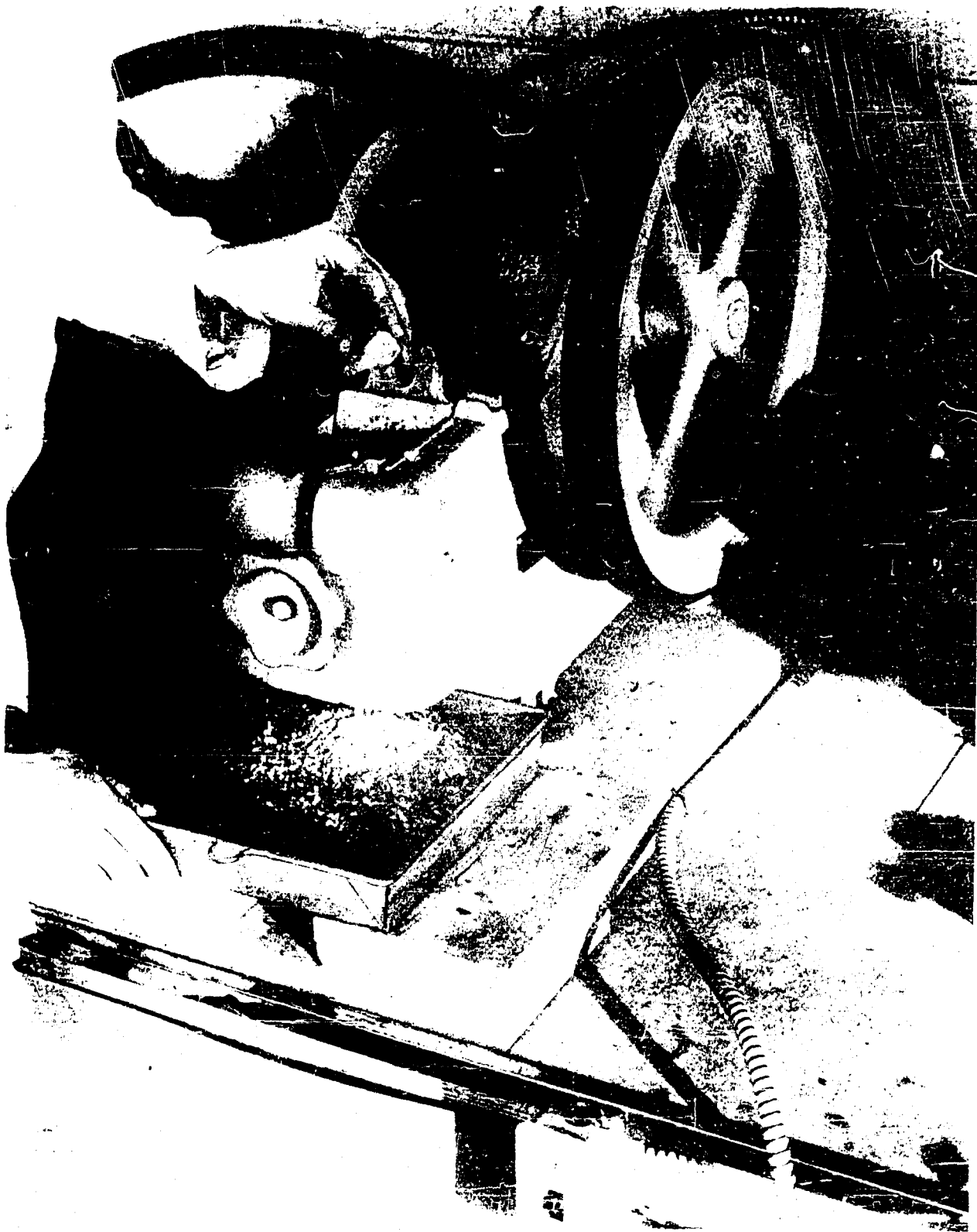


Figure 3.4. Soil and Rock Crusher



Figure 3.5. Soil and Rock Pulverizer



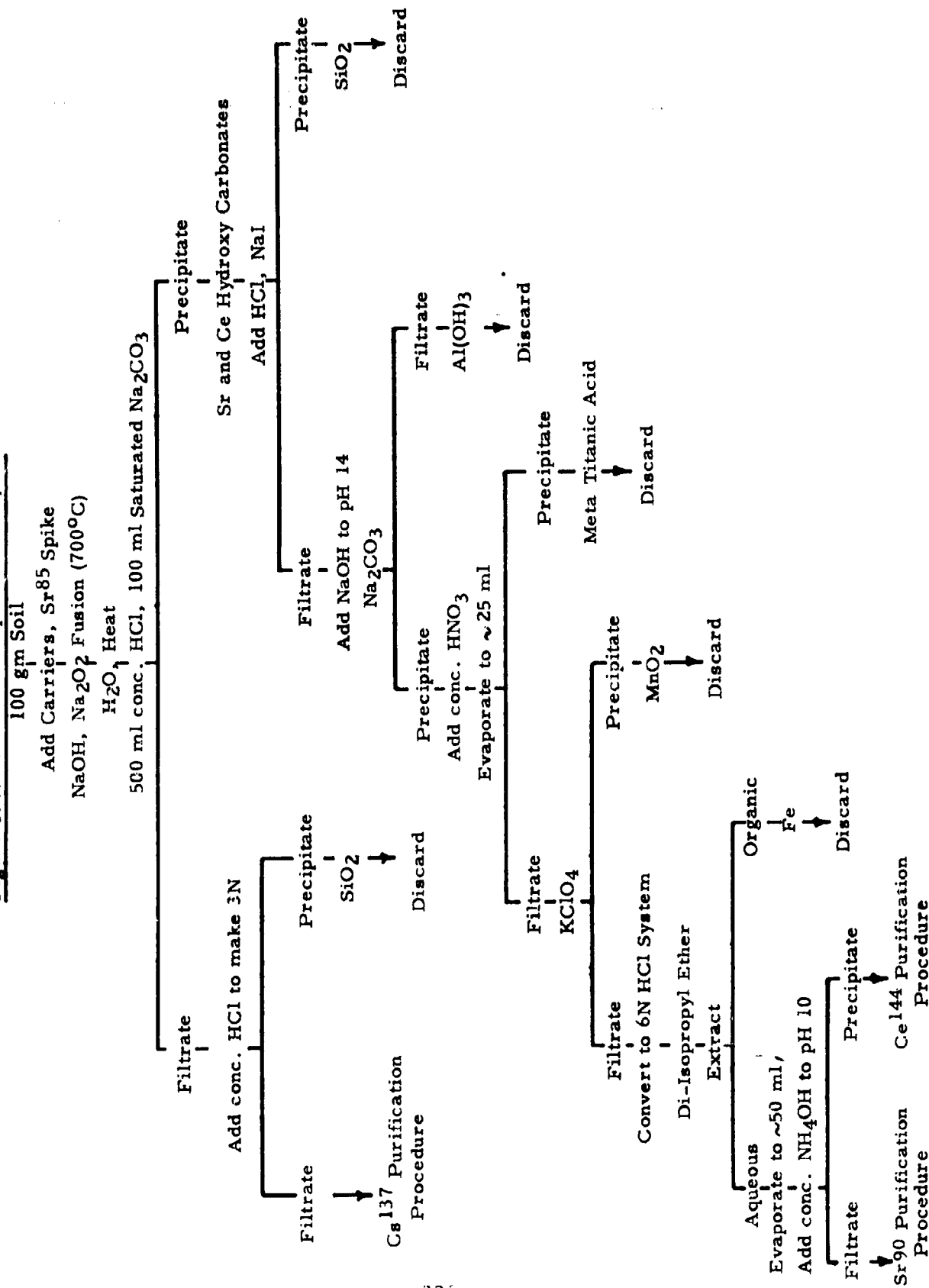
Figure 3.6. Patterson-Kelley Blender

THE RADIOCHEMICAL DETERMINATION OF STRONTIUM-90, RUTHENIUM-106, CESIUM-137 AND CERIUM-144 IN SOILS

The following is a description of the analytical methods for the radiochemical analysis of HASP soil samples. A sequential scheme of analysis was developed for strontium-90, cesium-137 and cerium-144 as shown in Figure 3.7. A separate aliquot was taken for the analysis of ruthenium-106. Considerable research was devoted to an unsuccessful attempt to include a plutonium analysis in the sequential scheme. Because of the very low activity levels (~ 1 dpm) associated with the maximum sample size which could be accommodated (~ 100 grams), and because of the relatively high concentrations of naturally occurring alpha emitters in the soil, a satisfactory plutonium analysis was not developed for the soil program.

Spectrographic analysis of a soil aliquot from each core showed that the naturally occurring cerium content varied from less than 10 ppm to 94 ppm, depending on the soil type. Therefore, appropriate corrections were applied to all cerium-144 chemical yields. The naturally occurring cesium content was also spectrographically determined but no cesium-137 chemical yield corrections were applied since no sample contained more than 6 ppm of cesium.

Figure 3.7. Outline of Sequential Analysis



The Sequential Separation of Strontium-90, Cesium-137 and Cerium-144¹

1. To a 100 gm aliquot of dry, homogenized soil sample contained in a 250 ml beaker, add 1 ml of Sr^{85} spike solution (approximately 25,000 cpm/ml) and 20 mg of strontium, cesium and cerium carriers. Mix thoroughly and dry in an oven at 110°C for 2 - 3 hours.
2. Add 200 gm of NaOH pellets to the dry soil sample and mix thoroughly.
3. Melt 100 gm of NaOH pellets in a 500 ml nickel crucible and rotate the crucible to coat the walls with melt as high as 1 1/2 inches from the top.
4. Cool the Ni crucible, transfer the soil-NaOH pellet mixture to the crucible and cover with 50 gm of NaOH.
5. Place the crucible on a tripod and heat with four Meeker burners. When the mixture begins to melt, stir with a glass rod. (CAUTION: some frothing will occur, but can be controlled by stirring and regulating heat.)
6. When the frothing has diminished, stir in 50 gm of Na_2O_2 and heat in a muffle furnace at 650°C for 1/2 hour. Remove the crucible from the furnace, add 25 gm of Na_2O_2 and heat in the furnace at 700°C for 1 hour.
7. Cool the crucible to room temperature and remove the flux by gently tapping the sides and bottom of the crucible.
8. Transfer the flux to a 2 liter beaker and add enough water to cover the melt. Add 400 ml of H_2O to the nickel crucible, place a cover glass over the top and heat on a hot plate until strong refluxing is evident. Combine the wash with the flux in the 2 liter beaker.
9. Heat the mixture until the large particles are broken, then heat for 1 hour with mechanical stirring to remove all traces of Na_2O_2 .
10. Cool, add 500 ml of concentrated HCl, 100 ml of saturated Na_2CO_3 and heat the solution for 1 hour with mechanical stirring.
11. Cool the mixture to room temperature and vacuum filter through a glass fiber filter paper contained in a 15 cm Buchner funnel. Wash the precipitate with hot H_2O to remove salts and reserve the filtrate for the cesium-137 purification procedure.
12. Transfer the precipitate and filter paper containing the strontium and cerium fraction to a 1 liter beaker. Wash the Buchner funnel with concentrated HCl until all of the precipitate is removed. Combine the wash and precipitate.
13. Add to the combined wash and precipitate 500 ml of concentrated HCl and heat the solution until the filter paper has disintegrated into small pieces.

14. Add 3 gm of NaI, place a cover glass over the beaker and heat the solution until I_2 vapors are no longer evident. Cool the solution in a cold water bath and filter through a 15 cm Whatman No. 41 filter paper contained in a Buchner funnel. Wash the residue with hot 6M HCl until colorless. Discard the residue.
15. Evaporate the filtrate and wash solution to a volume of approximately 300 ml and add NaOH until the pH is 14. Add 50 ml of saturated Na_2CO_3 , digest on a hot plate for 10 minutes, and filter the solution through a Buchner funnel containing 15 cm glass fiber filter paper. Wash the precipitate with 2N NaOH and filter to complete dryness. Discard the filtrate.
16. Transfer the precipitate and filter paper to a 600 ml beaker and add 150 ml of concentrated HNO_3 . Wash the Buchner funnel with concentrated HNO_3 and add the wash to the 600 ml beaker.
17. Boil the mixture on a hot plate until the filter paper is completely macerated. Filter the solution through a Buchner funnel containing a 9 cm glass fiber filter paper (Note 1) and wash the precipitate with 50 ml of H_2O . Discard the precipitate.
18. Transfer the filtrate to a clean 1 liter beaker and evaporate to about 25 ml (Note 2). Cool and filter the mixture through a Buchner funnel containing a 9 cm glass fiber filter paper. Wash the precipitate with 9N HNO_3 and discard the precipitate.
19. Transfer the filtrate to a 150 ml beaker, heat to boiling on a hot plate and add 1 gm of $KClO_4$.
20. Filter the mixture through a Buchner funnel containing a 9 cm glass fiber filter paper and wash the precipitate with 9N HNO_3 . Discard the precipitate.
21. Repeat steps 19 and 20.
22. Transfer the supernate to a clean beaker and evaporate to a small volume. Convert the nitric acid system to a hydrochloric acid system by the addition of concentrated HCl and heating on a hot plate until the red fumes of NO_2 are no longer evident.
23. Evaporate the solution to a small volume and add enough 6N HCl to bring the volume to 200 ml.
24. Transfer the solution to a 500 ml separatory funnel and wash the beaker with several ml of 6N HCl. Add the washings to the solution in the separatory funnel.
25. Add 25 ml of concentrated HCl, 200 ml of alcohol-free di-isopropyl ether and shake the mixture for 2 minutes. Allow the phases to separate and draw off the aqueous (lower) phase into a 600 ml beaker. Wash the ether fraction with two 100 ml portions of 6N HCl and combine the washings with the original solution (Note 3).
26. Evaporate the solution to about 50 ml, cool and add enough concentrated NH_4OH to bring the pH to 10. Cool the mixture to room temperature

and filter through a Buchner funnel containing a 9 cm Whatman No. 42 filter paper. Wash the precipitate with four 25 ml portions of 1N NH_4OH , filter the precipitate to complete dryness and reserve the precipitate for the Ce^{144} purification procedure.

27. Transfer the filtrate to a 1 liter beaker and reserve for the Sr^{90} purification procedure.

Note 1. Meta titanic acid will precipitate during filtration.

Note 2. Meta titanic acid will precipitate during evaporation.

Note 3 The ether fraction is reserved and purified for further use by distillation (boiling point 67.5°C).

Strontium-90 Purification Procedure²

- (a) To the filtrate from step 27 of the Sr^{90} , Ca^{137} and Ce^{144} sequential separation, add 200 ml of concentrated NH_4OH and 50 mg of Ca carrier. Heat on a hot plate for 20 minutes and add 100 ml of saturated Na_2CO_3 . Digest on a hot plate for 15 minutes, cool to room temperature and filter the precipitate through a Buchner funnel containing a 9 cm Whatman No. 52 filter paper. Wash the precipitate with 100 ml of 1N NH_4OH and discard the filtrate.
- (b) Dissolve the precipitate of $\text{SrCO}_3\text{-CaCO}_3$ in 100 ml of concentrated HCl and wash the filter paper with five 50 ml portions of hot 6N HCl .
- (c) Evaporate the solution to about 5 ml and transfer to a 40 ml centrifuge tube. Add 5 mg of Fe carrier, dilute to 10 ml with H_2O and add concentrated NH_4OH until $\text{Fe}(\text{OH})_3$ is completely precipitated. Centrifuge and transfer the supernate to a clean 40 ml centrifuge tube. Discard the precipitate.
- (d) Acidify the supernate with concentrated HCl , add 5 mg of Fe carrier and repeat step (c).
- (e) Acidify the supernate from step (d) with 6N HCl , add 20 mg of Ba carrier, 5 drops of alizarin indicator solution and adjust the pH with 6M NH_4OH until a color change from yellow to violet occurs (pH 6.8).
- (f) Add 5 ml of barium buffer solution (20% 6M HOAc - 80% 3M NH_4OAc) and heat nearly to boiling; add 1 ml of 1.5M Na_2CrO_4 (via a pipette), with stirring, and digest in a hot water bath until the BaCrO_4 settles out.
- (g) Cool the solution in a water bath, centrifuge, transfer the supernate to a 250 ml beaker and discard the precipitate.
- (h) Add 75 ml of concentrated NH_4OH , heat on a hot plate and add 75 ml of saturated Na_2CO_3 solution with stirring. Digest until the precipitate coagulates.
- (i) Centrifuge the mixture in a 40 ml glass centrifuge tube and discard the supernate. Wash the precipitate with two 10 ml portions of H_2O , centrifuge and discard the washings.
- (j) Dissolve the precipitate in 10 ml of 6N HNO_3 , boil the solution over a flame for about 2 minutes to remove excess CO_2 and add 5 mg of Fe carrier.
- (k) Add concentrated NH_4OH until $\text{Fe}(\text{OH})_3$ is completely precipitated, centrifuge and transfer the supernate to a clean 40 ml centrifuge tube. Discard the precipitate. Record the time of this $\text{Fe}(\text{OH})_3$ scavenge as the separation time for subsequent Y^{90} growth calculations.

- (l) Acidify the supernate with 6N HCl and add, via a pipette, 10 mg of yttrium carrier.
- (m) Transfer the solution to a 25 ml volumetric flask and dilute to volume with H_2O .
- (n) Pipette a 2 ml aliquot from the volumetric flask into a 10 ml test tube. Count the solution in the integral gamma counter for Sr^{85} activity and compare the count rate with a standard 2 ml aliquot of Sr^{85} spike solution to ascertain the radiometric strontium yield.
- (o) Quantitatively transfer the 2 ml aliquot used for radiometric yield and solution in the volumetric flask into a 40 ml centrifuge tube and allow to stand for at least twelve days to permit Y^{90} growth.
- (p) After equilibrium is established, add 7 to 8 drops of meta cresol purple indicator and make basic with 6M NH_4OH until one drop causes a color change from yellow to purple.
- (q) Digest in a hot water bath for about 10 minutes, cool, centrifuge and decant the supernate. Record the time and date of "milking."
- (r) Wash the $Y(OH)_3$ precipitate with 3 ml of H_2O , centrifuge and discard the wash.
- (s) Dissolve the precipitate in 2 ml of 1M HCl and 1.5 ml of 6M HNO_3 ; heat to boiling over an open flame and add 5 ml of saturated $(NH_4)_2C_2O_4$. Stir for several minutes and add gradually 10 ml more of saturated $(NH_4)_2C_2O_4$.
- (t) Digest in a hot water bath until the precipitate coagulates, cool and filter the $Y_2(C_2O_4)_3 \cdot 9H_2O$ on a previously weighed Whatman No. 42 filter disk using 10 ml of H_2O and finally 10 ml of anhydrous "anhydrol" as transfer agents. Dry in an oven at $100^\circ C$ for 10 minutes, cool to room temperature in a desiccator, weigh for chemical yield and mount on a standard brass planchet for beta counting.

Yttrium-90 Counting Procedure

The $Y_2(C_2O_4)_3 \cdot 9H_2O$ mount is counted in a low level counter. Each sample is counted once every 24 hours for three successive days. The counting time for each measurement is 8 hours. The activity at each mean counting time is corrected back to the milking time of Y^{90} using the theoretical half life of 64 hours. If the corrected activities agree to within one standard deviation of the counting error, the sample is considered radiochemically pure.

Cesium-137 Purification Procedure ^{3,4}

- (a) To the filtrate from step (11) of the sequential separation, add enough concentrated HCl to make the solution approximately 3N (SiO_2 will precipitate). Heat the mixture on a hot plate with mechanical stirring for 1 hour.
- (b) Cool to room temperature and filter the solution through a 24 cm Buchner funnel containing a Whatman No. 41H filter paper. Wash the SiO_2 alternately with 100 ml portions of hot 6N HCl and hot water until the silica is decolorized. Combine the washings and filtrate. Discard the SiO_2 precipitate.
- (c) Transfer the filtrate to a 3 liter beaker and neutralize the solution with NaOH pellets. Adjust the pH 5.5 with glacial acetic acid and cool the solution to room temperature.
- (d) Filter any precipitate through a Buchner funnel containing a Whatman No. 42 paper and wash the precipitate with 100 ml of hot water. Combine the wash and filtrate.
- (e) Transfer the filtrate and wash to a 3 liter beaker and cool to about 5°C in an ice bath with mechanical stirring.
- (f) Slowly add 100 ml of 15% sodium cobaltinitrite solution, with mechanical stirring and allow the mixture to stand for at least twelve hours in a cold water bath.
- (g) Decant and discard the supernate. Transfer the precipitate to a 40 ml glass centrifuge tube, centrifuge and discard the supernate.
- (h) Transfer the precipitate to a 250 ml beaker, and dissolve the precipitate in 75 ml of 6N HCl. Digest on a hot plate for 1 hour at moderate heat. Transfer the solution to a 40 ml glass centrifuge tube with 6N HCl and add 3 ml of 0.13M silicotungstic acid. Digest for 1/2 hour on a hot water bath, cool to room temperature, centrifuge and discard the supernate.
- (i) Wash the precipitate with two 10 ml portions of 6N HCl, centrifuge and discard the washings.
- (j) Dissolve the precipitate in 2 ml of 6N NaOH and 5 ml of H_2O . Centrifuge any precipitate of $\text{Co}(\text{OH})_2$ and transfer the supernate to a clean 40 ml glass centrifuge tube. Wash the precipitate with 5 ml of H_2O , centrifuge and combine the wash with the supernate. Discard the precipitate of $\text{Co}(\text{OH})_2$.
- (k) Adjust the acid concentration of the supernate to 6N with HCl to precipitate SiO_2 and WO_3 . Digest for 1/2 hour in a hot water bath, centrifuge and decant the supernate into a 100 ml beaker.
- (l) Dissolve the precipitate from step (k) in 2 ml of 6N NaOH, add 5 ml of H_2O and adjust the acid concentration to 6N with HCl. Centrifuge and decant the supernate into the 100 ml beaker.

- (m) Repeat step (l) and discard the precipitate.
- (o) Evaporate the combined solution in the 100 ml beaker to about 10 ml and transfer to a 40 ml centrifuge tube. Neutralize the solution with NaOH and precipitate Cs_2PtCl_6 by the addition of 3 ml of 10% chloroplatinic acid. Stir vigorously during addition.
- (p) Allow the mixture to stand for 1 hour, then centrifuge and discard the supernate.
- (q) Place the centrifuge tube in a hot water bath and dissolve the precipitate in a minimum amount of H_2O .
- (r) When the precipitate has completely dissolved, add 6 drops of hydrazine hydrate. Digest for 1/2 hour, cool, centrifuge and transfer the supernate to a 125 ml Erlenmeyer flask. Wash the Pt precipitate with two 5 ml portions of H_2O , centrifuge and combine the washings into the Erlenmeyer flask. Discard the precipitate.
- (s) To the combined supernate and washings in the Erlenmeyer flask, add 4 ml of aqua regia and evaporate the solution to dryness. Add another 4 ml of aqua regia and again evaporate to dryness.
- (t) Add 2 - 5 ml of 70% HClO_4 and heat to strong fumes of HClO_4 . Fume for 15 minutes, then cool the flask in an ice bath for 5 minutes. Add 25 ml of cold anhydrous ethyl acetate and cool for 15 minutes. Transfer the resultant CsClO_4 precipitate and ethyl acetate to a 40 ml centrifuge tube, centrifuge and discard the supernate. Wash the Erlenmeyer flask with 25 ml of cold anhydrous ethyl acetate, transfer the solution to the centrifuge tube, centrifuge and discard the wash.
- (u) Dissolve any remaining precipitate in the Erlenmeyer flask with 5 - 10 ml of H_2O and transfer the solution to the centrifuge tube. Digest in a hot water bath for 15 minutes to remove all traces of ethyl acetate.
- (v) Deposit the solution on a Bio Rex 40 cation exchange column (Note 1) at a flow rate of 1.5 ml/minute and wash the column with 100 ml of 0.2N HCl at the same flow rate. Strip the cesium from the column with 50 ml of 6N HCl, collecting the eluent in a 100 ml beaker (Note 2).
- (w) Evaporate the solution to about 10 ml, neutralize with 6N NaOH to a meta cresol purple end point. Add 3 ml of 10% chloroplatinic acid solution with vigorous stirring and allow to stand for 1 hour. Transfer the mixture to a 40 ml glass centrifuge tube, centrifuge and discard the supernate.
- (x) Slurry the precipitate in 5 ml of anhydrous "anhydrol" and filter onto a previously weighed Whatman No. 42 filter disk without applying suction, (Note 3); wash the precipitate with two 5 ml portions of anhydrous "anhydrol" applying a vacuum each time; oven dry at 100°C for ten minutes, cool in a desiccator and weigh as cesium chloroplatinate for chemical yield. Mount on a standard brass planchet for beta counting.

Cesium-137 Counting Procedure

The samples are counted in the low level beta counters. Radiochemical

purity is ascertained by counting the sample without an absorber and with an aluminum absorber of 9.77 mg/cm² thickness. If the absorber ratio agrees with the theoretical absorber ratio, the latter previously determined by counting absolute standards, the sample is accepted as radiochemically pure. Self-scattering self-absorption corrections are applied to convert to disintegrations per minute.

Note 1. The resin is conditioned in the following manner:

- (a) Soak the resin in H₂O for 24 hours
- (b) Transfer the resin to a column of 6 mm ID glass tubing, to a height of 10 cm
- (c) Wash the resin with three alternate washings of 100 ml of 0.2N HCl and 100 ml of H₂O

Note 2. At this point an additional cesium silicotungstate precipitation is performed on samples from lower depths (6 inches and below). The procedure is the same as in the precipitation of cesium silicotungstate in step (h) to step (m), then neutralize the solution and precipitate Cs₂PtCl₆ for mounting as in steps (w) and (x).

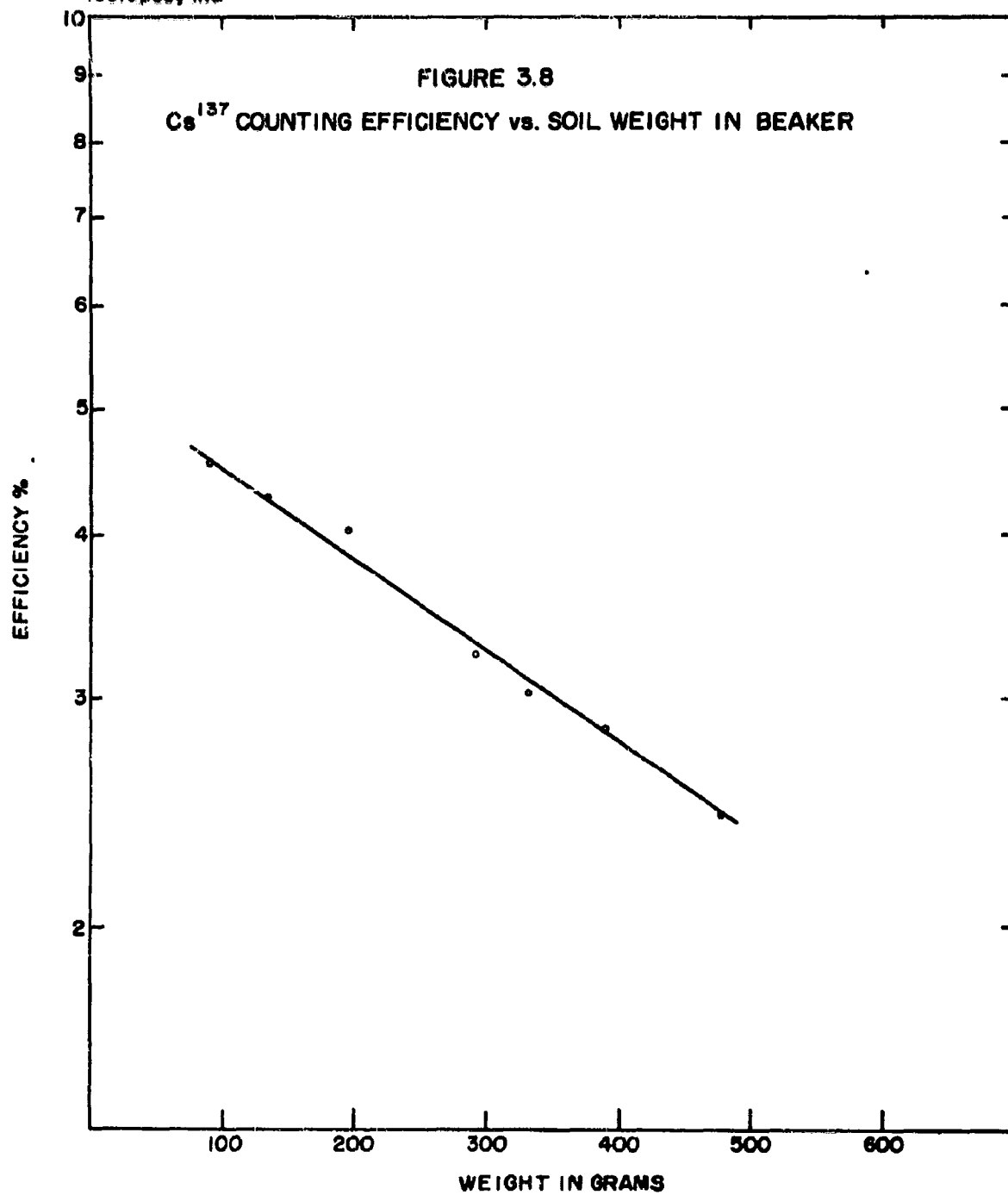
Note 3. The Cs₂PtCl₆ precipitate is a very fine powder and filtering without suction deposits the precipitate evenly on the surface of the filter disk with no tendency for seepage around the edge of the filtering column.

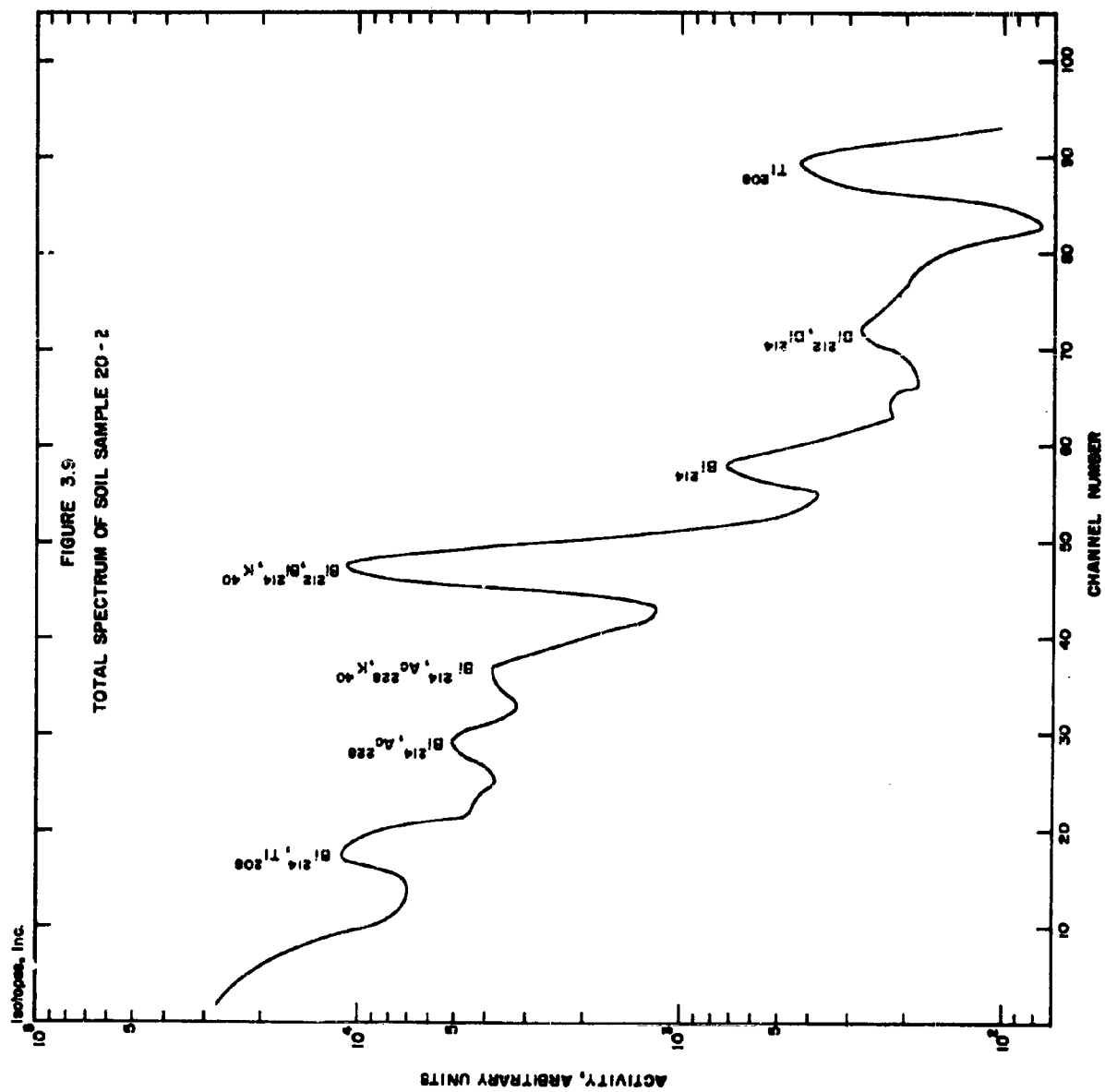
THE DETERMINATION OF CESIUM-137 IN SOILS BY GAMMA RAY SPECTROSCOPY⁵

Soil aliquots from depths no greater than two inches and ranging from 90 to 520 grams were analyzed for cesium-137 by gamma ray spectroscopy. The detector was an Isotopes, Inc. 3 inch by 3 inch NaI(Tl) crystal housed in a large lead cave as described in the radiometric techniques section of Part 1. The samples were counted in a 3 inch diameter 600 ml beaker placed directly on top of the crystal. The spectrometer had previously been calibrated for varying soil weights and the cesium-137 counting efficiency as a function of weight is shown in Figure 3.8.

To determine the effect of various soil densities, an experiment was conducted in which a standard cesium-137 spike solution was added to two different materials with densities of 0.64 and 1.6 grams/cc, respectively. The difference in efficiency using identical counting geometries was found to be only 7.0 percent. Since the densities of the soil samples were far less variable, absorption effects in the soils could account an error of no more than one or two percent at maximum.

The predominant radioactivity in soils at the present time is due to the natural products of the thorium and the uranium series and potassium-40 as shown for sample 20-2 in Figure 3.9. The 0.662 Mev photopeak of cesium-137 is completely obscured by the spectrum of these natural radioelements. To assay for cesium-137, it was necessary to resolve quantitatively the composite spectrum into its component parts. This was accomplished by subtracting the standard spectra of thorium, uranium and their daughters and potassium-40 from the gross spectrum all obtained under identical counting geometries.





The standard thorium spectra were obtained by blending a finely ground sample of monazite sand with an appropriate amount of powdered sodium phosphate and counting the mixture in the various physical geometries employed in the assay of the soil samples. The density of the sodium phosphate was about 1.3 grams per cc which was not greatly different from the density of the soils. The radioactive daughters in the thorium series were assumed to be in equilibrium with the parent nuclides. The appropriate thorium standard spectrum was subtracted from the gross composite sample spectrum by normalizing the two spectra to the 2.62 Mev photopeak of thallium-208. The resultant spectrum for sample 20-2 after the thorium subtraction is shown in Figure 3.10.

The standard uranium spectra were obtained by blending a finely ground sample of uraninite, which was known to be in equilibrium, with sodium phosphate according to the procedure described above for thorium. The appropriate uranium standard spectrum was subtracted from the resultant spectrum after the thorium subtraction by normalizing the two spectra to the 1.76 Mev photopeak of bismuth-214. The remaining spectrum after this second subtraction is shown in Figure 3.11. The irregular spectrum below the cesium-137 photopeak is a result of the presence of other fission products such as ruthenium-106 and the uncertainties involved in the mathematical subtractions of the other spectra.

The potassium-40 standard spectra were obtained by counting appropriate quantities of potassium acid phthalate in the various physical geometries normally employed in the assay of the soil samples. The proper potassium standard spectrum was subtracted from Figure 3.11 to yield the cesium-137 photopeak illustrated in Figure 3.12. The standard cesium-137 spectrum was normalized to this photopeak and the entire cesium-137 spectrum is represented in this figure. If the cesium-137 spectrum is subtracted from Figure 3.12, the remaining spectrum has little detail to permit any further

spectral resolution. The area beneath the 0.661 Mev photopeak was converted to disintegrations per minute by counting a soil sample spiked with a standard solution of cesium-137 under the various physical geometries employed.

The accuracy of the cesium-137 analysis by gamma ray spectroscopy was verified by comparing results obtained by this method with the data obtained by radiochemical separation of cesium. This comparison is summarized in Table 3.2 and in general shows good agreement. The limit of detection for soil samples assayed in beakers on top of the NaI(Tl) crystal was about 200 disintegrations per minute for a maximum sample size of 500 grams or 0.4 dpm/g. Although the annular type beaker described in Part I in which as much as 3 kilograms of soil was placed around the crystal was not employed in the analyses of these samples, the limit of detection of this arrangement was 175 disintegrations per 3 kilograms or 0.06 dpm/g.

Isotopes, Inc

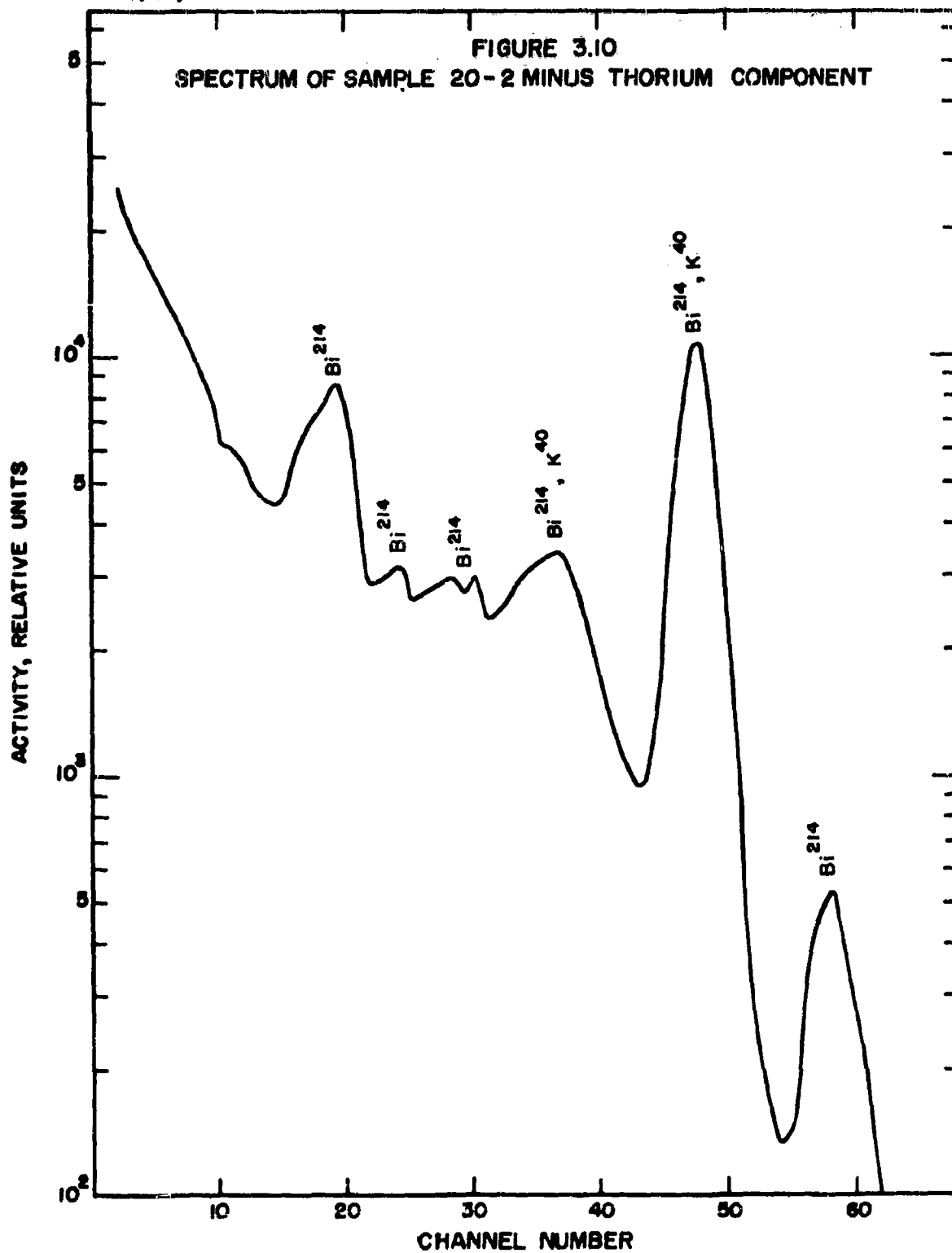
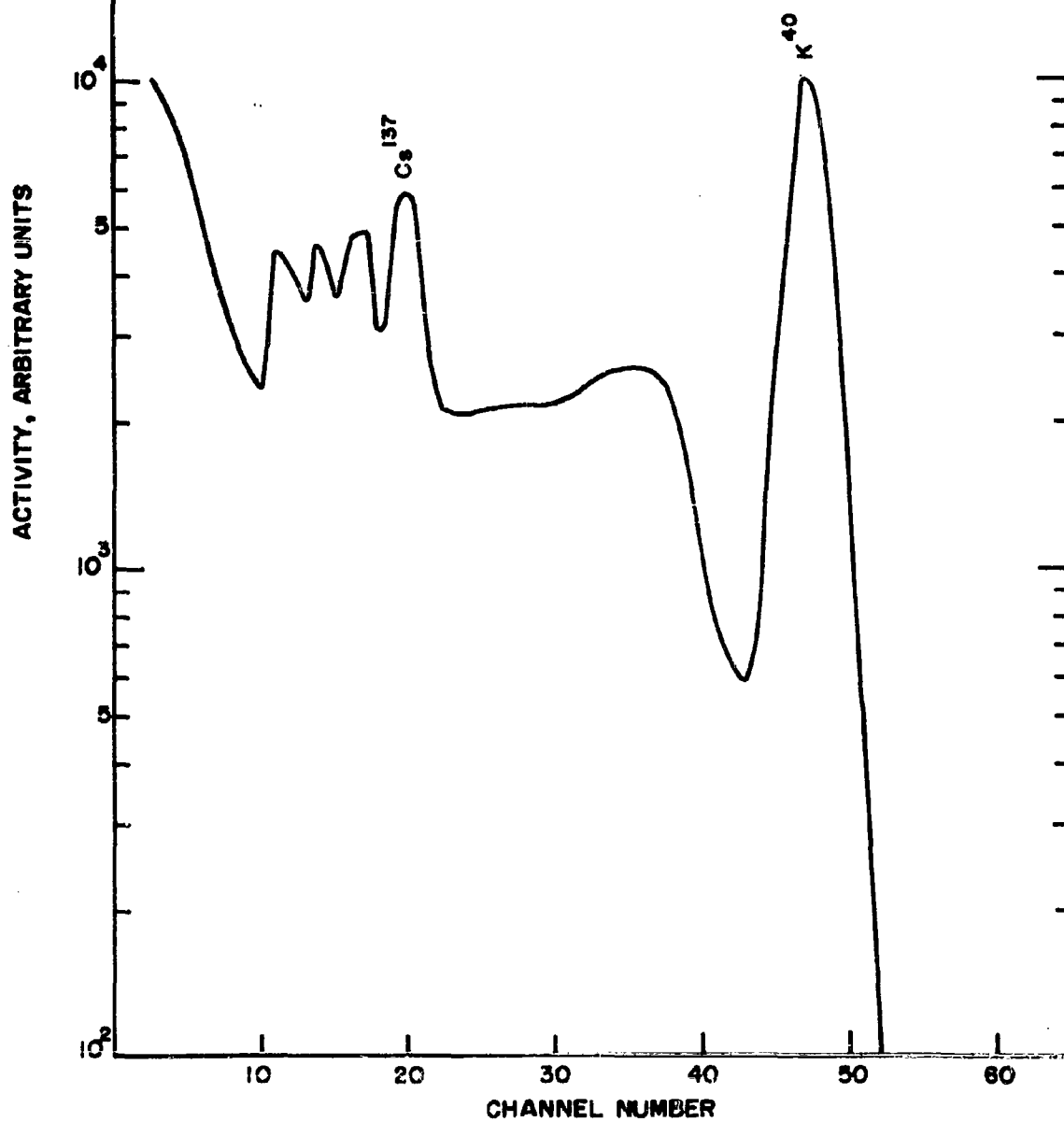


FIGURE 3.11

SPECTRUM OF SAMPLE 20-2 MINUS THORIUM AND U COMPONENTS



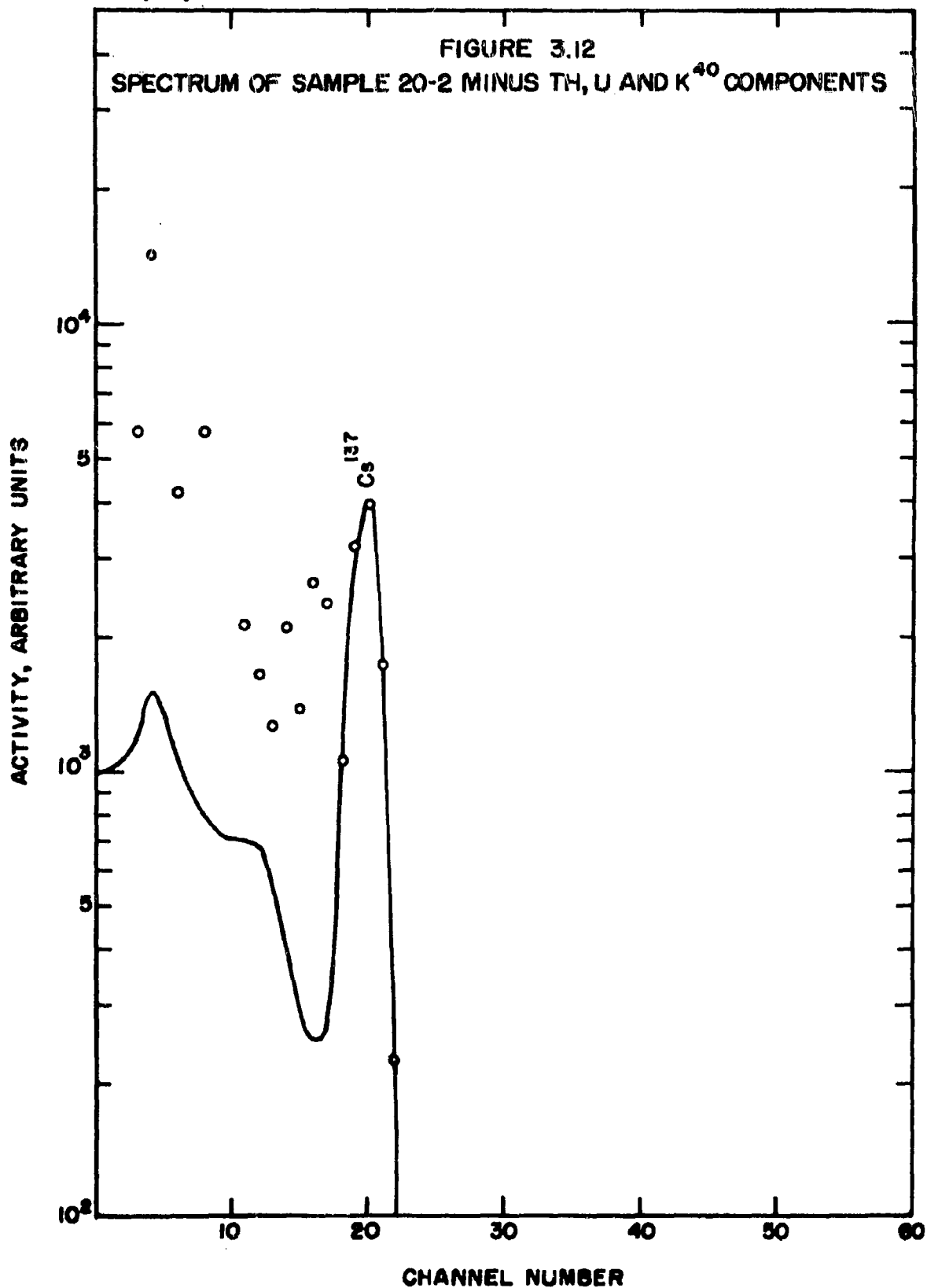


Table 3.2 Comparison of Cesium-137 Analyses by Gamma Ray Spectroscopy and Radiochemical Analysis

Sample No.	dpm Cs ¹³⁷ /100 grams	
	<u>Radiochemical Analysis</u>	<u>Gamma Ray Spectroscopy</u>
4-2	200 \pm 1.2%	195 \pm 2.0%
13-2	140 \pm 1.8%	142 \pm 2.3%
19-1	1510 \pm 1.2%	1550 \pm 0.6%
19-2	383 \pm 1.8%	369 \pm 1.1%

Cerium-144 Purification Procedure⁶

- (a) Remove the filter paper from the precipitate reserved for Ce^{144} analysis in step 26 of the sequential separation and dissolve the precipitate in 9N HNO_3 . Wash the filter paper with 9N HNO_3 and combine the wash and dissolved precipitate in a 250 ml beaker. Evaporate the solution to about 20 ml (Note 1).
- (b) Transfer the solution to a 250 ml separatory funnel containing 125 ml of freshly equilibrated methyl isobutyl ketone (Note 2). Wash the beaker with several ml of 9N HNO_3 and add the wash to the separatory funnel.
- (c) Add 5 ml of 2M NaBrO_3 and shake for 15 - 30 seconds. Withdraw the aqueous (bottom) phase and wash the organic phase with two 25 ml portions of 9N HNO_3 , each wash containing 1 ml of 2M NaBrO_3 (Note 2 and 3).
- (d) Back-extract the cerium by shaking the methyl isobutyl ketone phase with 10 ml of H_2O , containing 6 drops of 30% H_2O_2 (Note 2 and 4).
- (e) Withdraw the aqueous phase into a clean 50 ml beaker and neutralize by adding concentrated NH_4OH until a precipitate just appears. Acidify with 1.5 ml of 6N HNO_3 and dilute to 25 ml with H_2O .
- (f) Heat the solution just to boiling, add 5 ml of saturated $(\text{NH}_4)_2\text{C}_2\text{O}_4$, stir for several minutes and add gradually 10 ml more of saturated $(\text{NH}_4)_2\text{C}_2\text{O}_4$.
- (g) Digest the solution on a hot plate for about 10 minutes, cool to room temperature and filter the $\text{Ce}_2(\text{C}_2\text{O}_4)_3 \cdot 9\text{H}_2\text{O}$ on a Whatman No. 42 filter disk. Wash three times with 5 ml portions of H_2O and three times with 5 ml portions of acetone. Dry in an oven at 110°C for 20 minutes and cool to room temperature in a desiccator and beta count.
- (h) Chemical yield of cerium is determined, upon completion of counting, by dismounting the filter disk and plicofilm, and igniting at 850°C for 1 hour in a previously weighed (brought to constant weight) porcelain crucible. Cool in a desiccator, weigh and record the chemical yield of CeO_2 .

Cerium-144 Counting Procedure

The $\text{Ce}_2(\text{C}_2\text{O}_4)_3 \cdot 9\text{H}_2\text{O}$ mount is counted in a low level beta counter. Radiochemical purity is determined by first counting with an aluminum absorber of 224.3 mg/cm^2 thickness and then with a 412.7 mg/cm^2 absorber. The ratios of counting rates thus obtained are compared with ratios from absolute standards counted under the same conditions. If the sample ratio agrees

with the standard within the prescribed counting statistics, the sample is accepted as radiochemically pure.

Upon determination of chemical yield, the appropriate counter efficiency is applied in all Ce^{144} samples to convert to disintegrations per minute.

Note 1. If meta titanate precipitates at this point, filter the precipitate using a medium grade sintered glass funnel. Discard the precipitate.

Note 2. The equilibration of methyl isobutyl ketone (for use with two (2) samples) is performed in the following manner: to 400 ml of methyl isobutyl ketone add 400 ml of 9N HNO_3 containing 16 ml of 2M NaBrO_3 . Shake or stir for 5 minutes and remove the aqueous phase.

CAUTION: In extractions of strong HNO_3 solutions (6 to 12M) with methyl isobutyl ketone, considerable amounts of HNO_3 pass into the organic phase. It has been observed that such solutions of HNO_3 in methyl isobutyl ketone are unstable and will undergo a vigorous reaction after standing for a few hours. The methyl isobutyl ketone phases remaining after back-extraction with 10 ml of H_2O were observed to react similarly but only after standing for about 3 days. It is recommended, therefore, that the methyl isobutyl ketone not be equilibrated with HNO_3 until just before use and that it be washed thoroughly with water (three times with an equal volume) soon after use. It is also recommended that HNO_3 solutions which have been in contact with methyl isobutyl ketone be neutralized with NH_4OH prior to storing or discarding.

Note 3. Combine the aqueous phase and washings, and neutralize with NH_4OH before discarding.

Note 4. Wash the methyl isobutyl ketone three (3) times with 50 ml of H_2O before discarding. Also neutralize the washings before discarding.

Radiochemical Analysis of Ruthenium-106

1. Weigh 100 gms of dry homogenized soil in a 250 ml beaker and add 20 mg of ruthenium carrier. Mix thoroughly and dry in an oven at 110°C for 2-3 hours.
2. Add 200 gms of NaOH pellets to the dry soil sample, mix thoroughly and proceed as in steps 3 through 7 of the sequential separation of Sr^{90} , Cs^{137} and Ce^{144} in soils.
3. Transfer the melt to a 3 liter beaker and add 400 ml of H_2O . Add 400 ml of H_2O to the crucible, place a cover glass over the top and heat to boiling. Combine the crucible wash solution with the melt in the 3 liter beaker and heat for 1 hour, with mechanical stirring, to destroy all the Na_2O_2 .
4. Cool the beaker in a water bath and add concentrated HCl with continuous stirring until white lumps of $\text{Al}(\text{OH})_3$ appear.
5. Add more concentrated HCl until a yellow precipitate is obtained and then add an equal volume of concentrated HCl to make the solution approximately 6N.
6. Add 50 ml of 48% HBr and heat on a hot plate for 2 hours with mechanical stirring. Replace any volume lost through evaporation with 6N HCl .
7. Cool and filter the mixture through a 24 cm Buchner funnel using a Whatman No. 41H filter paper. Wash the SiO_2 precipitate with 150 ml portions of warm 6N HCl until the precipitate is decolorized. Discard the SiO_2 precipitate.
8. Transfer the filtrate to a 3 liter beaker and evaporate the solution on a hot plate to about 750 ml. Filter any salts onto a 15 cm Buchner funnel using a Whatman No. 42 filter paper. Wash the salts with warm 6N HCl until they are essentially decolorized. Discard the salts.
9. Transfer the filtrate to a clean 3 liter beaker and add an equal amount of H_2O to bring the solution to 3N in HCl .
10. Heat the solution to boiling and bubble H_2S gas through the solution for 15 minutes. Digest on a hot plate for 30 minutes, cool to approximately 50°C and filter the RuS_2 precipitate on a 9 cm Buchner funnel containing a Whatman No. 42 filter paper. Discard the filtrate.
11. Wash the precipitate with 100 ml of H_2O and discard the wash.
12. Transfer the precipitate and filter paper into a 250 ml distilling flask and water wash any remaining sulfide precipitate from the walls of the Buchner funnel into the distilling flask with a rubber policeman (Note 1).
13. Assemble the distilling apparatus as shown in Figure 3.13, cool the distilling flask in an ice bath and slowly add 30 ml of concentrated H_2SO_4 (Note 2).

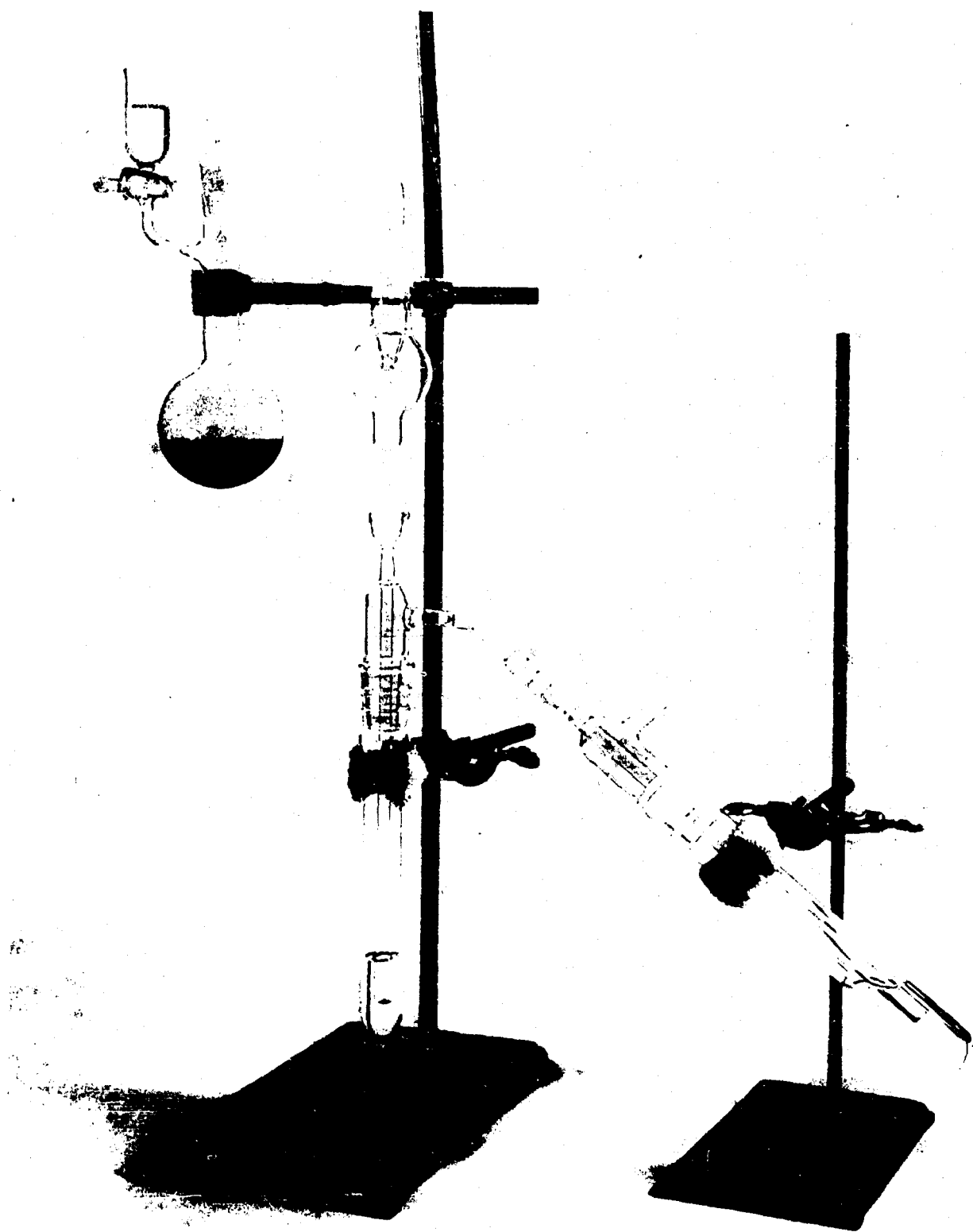


Figure 3.13. Ruthenium Distillation Apparatus

14. Through the addition funnel, add 5 ml of saturated NaBrO_3 and gently heat the flask over a flame (with swirling) for 10 minutes. Collect the volatile RuO_4 into two traps, each containing 30 ml of concentrated HCl .
15. Again cool the distilling flask, repeat the addition of 5 ml of saturated NaBrO_3 and apply heat (gently) for 10 minutes.
16. Repeat step 15 twice.
17. Transfer the $\text{Ru} - \text{HCl}$ distillate to a 250 ml Erlenmeyer flask and wash the traps with H_2O and 1N HCl . Combine the washings and distillate. Evaporate the solution on a hot plate in a fume hood to approximately 20 ml. (CAUTION: Br_2 evolved).
18. Cool and add powdered magnesium metal in small portions, swirling the flask after each addition, until the reduction to ruthenium metal is complete as indicated by a colorless solution.
19. After reduction is completed, transfer the mixture to a 40 ml glass centrifuge tube, centrifuge and discard the supernate.
20. Wash the ruthenium metal with 10 ml of 6N HCl and two 10 ml portions of H_2O . Centrifuge and discard the washings.
21. Slurry the precipitate with H_2O and filter onto a previously weighed Whatman No. 42 filter disk without applying a vacuum (Note 3); wash the precipitate with two 5 ml portions of acetone, dry in an oven at 100°C for ten minutes, cool in a desiccator and record the chemical yield of ruthenium metal.

Ruthenium-106 Counting Procedure

The Ru^{106} samples are counted in a low level beta counter.

The samples are counted without an absorber and with an aluminum absorber of 171.08 mg/cm^2 thickness. If the non-absorber - absorber ratio agrees with the previously determined standard absorber ratio within the prescribed counting statistics, the sample is accepted as radiochemically pure.

Appropriate counter efficiencies are applied to convert the count rate to disintegrations per minute.

Note 1. The volume in the distilling flask should not exceed 100 ml.

Note 2. Add the H_2SO_4 slowly so as to avoid charring of the filter paper.

Note 3. The ruthenium metal precipitate is a very fine precipitate and if suction is applied during filtration an irregular mount will result.

LIST OF REAGENTS

1. Carriers
 - (a) Strontium ($\text{SrCl}_2 \cdot 6\text{H}_2\text{O}$), 20 mg Sr/ml
 - (b) Cesium (CsCl_2), 20 mg Cs/ml
 - (c) Cerium (CeCl_3), 20 mg Ce/ml
 - (d) Ruthenium (Ru Metal), 30 mg Ru/ml
 - (e) Iron ($\text{FeCl}_3 \cdot 6\text{H}_2\text{O}$), 10 mg Fe/ml
 - (f) Calcium $[\text{Ca}(\text{NO}_3)_2 \cdot 4\text{H}_2\text{O}]$, 50 mg Ca/ml
 - (g) Barium ($\text{BaCl}_2 \cdot 2\text{H}_2\text{O}$), 20 mg Ba/ml
 - (h) Yttrium (Y_2O_3), 10 mg Y/ml
2. Sodium Hydroxide Pellets (NaOH)
3. Sodium Peroxide (Na_2O_2)
4. Saturated Sodium Carbonate (Na_2CO_3)
5. Sodium Iodide (NaI)
6. Potassium Perchlorate (KClO_4)
7. Di-isopropyl Ether (alcohol free) $(\text{CH}_3)_2\text{CHOCH}(\text{CH}_3)_2$
8. Alizarin Indicator (0.1% in ethanol)
9. Barium Buffer Solution (20% 6M HOAc - 80% 3M NH_4OAc)
10. Sodium Chromate (1.5M Na_2CrO_4)
11. Meta Cresol Purple Indicator Solution
12. Saturated Ammonium Oxalate $[(\text{NH}_4)_2\text{C}_2\text{O}_4]$
13. Sodium Cobaltinitrite $[15\% \text{Na}_3 \text{Co} (\text{NO}_2)_6]$
14. Silicotungstic Acid ($0.13\text{M SiO}_2 \cdot 12\text{WO}_3 \cdot 26\text{H}_2\text{O}$)
15. Chloroplatinic Acid ($10\% \text{H}_2\text{PtCl}_6 \cdot 6\text{H}_2\text{O}$)
16. Anhydrous Ethyl Acetate
17. Sodium Bromate (2M and saturated NaBrO_3)

18. Methyl Isobutyl Ketone (Hexone, $\text{CH}_3\text{COCH}_2\text{CH}(\text{CH}_3)_2$)
19. Hydrogen Bromide (48% HBr)
20. Hydrogen Sulfide (H_2S)
21. Magnesium Metal (70-80 Mesh)
22. Cation Exchange Resin (Bio Rex 40)
23. Acetone
24. Anhydrous "Anhydrol" (commercial product of denatured 95% ethyl alcohol available from C. P. Solvents, Inc., Newark, N. J.)

QUALITY CONTROL

The precision of radiochemical analysis of soil samples was determined by analysis of duplicate aliquots of several samples for each radionuclide of interest. The results, as summarized in Table 3.3, indicate that the precision of analysis for strontium-90 and ruthenium-106 was in the neighborhood of 10 percent, while the precision of the cerium-144 analysis was about 17 percent. It is felt that the greater uncertainty in the cerium-144 analysis may be due in part to the possibility of poor exchange between tracer cerium-144 and carrier. One split analysis is reported for cesium-137 because one-half of the other duplicate samples were lost during analysis.

Any sample cross contamination as well as contamination from minute residues from spike experiments was monitored by periodically processing a pre-1945 soil sample* in the same manner as the routine samples. Results of four samples monitored for each radionuclide indicate that all cesium-137 and ruthenium-106 blanks contained less than 1 DPM of contamination while three of the four blanks demonstrated less than 1 DPM of yttrium-90 activity. All blank samples contained about 2 DPM of cerium-144 contamination.

* Our gratitude to Dr. Ronald G. Menzel, Agricultural Research Service, Soil and Conservation Division, Beltsville, Maryland for a generous supply of pre-1945 soil.

Table 3.3 Duplicate Analyses

<u>Nuclide</u>	<u>Sample No.</u>		<u>DPM/100 gm</u>	<u>Avg DPM</u>	<u>+ Standard Deviation</u>
Sr ⁹⁰	7-4	A	24.0 \pm 3.4%	22.7	8.4%
		B	21.3 \pm 2.7%		
Sr ⁹⁰	8-6	A	2.35 \pm 3.7%	2.03	24.6%
		B	1.71 \pm 13.8%		
Sr ⁹⁰	11-3	A	43.9 \pm 0.8%	46.0	6.5%
		B	48.1 \pm 2.0%		
Sr ⁹⁰	17-6	A	2.80 \pm 5.3%	2.87	3.1%
		B	2.94 \pm 12.8%		
Sr ⁹⁰	18-5	A	29.4 \pm 4.2%	24.4	29.3%
		B	19.3 \pm 1.0%		
Sr ⁹⁰	20-2	A	66.9 \pm 3.8%	67.3	0.7%
		B	67.6 \pm 1.9%		
Average Sr ⁹⁰ Standard Deviation =					12.1%
Ru ¹⁰⁶	11-1	A	921 \pm 0.3%	927	0.9%
		B	933 \pm 1.2%		
Ru ¹⁰⁶	11-3	A	55.4 \pm 2.4%	54.7	0.2%
		B	53.9 \pm 5.5%		
Ru ¹⁰⁶	17-1	A	380 \pm 1.5%	405	8.7%
		B	430 \pm 1.2%		

Table 3.3 (continued)

<u>Nuclide</u>	<u>Sample No.</u>		<u>DPM/100 gm</u>	<u>Avg DPM</u>	<u>+ Standard Deviation</u>
Ru ¹⁰⁶	17-2	A	149 ± 1.9%	140	9.1%
		B	131 ± 1.2%		
Ru ¹⁰⁶	17-3	A	23.3 ± 12.7%	21.6	11.4%
		B	19.8 ± 9.2%		
Ru ¹⁰⁶	18-5	A	47.7 ± 1.6%	40.7	24.3%
		B	33.7 ± 2.0%		
Ru ¹⁰⁶	19-3	A	111 ± 1.4%	96.8	20.9%
		B	82.5 ± 1.7%		
Ru ¹⁰⁶	20-2	A	258 ± 1.4%	256	1.1%
		B	254 ± 1.5%		
Ru ¹⁰⁶	20-6	A	8.10 ± 4.7%	10.1	27.3%
		B	12.0 ± 4.7%		
Ru ¹⁰⁶	20-7	A	8.85 ± 6.5%	8.05	1.4%
		B	7.25 ± 7.2%		
<hr/>					
Average Ru ¹⁰⁶ Standard Deviation = 10.5%					
Ce ¹⁴⁴	11-3	A	19.3 ± 10.8%	16.8	21.5%
		B	14.2 ± 8.3%		
Ce ¹⁴⁴	17-3	A	32.3 ± 6.3%	28.5	18.9%
		B	24.7 ± 6.3%		

Table 3. 3 (continued)

<u>Nuclide</u>	<u>Sample No.</u>		<u>DPM/100 gm</u>	<u>Avg DPM</u>	<u>+ Standard Deviation</u>
Ce ¹⁴⁴	19-3	A	109 ± 4.8%	102	9.2%
		B	95.7 ± 4.3%		
Ce ¹⁴⁴	19-4	A	43.8 ± 9.2%	49.1	15.2%
		B	54.4 ± 2.3%		
Ce ¹⁴⁴	20-1	A	526 ± 3.7%	457	21.4%
		B	388 ± 2.4%		
Ce ¹⁴⁴	20-2	A	332 ± 3.0%	408	26.2%
		B	484 ± 2.7%		
<hr/>					
Average Ce ¹⁴⁴ Standard Deviation = 16.9%					
Cs ¹³⁷	20-2	A	163 ± 5.0%	170	5.8%
		B	177 ± 3.9%		

RESULTS AND DISCUSSION OF RADIOCHEMICAL DATA

In past studies^{7, 8} designed to determine the integrated world-wide fallout of strontium-90, one of the most important considerations which had to be borne in mind in the soil sampling procedures was the depth to which the core was taken. It was generally assumed after some preliminary studies had been conducted, that in 1956 and 1958 little strontium-90 had penetrated below a depth of six inches in the soil. Although this appeared to be a good assumption at that time it was realized that in due course some movement of the strontium-90 would occur in the soils in much the same manner as materials pass through an ion-exchange column. This comparison with ion-exchange columns can, of course, be extended to include different soils possessing different capacities for retention of strontium-90. It would be expected that the strontium-90 deposited as a result of world-wide fallout would be distributed with depth in a variable manner from soil to soil. Those soils possessing low cation exchange capacities would probably exhibit the most penetration of strontium-90 while those with a greater affinity for strontium-90 would tend to concentrate the nuclide to a greater extent in the uppermost sections of the soil. Thus a sandy soil might show relatively larger fractions of the total deposit at depth in a soil core compared to a clay or more loamy material. In addition to the chemical and physical properties of the soil itself and their effects on the distribution of strontium-90 with depth in the soil there are some obvious external parameters which can be important in these considerations. For example, if the adsorption of the radioactive nuclide by the soil from the deposited precipitation is a rate-controlled process, then the extent of the adsorption by the soil will depend on additional factors such as the permeability of the underlying strata and the rate of precipitation. Those materials which are poorly drained and have highly impermeable underlying

bedrock will retain the water containing the radioactivity for longer periods of time than well-drained soils, and thus the probability of equilibrium being attained between the liquid and solid phases will be enhanced for poorly-drained soils. Hence in the situation where two soils of equal cation exchange capacity are being considered, the soil which is poorly drained will tend to retain more of the radioactivity at levels nearer to the surface than the well-drained soil, where relatively rapid flow of the liquid phase through the material will tend to permit a more even distribution of the radioactivity with depth to be attained. Previous workers have endeavored to make the above considerations more quantitative by utilizing the concept of mass action. If we consider the simplest situation in which radioactive ion A^+ exchanges with soil mineral BX , the equation for this process may be written



and the rate constant K can be expressed as

$$K = \frac{[AX][B^+]}{[A^+][BX]}$$

Two general statements can then be made concerning K for two situations as follows.

First, the situation in which A^+ remains constant but BX varies, i.e., considering one radioactive nuclide strontium-90 and several different soil materials.

Second, the situation in which BX is constant but A^+ can vary, i.e., considering only one soil material but several different radioactive nuclides. It has been found⁹ in the first case that the rate constant K decreases in magnitude from clays through sandy clays to sands or, in more particular terms, K for montmorillonite > illite > kaolin > quartz. In the second case it has been generally found, for different ions in the same mineral or soil, that the values of K decrease from Ce > Cs > Sr > Ru. Thus, in a given soil, ruthenium might

be expected to be more evenly distributed with depth than strontium which in turn would penetrate to greater depths than cesium or cerium, and so on.

The above considerations are extremely important in the many problems presented by the world-wide fallout of radioactivity from weapons tests. As mentioned previously they can be of assistance in ascertaining the depth to which the soil ought to be sampled to ensure inclusion of all deposited fallout radioactivity. In addition, if these factors can be placed on a quantitative basis, it will permit more accurate evaluations of the dose to the human body from externally deposited gamma-emitting nuclides to be made, and, in addition, give us increased knowledge from which we may be able to predict future concentrations of fallout radioactivity in food products. Our aims in this limited and curtailed phase of the HASP program were to elucidate some of these factors and perhaps point the way to areas in which further work ought to be performed. Soils, varying from almost pure, well-drained sands to very poorly-drained, almost impermeable clays, were collected in New Jersey in summer 1960 for this purpose. Radiochemical analyses for strontium-90, ruthenium-106, cesium-137, and cerium-144 were performed on aliquots of soil taken at various depths within these soil cores. In addition it was hoped that another major soil type area could be studied in a similar manner. Soils were collected, therefore, in Kansas in late summer 1960 but unfortunately limited time and funds did not permit completion of this phase of the proposed work. On the credit side, however, considerable information was gleaned from our data on New Jersey soils and the project was certainly successful in this phase.

All results obtained from radiochemical analyses of the soil cores are given in Table 3.4. This table gives the depth profiles of strontium-90, ruthenium-106, cesium-137 and cerium-144 in eleven different soils from New Jersey and partial results from two soils collected in eastern Kansas. Included in the eleven soil sites

from New Jersey is one soil site which had been plowed in early 1960 and cultivated in the same year to compare with the same soil which had remained undisturbed. Analyses on the former core were performed to give some indication of the effect which man's activities have on the distribution of radioactivity with depth. Naturally this should result in a more even distribution of the radioactivity with depth, and this, in fact, proved to be the case (Collington Sandy Loam No. 5 and No. 4). All soils were carefully chosen in both states, and the selected areas had to satisfy certain stringent conditions. The chosen sampling sites had

- (a) to be in level areas so that no run-off from neighbouring areas could occur,
- (b) to have no objects, such as trees and buildings, in the immediate vicinity, which might shield them from precipitation, and
- (c) to have remained undisturbed by man for at least eight years prior to sampling in 1960 (with the exception of No. 5).

In addition we endeavoured to include soils which reflected a wide range in pH, organic content, permeability and drainage, texture, and chemical and mineral composition.

Columns 1, 2, and 3 in Table 3.4 give the depth of the sample from which an aliquot (usually 100g) was taken for radiochemical analyses. Depths are given in inches and in grams of soil. For conversion of the activities into surface concentrations (e.g. mc/mi^2), the volume of a cylindrical cross-section of 1 inch in height taken from the sampling corer is 823.5 cm^3 . All the weights reported are referred to this cylindrical corer which was used to obtain the contamination-free soil sample from the larger core taken in the field. It is noted that the weight of the top 1/2 inch section varies over a wide range. This is most likely a result of undulations in the surface of the soil sample, variations in, natural compaction, and also because this section includes some vegetation in the uppermost part. It is difficult, because of these effects, to determine

Table 3.4 Deposition of Strontium-90, Ruthenium-106, Cesium-137 and Cerium-144 in New Jersey and Kansas Soils in 1960

Sample No. 4 Collington Sandy Loam (Undisturbed) N. J.

A.	Depth		Nuclide Concentrations (dpm/100 g dry Wt)***				Nuclide Ratios			
	Inches	Dry Wt. (g)*	Wet Wt. (g)*	Sr ⁹⁰	Ru ¹⁰⁶	Cs ¹³⁷	Ce ¹⁴⁴	Ru ¹⁰⁶ /Sr ⁹⁰	Cs ¹³⁷ /Sr ⁹⁰	Ce ¹⁴⁴ /Sr ⁹⁰
	0-1/2	258	312	67.3	342	113	546	5.1	1.7	8.1
	1/2-1	532	646	63.6	251	200	411	3.9	3.1	6.5
	1-2	1217	1479	43.9	125	123	231	2.8	2.8	5.3
	2-3	1021	1230	25.3	59.3	86.2	85.2	2.3	3.4	3.4
	3-4	1171	1398	17.5	33.4	27.4	49.5	1.9	1.6	2.8
	4-6	2418	2738	12.7	25**	<4.2	39.6	2.0	< 0.3	3.1
	6-9	3863	4343	4.25	13.1	--	29**	3.1	--	6.8
	9-12	3503	3933	3.42	9.3	--	19.7	2.7	--	5.8

B.	Depth		Cumulative Activities (dpm)				
	Inches	Dry Wt. (g)	Wet Wt. (g)	Sr ⁹⁰	Ru ¹⁰⁶	Cs ¹³⁷	Ce ¹⁴⁴
	1/2	258	312	174	882	292	1409
	1	790	958	512	2217	1354	3596
	2	2007	2437	1046	3738	2851	6407
	3	3028	3667	1304	4343	3731	7277
	4	4199	5065	1509	4734	4052	7857
	6	6617	7803	1816	5338	<4154	8815
	9	10480	12146	1980	5844	--	9588
	12	13983	16079	2100	6169	--	10278

Sample No. 5 Collington Sandy Loam (Disturbed) N. J.

A.	Depth		Nuclide Concentrations (dpm/100 g dry Wt)***				Nuclide Ratios			
	Inches	Dry Wt. (g)*	Wet Wt. (g)*	Sr ⁹⁰	Ru ¹⁰⁶	Cs ¹³⁷	Ce ¹⁴⁴	Ru ¹⁰⁶ /Sr ⁹⁰	Cs ¹³⁷ /Sr ⁹⁰	Ce ¹⁴⁴ /Sr ⁹⁰
	0-2	2281	2648	29.9	36.6	39.8	61.5	1.2	1.3	2.1
	2-4	2563	2931	14.2	34.0	23**	63.7	2.4	1.6	4.5
	4-6	2653	3045	24.8	74.8	49.0	165	3.0	2.0	6.7
	6-9	3823	4462	14.2	50.8	<4.9	61.9	3.6	<0.3	4.4
	9-12	4103	4746	4.9	17.3	14.7	37.6	3.5	3.0	7.6

B.	Depth		Cumulative Activities (dpm)				
	Inches	Dry Wt. (g)	Wet Wt. (g)	Sr ⁹⁰	Ru ¹⁰⁶	Cs ¹³⁷	Ce ¹⁴⁴
	2	2281	2648	682	835	908	1403
	4	4844	5579	1046	1706	1582	3036
	6	7497	8624	1704	3688	2882	7413
	9	11320	13086	2247	5628	<3069	9779
	12	15423	17832	2449	6338	<3672	11321

Sample No. 7 Rutledge Fine Sandy Loam N. J.

A.	Depth		Nuclide Concentrations (dpm/100 g dry Wt)***					Nuclide Ratios		
	Inches	Dry Wt. (g)*	Wet Wt. (g)*	Sr ⁹⁰	Ru ¹⁰⁶	Cs ¹³⁷	Ce ¹⁴⁴	Ru ¹⁰⁶ /Sr ⁹⁰	Cs ¹³⁷ /Sr ⁹⁰	Ce ¹⁴⁴ /Sr ⁹⁰
0-1/2	228	364	116	345	244	1529	3.0	2.1	13.2	
1/2-1	474	650	90**	354	304	741	3.9	3.4	8.2	
1-2	1000	1343	56.6	120	140**	128	2.1	2.5	2.3	
2-3	1114	1442	21.3	44.7	49.3	62.5	2.1	2.3	2.9	
3-4	1394	1770	11.8	32.9	23**	22.1	2.8	1.9	1.9	
4-6	2380	2941	8.1	18.9	12.7	43.7	2.3	1.6	5.4	
6-9	3393	4233	5.5	12.9	7.9	17.5	2.3	1.4	3.2	
9-12	3618	4343	3.0	< 12.2	15.0	10**	< 4.1	5.0	3.3	

B.	Depth		Cumulative Activities (dpm)			
	<u>Inches</u>	<u>Dry Wt. (g)</u>	<u>Wet Wt. (g)</u>	<u>Sr⁹⁰</u>	<u>Ru¹⁰⁶</u>	<u>Cs¹³⁷</u>
1/2	228	364	264	787	556	3486
1	702	1014	691	2465	1997	6998
2	1702	2357	1257	3665	3397	8278
3	2816	3799	1630	4163	3946	8974
4	4210	5569	1794	4662	4267	9282
6	6590	8510	1987	5072	4569	10322
9	9983	12743	2174	5510	4837	10916
12	13601	17086	2282	< 5951	5380	11278

Sample No. 8 Marlton Sandy Loam, N. J.

A.	Depth		Nuclide Concentrations (dpm/100 g dry Wt.)***					Nuclide Ratios		
	Inches	Dry Wt. (g)*	Wet Wt. (g)*	Sr ⁹⁰	Ru ¹⁰⁶	Cs ¹³⁷	Ce ¹⁴⁴	Ru ¹⁰⁶ /Sr ⁹⁰	Cs ¹³⁷ /Sr ⁹⁰	Ce ¹⁴⁴ /Sr ⁹⁰
	0-1/2	220	306	366	889	858	2573	2.4	2.3	7.0
	1/2-1	409	522	109	161	240	282	1.5	2.2	2.6
	1-2	960	1180	37.7	98.3	47.1	62.9	2.6	1.2	1.7
	2-3	1178	1361	13.7	35.7	< 2.1	19.6	2.6	< 0.2	1.4
	3-4	1418	1668	6.5	18.8	< 5.6	5.0	2.9	< 0.9	0.8
	4-6	2468	2899	2.0	19.3	7.2	< 6.4	9.6	3.6	< 3.2
	6-10	5248	6436	1.0	4.7	4.0	< 4.8	4.7	4.0	< 4.8

B.	Depth		Cumulative Activities (dpm)				
	<u>Inches</u>	<u>Dry Wt. (g)</u>	<u>Wet Wt. (g)</u>	<u>Sr⁹⁰</u>	<u>Ru¹⁰⁶</u>	<u>Cs¹³⁷</u>	<u>Ce¹⁴⁴</u>
	1/2	220	306	806	1959	1890	5669
	1	629	828	1253	2617	2872	6822
	2	1589	2008	1615	3561	3323	7425
	3	2767	3369	1776	3981	< 3348	7656
	4	4185	5037	1869	4248	< 3428	7728
	6	6653	7936	1919	4724	< 3600	< 7885
	10	11901	14372	1974	4968	< 3813	< 8136

Sample No. 10 Lakewood Sand, N. J.

A.	Depth		Nuclide Concentrations (dpm/100 g dry Wt.)***				Nuclide Ratios		
			Sr^{90}	Ru^{106}	Cs^{137}	Ce^{144}	Ru^{106}/Sr^{90}	Cs^{137}/Sr^{90}	Ce^{144}/Sr^{90}
Inches	Dry Wt. (g)*	Wet Wt. (g)*							
0-1/2	409	415	29.5	165	318	620	5.6	10.8	21.0
1/2-1	632	640.5	37.2	82.8	81.0	129	2.2	2.2	3.5
1-2	1123	1148.5	13.4	47.1	6.8	17.5	3.5	0.5	1.3
2-3	1251	1281	20**	26.9	4.6	13.9	1.3	0.2	0.7
3-4	1240	1278	30.4	20.0	5**	15.2	0.7	0.2	0.5
4-6	2713	2761	8.5	8.6	5.7	<11.4	1.0	0.7	1.3
6-9	4003	4037	7.1	16.3	5**	33.4	2.3	0.7	4.7
9-12	4003	4065	5**	12.7	4.3	<17.1	2.5	0.9	<3.4

B.	Depth		Cumulative Activities (dpm)			
			Sr^{90}	Ru^{106}	Cs^{137}	Ce^{144}
Inches	Dry Wt. (g)	Wet Wt. (g)				
1/2	409	415	121	675	1302	2536
1	1041	1055.5	356	1198	1813	3351
2	2164	2204	506	1728	1890	3548
3	3415	3485	756	2064	1947	3722
4	4655	4763	1133	2312	2009	3910
6	7368	7524	1363	2544	2165	<4219
9	11371	11561	1649	3201	2367	<5556
12	15374	15626	1849	3713	2541	<6241

Sample No. 11 Leon Sand, N. J.

A.	Depth		Nuclide Concentrations (dpm/100 g dry Wt.)***				Nuclide Ratios		
			Sr^{90}	Ru^{106}	Cs^{137}	Ce^{144}	Ru^{106}/Sr^{90}	Cs^{137}/Sr^{90}	Ce^{144}/Sr^{90}
Inches	Dry Wt. (g)*	Wet Wt. (g)*							
0-1/2	306	406	327	927	1314	2003	2.8	4.0	6.1
1/2-1	387	451	92.6	183	206	182	2.0	2.2	2.0
1-2	1134	1256	46.0	54.6	37.0	16.7	1.2	0.8	0.4
2-3	1204	1285	11.4	22.1	9.4	7.9	1.9	0.8	0.7
3-4	1167	1255	14.5	10.2	28.9	10**	0.7	2.0	0.7
4-6	2741	2798	2.5	--	< 6.0	< 13.1	--	< 2.4	< 5.2
6-9	3833	4003	1**	--	--	< 15.9	--	--	< 15.9
9-12	4112	4235	1**	--	--	--	--	--	--

B.	Depth		Cumulative Activities			
			Sr^{90}	Ru^{106}	Cs^{137}	Ce^{144}
Inches	Dry Wt. (g)	Wet Wt. (g)				
1/2	306	406	1001	2837	4021	6129
1	693	857	1359	3545	4818	6833
2	1827	2113	1881	4166	5238	7024
3	3031	3398	2018	4432	5351	7119
4	4198	4653	2187	4551	5688	7236
6	6939	7451	2257	--	< 5851	< 7595
9	10772	11454	2295	--	--	< 8204
12	14884	15689	2336	--	--	--

Sample No. 13 Keyport Sandy Loam, N. J.

A.	Depth		Nuclide Concentrations (dpm/100 g dry Wt.)***					Nuclide Ratios		
	Inches	Dry Wt. (g)*	Wet Wt. (g)*	Sr ⁹⁰	Ru ¹⁰⁶	Cs ¹³⁷	Ce ¹⁴⁴	Ru ¹⁰⁶ /Sr ⁹⁰	Cs ¹³⁷ /Sr ⁹⁰	Ce ¹⁴⁴ /Sr ⁹⁰
0-1/2	118	127	67.4	357	--	808	5.3	--	--	12.0
1/2-1	546	621	48.6	226	140	545	4.6	2.9	--	11.2
1-2	1561	1775	30.7	54.4	35.7	78.7	1.8	1.2	--	2.6
2-3	1139	1303	11**	37.0	< 9.0	47.9	3.4	< 0.8	--	4.4
3-4	1483	1636	4.1	6.3	--	25.4	1.5	--	--	6.2
4-6	2823	3143	2.2	5.9	4.6	32.7	2.7	2.1	--	14.9
6-9	4203	4853	1.8	5**	--	6.8	2.8	--	--	3.8
9-12	3901	4463	2.3	3.9	3.8	10.0	1.7	1.6	--	4.3

B.	Depth		Cumulative Activities			
	Inches	Dry Wt. (g)	Wet Wt. (g)	Sr ⁹⁰	Ru ¹⁰⁶	Ce ¹⁴⁴
	1/2	118	127	80	421	--
	1	664	748	346	1655	--
	2	2225	2523	825	2504	--
	3	3364	3826	1053	2925	--
	4	4847	5462	1113	3019	--
	6	7670	8605	1176	3186	--
	9	11873	13458	1252	3396	--
	12	15774	17921	1343	3547	--

Sample No. 17 Woodstown Sandy Loam, N. J.

A.	Depth		Nuclide Concentrations (dpm/100 g dry Wt.)***					Nuclide Ratios		
	Inches	Dry Wt. (g)*	Wet Wt. (g)*	Sr ⁹⁰	Ru ¹⁰⁶	Cs ¹³⁷	Ce ¹⁴⁴	Ru ¹⁰⁶ /Sr ⁹⁰	Cs ¹³⁷ /Sr ⁹⁰	Ce ¹⁴⁴ /Sr ⁹⁰
	0-1	374	462	66.4	405	443	700	6.1	6.7	10.5
	1-2 1/8	1440	1703	22.8	140	86.4	123	6.1	3.8	5.4
	2 1/8-3 1/8	1326	1546	18.3	21.6	< 18.2	28.5	1.2	< 1.0	1.6
	3 1/8-4 1/8	1380	1553	24.0	6.9	4.0	31.1	0.3	< 0.2	1.3
	4 1/8-6 1/8	2722	3052	19.8	5.5	3.8	35**	0.3	< 0.2	1.8
	6 1/8-9 1/8	4204	4783	2.9	2.8	2.4	39.5	1.0	0.9	13.8
	9 1/8-13 1/8	5258	6281	1**	3.0	< 3.3	30.7	3.0	< 3.3	30.7

B.	Depth		Cumulative Activities			
	Inches	Dry Wt. (g)	Wet Wt. (g)	Sr ⁹⁰	Ru ¹⁰⁶	Ce ¹⁴⁴
	1	374	462	250	1516	2620
	2 1/8	1814	2165	578	3537	4391
	3 1/8	3140	3711	820	3818	4769
	4 1/8	4520	5264	1151	3900	5333
	6 1/8	7242	8316	1591	4064	6286
	9 1/8	11446	13099	1814	4183	7946
	13 1/8	16904	19380	1869	4350	9622

Sample No. 18 Buckle Silt Loam, N. J.

A.	Depth		Nuclide Concentrations (dpm/100 g dry Wt.)***					Nuclide Ratios		
	Inches	Dry Wt.(g)*	Wet Wt.(g)*	Sr ⁹⁰	Ru ¹⁰⁶	Cs ¹³⁷	Ce ¹⁴⁴	Ru ¹⁰⁶ /Sr ⁹⁰	Cs ¹³⁷ /Sr ⁹⁰	Ce ¹⁴⁴ /Sr ⁹⁰
	0-1/2	83	94.5	111	225	228	816	2.0	2.1	7.4
	1/2-1	235	286	92.4	223	180	606	2.4	1.9	6.6
	1-2	810	1020	86.6	165	407	293	1.9	4.7	3.4
	2-3	978	1226	42.6	86.2	69.9	142	2.0	1.6	3.3
	3-4	1057	1314	24.4	40.7	47.9	82.6	1.7	2.0	3.4
	4-6	2108	2648	13.3	<10.4	21.8	32.8	< 0.8	1.6	2.5
	6-9	3163	3980	2.3	11.8	11.3	20.5	5.1	4.9	8.8

B,	Depth		Cumulative Activities (dpm)			
Inches	Dry Wt.(g)	Wet Wt.(g)	Sr ⁹⁰	Ru ¹⁰⁶	Ce ¹³⁷	Ce ¹⁴⁴
1/2	83	94.5	92	187	189	677
1	318	380	309	712	612	2101
2	1128	1400	1010	2048	3909	4474
3	2106	2626	1427	2892	4593	5863
4	3163	3940	1685	3323	5099	6736
6	5271	6588	1965	< 3542	5559	7427
9	8434	10568	2038	< 3915	5916	8075

Sample No. 19 Croton Silt Loam, N. J.

A.	Depth		Nuclide Concentrations (dpm/100 g dry Wt.)***				Nuclide Ratios		
	Inches	Dry Wt. (g)*	Wet Wt. (g)*	Sr ⁹⁰	Ru ¹⁰⁶	Cs ¹³⁷	Ce ¹⁴⁴	Ru ¹⁰⁶ /Sr ⁹⁰	Cs ¹³⁷ /Sr ⁹⁰
0-1/2	100	179.5	193	2165	1507	6379	11.2	7.8	33.1
1/2-1	367	553.5	197	320	383	3866	1.6	1.9	19.6
1-2	1132	1540	47.8	96.8	43.7	102.4	2.0	0.9	2.1
2-3	1291	1721	32.9	29.9	<18.0	49.1	0.9	0.5	1.5
3-4	1217	1598	19.7	24.7	10**	--	1.3	0.5	--
4-6	1801	2875	10**	10.2	8.7	--	1.0	0.9	--
6-9	3588	4519	5.4	15.2	4.9	--	2.8	0.9	--

B.	Depth		Cumulative Activities (dpm)			
Inches	Dry Wt. (g)	Wet Wt. (g)	Sr ⁹⁰	Ru ¹⁰⁶	Cs ¹³⁷	Ce ¹⁴⁴
1/2	100	179.5	193	2165	1507	6379
1	407	733	917	3339	2914	20567
2	1599	2273	1458	4435	3409	21726
3	2890	3994	1883	4821	< 3641	22360
4	4107	5592	2123	5122	< 3763	--
6	5908	8467	2303	5305	< 3919	--
9	9496	12986	2495	5850	< 4095	--

Sample No. 20 Washington Loam, N. J.

A.	Depth		Nuclide Concentrations (dpm/100 g dry Wt)***				Nuclide Ratios			
	Inches	Dry Wt. (g)*	Wet Wt. (g)*	Sr ⁹⁰	Ru ¹⁰⁶	Cs ¹³⁷	Ce ¹⁴⁴	Ru ¹⁰⁶ /Sr ⁹⁰	Cs ¹³⁷ /Sr ⁹⁰	Ce ¹⁴⁴ /Sr ⁹⁰
	0-1/2	178	263.5	69.6	239	181	457	3.4	2.6	6.6
	1/2-1	466	616.5	67.2	256	170	408	3.8	2.5	6.1
	1-2	1112	1446	54**	134	65.9	177	2.5	1.2	3.3
	2-3	1089	1257	42.2	52.9	25**	73.6	1.3	0.6	1.7
	3-4	1170	1445	11.1	20.9	< 9.6	33.0	1.9	< 0.9	3.0
	4-6	2481	3045	3.6	10.0	< 9.0	18.1	2.8	< 0.3	5.0
	6-9	3215	4009	8.8	8.0	< 7.0	10**	0.9	< 0.1	1.1

B.	Depth		Cumulative Activities (dpm)			
<u>Inches</u>	<u>Dry Wt. (g)</u>	<u>Wet Wt. (g)</u>	<u>Sr⁹⁰</u>	<u>Ru¹⁰⁶</u>	<u>Ca¹³⁷</u>	<u>Ce¹⁴⁴</u>
1/2	178	263.5	124	425	322	813
1	644	880	438	1618	1114	2714
2	1756	2326	1038	3108	1847	4682
3	2845	3583	1498	3684	2119	5484
4	4015	5028	1628	3929	<2231	5870
6	6496	8073	1717	4178	<2455	6319
9	9711	12082	2001	4437	<2679	6641

Sample No. 28 Pratt Loamy Sand, (Kansas)

A.	Depth		Nuclide Concentrations (dpm/100 g dry Wt)***				Nuclide Ratios			
	Inches	Dry Wt. (g)*	Wet Wt. (g)*	Sr ⁹⁰	Ru ¹⁰⁶	Cs ¹³⁷	Ce ¹⁴⁴	Ru ¹⁰⁶ /Sr ⁹⁰	Cs ¹³⁷ /Sr ⁹⁰	Ce ¹⁴⁴ /Sr ⁹⁰
	0-1/2	162	221	244	891	5384	2596	3.7	22.1	10.6
	1/2-1	461	556	200**	348	90.4	603	1.7	0.5	3.0
	1-2	985	1111	204	117	34.3	103	0.6	0.2	0.5
	2-3	1095	1221	26.7	43.8	< 3.6	22.5	1.6	0.2	0.8
	3-4	1188	1301	63.5	27.1	0**	17.5	0.4	--	0.3
	4-6	2483	2813	10**	19.6	< 6.6	18*	2.0	< 0.7	1.8
	6-9	3613	4063	< 1.11	13.5	< 5.5	18.7	--	--	--

B.	Depth		Cumulative Activities (dpm)			
	Inches	Dry Wt. (g)	Wet Wt. (g)	Sr ⁹⁰	Ru ¹⁰⁶	Cs ¹³⁷
1/2	162	221	395	1443	8722	4206
1	623	777	1317	3047	9139	6986
2	1608	1888	3326	4199	9477	8001
3	2703	3109	3618	4679	<9516	8247
4	3891	4410	4372	5001	<9516	8455
6	6374	7223	4620	5488	<9681	8902
9	9987	11286	< 4660	5976	<9880	9578

Sample No. 29 Bethary Silt Loam, (Kansas)

A.	Inches	Depth	Dry Wt. (g)*	Wet Wt. (g)*	Nuclide Concentrations (dpm/100 g dry Wt.)***				Nuclide Ratios		
					Sr ⁹⁰	Ru ¹⁰⁶	Cs ¹³⁷	Ce ¹⁴⁴	Cs ¹³⁷ /Sr ⁹⁰	Ru ¹⁰⁶ /Sr ⁹⁰	Ce ¹⁴⁴ /Sr ⁹⁰
	0-1/2		182.5	297	181	374	801	1782	4.4	2.1	9.8
	1/2-1		452	549	117	271	279	550	2.4	2.3	4.7
	1-2		1154	1373	52.5	92.2	55.6	83.8	1.1	1.8	1.6
	2-3		1249	1477	--	45.8	<15.3	47.2	--	--	--

B.	Inches	Depth	Dry Wt. (g)	Wet Wt. (g)	Cumulative Activities (dpm)			
					Sr ⁹⁰	Ru ¹⁰⁶	Cs ¹³⁷	Ce ¹⁴⁴
	1/2		182.5	297	330	683	1462	3430
	1		634.5	846	859	1908	2723	5916
	2		1788.5	2219	1465	2972	3365	6883
	3		3037.5	3696	--	3544	<3556	7473

* Volume of 1 inch section = 823.5 ccs

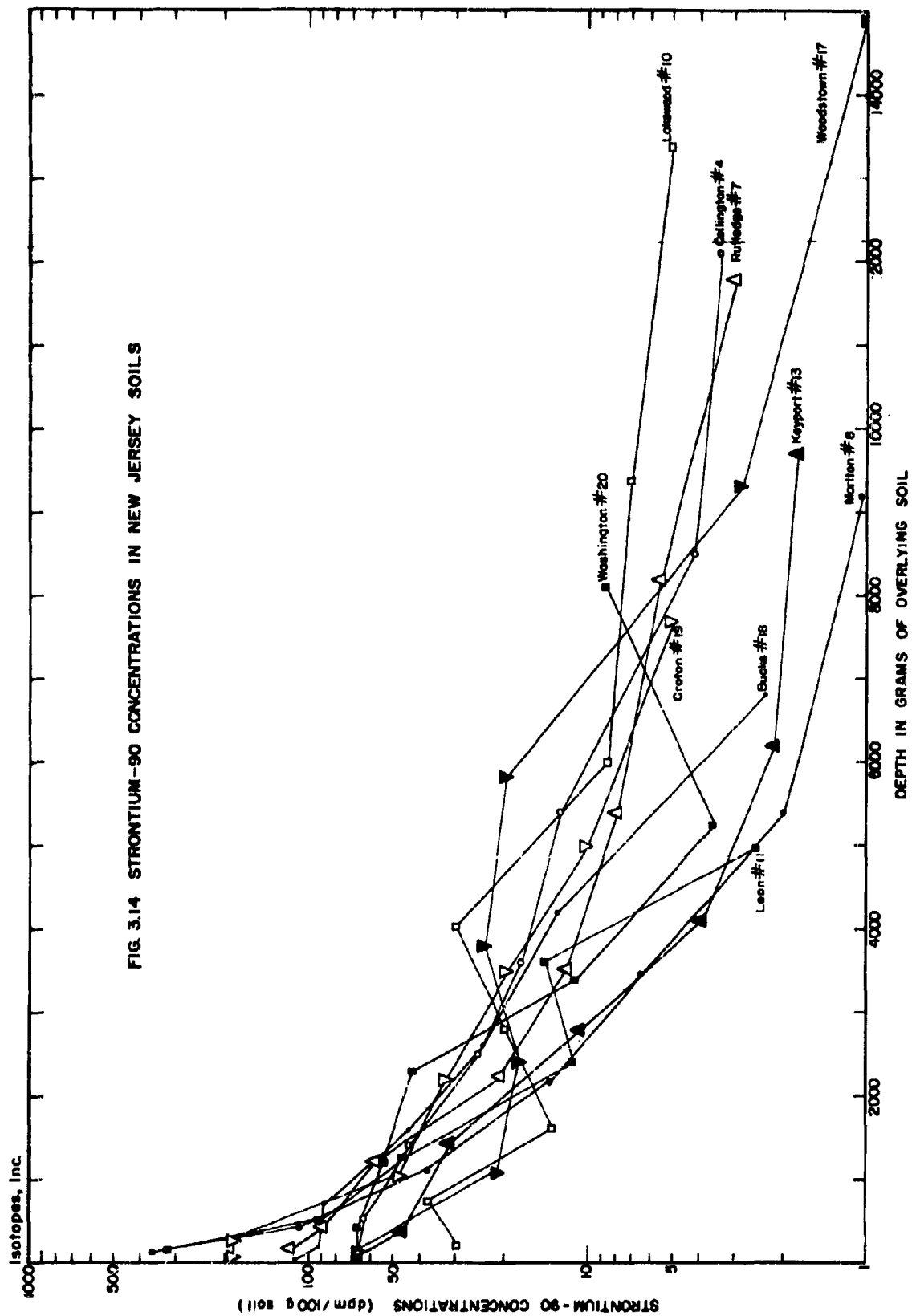
** Result interpolated

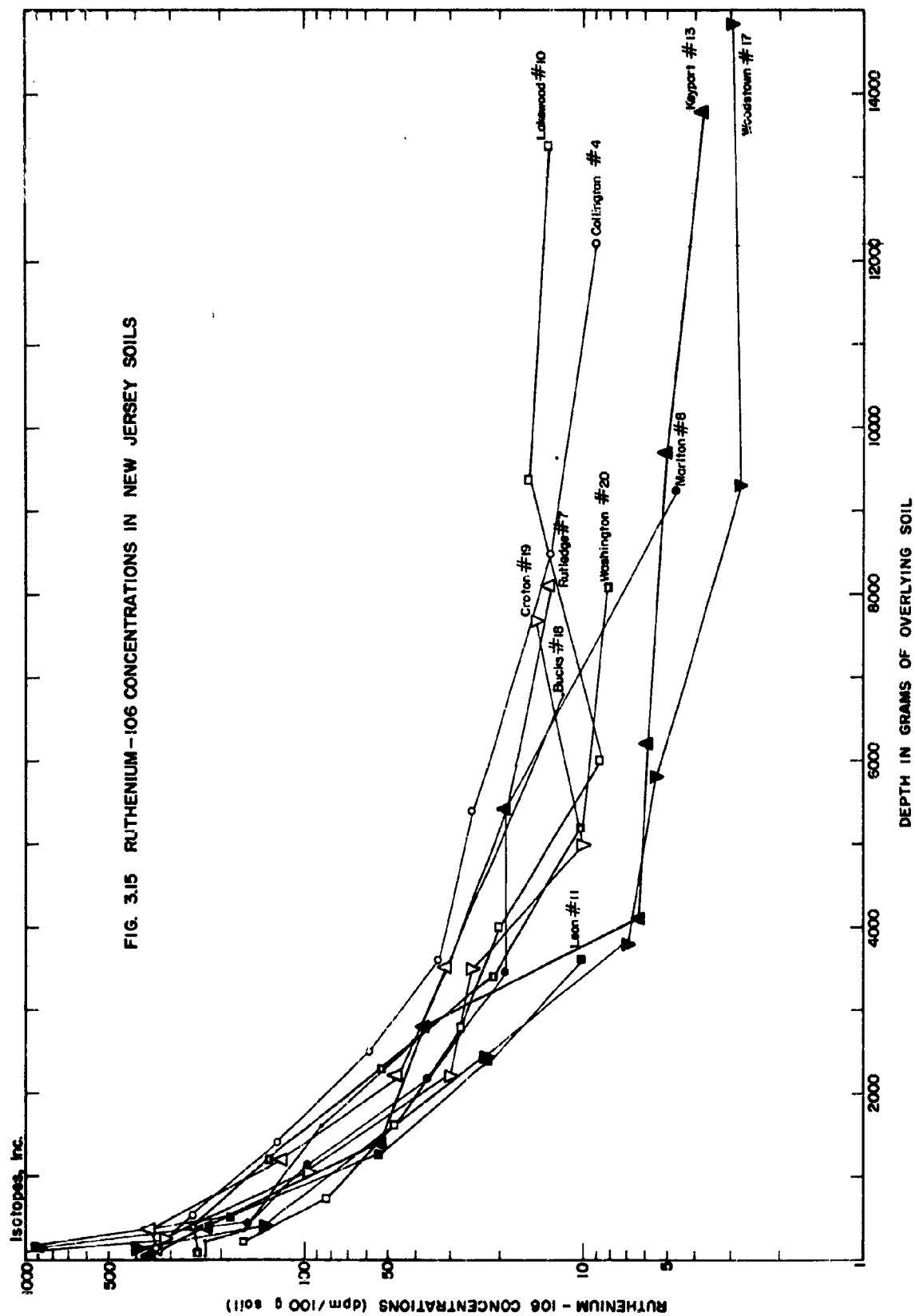
*** All activities corrected for radioactive decay to July 1, 1960

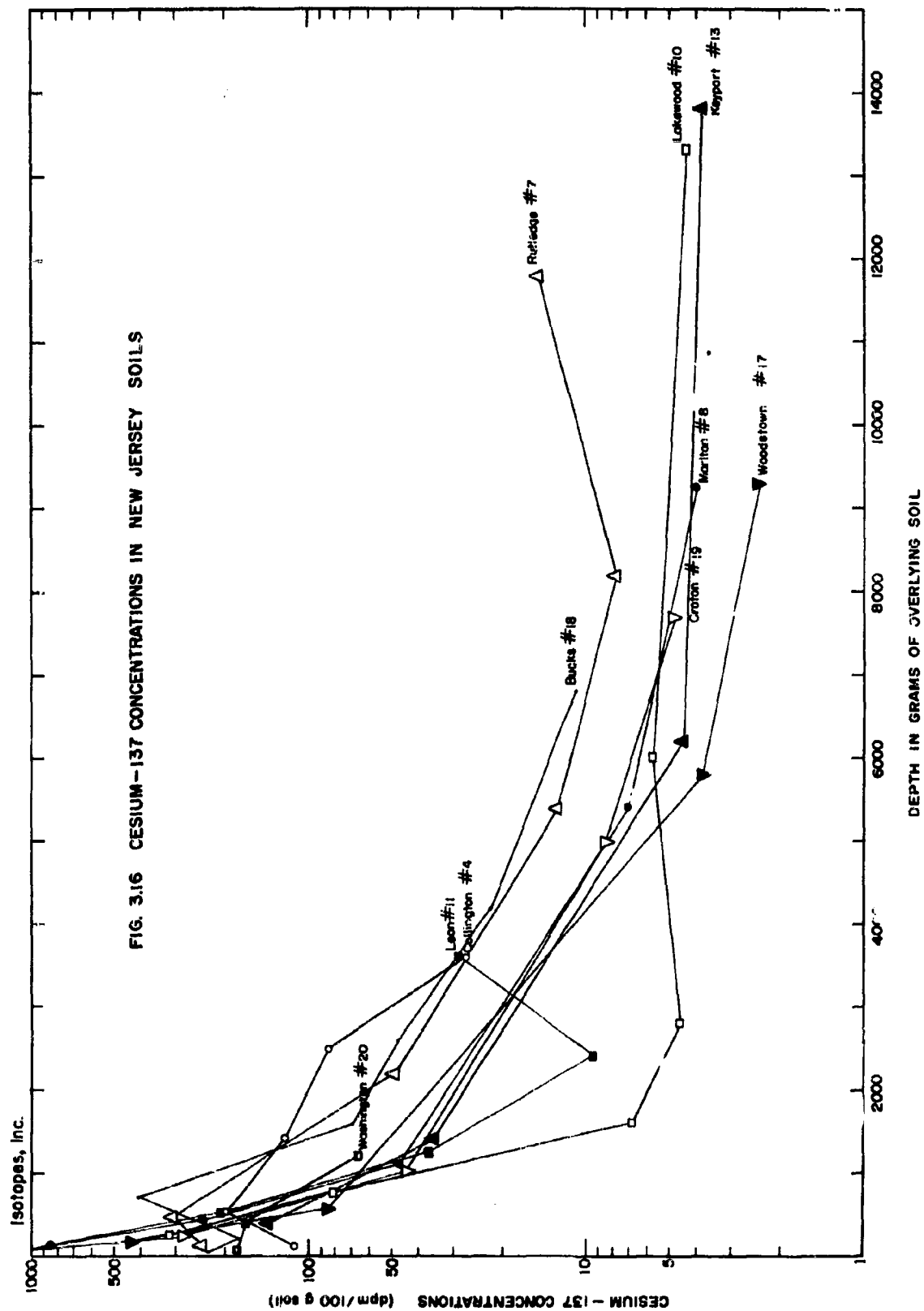
a depth of 1/2 inch in the core. For this reason the 0-1/2 inch section is somewhat arbitrary, and hence the advantages of expressing the depth in grams are apparent. This system of expressing the depth by the weight of a given sample in a soil core also allows a better intercomparison of results between cores. Columns 4, 5, 6 and 7 give the concentrations of strontium-90, ruthenium-106, cesium-137 and cerium-144 in dpm per 100g dry soil, all corrected for radioactive decay to 1 July 1960, and the remaining columns in the upper section of the table give the calculated results of the ratios of ruthenium-106, cesium-137 and cerium-144 respectively to strontium-90. In some examples it became necessary to interpolate certain nuclide concentrations because of analytical difficulties. The interpolated data were generally determined from plots of the logarithm of the nuclide concentrations as a function of depth in the core and assuming that there was a linear relationship between the above variables at depths between which a result was missing. When duplicate activity determinations were performed for a given depth the average value was given in Table 3.4. The lower half of Table 3.4 gives the cumulative deposits of the four nuclides at the indicated depths. Interpolated values, noted in the upper section of this table by an asterisk, were assumed in the summations of the activities.

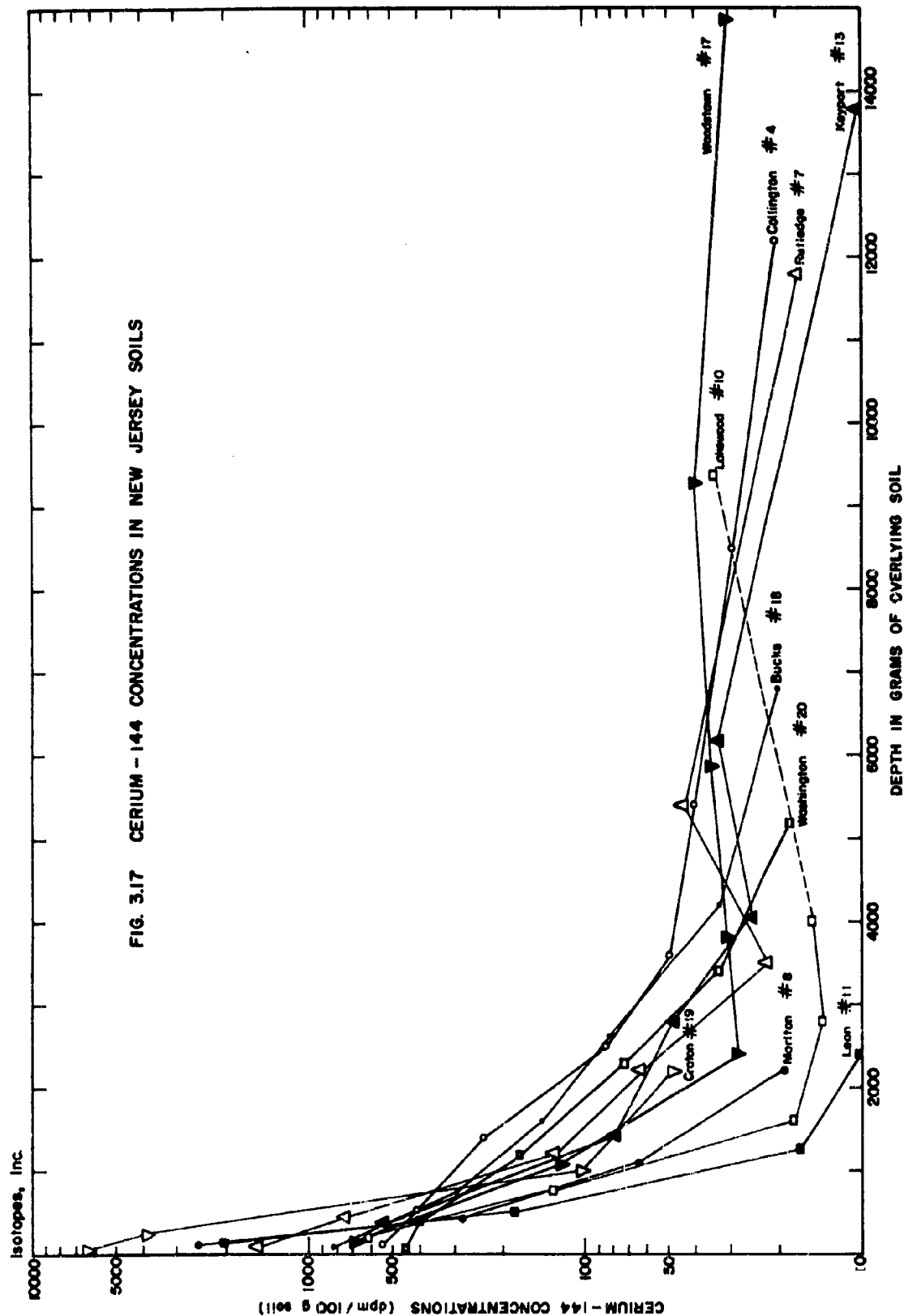
Variation of Concentrations of Nuclides With Depth In Soils

The results of the concentrations of strontium-90, ruthenium-106, cesium-137 and cerium-144 in New Jersey soils shown in Table 3.4 are plotted in Figures 3.14, 3.15, 3.16, and 3.17 as a function of depth in the soil cores. For all four nuclides it is apparent that there is a sharp decrease in concentration with depth. In general the concentrations drop by more than one order of magnitude in the first 6000 to 7000 grams of soil, which is equivalent to a depth in most soil









of about 6 inches. However, not all soils exhibit the same slope in the decrease of nuclide concentration with depth. For example, those soils possessing the highest concentrations of strontium-90 in the uppermost layer (Croton, Marlton and Leon soils) do not maintain this position, relative to the remaining soils, at greater depths. Rather, it is observed that at the 5000 gram depth the Marlton and Leon soils possess the two lowest strontium-90 concentrations, while the strontium-90 concentration in the Croton soil at this depth is intermediate in value. Those soils which have the lowest strontium-90 concentrations at the top of the core possess the highest concentrations at the 5000 gram depth. The Lakewood sand in particular is extremely interesting from this standpoint. Over a total depth of 12 inches the strontium-90 concentrations do not vary by more than a factor of six, while in the Leon sand and the Marlton sandy loam the concentrations decrease over a smaller depth interval by factors of about 100 and 300 respectively. The differences in behavior of the radioactive nuclides in the Leon, and Lakewood sands is quite remarkable since these two samples were collected within about 100 feet of each other. This general picture of the depth profiles of strontium-90 in New Jersey soils is similarly visible in the results of the other nuclide concentrations with only few exceptions. Again the rapid decrease in nuclide concentration with depth is clearly seen for ruthenium-106, cesium-137 and cerium-144. In addition it is observed that the soils with the highest concentrations of these three nuclides in the top layers are the Croton, Marlton and Leon, not necessarily in that order however. In terms of mineralogical composition these three samples vary widely. The Croton is a silt loam, the Marlton a sandy loam and the Leon is almost a pure sand. Thus we have encountered a broad range of base-exchange capacity in three soils. It is likely therefore that some factors other than the cation-exchange capacity of the soils play prominent parts in influencing the variability of the concentrations of these four nuclides with

depth in soils from New Jersey. Two likely factors are the permeability of the soil and the drainage properties of the sampled soil and the underlying strata. It is stated in the descriptions given in Table 3.1 that the Croton and Leon soils are poorly drained as a result of high water tables in the regions of the sampling sites. Rainwater does not soak through these soils very rapidly and thus there is a higher probability of the radioactivity being retained by the materials in the uppermost sections of the core. On the other hand the Marlton soil is well-drained and hence drainage is probably not the major factor governing the vertical profile of radioactivity in this case. However, it is noted that the Marlton soil is a moderate to poorly permeable material which results in a similar effect on the passage of water through the soil as does poor drainage. Moreover the Croton silt loam, in addition to its poor drainage properties, is also extremely slowly permeable. It is believed that the combination of these two factors results in this soil retaining a large portion of the total activity in the core in the top inch of material whereas in the Leon and the Marlton one of these factors, either poor drainage or low permeability, appears to be the overriding influence on the activity profile.

The average profile of activity in New Jersey soils is shown in Figure 3.18 for all four nuclides. Because there appears to be some question concerning the cerium results from the Croton samples these data were omitted from the average. Also the results from the disturbed sample of Collington sandy loam, No. 5, were omitted for obvious reasons. Figure 3.19 indicates the relative vertical profiles of activity concentrations which were obtained by expressing the activities over a given depth increment as a percentage of the cumulative activity at the 6000 gram depth, and converting these results to concentrations by dividing by the mass of soil in the depth increment.

If cesium-137 and strontium-90 concentrations are examined it is clear

that the cesium-137 curve has a steeper slope than the strontium-90 curve. This observation indicates, as expected, that strontium-90 penetrates to greater depths in the soil and is more mobile than cesium-137. Direct comparison of these two nuclides with the remaining two nuclides, ruthenium-106 and cerium-144, is complicated by the fact that the latter two possess much shorter radioactive half-lives (~ 1 year) than the former pair (~ 30 years). It is difficult to correct the observed concentrations of the short-lived nuclides at a given depth in soil because the age of the material at any point cannot be assessed accurately. However, because of the closeness of the half-lives of cerium-144 (285 days) and ruthenium-106 (1 year), some information on the movement of activity can be obtained from a comparison of the behavior of the two nuclides. The relative profiles of ruthenium-106 and cerium-144 (Figure 3.19) indicate higher concentrations of cerium-144 at the top of the soil core and a more rapid decrease in concentration than ruthenium-106 for the first 1000 g. Beyond this depth, however, it is noticeable that the ruthenium-106 concentrations continue to fall quite rapidly whereas the cerium-144 results tend to show a diminished rate of decrease. This is, at first sight, contrary to what would be expected to be the normal behavior of these nuclides in soil. Ruthenium has been shown to be relatively mobile, whereas cerium, because of its similarity in chemical properties to the rare earths, is quite immobile. If the ruthenium-106 and cerium-144 at the lower depths have similar dates of origin, correction for radioactive decay would enhance the divergence between the two profiles.

Three possible explanations can be advanced to clarify the anomaly. First, it is possible that the ruthenium-106 at depth is relatively much older than the cerium-144 fraction. Thus a greater radioactive decay correction factor for ruthenium-106 compared to cerium-144 would be necessary in the lower sections of the cores analyzed. The result of this correction would be to decrease the

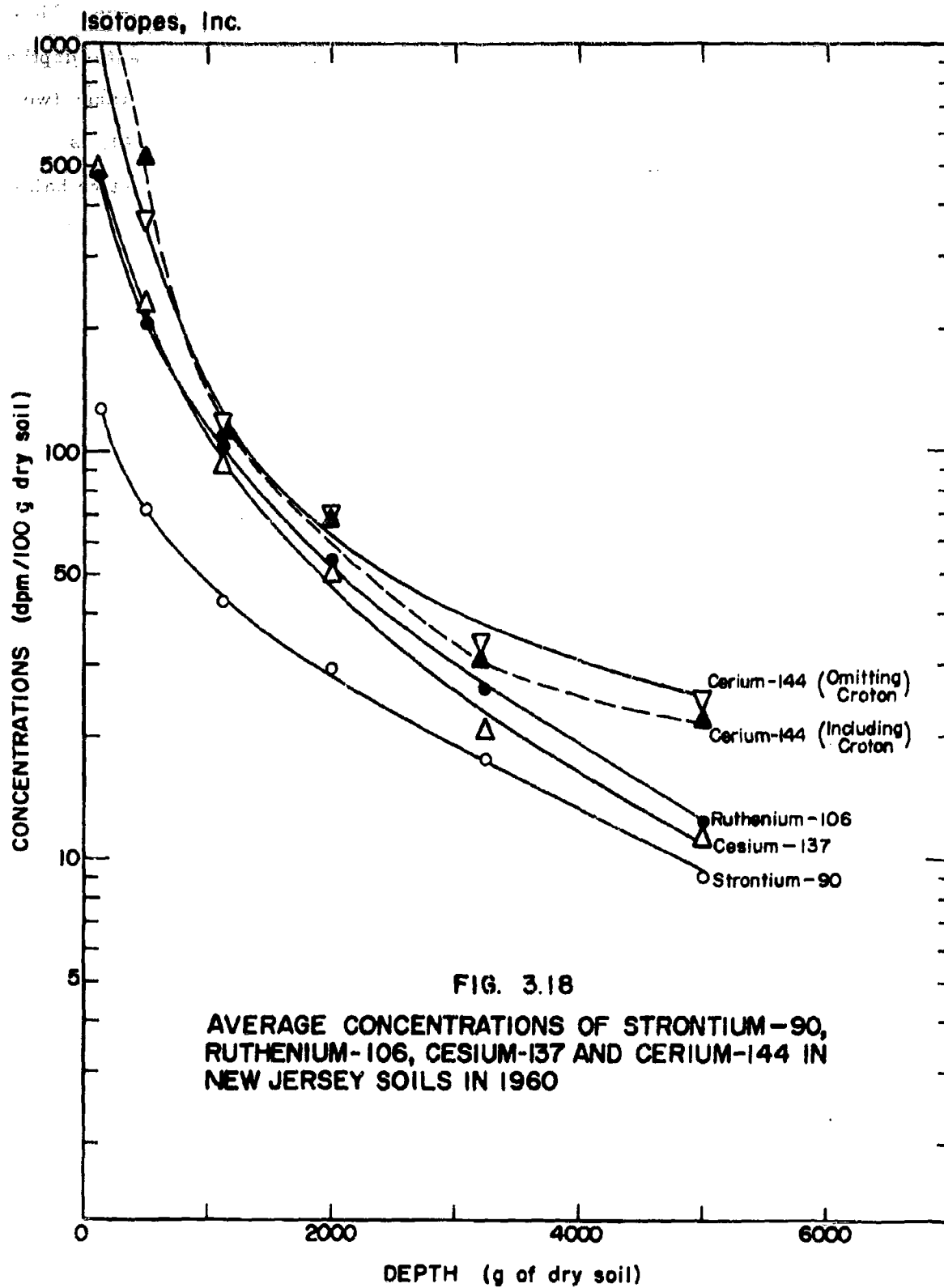
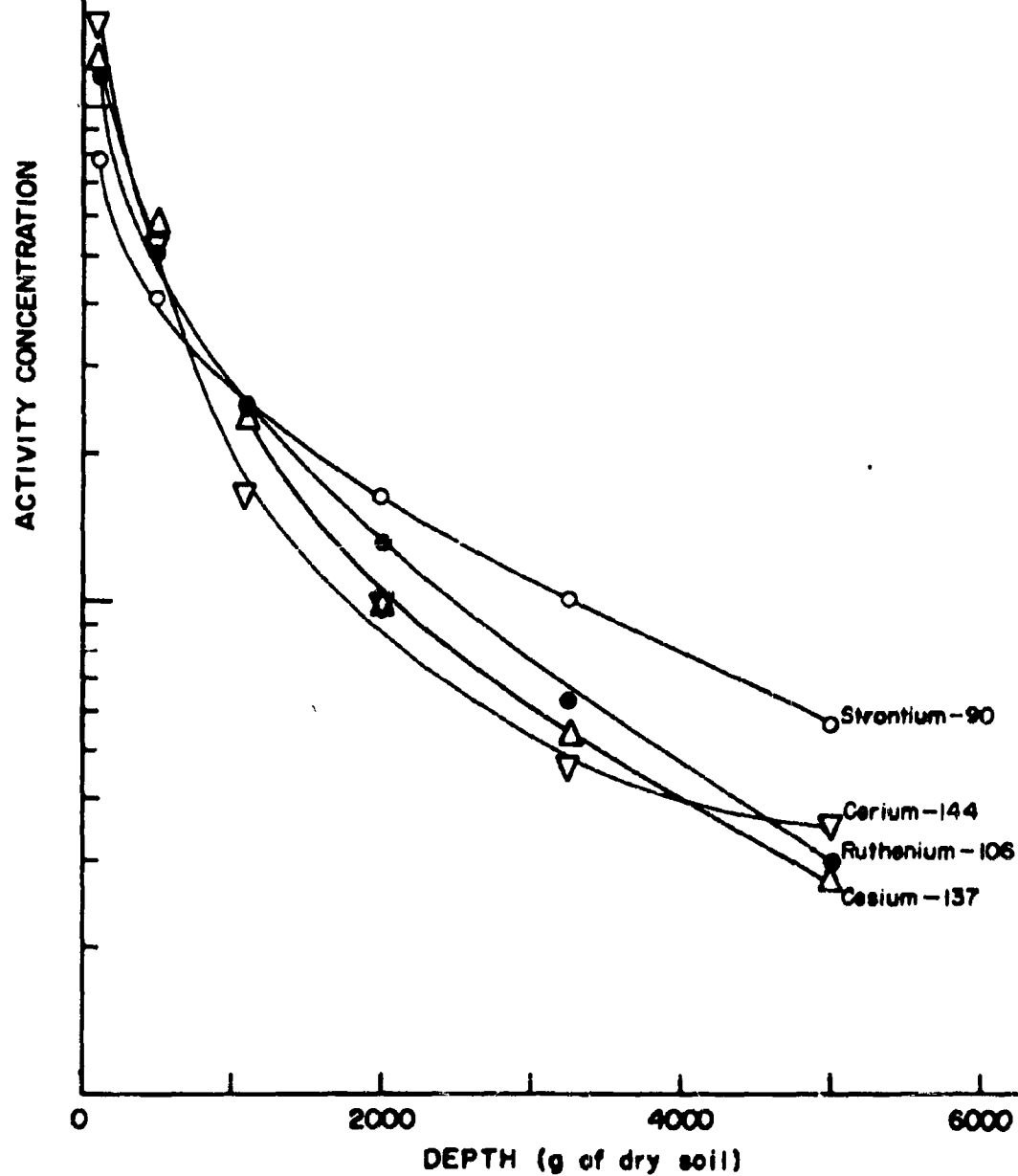


FIG. 3.18

AVERAGE CONCENTRATIONS OF STRONTIUM-90,
RUTHENIUM-106, CESIUM-137 AND CERIUM-144 IN
NEW JERSEY SOILS IN 1960

FIG. 3.19

RELATIVE VERTICAL PROFILES OF STRONTIUM-90, RUTHENIUM-106, CESIUM-137 & CERIUM-144 CONCENTRATIONS IN NEW JERSEY SOILS IN 1960



divergence' between the concentration curves at depths greater than 2000 grams and increase the differences between the two nuclides in the upper sections of the core. Such an explanation, however, is quite opposed to theories on movement of these elements in solution through soils and must therefore be considered unlikely at the present time. A second possible explanation is that the ruthenium-106 observed in the cores taken for analysis does not represent the actual amount deposited as fallout. Rather, because of the proven mobility of this nuclide under other conditions much of the deposited material may have passed on through the core so that it was never sampled. Since neither ruthenium-106 nor cerium-144 concentrations in precipitation have been assayed on a wide scale, this theory is difficult to disprove. Nevertheless, some assumptions were made concerning the cerium-144 and ruthenium-106 / strontium-90 ratios in precipitations since 1953, and estimates of the total deposits in soil in 1960 were made. Table 3.5 indicates how this calculation was performed. Even though gross assumptions were made about the source of nuclear debris deposited during the years prior to 1958, it is clear that the bulk of the cerium-144 and ruthenium-106 present in the soils on 1 July 1960 was deposited during the previous two year period. The ratios assumed for this two year interval are quite well known because data are available on the Ce^{144}/Sr^{90} ratios in air and precipitation.^{10, 11} Furthermore, the source of the fallout in New Jersey in this interval is also well-established, so that the Ru^{106}/Sr^{90} ratios may be estimated if the initial activity ratio of 24 at the time of detonation is assumed.¹² Comparison of the estimated values with the best values which can be calculated from the measured activities is presented in Table 3.6. It is encouraging to note the agreement between the observed and estimated deposits of the four radioactive nuclides examined. At the same time the agreement tends to remove the possibility that considerable quantities of ruthenium-106 penetrated to depths greater than 12 inches.

Table 3.5 Estimations of Cumulative Deposits of Ruthenium-106 and Cerium-144 in New Jersey Soils on July 1, 1960

Time of Deposition	Estimated Nuclide Ratios		Strontium-90 Deposited (mc/mi ²)	Estimated Deposits (mc/mi ²)		mc/mi ² remaining on July 1, 1960	
	Ce ¹⁴⁴ /Sr ⁹⁰	Ru ¹⁰⁶ /Sr ⁹⁰		Ce ¹⁴⁴	Ru ¹⁰⁶	Ce ¹⁴⁴	Ru ¹⁰⁶
1 July 53 - 1 July 54	6	10	4.2	25.2	42	0.1	0.5
1 July 54 - 1 July 55	14	18	9.5	133.0	171	1.2	3.8
1 July 55 - 1 July 56	15	12	10.9	163.5	130.8	3.1	5.8
1 July 56 - 1 July 57	20	10	11.5	230.0	115.0	10.4	10.4
1 July 57 - 1 July 58	20	10	13.1	262.0	131.0	28.3	23.6
1 July 58 - 1 July 59*	25	10	27.1	677.5	271.0	179.5	96.5
1 July 59 - 1 July 60**	4	5	7.2	28.4	36.0	18.2	25.6
			83.5			240.8	166.2

* Ratios estimated from ground level air ratio of Ce ¹⁴⁴/Sr ⁹⁰ measured by Lockhart et al ¹⁰

** Measured Ce ¹⁴⁴/Sr ⁹⁰ ratio in precipitation

Table 3.6 Comparison of Average Cumulative Activities in New Jersey Soils with Estimated Deposits (July 1, 1960)

<u>Nuclide</u>	<u>Estimated Deposit (mc/mi²)</u>	<u>Observed Average Deposit to Depth 14,000 g</u>
Strontium-90	83.5*	74.7
Ruthenium-106	166	169
Cesium-137	143**	155
Cerium-144	241	296 (omitting Croton)

* Calculated from rainfall data observed at Westwood, New Jersey and New York City

** Assumed cesium-137/strontium-90 ratio of 1.7

The third possible explanation, which may be the most likely, is that the cerium-144 concentrations at depth in the core could have been overestimated. Between the 4000 and 6000 gram depths, in the New Jersey soils, there were three samples for which only upper limits of the concentration could be estimated. When Figures 3.18 and 3.19 were plotted the maximum concentrations of cerium-144 were assumed and hence the average concentration for all soils is probably somewhat overestimated. In addition the problems associated with the measurement of low concentrations of ruthenium-106 and cerium-144 result in larger uncertainties in the data from the lower sections of the core. Hence some caution ought to be exercised in the interpretation of data obtained on samples taken from depths greater than 6 inches of soil.

Cumulative Deposits of Radioactivity in New Jersey Soils

Table 3.7 gives the average deposits of the four radioactive nuclides strontium-90, ruthenium-106, cesium-137 and cerium-144 in New Jersey soils. The depth at which 100 percent of the total amount of fallout radioactivity was assumed to be present was 14,000 grams of dry soil. With the possible exception of cerium-144, it appears from this table, and from Figure 3.20, that the assumption of 100 percent of the activity being present in the first 14,000 grams of dry soil (\sim 12 inches) is justified. For reasons cited above and from theoretical considerations described previously, it is probable that the average cumulative activity of cerium-144 at the 14,000 g depth is rather high. From Figure 3.20 it is apparent that there is a distinct tapering off in the rise of cumulative activity at 4000-6000 grams (\sim 4-6 inches), and beyond the 6 inch depth there is only a small increase in the average total activity of each nuclide present in New Jersey soils. The average percentages of the total activity in the

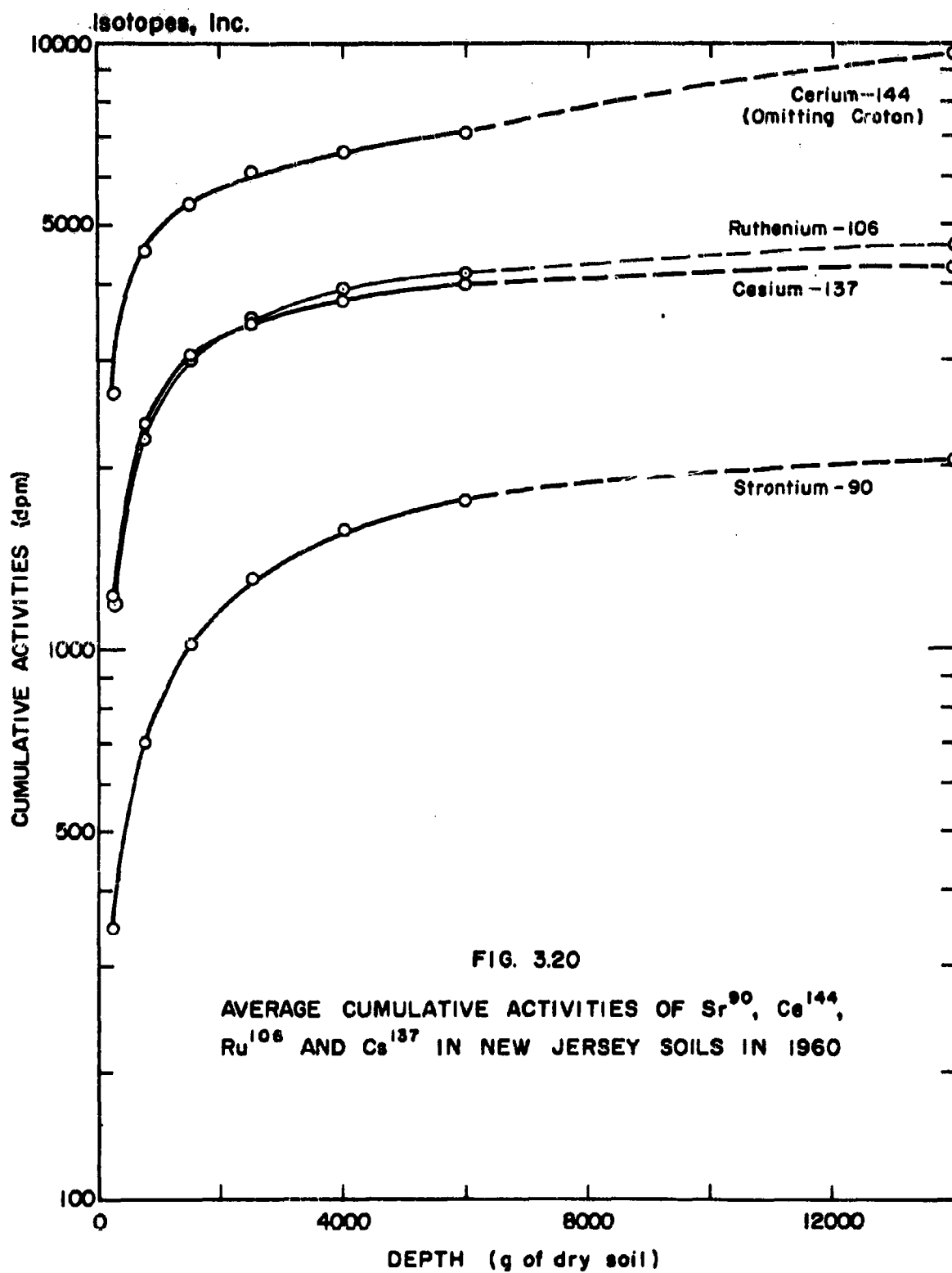


FIG. 3.20

AVERAGE CUMULATIVE ACTIVITIES OF Sr^{90} , Cs^{144} ,
 Ru^{106} AND Cs^{137} IN NEW JERSEY SOILS IN 1960

soil samples (to 14,000 g) are given in Table 3.8. It must be remembered that not all soils were sampled to 14,000 g and in these particular examples the cumulative activity had to be estimated. The estimated values were obtained by reasonable extrapolation of the curves shown in Figures 3.14 through 3.17 for each nuclide, and it is believed that these extrapolations do not introduce any large errors in the calculated quantities of the average total fallout in New Jersey soils.

The analyses of soils for the purpose of estimating world-wide integrals of strontium-90 have usually been performed to a depth of 6 inches. During 1959 this depth was extended to 9 inches for most soil samples to ensure complete recovery of the deposited strontium-90. From Table 3.8 and Table 3.9 it appears, when many different soil types are assayed, that the amount of strontium-90 in underlying depths when sampling is conducted to 9 inches is about 5 percent. Of course this fraction varies, as can be seen in the results shown in Table 3.4. The Lakewood sand, for example, has approximately 11 percent of the total strontium-90 below 9 inches, and the Washington loam has about 14 percent present below 9 inches, while the Leon sand appears to have a maximum of 2 percent of the cumulative activity in the core between 9 and 12 inches. Data, comparable with the above, have been obtained by Schulert et al¹³ for soils collected in the New York City area in 1958. Their results suggest that, for "average" soils, about 80 percent of the strontium-90 was retained in the upper 2 inches and at least 95 percent in the upper 6 inches in 1958. Our results yield 54.5 percent and 88.4 percent for the same depths but in 1960. Although Schulert et al¹³ reported that their data indicated relatively slow migration of strontium-90 between 1954 and 1958 our data when compared to the results of Schulert et al for 1958, do suggest that some movement has occurred in the period 1958-1960.

Other studies of the distribution and movement of strontium-90 in soils

Table 3.7 Variability of Cumulative Activities of Strontium-90, Ruthenium-106, Cesium-137 and Cerium-144 in New Jersey Soils (July 1, 1960)

<u>Nuclide</u>	<u>Average Cumulative Activity at 14,000 g (dpm)</u>	<u>Standard Deviation (Percent)</u>	<u>Average Deviation (Percent)</u>
Strontium-90	2072	16.9	13.1
Ruthenium-106	4677	21.1	17.5
Cesium-137	4290	32.5	27.2
Cerium-144	8190	20.5	15.6

Table 3.8 Average Percentages of Total Activity in Soils as a Function of Depth

<u>Nuclide</u>	<u>Depth (grams dry soil)</u>						
	<u>250</u>	<u>750</u>	<u>1500</u>	<u>2500</u>	<u>4000</u>	<u>6000</u>	<u>14,000</u>
Strontium-90	16.7	34.1	49.6	63.6	76.4	85.1	100
Ruthenium-106	25.6	47.8	64.5	76.1	84.6	89.9	100
Cesium-137	28.7	55.3	71.7	80.9	88.2	93.4	100
Cerium-144	32.4	55.4	66.3	74.8	80.9	87.0	100

Table 3.9 Average Vertical Profile of Strontium-90 in New Jersey Soils

<u>Depth (Inches)</u>	<u>Percentage of Cumulative Activity at 12 Inches Depth</u>
1/2	15.4
1	31.3
2	54.5
3	68.8
4	78.7
6	88.4
9	95.6
12	100

have been made. Thornthwaite¹⁴ endeavoured to explain the observed vertical profiles of fallout strontium-90 in New York City soils during the period 1955-1959 on the basis of a mathematical model. Only limited agreement was obtained between the observed and calculated values. Miller and Reitemeier¹⁵ have conducted laboratory experiments with different soils ranging from sands through clay loams to determine the movement of strontium-89 in these media under varying conditions. In general they found more movement in the sandy loam than in the clay or silt loams. This finding is in agreement with our results for soils which were relatively well-drained and differed only in their cation-exchange capacities and permeabilities.

Variability of the Total Deposits of Radioactivity in New Jersey Soils

Tables 3.7 and 3.8 give the cumulative deposits of strontium-90, ruthenium-106, cesium-137 and cerium-144 in New Jersey soils. Table 3.8 also indicates the "standard deviation" of the cumulative activities. The term standard deviation can only be applied to a normal distribution, and since only the results from ten samples from the state of New Jersey contribute to the determination of the average and its standard deviation, the use of these calculations is questionable. However, it serves to give some picture of the degree of variability in this area. Perhaps a more meaningful expression is the range of cumulative activities and the average deviations from the mean which were found. With the exception of the cerium-144 results determined for the Croton soil, in no area did the maximum and minimum cumulative activities differ by more than a factor of three. For strontium-90, ruthenium-106 and cerium-144 the extremes were within a factor of 2 of each other, while for cesium-137 the extreme results were within a factor of 2.5 of each other. Alexander⁷ has

presented data which are somewhat comparable to our results. In 1958 several pairs of soil sites 1 to 25 miles apart were selected for sampling. Analytical determinations of strontium-90 on duplicates of the same soil samples agreed to within $0.72 \text{ mc strontium-90/mi}^2$, while the variation between sites in the same general area averaged 1.64 mc/mi^2 . Thus difference in deposition between similar sites was approximately 1.0 mc/mi^2 when the deposits of strontium-90 ranged from 4 to 45 mc/mi^2 with an average of 13.7 mc/mi^2 . A maximum difference between two sites was observed at Tokyo, Japan where one site yielded a deposit of 30.8 mc/mi^2 and the second site yielded 23.5 mc/mi^2 . The percentage average deviation of strontium-90 from the mean at soil sites sampled by Alexander was thus 12.0 percent, compared with our average deviation of 13.1 percent for sites situated up to 100 miles apart. Our average deviation from the mean for duplicate radiochemical determinations was 8.3 percent, compared to Alexander's result of 5.3 percent. Excellent agreement has been found, therefore, both for radiochemical assays and for the heterogeneity of the strontium-90 deposit over a large area. Further work by Alexander et al⁸ for soils collected during the period 1956 through 1959 led to the conclusion that on the average the error in analytical reproducibility was less than 10 percent for the majority of soils assayed. This additional work further substantiated the conclusions based on the 1958 results alone.

Variability of Nuclide Ratios Within Soils

The variability of the concentrations with depth (and hence the nuclide ratios) of the four nuclides examined in the present study was discussed in a previous section. In this discussion we are concerned more with the ratios of the cumulative deposits of each nuclide.

The cesium-137/strontium-90 ratio is the quantity of most interest because it has a direct bearing on the questions of fractionation of nuclear debris and the radiological hazard from externally deposited gamma emitting nuclides such as cesium-137. The ratio of cesium-137/strontium-90 in the cumulative deposits to a depth of 14,000 g (\sim 12 inches) is 2.1 ± 0.8 which is in accord with an initial activity ratio of 1.87 for the fast fission of uranium-238¹² and a value of 1.7 ± 0.5 determined from the analyses of air filter samples collected in the HASP program. Other analyses of soils for cesium-137 by Gustafson¹⁶ have been performed. Combined with the strontium-90 results, which were determined by HASL, Gustafson obtained an average value for the cesium-137/strontium-90 ratio down to a depth of 6 inches of 1.62 ± 0.34 . Also, Gustafson recently reported that the cesium-137 concentration in soil near Argonne at the end of 1959 was approximately 200 mc/mi² compared to our average deposition in New Jersey of 155 mc/mi².

There has been considerable speculation regarding the use of cesium-137 measurements as a means of quickly determining the strontium-90 contents of soils. From our studies it is clear that this would only be possible if the soil was sampled to sufficient depth. Table 3.10 indicates how the average cesium-137/strontium ratio in New Jersey soils varies with depth, and it can be seen that if soils were sampled to about 1 inch depth (to about 1500 g), the strontium-90 deposit calculated from the measured cesium-137 deposit could be overestimated by at least 50 percent. This discrepancy could quite easily be much greater and will depend on the type of soil being analyzed, as was discussed briefly in preceding sections. For example in the Lakewood sand the ratio of the cumulative deposits of cesium-137 to strontium-90 was 10.8 in the first half inch of soil, and greater than 5 in the first one inch. In one of the Kansas samples, the Pratt loamy sand, cesium-137/strontium-90 ratios of 22 for the first half inch and 7 for

the top one inch were observed. The limitations of using a quick cesium-137 determination to assess the corresponding strontium-90 content in a given sample are therefore quite clear.

The ratios of the cumulative deposits of other nuclides to strontium-90 in New Jersey soils are given in Table 3.11. Although these results agree quite well with our predicted ratios given in Table 3.5, there are some large discrepancies between our results and those of Gustafson, reported by Alexander, Hardy and Hollister for 1959 soil analyses at Argonne¹⁷. According to Alexander et al¹⁷, the ruthenium-106 and cerium-144 deposits at Argonne in July 1959 were 1202 mc/mi² and 1812 mc/mi² respectively. If it is assumed that the deposition of these nuclides during the period July 1959-1960 was practically nil, the amounts of radioactivity present in July 1960 would be approximately 600 mc/mi² for ruthenium-106 and about 750 mc/mi² for cerium-144 after correction is made for radioactive decay.* For the same time in 1960 our results yield deposits of 109 mc/mi² for ruthenium-106 and 296 mc/mi² for cerium-144. Thus the results predicted from Gustafson's data are factors of 3.5 and 2.5 higher than our data for ruthenium-106 and cerium-144 respectively. From Table 3.5 it is possible to estimate deposits of these nuclides for September 1958 which may be compared with Gustafson's data for the same time. Inspection of Table 3.5 indicates that the agreement is good between our estimated data and Gustafson's results of 210 mc/mi² for ruthenium-106 and 270 mc/mi² for cerium-144. The major discrepancy lies therefore in the deposits estimated for early 1959. During the period September 1958-July 1959 the Argonne data indicate increases in ruthenium-106 deposition of 1000 mc/mi², cerium-144 - 1542 mc/mi² and

* Gustafson¹⁸ recently reported deposits of 790 mc/mi² and 1160 mc/mi² of ruthenium-106 and cerium-144 respectively for 1 July 1960.

Table 3.10 Average Cesium-137/Strontium-90 Ratios with Depth in New Jersey Soils

<u>Depth Increment (g dry soil)</u>	<u>Cs¹³⁷/Sr⁹⁰ Ratio in Increment</u>	<u>Cumulative Cs¹³⁷/Sr⁹⁰ Ratio</u>
0-250	3.6	3.6
250-750	3.2	3.4
750-1500	2.2	3.0
1500-2500	1.4	2.6
2500-4000	1.2	2.4
4000-6000	1.2	2.3
6000-14000	0.9	2.1

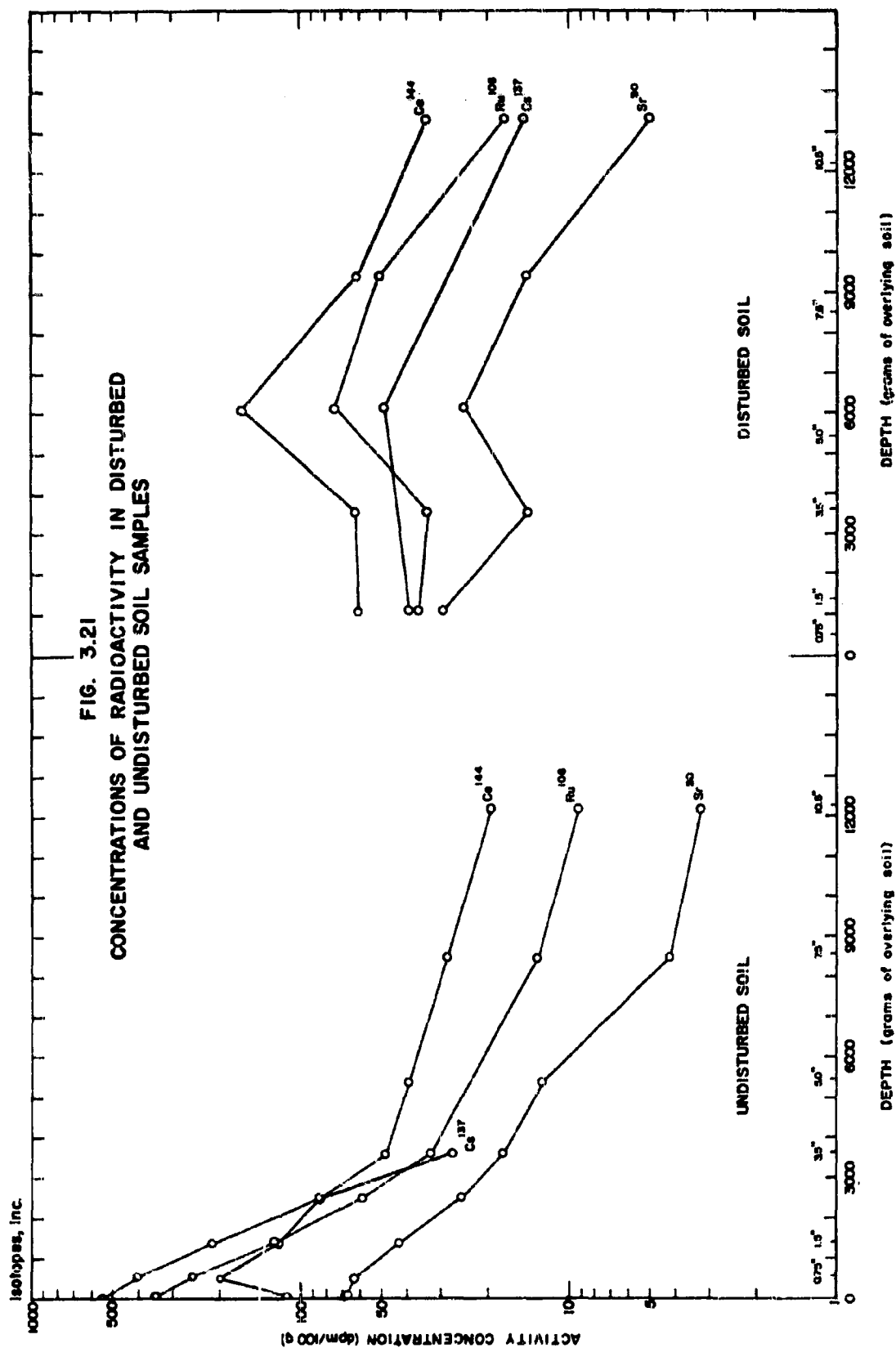
Table 3.11 Average Nuclide Ratios of Cumulative Activities in New Jersey Soils

<u>Nuclides</u>	<u>Cumulative Activity Ratio (dpm/dpm at 14,000 g depth)</u>
Cesium-137/Strontium-90	2.1 \pm 0.8
Ruthenium-106/Strontium-90	2.3 \pm 0.6
Cerium-144/Strontium-90	4.0 \pm 1.0

cesium-137 - 70 mc/mi². It appears safe to assume, in view of the fairly good agreement between our cesium-137 determinations, that the strontium-90 deposition during the above period was between 35 and 40 mc/mi². Hence, the Argonne measurements lead to results of 25-30 for the ratio of ruthenium-106 to strontium-90 and 38-45 for the ratio of cerium-144 to strontium-90 even if radioactive decay is not allowed for during the 9 month period. The activity production ratio for ruthenium-106/strontium-90 is 25 and for cerium-144/strontium-90 it is 55. In the case of ruthenium-106, therefore, the results from Argonne appear to be rather high for the 1958-59 period. For cerium-144, it is quite well established that it is fractionated in ground bursts, and thus a value of 38-45 for the cerium-144/strontium-90 ratio is probably high for early 1959. In addition the data of Lockhart et al¹⁰ suggest that the ratio at this time should be in the region of 20-25, which is a factor of two or more lower than the Argonne results suggest for the same period, when corrections for decay are applied. In conclusion, therefore, the weight of evidence appears to suggest that the results for the deposition of ruthenium-106 and cerium-144 during late 1958 and early 1959 at Argonne are much higher than expected on the basis of both theoretical and practical considerations. It must also be noted that the ratios of the deposits of short-lived nuclides, including zirconium-95-niobium-95, which were deposited at Argonne in 1959 are internally consistent with respect to the production ratios of the isotopes from the fast fission of uranium-238.

Distribution of Radioactivity in Disturbed and Undisturbed Soils

For the purpose of examining the effects of man's agricultural activities on the distribution of radioactivity in soils, two soil cores were collected in New Jersey. One sample (No. 4) was collected in a field which had been cultivated



regularly and at the time of sampling was under corn. The undisturbed sample (No. 5) was taken from the same soil (Collington sandy loam) in an adjacent field which had not been cultivated for at least 8 years, but which retained all the other characteristics of the first sample. The results of the analysis for the four nuclides are shown graphically in Figure 3.21.

Cultivation of the soil has obviously had a marked effect on the distribution of radioactivity. No longer are the steep decreases in concentration of the nuclides with depth clearly visible in the disturbed soil. Rather it is apparent that considerable homogenization of the activity in the core has occurred. The mixing, which undoubtedly was caused by periodic plowing of the soil, was apparently not complete. There are tendencies for the concentrations of all four nuclides to peak at about 5 inches depth, which is probably explained by the placing at this depth of considerable amounts of material from the top layers of the soil. Since the plowing occurred at the end of 1959 and most of the short-lived nuclides were deposited in the spring of 1959 (see Table 3.5) this explanation seems feasible. Average concentrations at the bottom of the core, i. e., between 5 and 12 inches, are somewhat higher in the plowed material than in the undisturbed soil. This too is probably the result of plowing and possibly the added effect of nuclide movement caused by water passing through the soil matrix. It certainly cannot be attributed to any additional amounts of radioactivity being present in the plowed soil, as can be seen in the results of Table. 3.4.

Application of Results to World-Wide Fallout of Strontium-90 and the External Hazard from Fallout Radioactivity

Many of the implications of the present study to the question of the world-wide fallout of strontium-90 have been mentioned in previous sections. The points

of greatest import are probably the distribution of radioactivity with depth and the variability of the cumulative deposits of the nuclides over a given area. Over an area the size of the State of New Jersey (7500 mi^2) it was determined that the average deviation of strontium-90 from the mean of ten samples (area $\sim 5 \text{ ft}^2$) was about 13 percent. This uncertainty is quite small, and since it includes the errors in radiochemical determination in addition to the uncertainties in sampling, it is felt that the strontium-90 deposit in New Jersey is quite well-established. It is difficult to ascertain the quantity of strontium-90 deposited in eastern Kansas from the limited data which are available. Nevertheless the strontium-90 and cesium-137 cumulative activities are apparently considerably higher than in New Jersey, but the concentrations of ruthenium-106 and cerium-144 are approximately equal to the deposits in New Jersey. This observation could be explained by the fact that the eastern sections of Kansas have probably received a larger fraction of their total fallout from lower yield shots detonated in the Nevada desert. Any short-lived activity from these sources has most likely decayed to only a small fraction of the original deposit, and the predominant contribution to the ruthenium-106 and cerium-144 activities is probably world-wide fallout from high yield shots in the megaton range. The possibility that this extra activity ($\sim 80 \text{ mc/mi}^2$ for strontium-90) is entirely Nevada debris seems rather remote, however, in view of other soil results from neighboring states¹⁹. Any further conclusions at this time regarding this high deposition in eastern Kansas would be unwarranted until we have more extensive data on this point.

As far as depth considerations are concerned, it will be necessary in the next 2 years to sample soils to at least 9 inches to ensure recovery of at least 90 percent of the total strontium-90. Although it is not yet possible to describe accurately the future redistribution of fallout strontium-90 with time as a result of water movement, it is believed that careful studies will enable this factor to be

established in 2 or 3 years. Of course the extent of the redistribution will depend on soil type and it may be necessary to sample sandy soils to depths greater than 12 inches to ensure complete recovery of the activity, particularly strontium-90.

Some of the factors governing the vertical profiles of activities within soil cores have been discussed. These factors included the type of soil, permeability and drainage as three of the most important. One other possibility namely the organic content of the material, was not examined in great detail. The influence of this variable is, however, rather difficult to pursue with the small number of types of soils which were analyzed in the present program. The Rutledge fine sandy loam is the only soil in the group which possesses an abnormally high content of organic material. Unfortunately this property is combined with poor drainage characteristics in this particular soil. This leads to relatively high concentrations of the four radioactive nuclides in the top part of the core. Since the latter feature itself appears to have a marked effect on the distribution of radioactivity, the influence of organic content may be somewhat obscured in our results.

The fallout deposit of gamma-emitting nuclides in soil constitutes an external source of radiation to the human body but, because of the added radioactivity which is present from natural sources, the concentrations of the former are difficult to measure directly. The dose rates etc. from fallout have also to be obtained indirectly since they cannot be measured in the field. Consequently several theoretical mathematical expressions have been derived which express the dose rate to a human being from a given deposit of radioactivity distributed in some manner in the soil. Various assumptions have been made regarding this distribution of radioactivity in the ground, the build-up factors from scattering of the radiation and the shielding factors, such as the effect of buildings,

in obtaining these equations. The final expressions for the dose rate must, therefore be approximate since little experimental work is available to verify these assumptions.

The expression given by the U. N. ²⁰ for the computation of the exposure dose rate from deposited fission products is based on the uniform distribution of the activity over an infinite plane. The equation is

$$I = C \times \bar{E}_\gamma \times F_D ,$$

where

I is dose rate to the gonads in m rad/year,

\bar{E}_γ is average gamma ray energy (MEV) and

F_D is activity of deposit in mc/mi².

C is approximately equal to 0.04. For the above units for a deposit of 1000 mc/mi² of fission products with an average gamma-ray energy of 0.5 MEV the "infinite plane" dose rate is about 20 m rad/year or 2.3 μ rad/hour. In New Jersey soils we determined an activity of 620 mc/mi² from three of the major contributors to the external gamma dose. Thus the dose rate to the gonads from these three nuclides alone is less than 2 μ rad/hour. Gustafson¹⁸, utilizing a modification of the above formula, found a dose rate which is about one third the result reported here. The maximum permissible radiation exposure recommended by the NCRP²¹ for external exposure of the gonads is 0.5 rems multiplied by the number of years beyond age 18. Thus the dose rate calculated by us, for the three nuclides analyzed, is about 3 percent of MPD rate in 1960 for people older than 18.

CONCLUSIONS

In summary the following conclusions may be drawn regarding the deposition of strontium-90, ruthenium-106, cesium-137 and cerium-144 in New Jersey soils.

1. The average deposits of the above four nuclides in New Jersey were about 75, 160, 155 and 295 mc/mi² respectively on 1 July 1960. These values are in agreement with results for this area predicted on the basis of results of fission product determinations in precipitation and ground-level air.
2. Some discrepancies are observed between the concentrations of the short-lived fission products ruthenium-106 and cerium-144 in the New Jersey and Chicago areas.
3. The average deviation of the cumulative deposits in New Jersey, calculated from the results of analyses of 11 cores, is about 15 percent for strontium-90, ruthenium-106 and cerium-144. Cesium-137 results reflect a higher deviation of about 27 percent. With the exception of one soil the maximum and minimum cumulative activities for a given nuclide did not vary by more than a factor of three for all soils."
4. Vertical profiles of radioactivity within soils vary considerably and can be correlated with certain physical parameters. Permeability and drainage characteristics of the soil and underlying strata appear to have profound influences on the distribution of radioactivity with depth.
5. In the "average" New Jersey soil in 1960 about 55 percent of the total deposit of strontium-90 is contained in the top 2 inches, about 79 percent in the top 4 inches and about 96 percent in the top 9 inches. These values contrast quite sharply with similar data observed by Schulert et al for soils collected in the same general area in 1958.
6. As expected strontium-90 appears to have penetrated to greater depths in the soils, on the average, than the other comparable long-lived nuclide cesium-137. Because of the difficulties involved in correcting the observed activities of cerium-144 and ruthenium-106 for radioactive decay, the relative mobilities of these nuclides are somewhat obscured. Nevertheless, while ruthenium-106 shows relatively more penetration in the tops of the cores than cerium-144, the profile is inexplicably reversed at greater depths.
7. From the radiological hazard point of view the combined activities of the three gamma-emitting nuclides yield a dose rate which is less than 3 percent of the external dose rate recommended by the NCRP for the general populace. This level of activity will, of course, decrease rather rapidly with time as the radioactivity decays.

REFERENCES

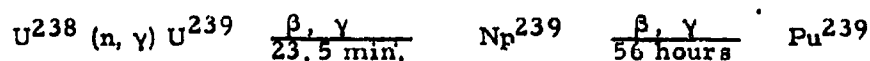
1. Hillebrand, W. F., and Lundell, G. E., "Applied Inorganic Analysis," (J. Wiley and Sons, New York, 1953) Second Edition, Part III, P. 838.
2. Turk, E., "A Modified Radiochemical Strontium Procedure," ANL-5184 Dec. 1953.
3. Sugihara, T. T., James, H. I., Troianello, E. F., and Bowen, V. T., Anal. Chem. 31, 44 (1959).
4. Niday, J. B., "Radiochemical Procedures in Use at the University of California Radiation Laboratory," (Livermore), UCRL-4377.
5. Gustafson, F. F., Marinelli, L. D., and Brar, S. S., Science, 127, 1240 (1958).
6. Glendenin, L. E., Flynn, K. F., Buchanan, R. E. and Steinberg, E. P., Anal. Chem., 27, 59 (1955).
7. Alexander, L. T., Statement for the Joint Committee on Atomic Energy, 86th Congress, U. S. Government, P. 278, May 1959.
8. Alexander, L. T., Jordan, R. H., Dever, R. F., Hardy, Jr., E. P., Hamada, G. H., Machta, L., and List, R. J., "Strontium-90 on the Earth's Surface," HASL-88, USAEC, July 1, 1960.
9. Higgins, G. H., "Evaluation of the Ground-Water Contamination Hazard from Underground Nuclear Explosions," J. Geophys. Research, 64, 1509 (1959).
10. Lockhart, Jr., L. B., Patterson, Jr., R. L., Saunders, Jr., A. W., and Black, R. W., "Fission Product Radioactivity in the Air along the 80th Meridian (West) during 1959," NRL Report 5528, August 15, 1960.
11. Walton, A., "Studies of Nuclear Debris in Precipitation," Isotopes, Inc. 6th Progress Report Contract AT(30-1)-2415, USAEC, January 31, 1961.
12. Katcoff, S., Nucleonics, 16, No. 4, 78 (1958).
13. Schulert, A. R., Kulp, J. L., and Broecker, W. S., "Distribution of Nuclear Fallout," Annual Report to USAEC, Contract AT(30-1)-1656, October 1, 1959.
14. Thornthwaite, C. W., Mather, J. R., and Nakamura, J. K., "Movement of Radiostrontium in Soils," Science, 131, 1015 (1960).
15. Miller, J. R., and Reitemeier, R. F., "Rate of Leaching of Radiostrontium through Soils by Simulated Rain and Irrigation Water," U. S. Dept. Agr. ARS Research Rept. No. 300, (1957).

16. Gustafson, P. F., "Cesium-137 in Soils," *Science*, 130, 1404 (1959).
17. Alexander, L. T., Hardy, Jr., E. P., and Hollister, H. L., "Radioisotopes in Soils: Particularly with Reference to Strontium-90," Published in *Radioisotopes in the Biosphere* by University of Minnesota 1960.
18. Argonne National Laboratory Soil Data, Radiological Health Data, Quarterly Report, January, 1961.
19. Walton, A., "Studies of Nuclear Debris in Precipitation," Isotopes, Inc., 5th Progress Report, Contract AT(30-1)-2415, USAEC, October 15, 1960.
20. Report of United Nations Scientific Committee on the Effects of Atomic Radiation (UNSCEAR), New York 1958.
21. "Maximum Permissible Body Burdens and Maximum Permissible Concentrations of Radionuclides in Air and in Water for Occupational Exposure," Handbook 69, National Bureau of Standards, U. S. Department of Commerce, June 5, 1959.

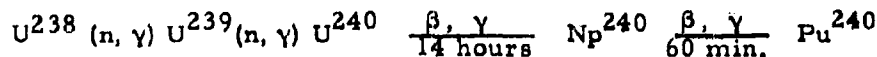
CHAPTER 4

PLUTONIUM IN MAN AND ENVIRONMENT

Fallout plutonium does not result directly from the fission reaction occurring in a nuclear detonation. However, it is produced in a nuclear detonation as the result of the radiation capture process of the uranium-238 present in the device. In this process, neutrons which are released by the fission reaction are absorbed by the uranium-238 with the subsequent emission of gamma rays to form uranium-239. Uranium-239 decays with a 23.5 minute half-life to neptunium-239 which in turn decays with a 56 hour half-life to plutonium-239, i.e.



Actually there are two significant nuclides of plutonium which are produced. Plutonium-240 is also generated as the result of successive neutron capture of uranium-238, i.e.



The radiation characteristics of plutonium-239 and plutonium-240 are given in Table 4.1. Both isotopes are alpha emitters with similar energies of emission. They have the same chemical characteristics, and it is impossible by normal radiometric assay techniques to differentiate between the two. Consequently the total plutonium in a sample is usually measured without reference to its isotopic composition. Although the half-life of plutonium-240 is about 1/4 that of plutonium-239, radioactive decay of plutonium-240 will not be significant for many years since its half-life is 6,600 years.

Mode of Entry into Humans

Plutonium has always been considered an extremely hazardous radioactive nuclide as far as incorporation into biological systems is concerned

Table 4.1 Radiation Characteristics of Plutonium-239 and Plutonium-240

<u>Isotope</u>	<u>Half-Life</u>	<u>Emissions</u>
Plutonium-239	24,300 Years	γ 5.15, 5.14, 5.10 Mev γ 0.052, 0.039, Mev
Plutonium-240	6,600 Years	γ 5.16, 5.12 Mev γ 0.045 Mev

Once in the blood stream, it has been described as a bone seeker with 85 percent of the absorbed plutonium being fixed in the skeleton and largely retained throughout the lifetime of the animal¹. However, the liver, kidney, and lymph nodes have also been observed as sites of plutonium deposition². Since the apparent half-time of plutonium elimination from the skeleton in man is about 200 years, it is accumulated by the body on absorption.

Two modes of entry of fallout plutonium into man have been considered, namely ingestion and inhalation. To evaluate ingestion as a mode of entry, the plutonium was traced through the ecological cycle from soils to man. Since plutonium is tightly bound when deposited in soil and is chemically unrelated to any of the essential nutrients of plants, its incorporation into plant metabolism was considered unlikely. In studying the absorption of plutonium by barley from a sandy soil, Rediske³ reported that the ratio of plutonium concentration in dry plant material to the concentration in the soil was 9×10^{-4} . When domestic animals ingest such plant food, there is an additional 10^{-4} discrimination factor in meat and dairy products. Langham¹ reported that "the over-all discrimination in going through the ecological cycle from soils to man is at most 5×10^{-8} ". With such a large discrimination, it was concluded that a significant degree of incorporation of plutonium fallout into man via the ecological chain was quite unlikely. However, Langham added that "incorporation via inhalation and direct fallout on vegetation, although insignificant also, probably would be much greater than incorporation via ecological transport."

To further evaluate inhalation as a mode of entry of fallout plutonium into man, the mechanism describing the pulmonary deposition, retention and turnover must be known. The Harriman Conference on Permissible Dose⁴ adopted a lung model in an attempt to simplify the many factors involved. Basically the model assumes that 75 percent of all inhaled particles are deposited

in the respiratory tract. Approximately 50 percent of those inhaled are removed by ciliary action and swallowed. The elimination of these particles by this process is considered to be independent of solubility and to occur with a half-time of about 20 days. Of the 25 percent remaining, two possibilities are considered: (a) if the substance is readily soluble, it is assumed to be taken up quickly into the body; (b) if the material is insoluble, it is assumed that half will be eliminated from the lungs by way of the tracheo-bronchial tree and be swallowed, while the rest, namely, 12.5 percent of the initial amount inhaled, is considered to remain in the lung with a half life of 120 days.

Stannard⁵ has investigated inhalation hazards and has concluded that the accumulation of material in pulmonary lymph nodes on a per gram of tissue basis, particularly after prolonged inhalation exposure, may greatly exceed that in the lung. He has shown that in controlled experiments with animals the dpm of plutonium per gram of pulmonary lymph node tissue is higher by factors of 10 or more than the corresponding dpm per gram of lung tissue. This is analogous to the reports from medical authorities that radioactive colloidal gold concentrates in the lymph nodes when injected into patients for therapeutic or diagnostic purposes⁶. Stannard concluded further that the lymph nodes may limit exposure under many conditions and that calculation of maximum permissible doses on this basis may be required. Bair⁷ found somewhat comparable results from the intratracheal administration of plutonium oxide in dogs. Ten days after exposure, the plutonium dpm per gram of pulmonary lymph nodes was already about 0.1 percent of the value for the lungs, indicating that the pulmonary lymph nodes rapidly accumulate plutonium. Bair also noted plutonium was translocated from the lungs to the ovaries and bones.

Environmental Levels

Baus⁸ has shown that the average strontium-90 concentration in ground level air for Washington, D. C. in mid 1957 was about 1.5 dpm per 100 standard cubic meters. Using the Pu/Sr⁹⁰ dpm ratio of 0.018 obtained from the HASP analyses⁹ of stratospheric air, the plutonium concentration for ground level air is calculated to have been 0.027 dpm/100 SCM. The AEC regulations in Part 20 Title 10 of the Federal Register specify that the maximum permissible concentration of soluble plutonium (either plutonium-239 or plutonium-240) in air for the general population is about 1.4 dpm/SCM when bone is considered to be the critical organ. The plutonium concentration calculated above (0.027 dpm/100 SCM) represents approximately 0.2 percent of MPC.

Since man breathes at an average rate of 20 standard cubic meters per day, he inhaled about 0.0054 dpm of plutonium per day in mid 1957. According to the Harriman lung model, 62.5 percent of the plutonium is eliminated from the lungs with a 20 day half-life, while 12.5 percent of the plutonium remains in the lung with a 120 day half life. It was further assumed that at equilibrium, the elimination rate from the lungs by each process is equal to the deposition rate. Therefore:

$$0.625 \times 5.4 \times 10^{-3} \text{ dpm Pu eliminated/day} = \frac{0.693}{20 \text{ days}} \times (\text{dpm Pu})_1 \text{ in lung} \quad (4.1)$$

$$0.125 \times 5.4 \times 10^{-3} \text{ dpm Pu eliminated/day} = \frac{0.693}{120 \text{ days}} \times (\text{dpm Pu})_2 \text{ in lung} \quad (4.2)$$

Solving the above equations for the plutonium activity in the lungs yields 0.097 and 0.117 dpm by process 1 and 2 respectively. Their sum representing the total lung burden is 0.21 dpm. Since the weight of the lungs is about 1000 grams, the plutonium concentration in human lungs in mid 1957 calculated from the Harriman lung model was 0.21×10^{-3} dpm/gram of tissue. This concentration

can be translated to percent of maximum permissible dose by the following derivation:

NBS Handbook 69¹⁰ proposes a maximum annual dose of 15 rems for most individual organs of the body and 5 rems for the gonads or the whole body for occupational workers. By applying a 1/10 reduction of this dose for the general population, the plutonium concentration in most individual organs can be converted to percent of maximum permissible dose to that organ by multiplying the $\frac{\text{dpm Pu}}{\text{g of tissue}}$ by a factor which converts the alpha energy per disintegration per minute to rems per year and dividing by the MPD in rems per year. This gives

$$\frac{\text{dpm Pu}}{\text{g of tissue}} \times 28.8 = \% \text{ of MPD to organ.} \quad (4.3)$$

Since the MPD to the gonads is 1/3 that of most individual organs:

$$\frac{\text{dpm Pu}}{\text{g of gonads}} \times 86.4 = \% \text{ of MPD to gonads.} \quad (4.4)$$

According to equation 4.3, the 0.21×10^{-3} dpm Pu/gram of lung tissue calculated above represents about 0.01 percent of MPD to the lungs.

Based on these measurements and calculations, and in view of the rapid accumulation of plutonium in the pulmonary lymph nodes, inhalation of fallout plutonium was considered to be a significant mode of entry into the body and further investigation appeared warranted. Eight samples, selected at random from the library of daily air samples from the Washington, D. C. area, and collected from March through June 1959 were made available to Isotopes, Inc. by Dr. L. B. Lockhart, Jr. of the U. S. Naval Research Laboratory. The plutonium analyses of these filter paper samples gave an average value of about 0.14 dpm/100 SCM which is a factor of 5 greater than the value calculated for mid-1957. This agrees with the British estimate of 0.2 dpm/100 SCM for this

period¹¹. The spring 1959 ground level air concentration of plutonium represents about 1 percent of MPC for the general population. Using this most recent concentration in equations 4.1 and 4.2 yields 0.48 dpm respectively, or a total lung burden of 1.06 dpm. This burden corresponds to about 0.05 percent MPD in the lungs. As a result of these estimates and measurements, a cursory investigation of plutonium in human and animal tissue was undertaken.

Analytical Procedure

After the wet weight of the sample was determined, the sample was ashed in an evaporating dish over a Meeker burner. The residue was ignited in a muffle furnace at 650°C for 8 hours or until all the carbon was burned off. The ash was fused with 5 grams of sodium carbonate at 950°C for 1/2 hours. The cooled melt was dissolved in hydrochloric acid and diluted to 250 ml for analysis as follows; any undissolved silicious material was washed and discarded.

1. Adjust pH of sample solution to 1 with conc. NH_4OH ; add 10 ml of 5% $\text{NH}_2\text{OH}\cdot\text{HCl}$ and wait 10 minutes for reduction to Pu^{+3} .
2. Add 2 ml of saturated $\text{Bi}(\text{NO}_3)_3$ solution and conc. NH_4OH dropwise with stirring until BiPO_4 precipitates. The pH of the supernate must not be greater than 1.5; adjust if necessary with the dropwise addition of conc. HCl .
3. Digest the precipitate at room temperature for 1/2 hour; aspirate the supernate to about 50 ml. above the precipitate and discard the supernate.
4. Transfer the mixture to a Lusteroid tube, centrifuge and discard the supernate. Wash down the sides of the beaker which contained the precipitate with 10 ml of 5 N HCl and heat. Transfer the HCl wash from the beaker to the Lusteroid tube to dissolve the BiPO_4 precipitate. Wash the beaker with another 2 ml of 5N HCl and combine in the Lusteroid tube. (Note 1).
5. Add 1 ml of lanthanum carrier (2 mg/ml), 2-4 drops of 5% $\text{NH}_2\text{OH}\cdot\text{HCl}$ and wait 10 minutes.
6. Add conc. HF to make the final solution 2.5 molar in HF (Note 2). Digest the precipitate in a hot water bath for 5 minutes, centrifuge and discard the supernate.

7. Wash the LaF_3 precipitate with 2.5 M HF-HNO_3 solution and discard the wash.
8. Slurry the precipitate with 1 ml. of saturated boric acid solution and transfer to a 50 ml. beaker with 7N HNO_3 . Wash the Lusteroid with 7N HNO_3 and combine with the solution in the beaker.
9. Heat the solution and adjust the acidity to 7N HNO_3 . Continue with step 5 of the plutonium procedure in Part I, Chapter 3 in which the solution is added to the anion exchange column.

Notes

1. If the sample has a high calcium content as in the case of bones, a second precipitation must be performed. CaF_2 precipitates during the LaF_3 scavenge and the calcium interferes with the efficiency of the ion exchange column. The chemical yield of plutonium in an analysis employing two Bi PO_4 precipitations is $72.1 \pm 5.4\%$ as compared to a $83.7 \pm 4.0\%$ yield for an analysis involving only Bi PO_4 precipitation.
2. If some iron has been carried through with the Bi PO_4 precipitation, sufficient HF must be added to complex it. When all of the iron is complexed, the solution should be decolorized.

The electroplated disks were assayed by using ZnS scintillation counters. The spectra of several samples were determined by alpha particle spectroscopy, and they exhibited pure plutonium-239 and/or 240 with no other alpha contamination. Since the plutonium activities in the samples which were analyzed were generally low, extreme caution was exercised to eliminate possible contamination of the sample during the analytical processing. Reagent blanks were processed concurrently with samples to monitor the contamination level if any existed. In addition, lung tissue autopsied prior to 1945* was processed to represent ideal tissue blanks. In all cases, the blank samples reflected no detectable alpha activity.

* Made available through the courtesy of Col. J. M. Blumberg, Deputy Director Armed Forces Institute of Pathology, Washington 25, D. C.

Human Tissue Analyses

The results of the human tissue analyses are reported in Table 4.2. The errors accompanying the data represent one standard deviation of the counting error. All samples were obtained in the New York metropolitan area. The sample solution obtained from a 1959 lung sample was split and each aliquot analyzed separately to reflect the reproducibility of the radiochemical procedure. Analyses of other duplicate samples and standards in which the counting errors were minimal gave an average precision of better than ± 5 percent. The composite organs in group 1 consisted of combined samples from six cadavers whose age at time of death was at least 70 years.

The most striking result obtained from the analyses of the human tissue is the high percentage of the maximum permissible dose (MPD) delivered to the lungs, pulmonary lymph nodes and gonads by the plutonium deposited in these organs. This is particularly emphasized by comparison to the average percent of MPD delivered by Sr^{90} to the adult skeleton. Kulp¹² has reported that the average Sr^{90} concentration in adult bone in 1957 for Western culture in the Northern Hemisphere was about 0.30 $\mu\text{pc/g Ca}$ or about 0.15 percent of MPD. The percent of MPD for plutonium in lungs, pulmonary lymph nodes and gonads ranges from 1/3 to about 10 times this percent of Sr^{90} MPD to the skeleton. The gonad burden raises the question of genetic effects in addition to possible somatic effects.

The distribution of total plutonium measured in the human organs supports the theory that inhalation is the significant mode of entry of fallout plutonium into man. In the composite organs of group 1, only one lung from each cadaver was analyzed, so that the activity (4.1 DPM) for the total lung sample should be doubled when comparing the plutonium content of the various organs. It is clear that the total activity of plutonium in the lungs is about 10 times greater

Table 4.2 Plutonium Analyses of Human Tissue

<u>Sample*</u>	<u>Year of Death</u>	<u>Sample Weight (g)</u>	<u>DPM \pm Stnd. Dev.</u>	<u>DPM/g of Tissue \pm Stnd. Dev. (10⁻³)</u>	<u>%MPD \pm Stnd. Dev.</u>
lung - 1	1953	950	0.409 \pm 0.030	0.430 \pm 0.037	0.012 \pm 0.001
lung - 2	1954	1000	0.760 \pm 0.062	0.760 \pm 0.062	0.022 \pm 0.002
lung - 3	1958	398	4.75 \pm 0.44	11.9 \pm 1.1	0.34 \pm 0.03
tracheo-hilar lymph nodes - 3	1958	3.4	0.22 \pm 0.11	65 \pm 32	1.9 \pm 0.9
lung - 4A	1959	450	0.565 \pm .007	1.25 \pm 0.17	0.036 \pm 0.005
4B	1959	450	0.611 \pm .077	1.36 \pm 0.17	0.39 \pm 0.005
<u>Composite Organs - Group 1</u>					
lung	1959	2340	4.06 \pm 0.39	1.74 \pm 0.17	0.050 \pm 0.005
pulmonary lymph nodes	1959	53.6	0.57 \pm 0.21	11 \pm 4	0.32 \pm 0.11
spleen	1959	889	1.02 \pm 0.19	1.15 \pm 0.21	0.033 \pm 0.006
kidney	1959	949	0.94 \pm 0.13	0.99 \pm 0.22	0.028 \pm 0.006
gonad	1959	96	0.76 \pm 0.18	7.9 \pm 1.9	0.68 \pm 0.16

* Samples collected from 1953 to 1958 were made available by Dr. Arthur Schultert, Lamont Geological Observatory, Palisades, New York

Samples recovered in 1959 were supplies by Dr. Roth, Head Pathologist, Bergen Pines Hospital, Oradell, N.J.

than any other organ measured. Further, the high activity per gram in the pulmonary lymph nodes (a factor of about 6 greater than the corresponding lungs) correlates with theories predicting that the plutonium deposited in the lungs will concentrate in the lymph system. This argues that the pulmonary lymph nodes may be the critical organ as far as plutonium inhalation is concerned. It is interesting to note that the values of plutonium found in the lungs autopsied in the spring of 1959 agree with a predicted value of 1 dpm per gram calculated from the Harriman lung model of pulmonary deposition and the measured air concentrations.

Animal Tissue Analyses

The results of the animal tissue analyses are reported in Table 4.3. The samples comprising the steer number 1 organs were recovered from the same animal by making arrangements with a local slaughterhouse. All other samples in Table 4.3 were purchased in supermarkets in the northern New Jersey area during the fall of 1958 and the spring of 1959. In the stewing beef samples numbers 3 and 4, the fluid was drained from the meat and each fraction analyzed separately.

The plutonium activities per gram of beef spleen, stewing beef and particularly the fluid extract from the stewing beef samples are relatively high. Stewing beef samples are extracted from the shoulder of the animal in the vicinity of the thoracic duct. Since these samples are all associated with the lymph system, there is an apparent correlation between high plutonium content and this system.

The one steer lung analyzed contained about the same amount of plutonium per gram as did human lung. Unfortunately, this steer lung was not recovered from the same animal as the number 1 group of samples. Therefore,

no definitive correlation between total plutonium burden and organ can be made to delineate the mode of entry of the plutonium into the animal. However, the high concentrations of plutonium in the spleen and stewing beef samples offer curious data which may be difficult to explain solely on the basis of an inhalation mode of entry.

The general level of plutonium found in the other tissue in Table 4.3 reflects its somewhat ubiquitous nature. The percent of MPC for ingestion of these meat products by the general population is also included in Table 4.3. Although the concentrations approach one percent in the spleen and stewing beef samples, the general levels are of no real significance as far as ingestion hazards of the total diet are concerned. This has also been demonstrated by the plutonium analysis of several total diet samples which were collected by Consumers Union in their study of Sr^{90} during 1959¹³. The highest concentration of plutonium found in these samples (0.095 dpm/kg) represents only 10^{-3} percent of MPC for continuous ingestion by the general population.

Miscellaneous Sample Analyses

The common occurrence of low levels of plutonium is further indicated by the analyses of miscellaneous samples reported in Table 4.4. The plutonium concentration of the alfalfa may be indicative of its concentration in other forms of vegetation. Since the ash weight of wheat is about 2 percent of the raw vegetation, the specific activities reported range from about 0.02 to 0.15 percent of MPC for plutonium ingestion.

Strontium-90 analyses were also performed on the miscellaneous samples, and the Pu/Sr^{90} ratio is reported in Table 4.4. The ratio obtained from the rain sample compares favorably with the ratio obtained from the stratospheric and ground level air samples. The ratios for the alfalfa and

Table 4.3 Plutonium Analyses of Animal Tissue

Sample	Time of Collection	Sample Weight (g)	DPM \pm Std. Dev.	DPM/g \pm Std. Dev. (10^{-3})	% MPC \pm Std. Dev.
Steer No. 1 Organs	Spring 1959				
spleen		453	41.7 \pm 6	92.1 \pm 3.5	0.84 \pm 0.03
liver		482	3.11 \pm 0.37	6.45 \pm 0.77	0.059 \pm 0.007
heart		609	2.01 \pm 0.31	3.30 \pm 0.51	0.033 \pm 0.004
Steer lung	Spring 1959	381	0.71 \pm 0.16	1.9 \pm 0.4	0.017 \pm 0.004
Stewing Beef Samples	Fall 1958 thru Spring 1959				
1		516	35.5 \pm 1.6	68.8 \pm 3.1	0.62 \pm 0.03
2		462	46.4 \pm 2.2	100 \pm 5	0.91 \pm 0.04
3		540	16.0 \pm 0.7	27.8 \pm 1.3	0.25 \pm 0.01
a) Tissue		432	1.29 \pm 0.24	2.99 \pm 0.56	
b) Fluid		32.6	13.7 \pm 0.7	420 \pm 21	
4		270	1.42 \pm 0.33	5.26 \pm 1.22	0.048 \pm 0.011
a)		213	0.64 \pm 0.12	3.0 \pm 0.6	
b)		18.4	0.78 \pm 0.31	42 \pm 17	
Pork Liver (average of 5 Samples)	Fall 1958 thru Spring 1959	390	1.75 \pm 0.73	4.48 \pm 1.87	0.041 \pm 0.017

Table 4.4 Miscellaneous Plutonium Analyses

Sample* Type	Sample Weight (g)	Sample dpm ± Std. Deviation	dpm/g ± Std. Deviation (10 ⁻³)	Pu/Sr ⁹⁰
Alfalfa Ash I	5.6	9.92 ± 0.96	1770 ± 170	0.12
Alfalfa Ash II	4.2	4.03 ± 0.39	960 ± 93	0.15
Wheat Ash I	5.3	1.49 ± 0.27	281 ± 51	0.046
Wheat Ash II	5.2	7.75 ± 0.51	1490 ± 100	0.114
Wheat Ash III	5.91	1.11 ± 0.18	188 ± 30	0.057
Wheat Ash IV	5.24	0.996 ± 0.149	190 ± 28	0.060
Rain	5000	1.98 ± 0.30	0.396 ± 0.060	0.028

* The alfalfa and wheat ash samples were harvested in 1958 and were supplied by Dr. John Harley, Director Health and Safety Laboratory, AEC, New York.

The rain sample was collected in the spring of 1959 on the roof of Isotopes, Inc.

wheat ash samples are a factor of 2 to 5 times greater. This discrimination against strontium-90 is most probably the result of the foliar uptake mechanism of plant contamination. The fallout plutonium was deposited on the leaves of the plant and was retained to a greater degree than the strontium-90.

Summary

These data, particularly the results from the human tissue analyses, have shown that fallout plutonium has entered the biosphere and man, and that inhalation is the principal mode of entry into man. In addition, it appears that the pulmonary lymph nodes should be considered in the assignment of the critical organ as far as inhalation of plutonium is concerned. As a result of the moratorium of nuclear weapons, the rate of fallout and, therefore, the plutonium concentration in ground level air have markedly decreased. Barring an unexpectedly high resuspension of surface deposited fallout, there is probably no hazard associated with fallout plutonium at the present time. It is unfortunate that a more extensive program was not undertaken during 1959 and 1960 when a precise assessment of the hazard from plutonium in nuclear weapons fallout could have been made.

It is possible that one aspect of this investigation may still be exploited to good advantage. A great deal of research has been directed toward the metabolism and fate of plutonium in a living system. Extensive laboratory tests with animals are still in progress to probe deeper into this study. No matter how successful these studies are, there remains the enormous extrapolation of the results from the laboratory test animals to the ultimate biological system of concern, i. e. man. The presence of plutonium in man as a result of nuclear weapons testing offers a unique opportunity to study the metabolism and translocation of this element within the body. The results of this cursory

investigation prove unquestionably that this sort of a program could have been conducted two years ago by combining autopsy samples. Since the biological half life of plutonium is long, it is likely that current autopsy material, in perhaps slightly larger composites, could still offer the same opportunity for study.

REFERENCES

1. Langham, W., and Anderson, E. C., Bulletin of the Swiss Academy of Medical Sciences, 14, 434 (1958).
2. Williams, K., "Studies of the Toxicology of Plutonium," AERE-R2970 (1959)
3. Rediske, J. H., Cline, J. R., and Selders, A. A., Hanford Atomic Energy Works Report HW-36734 (1955).
4. Langham, N. H., Am. Ind. Hyg. Assoc. Quarterly, 17, 305 (1956).
5. Stannard, J. N., Second United Nations International Conference on the Peaceful Uses of Atomic Energy A/Conf. 15/P/738 U.S.A. (1958).
6. Roth, D., Head Pathologist, Bergen Pines County Hospital, Oradell, N.J. Private Communication (1959).
7. Bair, W. J., Hanford Atomic Products Operations Report, HW-56636 (1958).
8. Paus, R. A., Patterson, R. L. Jr., Saunders, A. W. Jr., and Lockhart, L. B. Jr., Naval Research Laboratory Report 5239 (1958).
9. "Second Technical Report of the High Altitude Sampling Program", Isotopes, Inc. (1959).
10. "Maximum Permissible Body Burdens and Maximum Permissible Concentrations of Radionuclides in Air and Water for Occupational Exposure", U. S. Department of Commerce, National Bureau of Standards Handbook 69, U. S. Government Printing Office, Washington 25, D. C. (1959).
11. Pierson, D. H., Crooks, R. N., and Fisher, E. M. R., AERE-M620 (1960).
12. Kulp, J. L., Schulert, A. R., and Hodges, E. J., Science 132, 448 (1960).
13. Consumer Reports, June 1960.